OBSERVABLE CONSTRAINTS ON GALACTIC CHEMICAL EVOLUTION USING A UNIFORM SAMPLE OF OPEN CLUSTERS

by

JOHN R DONOR III

Bachelor of Arts, 2014
Austin College
Sherman, TX

Master of Science, 2017
Texas Christian University
Fort Worth, TX

Submitted to the Graduate Faculty of the
College of Science and Engineering
Texas Christian University
in partial fulfillment of the requirements
for the degree of

Doctor of Philosophy

August 2020

ACKNOWLEDGEMENTS

I would like to thank my wife, Rachel, for her constant support. I would like to thank my parents, whose financial support and lifelong guidance have been essential to my success. I would also like to thank my adviser for his guidance and advocacy on my behalf. Finally I would like to thank my colleagues, current and graduated, for their support and comradery.

This material is based upon work supported by the National Science Foundation under award AST-1311835 and AST-1715662.

This research made use of Astropy, a community-developed core Python package for Astronomy (Astropy Collaboration, 2013).

This publication makes use of data products from the Two Micron All Sky Survey, which is a joint project of the University of Massachusetts and the Infrared Processing and Analysis Center/California Institute of Technology, funded by the National Aeronautics and Space Administration and the National Science Foundation.

This publication makes use of data products from the Wide-field Infrared Survey Explorer, which is a joint project of the University of California, Los Angeles, and the Jet Propulsion Laboratory/California Institute of Technology, funded by the National Aeronautics and Space Administration.

Funding for the Sloan Digital Sky Survey IV has been provided by the Alfred P. Sloan Foundation, the U.S. Department of Energy Office of Science, and the Participating Institutions. SDSS acknowledges support and resources from the Center for High-Performance Computing at the University of Utah. The SDSS web site is www.sdss.org.

SDSS is managed by the Astrophysical Research Consortium for the Participating Institutions of the SDSS Collaboration including the Brazilian Participation Group, the Carnegie Institution for Science, Carnegie Mellon University, the Chilean Participation Group, the French Participation Group, Harvard-Smithsonian Center for Astrophysics, Instituto de Astrofsica de Canarias, The Johns Hopkins University, Kavli Institute for the Physics and Mathematics of the Universe (IPMU) / University of Tokyo, Lawrence Berkeley National Laboratory, Leibniz Institut fr Astrophysik Potsdam (AIP), Max-Planck-Institut fr Astronomie (MPIA Heidelberg), Max-Planck-Institut fr Astrophysik (MPA Garching), Max-Planck-Institut fr Extraterrestrische Physik (MPE), National Astronomical Observatories of China, New Mexico State University, New York University, University of Notre Dame, Observatrio Nacional / MCTI, The Ohio State University, Pennsylvania State University, Shanghai Astronomical Observatory, United Kingdom Participation Group, Universidad Nacional Autnoma de Mxico, University of Arizona, University of Colorado Boulder, University of Oxford, University of Portsmouth, University of Utah, University of Virginia, University of Washington, University of Wisconsin, Vanderbilt University, and Yale University.

Contents

1 Introduction **1**

1.1 General Scientific Introduction 1
1.1.1 Open Star Clusters 1
1.1.2 Chemical Abundances in Astronomy 3
1.1.3 Stellar Nucleosynthesis 5
1.2 Probing Galactic Evolution 7
1.2.1 Galactic Chemical Modeling 8
1.2.2 Observing the Galactic Abundance Gradient 9
1.2.3 The Evolution of the Abundance Gradient 11
1.2.4 On Radial Migration 12

2 Methodology and the Very High Quality Sample **14**

2.1 OCCAM Target Selection 14
2.2 Analysis 18
2.2.1 OCCAM Observed Stars in SDSS4 DR14 18
2.2.2 OCCAM Membership Criteria 19
2.2.3 Measured Cluster Bulk Abundances 24
2.3 Cluster [Fe/H] in Comparison to previous work 24
2.3.1 NGC 2682 (M67) 25
2.3.2 NGC 188 25
2.3.3 NGC 6791 26
2.3.4 NGC 2420, NGC 6819, and NGC 7789 26
2.3.5 APOGEE DR14 vs. Literature Trends 27
2.4 Galactic Metallicity Gradients 27
2.4.1 Error Analysis 28
2.4.2 NGC 6791 and the metallicity gradient 29
2.4.3 Distance Effects on the Gradient 30
2.4.4 Comparison to Previous Work 33
2.5 Other Elements Beyond [Fe/H] 36
2.5.1 OCCAM DR14 Calibration Sample 38
2.5.2 Galactic Gradients in Other Elements 39

3 Evolution of Galactic Chemical Trends **44**
3.1 Data . . . 45
3.2 Methods . . . 50
3.2.1 Membership Analysis . . . 50
3.2.2 Visual Quality Check . . . 50
3.2.3 Data Access - SDSS Value Added Catalog . . . 52
3.3 The OCCAM DR16 Sample . . . 54
3.3.1 Modifications to the High Quality Sample . . . 55
3.3.2 Comparison to previous work . . . 56
3.4 Measuring Galactic Trends . . . 59
3.4.1 Choosing a Distance Catalog . . . 59
3.4.2 Fitting Galactic Abundance Gradients . . . 61
3.5 The Galactic Metallicity Gradient . . . 62
3.6 Galactic Trends for Other Elements . . . 65
3.6.1 Galactic Trends for α-Elements . . . 65
3.6.2 Galactic Trends for Iron-Peak Elements . . . 66
3.6.3 "Odd-z" Gradients . . . 69
3.7 The Evolution of Galactic Abundance Gradients . . . 71
3.7.1 Iron . . . 71
3.7.2 Other Elements . . . 74
3.7.3 The Evolution of [X/Fe] Gradients . . . 76

4 Characterizing Open Cluster Radial Migration **79**
4.1 Deriving Birth Radius from a Model . . . 79
4.2 Implications from the Model . . . 83

5 Conclusions **85**

A Table 2.1: OCCAM sample from APOGEE data used for membership analysis – Full Version **89**

B Table 2.6: DR14 OCAAM Open Cluster Member Star Abundances – Full Version **112**

C Table 3.1: OCCAM DR16 Sample - Basic Parameters – Full Version **135**

D Table 3.2: OCCAM DR16 Sample - Detailed Chemistry – Full Version **141**

E Figure Set For Figure 2.2 **153**

Vita

Abstract

List of Figures

1.1 Color-Magnitude Diagram (CMD) for an open cluster with an isochrone fit. J-magnitude, shown on the y-axis, is brightness, measured with the 2MASS J filter, J-K, shown on the x-axis, is the difference in 2MASS J magnitude and 2MASS K_S magnitude, referred to as a "color". 2

2.1 Sample analysis for the cluster King 7 utilizing 2MASS+WISE data (Frinchaboy et al. 2010). a) Galactic latitude and longitude for all stars (gray) within the $2R_{cl}$ area to be analyzed, stars selected to be likely members from the photometry extinction analysis are shown in black. Prime APOGEE targets are circled. b) Distribution of A_{K_s} for all stars in the NGC 6802 sample area, black points denote stars with $1.1R_{cl}$ within the determined mean cluster A_{K_s} range. c) Color-magnitude diagram (CMD) for all stars in the analysis area (gray). The dashed box denotes the SDSS-III/APOGEE target selection region. Black points denote stars selected as likely members from their A_{K_s}. d) CMD of only likely cluster members overplotted with the Padova Isochrone (Marigo et al. 2008) using the clusters parameters from Dias et al. (2002). Circled stars denote identified high-probability stars for APOGEE target selection (also see the sky distribution (a)). 16

2.2 A summary of the membership analysis for open cluster NGC 7789. The complete figure set (19 images) is available in Appendix E. (a) The *Gaia* CMD (Gaia Collaboration et al. 2018, Riello et al. 2018), with proper motion members shown in black, others in gray. Likely APOGEE members are shown as orange stars, non-members as blue squares, and APOGEE stars passing an RV and proper motion membership cut, but failing a $\log(g)$ cut for metallicity reliability are shown as red circles. (b) The $T_{eff} - \log(g)$ diagram for the cluster with an isochrone based on MWSC Catalog ages (Kharchenko et al. 2013) shown for reference. Error bars shown are characteristic, and a possible global offset in $\log(g)$ is seen. (c) The cluster area on the sky. (d) A contour plot of the 2D Gaussian fit to the kernel smoothed proper motions. Contours show 1σ intervals. (e) The Gaussian kernel density convolution in RV, with a Gaussian fit shown in orange. (f) The Gaussian kernel density convolution in [Fe/H], with a Gaussian fit shown in orange. 21

2.3 A comparison to commonly studied clusters in the literature (Δ[Fe/H] = literature–OCCAM). The gray bar indicates the internal 1σ standard deviation for stars in each cluster from our data. 25

2.4 The high reliability metallicity gradients using APOGEE clusters. Dotted lines are shown for reference at $R_{\odot} = 8$ kpc and [Fe/H] = 0 dex. (a) shows the entire sample and (b) shows the sample with the very metal-rich NGC 6791 removed. 28
2.5 The galactic metallicity gradient computed using values from the Dias Catalog (Dias et al. 2002), the MWSC Catalog (Kharchenko et al. 2013), inverse-parallax (Gaia Collaboration et al. 2018, Lindegren et al. 2018), and the Bailer-Jones catalog (Bailer-Jones et al. 2018). 31
2.6 The Galactic abundance trend (R_{GC} vs.[Fe/H]) assuming $R_{GC,\odot} = 8.0$ kpc. Our sample (dark blue triangles) is shown along with a literature sample from Reddy et al. (2016) (light blue points), and clusters analyzed by (Reddy et al. 2012; 2013; 2015; 2016, R16) (orange points). 35
2.7 Comparison of individual elemental abundances using the APOGEE calibration clusters with available comparison elements in the other literature studies. Clusters are color-coded by analysis group: *dark blue* for Reddy et al. 2013; 2016, *light blue* for Jacobson et al. 2011, *green* for Bragaglia et al. 2001, *orange* for Carraro et al. 2006, and *red* for O'Connell et al. 2018 (submitted). 38
2.8 Galactic Trend for our sample for the α elements (O, S, Mg, Si, Ca) from DR14. 40
2.9 Galactic trend for our sample for the iron-peak (V, Co, Mn, Cr, Ni) elements from DR14. Clusters with very large uncertainties are not included in the fit (N reflects only those included in the fit), but are shown for reference as blue dots. 41

3.1 Five example color-magnitude diagrams of open clusters analyzed in the study, with cluster name and quality designation from Table 3.1 . *Gaia* stars within twice the cluster radius are shown; stars identified as PM members and inside the cluster radius are blue. Non-member stars are shown as a Hess diagram in grey except for Chupina 5 where actual stars are shown. The OCCAM pipeline-identified APOGEE members are shown as orange stars. 51
3.2 The full OCCAM DR16 sample plotted in the Galactic plane. Square points are "high quality" clusters, triangles are the lower quality clusters. The colorbar shows [Fe/H]. The concentric circles show $R_{GC} = 8$, 16, & 24 kpc 54
3.3 The difference in reported [Fe/H] from DR14 to DR16 for the 19 clusters from 2. A characteristic error-bar is shown. 56
3.4 Similar to Figure 3.3 but for other elements. Characteristic error bars are shown. Datapoints are colored by their [Fe/H] as reported in APOGEE DR16 57
3.5 The difference between the metallicities in the LAMOST (from Zhang et al. 2019) and APOGEE surveys for open clusters in common. The color bar indicates the number of APOGEE stars in the cluster (saturating at 5). The square symbols denote clusters with a single star in Zhang et al. (2019). 58

3.6 [Fe/H] vs R_{GC} trends measured using different distance determinations. This is similar to an analysis performed in 2, but we have added measurements from Cantat-Gaudin et al. (2018) where available. The colorbar shows the number of APOGEE stars per cluster, saturating at 5. 60
3.7 The full high quality sample Galactic [Fe/H] versus R_{GC} trend, with a 2-line fit (described by Eq. 3.1). Clusters flagged with quality "0" are shown as light blue circles. The color bar indicates the number of member stars per cluster, saturating at 5. 63
3.8 The "corner plot" showing correlations between the 4 free parameters of the 2-line abundance gradient fit shown in Figure 3.7 64
3.9 The [X/Fe] vs R_{GC} trend for α elements. As before the color bar indicates number of member stars, saturating at 5. 67
3.10 The [X/Fe] vs R_{GC} trend for iron-peak elements. Light blue circles are clusters that have an [X/Fe] abundance reported but σ [X/Fe] ≥ 0.2 dex. 68
3.11 The [X/Fe] vs R_{GC} trend for the "odd-z" elements reported in APOGEE DR16. As before, the color bar indicates number of members and light blue circles are clusters with very high uncertainty in that element. 70
3.12 The Galactic [Fe/H] vs R_{GC} trend in 4 age bins, showing the general decrease in steepness over time. 72
3.13 A summary of Galactic metallicity gradients measured in mono-age populations from the literature. 73
3.14 OCCAM IV clusters (red) plotted with the pure chemical evolution model of Chiappini (2009) (blue line) and the MCM chemo-dynamical simulation (Minchev et al. 2013; 2014), seperated into the age bins used previously. . 75
3.15 Gradients measured in four age bins as for Figure 3.12 are plotted for each element. The points increase in size from youngest to oldest; the color indicates number of clusters used to measure each gradient. 76

4.1 A reproduction of Figure 11 from C20, but with updated distances and ages from Cantat-Gaudin et al. (2020). We also color the points by their computed Z-max; the maximum distance a cluster will move away from the Galactic plane during its orbit. 80
4.2 Similar to Figure 4.1 but using the OCCAM high-quality sample. 81

E.1 Summary for NGC 6791 154
E.2 Summary for NGC 6819 155
E.3 Summary for NGC 6811 156
E.4 Summary for Berkeley 53 157
E.5 Summary for NGC 7789 158
E.6 Summary for FSR 0494 159
E.7 Summary for NGC 188 160
E.8 Summary for IC 166 161
E.9 Summary for Berkeley 66 162
E.10 Summary for NGC 1245 163
E.11 Summary for King 7 164

E.12 Summary for NGC 1798 165
E.13 Summary for NGC Berkeley 17 166
E.14 Summary for Berkeley 71 167
E.15 Summary for Teutsch 51 168
E.16 Summary for King 5 169
E.17 Summary for NGC 2158 170
E.18 Summary for NGC 2420 171
E.19 Summary for NGC 2682 172

List of Tables

2.1 OCCAM sample from APOGEE data used for membership analysis . . . 20
2.2 OCCAM Data Sample . . . 23
2.3 A summary of reported spectroscopic metallicity gradients. . . . 30
2.4 R_{GC} calculated using different distance sources . . . 33
2.5 OCCAM DR14 Cluster Abundances . . . 34
2.6 DR14 OCAAM Open Cluster Member Star Abundances . . . 37
2.7 DR14 OCCAM Abundance Comparison to Literature . . . 42

3.1 OCCAM DR16 Sample - Basic Parameters . . . 48
3.2 OCCAM DR16 Sample - Detailed Chemistry . . . 49
3.3 A summary of the individual star data included in the DR16 OCCAM VAC 53

4.1 Comparison of Netopil et al. (2016) and APOGEE migration results . . . 84

A.1 OCCAM sample from APOGEE data used for membership analysis (Full) 89

B.1 DR14 OCAAM Open Cluster Member Star Abundances (Full) . . . 113

C.1 OCCAM DR16 Sample - Basic Parameters (Full) . . . 136

D.1 OCCAM DR16 Sample - Detailed Chemistry (Full) . . . 142

List of Abbreviations

R_{GC}	Galactocentric radius, in cylindrical coordinates
R_{guide}	Galactocentric guiding radius
R_{birth}	Galactocentric birth radius
CMD	Color Magnitude Diagram
RV	Radial Velocity (Doppler velocity)
RA	Coordinates of Right Ascension
Dec	Coordinates of Declination
PM	Proper motion (an object's velocity in RA and Dec)
kpc	kiloparsec
SNe (Ia/II)	supernovae (type Ia/type II)
$M_{\odot}$	Solar mass (the mass of the sun)
[Fe/H]	metallicity (on a log scale, relative to the sun)
[X/Fe]	relative abundance of element X to Fe, also on a log scale
α-elements	elements built up with alpha-particles (O, Mg, Si, S, Ca)
APOGEE	Apache Point Observatory Galactic Evolution Experiment
SDSS	Sloan Digital Sky Survey
OCCAM	Open Cluster Chemical Abundance and Mapping Survey
2MASS	2 Micron All Sky Survey
WISE	Wide-field Infrared Survey Explorer
RJCE	Rayleigh Jeans Color Excess
MWSC	Milky-Way Star Cluster Catalog (Kharchenko et al. 2013)
A_{K_s}	extinction in the 2MASS K_s band
$E(H-4.5\mu\text{m})$	color excess in the $H-4.5\mu$m color
ASPCAP	APOGEE Stellar Parameter and Chemical Abundance Pipeline
MCM	Minchev, Chiappini, & Martig
DR14	14^{th} Data Release from SDSS
DR16	16^{th} Data Release from SDSS
VAC	SDSS Value Added Catalog
NGC	New General Catalog (Dreyer 1888)

Chapter 1

Introduction

1.1 General Scientific Introduction

1.1.1 Open Star Clusters

Stars form when a cloud of gas collapses under its own gravity. Generally, these gas clouds are hundreds or thousands of times the mass of the Sun, resulting in the formation of hundreds or thousands of stars. Stars formed from the same cloud are gravitationally bound and consequently they move through the Galaxy as group. These groups of stars are called open clusters.

Open clusters are often studied using color-magnitude diagrams (CMDs). Magnitude, the astronomical measurement of apparent brightness, is usually measured by counting how many photons from a star fall on a detector. Magnitude is typically measured with a well-calibrated bandpass filter over the detector, for example the "H" bandpass filter blocks any light outside of the range $1.5 < \lambda < 1.8$ μm. The difference in magnitudes

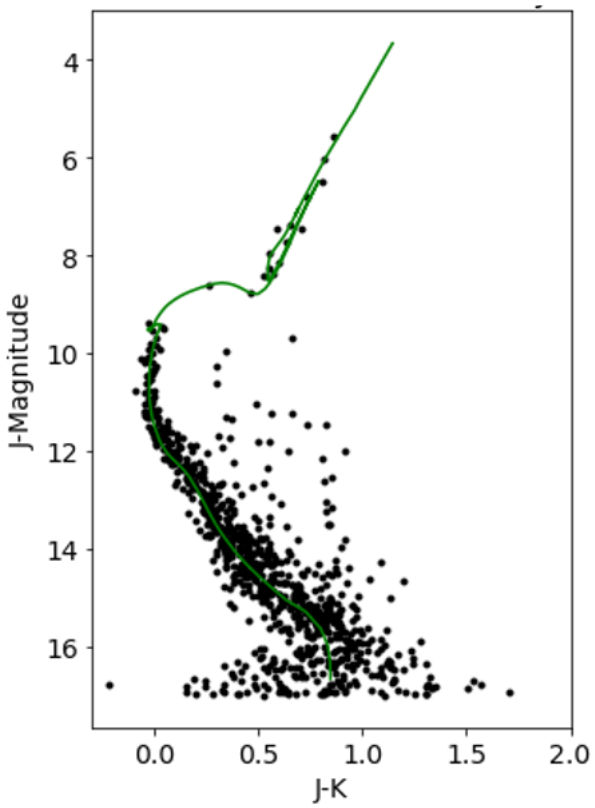

Figure 1.1: Color-Magnitude Diagram (CMD) for an open cluster with an isochrone fit. J-magnitude, shown on the y-axis, is brightness, measured with the 2MASS J filter, J-K, shown on the x-axis, is the difference in 2MASS J magnitude and 2MASS K_S magnitude, referred to as a "color".

measured with two different bandpass filters is called a "color", and is in fact a numerical representation of a color. Figure 1.1 shows an example CMD using the J and K bandpass filters.

The green line in figure Figure 1.1 is an isochrone. A single isochrone model is generated by evolving a population of stars of varying masses, but uniform chemical composition, for a set period of time. If an isochrone models a star cluster CMD well, as in Figure 1.1, it is likely the stars in that cluster match the chemical composition and age of the isochrone.

Isochrone models are generated from stellar evolution models, thus the intrinsic brightness, or "absolute magnitude" of the stars in the model is known. To match a cluster, the magnitudes must be changed to reflect the apparent magnitude observed for the cluster stars. Since brightness decreases as $\frac{1}{r^2}$, where r is the distance to the object, if both the apparent magnitude and absolute magnitude are known, the distance can be found. Thus an isochrone model that fits a cluster can provide both an age and distance estimate for that cluster.

1.1.2 Chemical Abundances in Astronomy

Spectroscopy is a powerful tool for astronomers. A spectrograph disperses light according to its wavelength, typically using a diffraction grating, onto a detector. The detector is calibrated carefully such that the wavelength of light falling on each pixel is known, allowing the amount of light at each wavelength to be measured. The resulting measurement of "amount of light" vs wavelength is referred to as a spectrum.

It is now well understood that atoms and molecules absorb and emit light at specific wavelengths. These wavelengths have been precisely measured in the laboratory for every known element. When observing astronomical objects such as stars, we look for patterns in their spectra corresponding to specific elements. For example we know from lab measurements that calcium absorbs light at 8498 Å, 8542 Å, and 8662 Å, creating a very distinctive feature. If this feature is seen in a star, it is therefore evidence of calcium. Since stars are moving at a relatively large velocity compared to the Earth (generally measured in km s^{-1}), this pattern is usually seen at slightly bluer or slightly

redder wavelengths. Measuring the difference allows for the computation of a Doppler velocity along the line of sight, referred to as radial velocity (RV).

To actually measure the relative abundance of an element in a star, a model of the stellar atmosphere is used. This model incorporates the temperature of the atmosphere, relative gravitational pull at the surface of the star, and the various atomic and molecular species to be measured. Absorption at a particular wavelength is referred to as an absorption "line", and the list of features to be measured in a star is typically referred to as a "line list". It is common to include many lines for a given element to increase the accuracy of the measured abundance. To measure the abundance of an element, the number of atoms in the model atmosphere is varied until the amount of light absorbed for a given line (or set of lines) matches the observed line(s).

1.1.2.1 Metallicity and [Fe/H] Notation

When the appropriate abundance for the model atmosphere is found, the abundance is commonly reported in a bracket notation, for example [Fe/H], defined in Equation 1.1.

$$[Fe/H] \equiv \log_{10}\left(\frac{N_{Fe}}{N_H}\right)_{\star} - \log_{10}\left(\frac{N_{Fe}}{N_H}\right)_{\odot} \tag{1.1}$$

This notation may seem odd at a glance but is convenient on astronomical scales. Critically, it is a relative scale. That is to say: [Fe/H] is independent of the exact amount of iron or hydrogen in the object being measured. So a $0.1M_{\odot}$ star with the same [Fe/H] as a $5M_{\odot}$ star has many fewer hydrogen *and* many fewer iron atoms, but their ratio is the same; iron is relatively equally abundant in both stars. The scale is

further convenient when considering how much chemical abundance varies in astronomy. Stars with [Fe/H]$= -2$ (100 times less abundant than the sun) are common, as are stars with [Fe/H]=0.3 (2 times more abundant than the sun). When measuring elements besides iron, it is common to use the same notation, but compare to iron instead of hydrogen. Using "X" to represent a given element:

$$[X/Fe] \equiv \log_{10}\left(\frac{N_X}{N_{Fe}}\right)_\star - \log_{10}\left(\frac{N_X}{N_{Fe}}\right)_\odot \tag{1.2}$$

Understanding the usefulness of [X/Fe] notation requires a brief discussion of stellar life-cycles and nucleosynthesis; we do so below.

Finally a note on units. Since [Fe/H] is fundamentally a ratio, it is formally unitless. However it is often useful to refer [Fe/H] measurements or differences in measurements with some unit, and for this purpose astronomers often use "dex", in reference to the base 10 logarithm.

1.1.3 Stellar Nucleosynthesis

As matter cools after the big bang, the universe is filled with hydrogen and some helium. Heavier elements are all formed by stars. During their lives, the massive gravitational pressures in the cores of stars fuse light elements into heavier elements, creating the energy that keeps gravity from collapsing them, the same energy seen as star light. In the Sun, the pressure is only enough to fuse hydrogen into helium. Some stars will eventually produce enough pressure in their cores to fuse elements as heavy as iron. But once a star reaches this stage in its life, it quickly switches to forming nickel, which requires more

energy to fuse than the fusion reaction gives off. Once nickel fusion begins, the star can no longer fight off the impending gravitational collapse, and the star collapses rapidly, leading to a supernova.

Supernovae (SNe) are incredibly energetic events, with a sea of sub-atomic particles moving at incredible velocities; an environment ripe for building up heavier nuclei. We now understand supernovae to be the source of the vast majority of heavier elements. Supernovae come mainly in two varieties: massive stars collapsing, as mentioned before, dubbed type II SNe, and white dwarfs slowly accreting enough mass to collapse, dubbed type Ia SNe. The nucleosynthetic yields from these explosions are an area of active research (e.g., Nomoto et al. 2013). In general, type II SNe produce nearly all magnesium and a majority of other "alpha" elements (atoms that build up via the fusion of alpha particles, $^4_2$He nuclei). Type Ia SNe produce more iron than type II SNe, and a majority of the "iron-peak" elements: Cr, Mn, Fe, Co, and Ni, so called due to their relatively similar nucleosynthetic origins.

During star formation, stars of a variety of masses are formed. Usually at least a handful of very massive stars will form, live short lives, and die as SNe. In their deaths, they enrich any surrounding gas, meaning the next generation of stars will be more abundant in the various elements produced by the supernova. Stars that aren't quite massive enough to collapse as type II SNe will form white dwarfs and if they can eventually accrete enough mass, they will eventually explode as type Ia SNe; a process that typically takes at least one billion years. In either case, star formation enriches surrounding gas with iron and other elements. This means that a star with a fairly high [Fe/H] will also have a fairly high [Mg/H], or [Mn/H]. It is thus often more convenient

to measure abundances relative to iron, e.g., [Mg/Fe].

For a sense of scale, it is very unusual to measure an [Mg/Fe] as low as -1 (10x less abundant than the sun), while it is somewhat common to measure [Mg/Fe]= 0.4. Compare to [Fe/H], where it is uncommon to measure [Fe/H]= 0.4, but somewhat common to measure [Fe/H]= -2. These scales are both very reasonable in the context of star formation and stellar nucleosynthesis.

1.2 Probing Galactic Evolution

Understanding the detailed evolution of galaxies is one of the largest areas of research in astronomy, encompassing a variety of sub-fields. Studies of distant galaxies provide snapshots of entire galaxies, helping us understand structures like spiral arms. Since light from very far away galaxies takes billions of years to reach us, studying galaxies at vastly different distances can allow us to explore them at different points in their lives.

Detailed chemical studies of distant galaxies are nearly impossible however; even carefully planned integral field unit spectroscopy provides no more than ~ 100 datapoints for an entire galaxy (e.g., Bundy et al. 2015)[1]. Within our own galaxy though, we can make chemical measurements of millions of individual stars, among other tracers, to piece together a detailed portrait of Galactic chemistry. If enough tracers are observed for which an age can be accurately determined, they can be split up to study how the chemistry of the Galaxy has changed over time as well.

[1]Of course these observations are still very powerful, especially when there are thousands to compare, as in Bundy et al. (2015), or when they are interpreted in context with our Galaxy.

1.2.1 Galactic Chemical Modeling

Galactic chemical evolution (GCE) models attempt to reproduce the observed chemical abundance trends in the Galaxy. They account for processes we know vary between galaxies (by studying distant galaxies), such as star-formation rate and gas infall rate. By varying some number of input parameters such that the current day chemical trends match observed trends, these models attempt to reconstruct the history of the Galaxy.

Recent models, such as the Chiappini (2009) model, often include a large gas infall early in the life of the Galaxy, but account for the steady accretion of more gas in recent times. By taking into account feedback processes, such as supernovae, these models increasingly accurately predict the observed distribution of stellar chemical abundances.

Minchev et al. (2013; 2014, MCM) use a more complicated simulation (focusing on gravitational interaction of gas and dark matter in galaxies) to track the movement of "particles"[2] along with the chemical evolution model of Chiappini (2009). This is necessary to account for the radial migration of massive objects, which has been shown to move stars far from their birth radius (e.g., Hayden et al. 2015).

The MCM model finally provides a full, 3 dimensional portrait of the evolution of the Galaxy. Such models predict quantifiable observable constraints, such as the rate of change of chemical enrichment moving away from the center of the Galaxy (d[Fe/H]/dR_{GC}), dubbed the Galactic metallicity gradient. The evolution of this trend over time is an even more valuable, and likely more reliable constraint, as will be discussed in §3.7.1. Indeed it is now common to split observational results into age bins

[2]Here "particle" refers the smallest resolved unit in their simulation, in this case $\sim$ 150 pc in size, with a mass of $10^{4-5} M_{\odot}$.

when comparing with GCE models (e.g., Anders et al. 2017, Casamiquela et al. 2019). A key question then in comparing to galactic evolution models is: what are the abundance gradients in the Galactic disk, and how do they vary as a function of the age and location of the tracer population?

1.2.2 Observing the Galactic Abundance Gradient

Star clusters provide an age-datable tracer for measuring the growth and evolution of the Galaxy, and have been used to measure the Galactic radial abundance gradient since the Janes (1979) study. The Galactic abundance gradient tends to be fit by a single linear gradient (e.g. Friel & Janes 1993, Friel 1995, Carraro et al. 1998, Friel et al. 2002), though the usage of two intercepting linear functions is becoming increasingly common (e.g. Bragaglia et al. 2008, Sestito et al. 2008, Friel et al. 2010, Carrera & Pancino 2011, Reddy et al. 2016).

Galactic trends in elements besides iron have been reported (e.g., Yong et al. 2005, Friel et al. 2010, Jacobson et al. 2011). Trend lines are commonly fit for α-elements (e.g., Carrera & Pancino 2011, Yong et al. 2012, Reddy et al. 2016), and in some cases for other elements, such as [Ni/Fe], [Cr/Fe], and [V/Fe] (Casamiquela et al. 2019) or [Na/Fe] and [Al/Fe] (Yong et al. 2012). There is a growing consensus that there is a mild positive [α/Fe] versus R_{GC} trend in the inner galaxy, similar to some chemodynamical model predictions (see Minchev et al. 2014).

Recent work using open clusters has consistently found a metallicity gradient (d[Fe/H]/dR_{GC}) between roughly -0.05 dex kpc^{-1} (Reddy et al. 2016) and -0.09 dex kpc^{-1} (Yong et al.

2012, Friel 1995, Carraro et al. 1998) for clusters between 6 kpc $< R_{GC} <$ 14 kpc. Others have reported qualitatively similar trends, but do not quote a metallicity gradient measurement (Donati et al. 2015, Magrini et al. 2015; 2017, Casamiquela et al. 2017). But while the general negative shape of the abundance trend is well agreed upon, no consensus has been reached on the steepness of the gradient. Carrera & Pancino (2011) shed some light on this discrepancy by showing the difference between a gradient measured to R_{GC} = 12.5 kpc (-0.070 ± 0.005) and all the way to R_{GC} = 25 kpc (-0.046 ± 0.010); Frinchaboy et al. (2013) show a similar discrepancy using [M/H].

Another unavoidable problem that has made this measurement difficult is systematic offsets between studies of chemical abundance and distance. This inevitably introduces some systematic uncertainties when a compilation of results from the literature is used. Recent work has sought to correct for systematic uncertainties uncertainties by "homogonizing" their samples. Reddy et al. (2016) take equivalent width measurements from the literature, but use a uniform line list for their analysis. (Netopil et al. 2016) homogenized a large photometric sample using a literature compilation of high-resolution spectroscopic studies, however they do not homogenize the spectroscopic studies.

This work presents an important contribution to the field by utilizing a homogeneous spectroscopic data set, with all stars observed by the same telescope and analyzed with the same abundance analysis pipeline: the Apache Point Observatory Galactic Evolution Experiment (APOGEE; Majewski et al. 2017). In Chapter 2 we present a high reliability sample of stars from APOGEE Data Release 14 (DR14) that are open cluster members along with bulk cluster parameters, and we use this sample, the Open Cluster Chemical Abundance and Mapping (OCCAM) sample, to measure Galactic abundance gradients.

1.2.3 The Evolution of the Abundance Gradient

Since open clusters can range in age from a few Myr to more than 6 Gyr, they also provide a unique opportunity to study the evolution of Galactic abundance gradients. A number of authors have measured metallicity gradients for open clusters in various age bins (e.g., Carraro et al. 1998, Friel et al. 2002, Jacobson et al. 2011, Carrera & Pancino 2011, Cunha et al. 2016), and while all studies agree that the gradient is shallower for younger clusters, further comparison is difficult due to a somewhat heterogeneous choice of age bins; there does not seem to be a consensus as to the measured gradient for clusters of any given age range.

Indeed, there are indications the picture is even more complicated. While open clusters have the advantage of precise age estimates, there are complexities that must be considered when using them to probe Galactic evolution. Anders et al. (2017) suggest open clusters in the inner galaxy are more likely to be broken up, leading to samples significantly biased towards younger clusters.

In Chapter 3, we will present the expanded OCCAM sample based on results from the Sloan Digital Sky Survey (SDSS) IV Apache APOGEE 2 (Majewski et al. 2017) Data Release 16 (DR16) (Ahumada et al. 2019, Jönsson et al., *submitted*). We discuss this sample in comparison to the very high quality sample that used SDSS IV DR14 results (Chapter 2), as well as other results from the literature. We then explore Galactic trends in [Fe/H], α elements, iron-peak elements, and all other elements reported by APOGEE as a function of Galactocentric distance. We finally break the sample in age bins to explore changes in radial abundance trends over time.

1.2.4 On Radial Migration

The gradual movement of stars away from their birth radius in the Galaxy has long been predicted by simulations (e.g., Raboud et al. 1998). There is now strong observational evidence of radial migration in stellar populations as well; Hayden et al. (2015) found good agreement between observations and the MCM model. The effects of radial migration have been characterized fairly well. Minchev et al. (2018) prescribe a formula for estimating the birth radius of a given star which agrees reasonably well with observations.

It is not clear if clusters migrate in the same way as stars. Stars can migrate inward or outward a considerable distance, interacting mainly with the gravitational potential of spiral arms (e.g., Sellwood 2014). However, an open cluster is not a dense point-like mass; open clusters are multiple parsecs across with hundreds or thousands of stars interacting gravitationally. Therefore, the interaction of an open cluster with a spiral arm is much more complicated than an individual star. Spiral arms are more dense near the center of the Galaxy, so a cluster migrating inward is more likely to encounter them.

It is not unlikely then that clusters migrating inward are more likely to be disrupted by interactions with spiral arms. This explanation is offered by Anders et al. (2017). This prediction is bolstered by the relative lack of older star clusters. In any catalog of star clusters (e.g., Dias et al. 2002, Kharchenko et al. 2013, Cantat-Gaudin et al. 2020), there are vastly more clusters younger than 1 Gyr than older.

Simulations are of little help for this problem. With particle sizes on the order of the mass of a star cluster ($10^{4-5} M_{\odot}$), simulations cannot predict the dissolution of a cluster. Another key question is then: do clusters participate in radial migration in the Galactic

disk, and what effect does this have on analysis of Galactic Chemical Trends? In Chapter 4, we will explore recent efforts to quantify star cluster migration.

Chapter 2

Methodology and the Very High Quality Sample

2.1 OCCAM Target Selection

The OCCAM survey includes targets selected in two different ways. First, we selected known members of a subset of open clusters that were observed for calibration purposes. Stars with previous abundance determinations (e.g., Cohen 1980, Origlia et al. 2006, Carretta et al. 2007, Carraro et al. 2006, Bragaglia et al. 2001, Yong et al. 2005, Tautvaišiene et al. 2000, Pancino et al. 2010, Basu et al. 2011, Smith & Suntzeff 1987) and/or high quality RV-based membership studies (e.g., Hole et al. 2009, Geller et al. 2008; 2010, Mermilliod et al. 2008) were targeted. These calibration cluster targets can be identified in DR14 though a specific targeting flag (*apogee_target2* = 10 and/or *apogee2_target2* = 10; Zasowski et al. 2013; 2017). The second method selected "likely" cluster targets

based upon their location in the cluster color-magnitude diagram (CMD) using the colors in the surveys 2MASS (Cutri et al. 2003) and WISE (Wright et al. 2010).

The combination of 2MASS and *WISE* photometry allows for a direct assessment of the line-of-sight reddening to any particular star. The long wavelength regime of spectral energy distributions (SEDs) of stars have the same Rayleigh-Jeans shape, equivalent to saying that the Vega-based, *intrinsic* colors of all stars are nearly constant for the correct combination of filters, as seen in Figure 5 of Majewski et al. (2011). Thus, the *observed* mid-IR colors contain information on the reddening to a star *explicitly*, whereas the NIR SEDs contain information on the stellar types.

By assuming constancy of the intrinsic stellar ($H-4.5\mu$m) colors in the Rayleigh-Jeans regime, $E(H-4.5\mu\text{m})$, the "color excess" caused by dust along the line of site for the ($H-4.5\mu$m) color, is derived directly from the observed ($H-4.5\mu$m) color (Majewski et al. 2011). The spread from different populations in a cluster, red giant branch, red clump and main sequence, is minimized for this combination yielding an intrinsic spread of less than 0.09 mag in color for all but the reddest and bluest stars. Since the primary purpose in using this technique is to "clean" the cluster from the field, small systematics are not a concern. Also, the reddest main sequence stars that would belong to a cluster are too faint for these surveys.

Frinchaboy et al. (2010) devised a technique to utilize the extinction (A_{K_S}) derived from the Rayleigh-Jeans Color Excess (RJCE) technique to distinguish and isolate cluster stars from foreground and background contamination. This technique consists of isolating a region of approximately twice the cluster's catalog radius (R_{Dias}; Dias et al. 2002) and dividing it into five regions (see Figure 2.1a). We utilize four "field" regions and the

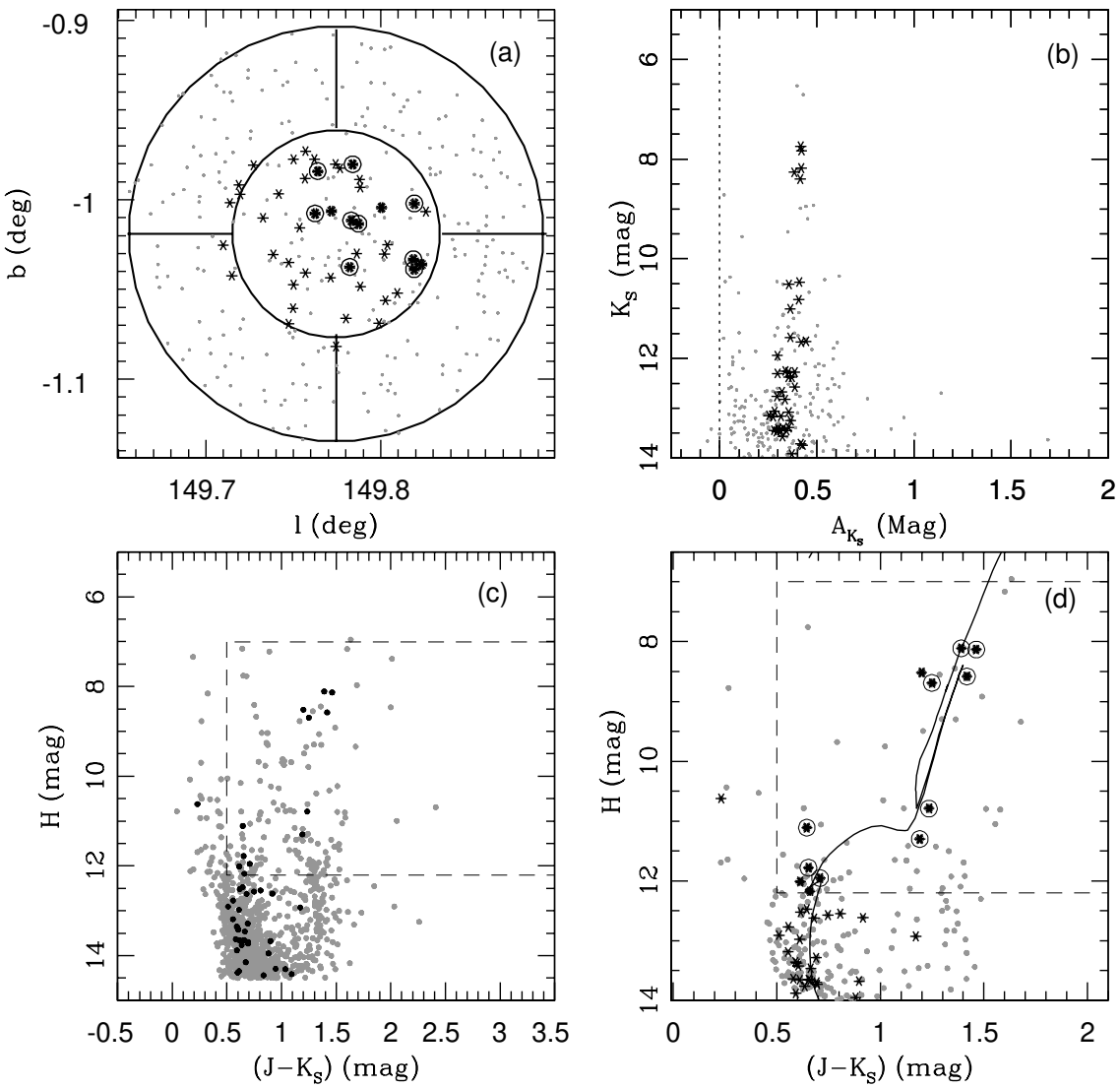

Figure 2.1: Sample analysis for the cluster King 7 utilizing 2MASS+WISE data (Frinchaboy et al. 2010). a) Galactic latitude and longitude for all stars (gray) within the $2R_{cl}$ area to be analyzed, stars selected to be likely members from the photometry extinction analysis are shown in black. Prime APOGEE targets are circled. b) Distribution of A_{K_s} for all stars in the NGC 6802 sample area, black points denote stars with $1.1R_{cl}$ within the determined mean cluster A_{K_s} range. c) Color-magnitude diagram (CMD) for all stars in the analysis area (gray). The dashed box denotes the SDSS-III/APOGEE target selection region. Black points denote stars selected as likely members from their A_{K_s}. d) CMD of only likely cluster members overplotted with the Padova Isochrone (Marigo et al. 2008) using the clusters parameters from Dias et al. (2002). Circled stars denote identified high-probability stars for APOGEE target selection (also see the sky distribution (a)).

cluster region (radius = R_{Dias}). The field is divided in order to account for dust clouds and any other source of background variability.

We subtract the median area-scaled "field" star density from the "cluster" star numbers within a given A_{K_s} range, and scan this range across all available A_{K_s} values that have at least 15 stars (see Figure 2.1b). The window of extinction with the highest concentration of stars within the inner radius will reveal the cluster (Figure 2.1c & d). We then optimize the cluster isolation surveying a grid of A_{K_s} width, A_{K_s} stepsize, and allowed $\sigma_{A_{K_s}}$ values.

We present a demonstration of this technique utilizing the cluster King 7, shown in Figure 2.1. Figure 2.1a first shows the area explored by our analysis in Galactic latitude and longitude. As described above, we selected likely cluster members utilizing the A_{K_s}, as shown in Figure 2.1b. For King 7, we find a low, but non-negligible extinction or reddening to the cluster. A CMD of this cluster (Figure 2.1c) is generated which highlights the member stars with A_{K_s} values within the selected window of extinction, where the dashed box denotes the area where the SDSS/APOGEE project selects targets ($8.0 < H < 12.2$ and $J - K_S \geq 0.5$). Finally, we compare our "cleaned" cluster CMD to the Padova isochrone (Bressan et al. 2012) utilizing catalog values (Dias et al. 2002) for King 7 and find a good match. By comparing the CMD with isochrone values, when available, we are able to isolate candidate open cluster stars with a high probability for membership. The APOGEE project requires this cleaning for most clusters for three reasons. 1) Most open clusters are found at low Galactic latitude and thereby are heavily contaminated with field stars. 2) Due to the large SDSS telescope field of view (Gunn et al. 2006), the minimum fiber-to-fiber distance is fairly large (≥ 1 arcmin), which only

allows for the targeting of a handful of stars ($\sim 5-10$) per cluster for the most poorly studied, distant, and reddened clusters. 3) Prior to *Gaia* the proper motion data required for high-quality reliable membership determinations were only available for a few clusters. Likely open cluster members selected by this method are identified in DR14 (Abolfathi et al. 2018), and previous DRs (10,12,13) through specific targeting flag (*apogee_target1* = 9 and/or *apogee2_target1* = 9; Zasowski et al. 2013; 2017)[1].

2.2 Analysis

2.2.1 OCCAM Observed Stars in SDSS4 DR14

The primary spectroscopic data for OCCAM comes from the APOGEE survey (Majewski et al. 2017), which is part of the SDSS III and IV surveys (Eisenstein et al. 2011, Blanton et al. 2017), utilizing the 2.5m Sloan Foundation telescope (Gunn et al. 2006) at Apache Point Observatory. APOGEE is a near-infrared (1.514 μm to 1.696 μm) spectroscopic survey, primarily focusing on the galactic disk (Zasowski et al. 2013; 2017). The survey uses multi-fiber spectrographs (Wilson et al. 2012), allowing for simultaneous observations of 300 stars.

The APOGEE data reduction pipeline (Nidever et al. 2015, Holtzman et al. 2015) provides high precision RVs. Stellar parameters (T_{eff} , $\log g$, [M/H], [C/M], [N/M], [α/M]), and detailed abundances for individual elements, such as, Fe, C, N, O, Al, Si, Ca, Ni, Na, S, Ti, Mn, K, and Cu, are derived automatically by the APOGEE Stellar

[1]We did not limit our analysis to stars with just these targeting flags. Random field stars and additional specific targeted cluster programs, and other calibration flags may also apply to the targets analyzed here.

Parameter and Chemical Abundance Pipeline (ASPCAP) pipeline (García Pérez et al. 2016). The APOGEE survey provides the *uniform* chemical data and reduction pipeline that underpin this study of open cluster members.

The targets selected for analysis were observed from August 2011 to July 2014 (APOGEE-1), and from July 2014 to July 2016 (APOGEE-2). These data were released as part of the 14th Data Release of SDSS (DR14; Abolfathi et al. 2018), which included APOGEE data for over 250,000 stars. All APOGEE data, from the beginning of APOGEE-1, were reduced using the latest data reduction pipeline (full description of this pipeline is presented in Holtzman et al. (2018)). For this study, we analyzed all stars within 2× the cluster radius (Kharchenko et al. 2013) for 19 clusters that resulted in a sample of 1361 stars. This entire sample is listed in Table 2.1 for reference, along with our final membership probabilities and a classification for each star (§2.2.2).

2.2.2 OCCAM Membership Criteria

Using the stellar radial velocities and derived metallicities as initial discriminators, APOGEE data alone can provide a first guess at cluster membership based on the "bulk" RV and [Fe/H] for the cluster region on the sky and comparing each star to the average values. We then further constrain the membership using proper motions measured by *Gaia* (Gaia Collaboration et al. 2016; 2018, Lindegren et al. 2018).

2.2.2.1 Quantifying Membership Probability

The "bulk" behavior is found by convolving all measurements using a Gaussian kernel smoothing routine, based on the methods from Frinchaboy & Majewski (2008). The

first analysis is in RV. In order to distinguish the cluster from field stars, 2 samples are computed: (1) stars within 2 cluster radii (from Kharchenko et al. 2013, except where we enforced a minimum radius of 5 arcminutes) of the cluster center, and (2) stars between 1 and 2 cluster radii of the center. The results from the "outer" stars are subtracted from the "total" result, leaving a peak where the cluster stars fall, as seen in Figure 2.2e (in blue).

Table 2.1: OCCAM sample from APOGEE data used for membership analysis

Cluster name	2MASS ID	RV (km s^{-1})	[Fe/H] (dex)	μ_α (mas yr^{-1})	μ_δ (mas yr^{-1})	RV Prob	[Fe/H] Prob	PM Prob	Memb
NGC 6819	2M19401402+4016306	−56.4±0.0	+0.06±0.01	−5.85±0.03	−9.04±0.03	0.00	0.00	0.00	NM
NGC 6819	2M19401466+4004598	−18.9±0.0	−0.03±0.01	+50.96±0.04	+99.82±0.04	0.00	−1.00	0.00	NM
NGC 6819	2M19401937+4015495	−52.3±0.2	−0.35±0.01	−5.93±0.03	−6.26±0.03	0.00	0.00	0.00	NM
NGC 6819	2M19402284+4006008	−50.3±0.1	−0.34±0.01	−1.60±0.03	−2.91±0.03	0.00	0.00	0.00	NM
NGC 6819	2M19403569+4005038	+2.7±0.1	−0.45±0.01	−3.76±0.03	−3.46±0.03	0.00	0.00	0.00	NM
NGC 6819	2M19403684+4015172	+2.1±0.0	+0.15±0.01	−3.00±0.03	−3.66±0.03	0.00	0.00	0.54	NM
NGC 6819	2M19404262+4003043	−35.2±0.1	+0.07±0.01	−4.36±0.04	−19.13±0.04	0.00	0.00	0.00	NM
NGC 6819	2M19404341+4020235	−11.8±16.3	−0.01±0.01	+0.65±0.09	−3.89±0.09	0.00	−1.00	0.00	NM
NGC 6819	2M19404803+4008085	+2.4±0.1	+0.09±0.01	−2.98±0.04	−3.83±0.04	1.00	0.82	0.94	GM
NGC 6819	2M19404965+4014313	+3.1±0.0	+0.12±0.01	−2.84±0.03	−3.72±0.03	0.96	0.94	0.70	GM
NGC 6819	2M19405020+4013109	+4.3±0.0	+0.15±0.01	−3.03±0.04	−3.84±0.04	0.67	0.59	0.85	GM
			.....						

[a] Table 2.1 is published in its entirety in Appendix A, with 1361 stars.

The process is repeated for [Fe/H], seen in Figure 2.2f (in blue) this time subtracting the stars farther than 3σ from the cluster RV previously identified from the whole field (σ is small in practice, thus 3σ is appropriate for keeping cluster stars without including field stars incidentally close in RV space). If there are at least two APOGEE stars that are cluster members, the smoothing routine will leave behind a larger peak where their values combined. The shape is approximately Gaussian, so a Gaussian profile is fit for both RV and [Fe/H]. When normalized, this Gaussian fit can be used as a membership probability distribution in RV or [Fe/H] space, seen in Figure 2.2e & f (overlaid in orange).

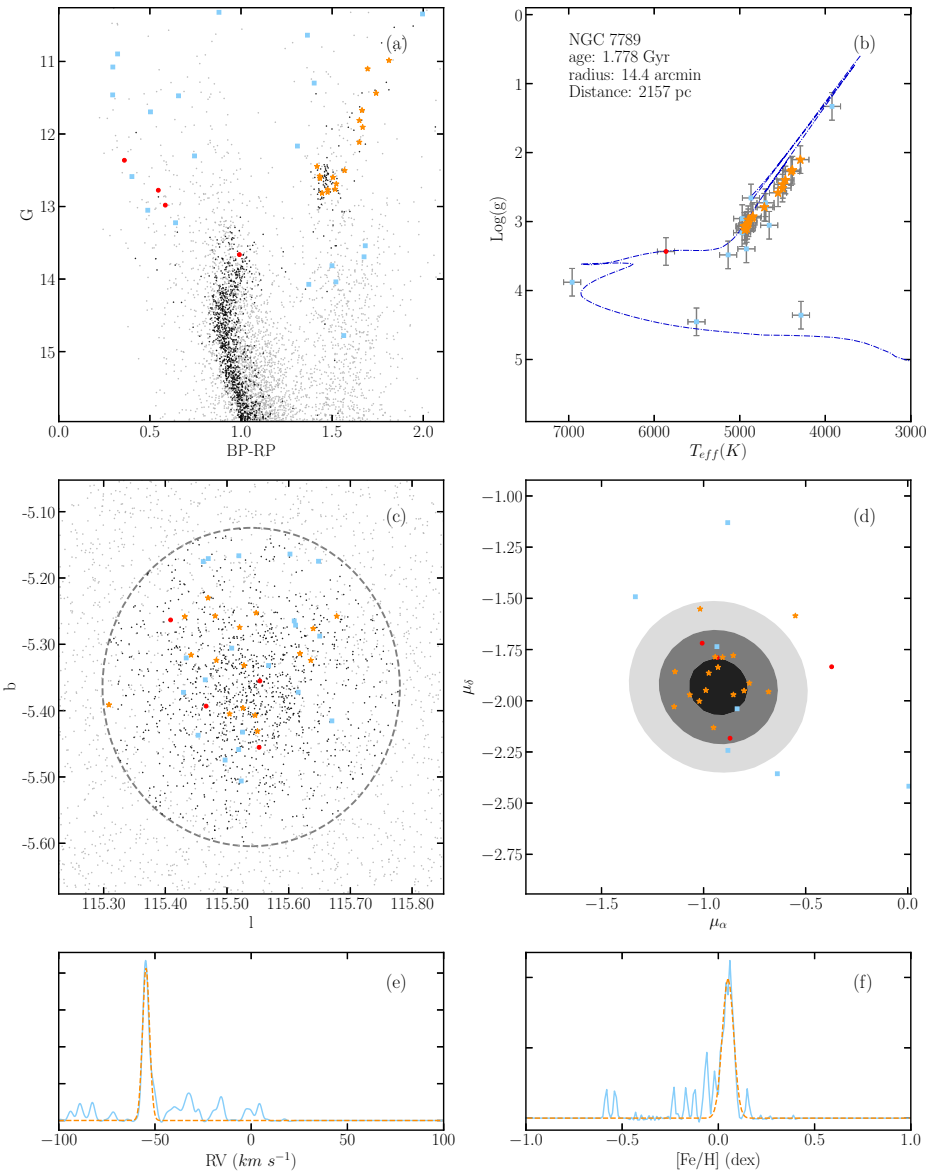

Figure 2.2: A summary of the membership analysis for open cluster NGC 7789. The complete figure set (19 images) is available in Appendix E. (a) The *Gaia* CMD (Gaia Collaboration et al. 2018, Riello et al. 2018), with proper motion members shown in black, others in gray. Likely APOGEE members are shown as orange stars, non-members as blue squares, and APOGEE stars passing an RV and proper motion membership cut, but failing a $\log(g)$ cut for metallicity reliability are shown as red circles. (b) The $T_{eff} - \log(g)$ diagram for the cluster with an isochrone based on MWSC Catalog ages (Kharchenko et al. 2013) shown for reference. Error bars shown are characteristic, and a possible global offset in $\log(g)$ is seen. (c) The cluster area on the sky. (d) A contour plot of the 2D Gaussian fit to the kernel smoothed proper motions. Contours show 1σ intervals. (e) The Gaussian kernel density convolution in RV, with a Gaussian fit shown in orange. (f) The Gaussian kernel density convolution in [Fe/H], with a Gaussian fit shown in orange.

Using proper motion data from *Gaia* DR2 (Gaia Collaboration et al. 2016; 2018, Lindegren et al. 2018), a 2-dimensional Gaussian smoothing routine is applied in the 2-dimensional proper motion space (proper motion in right ascension and proper motion in declination). Again, 2 samples are computed: (1) all stars within twice the cluster radius and (2) stars outside the cluster's radius, then the outside sample (2) is subtracted from the full sample (1). A 2D Gaussian is fit to the remaining peak and membership probabilities are assigned, shown in Figure 2.2d.

Finally, a 3σ criterion is adopted for likely membership: a star with parameters falling within 3σ of the cluster mean in [Fe/H], RV, and proper motion is considered a likely member of the cluster. Due to diffusion effects that are present in the abundances of main-sequence and turn-off stars (Souto et al. 2018), and the lack of calibrated DR14 abundances for dwarfs observed in the APOGEE survey (Holtzman et al. 2018, Abolfathi et al. 2018), we restricted our final sample to stars having $\log(g) \lessapprox 3.7$. Stars passing an RV and proper motion membership cut but falling above the $\log(g) \approx 3.7$ cut are identified as dwarf members ("DM")[2], while those falling below the $\log(g)$ cut are identified as giant members ("GM"). Only the giant members are included in the final OCCAM sample. All stars not falling into either the DM or GM category are identified as non-members ("NM"). Table 2.1 shows the sample of stars used, with the relevant stellar parameters used and final membership determinations. The 19 clusters studied in this work were chosen because they had at least 4 member *giant* stars.

[2]We note the existence of a few stars with missing calibrated $\log(g)$ values that consequently fail our $\log(g)$ cut, even though they are likely giant members, which result in a "dwarf member" (DM) classification.

2.2.2.2 Verifying Membership

Figure 2.2a shows the CMD for NGC 7789, with identified APOGEE members shown in orange and non-members in blue; 2.2c shows the cluster area on the sky for reference. While some members may have been falsely rejected, obvious non-members are clearly rejected. The $T_{eff} - \log(g)$ diagram in Figure 2.2b shows likely members where they are expected. Figure 2.2d shows a proper motion contour plot, from the 2D Gaussian fit discussed above, that shows members where they are expected. Figure 2.2d also shows some proper motion members rejected for RV and/or metallicity.

All APOGEE cluster and star data, including membership probabilities and abundances plus bulk cluster properties, were released as part of a SDSS DR14 mini-data release in July 2018. The catalogs are available at: `http://www.sdss.org/dr14/data_access/value-added-catalogs/`

Table 2.2: OCCAM Data Sample

Cluster name	l (deg)	b (deg)	Radius (')	Age Gyr	R_{GC} (kpc)	μ_α (mas yr^{-1})	μ_δ (mas yr^{-1})	RV (km s^{-1})	[Fe/H] (dex)	Member stars
NGC 6791	69.9658	+10.9080	6.3	4.42	7.70	−0.42±0.25	−2.28±0.29	−47.3±1.4	+0.42±0.05	31
NGC 6819	73.9834	+8.4882	6.9	1.62	7.70	−2.92±0.18	−3.86±0.20	+2.4±1.7	+0.11±0.03	36
NGC 6811	79.2233	+12.0047	7.2	0.64	7.87	−3.39±0.17	−8.78±0.18	+7.8±0.3	−0.01±0.02	4
Berkeley 53	90.3051	+3.7555	7.5	1.23	8.90	−3.77±0.39	−5.69±0.34	−36.3±0.5	−0.00±0.02	5
NGC 7789	115.5392	−5.3644	14.4	1.84	9.13	−0.93±0.19	−1.93±0.20	−54.7±1.3	+0.05±0.03	17
FSR 0494	120.0882	+1.0206	5.7	2.00	10.60	−2.45±0.48	−0.65±0.48	−63.3±1.5	+0.01±0.02	5
NGC 188	122.8416	+22.3840	17.7	4.47	9.06	−2.31±0.19	−0.96±0.16	−41.5±1.1	+0.14±0.03	13
IC 166	130.0502	−0.1616	7.5	1.00	11.47	−1.46±0.15	+1.13±0.28	−40.5±1.5	−0.06±0.02	15
Berkeley 66	139.4199	+0.1803	3.3	1.41	11.55	−0.14±0.61	+0.01±0.69	−50.1±0.3	−0.13±0.02	6
King 5	143.7732	−4.2760	8.4	1.23	10.01	−0.26±0.28	−1.16±0.29	−44.3±1.5	−0.11±0.02	5
NGC 1245	146.6533	−8.9081	11.4	1.06	10.66	+0.52±0.23	−1.57±0.19	−29.2±0.8	−0.06±0.02	23
King 7	149.7993	−1.0215	11.1	0.71	10.54	+1.07±0.55	−1.21±0.42	−11.9±2.0	−0.05±0.02	4
NGC 1798	160.6994	+4.8502	5.4	2.00	12.50	+0.89±0.33	−0.33±0.31	+2.0±1.7	−0.18±0.02	9
Berkeley 17	175.6574	−3.6494	7.2	3.98	11.08	+2.55±0.41	−0.32±0.27	−73.4±0.4	−0.11±0.03	7
Berkeley 71	176.6384	+0.8936	4.8	1.05	11.51	+0.68±0.36	−1.62±0.46	−8.7±2.3	−0.20±0.03	7
Teutsch 51	182.7401	+0.4760	2.7	0.53	11.68	+0.56±0.29	−0.34±0.34	+17.0±1.4	−0.28±0.03	5
NGC 2158	186.6394	+1.7807	8.4	2.14	12.41	−0.18±0.32	−2.01±0.25	+27.5±1.5	−0.15±0.03	18
NGC 2420	198.1134	+19.6318	7.5	2.32	10.25	−1.19±0.22	−2.13±0.18	+74.2±0.5	−0.12±0.02	15
NGC 2682	215.6906	+31.9221	33.0	3.43	8.60	−10.97±0.24	−2.95±0.24	+33.8±1.0	+0.07±0.03	35

2.2.3 Measured Cluster Bulk Abundances

A "high reliability" criterion is adopted for a cluster to be included in our sample: 4 or more likely member stars, as determined above. This resulted in a total sample of 259 member stars in 19 clusters used for the analysis of galactic abundance gradients.

The final value for [Fe/H] used for computing metallicity gradients is taken to be the mean metallicity of the likely members. The uncertainty on this value is taken to be the standard deviation of the mean metallicity for the cluster. We note that the uncertainties in the metallicities for the individual stars as reported in DR14 are typically ~ 0.01 dex, which may be an underestimation. We therefore disregard these uncertainties in our consideration of the uncertainty in the cluster metallicity. We find the majority of clusters have an uncertainty of 0.02-0.03 dex, with the exception of one cluster (King 7), which has a standard deviation of only 0.01; we therefore enforce a more conservative 0.02 dex uncertainty for this cluster. Our final sample, assuming a solar distance to the Galactic center of 8 kpc and using the median distance to likely members (stellar distances are taken from Bailer-Jones et al. 2018; this is discussed in detail in §2.4.3), is presented in Table 2.2.

2.3 Cluster [Fe/H] in Comparison to previous work

In order to place our results in the context of previous work, we conducted a detailed comparison of well-studied clusters from the literature: NGC 188, NGC 2682, NGC 2420, NGC 6791, NGC 6819, and NGC 7789, presented in Figure 2.3 and discussed below.

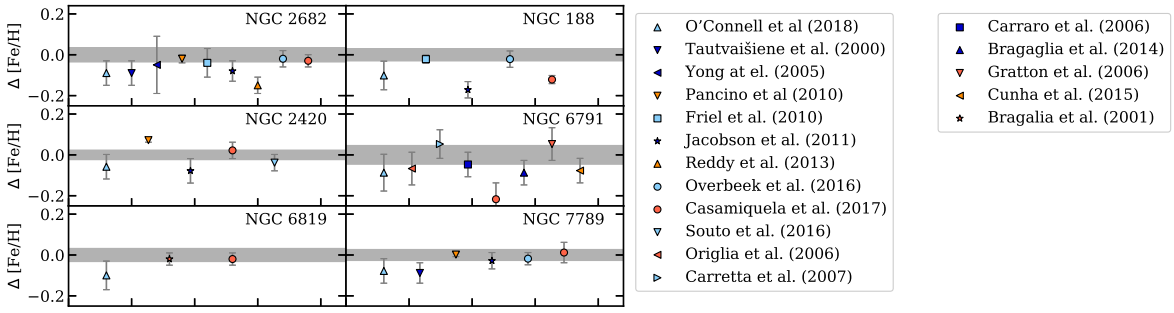

Figure 2.3: A comparison to commonly studied clusters in the literature (Δ[Fe/H] = literature–OCCAM). The gray bar indicates the internal 1σ standard deviation for stars in each cluster from our data.

2.3.1 NGC 2682 (M67)

Figure 2.3 shows that all of the literature values (O'Connell et al. submitted; Tautvaišiene et al. 2000, Yong et al. 2005, Pancino et al. 2010, Friel et al. 2010, Jacobson et al. 2011, Reddy et al. 2013, Casamiquela et al. 2017) for M67 agree within quoted uncertainties, except for the lowest metallicity value from Reddy et al. (2013), in which the authors note a possible metal-poor offset from the literature. The mean difference from the literature values is Δ[Fe/H]$= -0.06 \pm 0.04$ dex for this cluster.

2.3.2 NGC 188

We find that three studies (O'Connell et al. submitted; Friel et al. 2010, Overbeek et al. 2016) are in agreement with our results, however we find significant differences with Jacobson et al. (2011) and Casamiquela et al. (2017). The mean difference from the literature is Δ[Fe/H]$= -0.09 \pm 0.06$ dex for this cluster, the highest of the commonly studied clusters analyzed.

2.3.3 NGC 6791

We find general agreement with all but one of the literature values considered (Casamiquela et al. 2017, finds a significantly lower metallicity), and note the majority of literature values (O'Connell et al. submitted; Origlia et al. 2006, Carretta et al. 2007, Carraro et al. 2006, Bragaglia et al. 2014, Cunha et al. 2015) again fall slightly below ours, with a mean difference from the literature of Δ[Fe/H]$= -0.06 \pm 0.08$ dex. We hypothesize that this may be due to a poor calibration in the metal-rich end of the APOGEE calibrations, as Cunha et al. (2015) using APOGEE spectra of many of the same stars for a detailed individual analysis found a lower metallicity ([Fe/H] = 0.34 $\pm$ 0.06) as compared with our DR14 pipeline value ([Fe/H] = 0.42 $\pm$ 0.05). We note, however, that Cunha et al. (2015) used an older version of the ASPCAP line list than the DR14 results, and that the Cunha et al. (2015) results agree within the uncertainties given the changes in the line list.

2.3.4 NGC 2420, NGC 6819, and NGC 7789

Nearly all of the literature results are in good agreement with ours, with the exception of Pancino et al. 2010 for NGC 2420, which quotes particularly small errors. The other results (O'Connell et al. submitted; Jacobson et al. 2011, Casamiquela et al. 2017) are consistent within their uncertainties, and we note in particular the close agreement with Souto et al. 2016, who completed a by-hand analysis of the same APOGEE spectra of 12 giant stars in cluster. The mean differences from the literature are -0.02 ± 0.05, -0.05 ± 0.04, and -0.03 ± 0.04 for NGC 2420, NGC 6819 (O'Connell et al. submitted;

Bragaglia et al. 2001, Casamiquela et al. 2017), and NGC 7789 (O'Connell et al. submitted; Tautvaišiene et al. 2000, Pancino et al. 2010, Jacobson et al. 2011, Overbeek et al. 2016, Casamiquela et al. 2017) respectively.

2.3.5 APOGEE DR14 vs. Literature Trends

The comparison for NGC 188, NGC 6791, and NGC 2682 clearly shows the majority of literature values are more metal poor than our adopted values. The other clusters agree on the direction of the offset, but suggest it is not severe. Jönsson et al. (2018) compared to optical studies for 525 stars in common with APOGEE. They find an average difference (in the sense literature – APOGEE) of -0.04 ± 0.010 dex. From our comparison of 6 open clusters to 17 studies in the literature (Figure 2.3), we find a mean difference (in the sense literature – APOGEE) of Δ[Fe/H]$- = 0.05 \pm 0.06$. Both our analysis and the analysis of Jönsson et al. (2018) suggest the possibility of a *slight* global metal-rich offset in the APOGEE DR14 sample, but both analyses are consistent with no offset from the literature. Still, we emphasize that when using only the APOGEE DR14 sample for analysis, any global offset, minor or otherwise, will have no significant effect on the results of a *gradient* measurement.

2.4 Galactic Metallicity Gradients

The uniform OCCAM sample of 259 member stars in 19 open clusters was used to measure the Galactic metallicity gradient. The sample covers the disc from $R_{GC} \approx 7$ to 13 kpc with no major gaps.

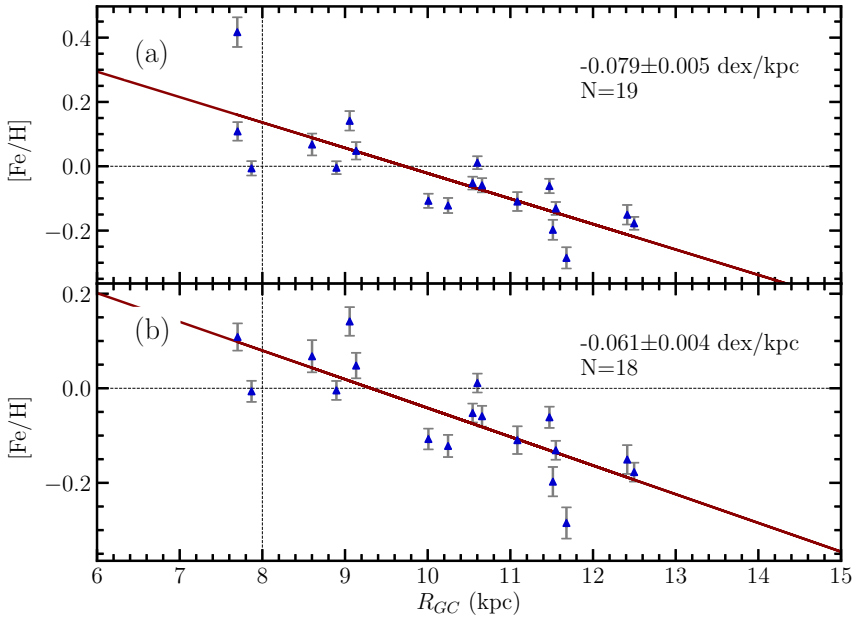

Figure 2.4: The high reliability metallicity gradients using APOGEE clusters. Dotted lines are shown for reference at $R_{\odot} = 8$ kpc and [Fe/H] = 0 dex. (a) shows the entire sample and (b) shows the sample with the very metal-rich NGC 6791 removed.

In addition to uniform abundances, a uniform R_{GC} analysis is desirable. We considered 4 sources for cluster distances, discussed in detail in §2.4.3. We use distances computed from the Bailer-Jones Catalog (Bailer-Jones et al. 2018) for the gradients we present below.

2.4.1 Error Analysis

The scatter in the abundance gradients necessitates some reliable determination of the uncertainty in any quoted gradient. A re-sampling routine is used to estimate the error in gradients. The gradient is determined 2000 times, each time using a randomly determined [Fe/H] for each cluster, sampled from a standard normal distribution within their uncertainties. The mean of the resulting sample of 2000 gradients is adopted, and

the standard deviation is taken as the uncertainty. A check was made against the χ^2 minimum error for a straight line fit in each case; it was found that in every case, our error estimation was larger than this minimum. These are the uncertainties quoted for all the gradients we present.

2.4.2 NGC 6791 and the metallicity gradient

The overall metallicity gradient with the entire sample included, is found to be -0.079 ± 0.005 dex kpc^{-1} (Figure 2.4a). We note that NGC 6791 is very metal rich, fairly old, and relatively far from the Galactic plane. Previous work using APOGEE data has suggested it likely migrated to its current location (Linden et al. 2017). Since it is likely not representative of the region of the Galaxy in which it currently resides, we exclude it from further analysis. Previous work including NGC 6791 such as Carraro et al. (1998), Friel et al. (2002), used a much lower value for [Fe/H] (+0.19 dex and +0.11 dex respectively), low enough to be in disagreement with most recent studies. Even Reddy et al. (2016) used a lower value for NGC 6791 (+0.24 dex). Jacobson et al. (2011) note that it strongly influences the gradient. Removing NGC 6791 gives a final metallicity gradient, from the full OCCAM high-reliability sample, of -0.061 ± 0.004 dex kpc^{-1} (Figure 2.4b).

Table 2.3: A summary of reported spectroscopic metallicity gradients.

Study	dex kpc^{-1}	# study	# total	range (kpc)
Carraro et al. (1998)	-0.085 ± 0.008	0	37	7–16
Friel et al. (2002)	-0.06 ± 0.01	24	39	7–16
Carrera & Pancino (2011)[a]	-0.070 ± 0.010	9	89	6–12.5
Jacobson et al. (2011)	-0.085 ± 0.019	10	19	9–13
Yong et al. (2012)[a]	-0.09 ± 0.01	5	49	6–13
Reddy et al. (2016)[a]	-0.052 ± 0.011	28	79	5–12
This Study	-0.061 ± 0.004	18	18	7–12

[a] These studies fit a two-function gradient. We quote only the gradient measured for the inner sample, as we only discuss this measurement.

2.4.3 Distance Effects on the Gradient

The metallicity gradients are highly susceptible to systematic differences in the distance values used. We considered 4 sources of distances: 1) the Dias Catalog (Dias et al. 2002), which is a compilation of distances from the literature, 2) the MWSC Catalog (Kharchenko et al. 2013), which independently measured distances to each cluster, 3) inverse-parallax (Gaia Collaboration et al. 2018, Lindegren et al. 2018), accounting for a 0.08 milli-arcsecond offset (Stassun & Torres 2018), and 4) the Bailer-Jones catalog (Bailer-Jones et al. 2018), which used the same parallax measurements combined with a geometric prior to compute distances to nearly every star in *Gaia* DR2. Table 2.4 shows a summary of R_{GC} using these 4 sources for distance, while Figure 2.5 shows the d[Fe/H]/dR$_{GC}$ gradient computed using different distance catalogs/methods.

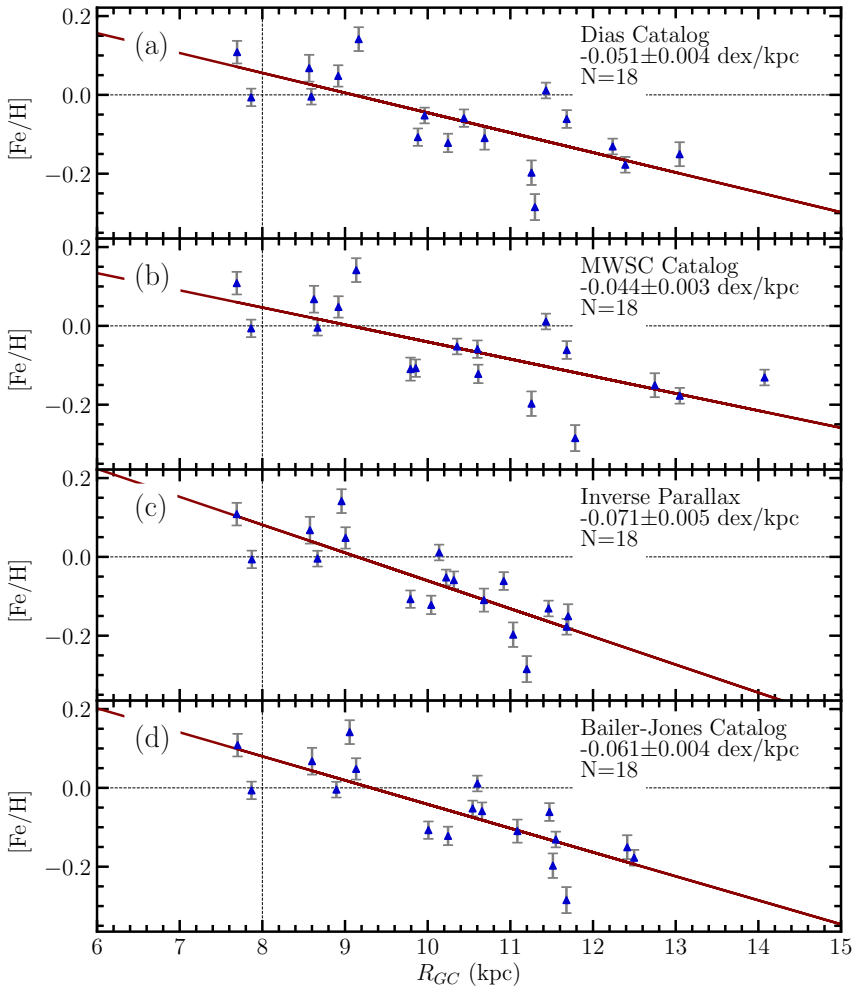

Figure 2.5: The galactic metallicity gradient computed using values from the Dias Catalog (Dias et al. 2002), the MWSC Catalog (Kharchenko et al. 2013), inverse-parallax (Gaia Collaboration et al. 2018, Lindegren et al. 2018), and the Bailer-Jones catalog (Bailer-Jones et al. 2018).

Not surprisingly, the parallax and Bailer-Jones et al. (2018) distances are fairly similar, at least for relatively nearby clusters, yet still: the gradient measurements are incompatible. The Dias Catalog and MWSC Catalog distances are similar for a number of clusters, but for clusters at higher R_{GC} they tend to be larger than (Bailer-Jones et al. 2018) or parallax, leading to a shallower gradient result for both catalogs. The Dias Catalog and MWSC Catalog gradients are barely in agreement within the uncertainties.

The MWSC Catalog recomputed distances for every cluster, and thus is internally consistent. The parallax distances and (Bailer-Jones et al. 2018) distances are internally consistent as well. But there is a clear discrepancy between these 3 data sets. The Bailer-Jones geometric distances should be the most accurate for nearby clusters, since they are based on *Gaia* parallaxes. Considering clusters within 7 kpc $< R_{GC} <$ 10 kpc, the MWSC Catalog distances are in good agreement with Bailer-Jones distances. For some more distant clusters, significant discrepancies exist (e.g Berkeley 66 and Berkeley 17), while many remain in good agreement. At this time, we have no strong evidence to distrust one catalog over the other at larger distances, but a decision must be made. Looking at the 2 clusters with very discrepant MWSC Catalog distances (Berkeley 66 and Berkeley 17), we see they also disagree significantly with the Dias Catalog, so for this study, we adopt distances from (Bailer-Jones et al. 2018).

Table 2.4: R_{GC} calculated using different distance sources

Cluster name	R_{GC} Dias (kpc)	R_{GC} MWSC (kpc)	R_{GC} Parallax (kpc)	R_{GC} Bailer-Jones (kpc)
NGC 6791	7.83	7.80	7.57	7.70
NGC 6819	7.69	7.69	7.69	7.70
NGC 6811	7.86	7.86	7.87	7.87
Berkeley 53	8.59	8.67	8.67	8.90
NGC 7789	8.92	8.92	9.01	9.13
FSR 0494	11.43	11.43	10.14	10.60
NGC 188	9.17	9.14	8.96	9.06
IC 166	11.68	11.68	10.92	11.47
Berkeley 66	12.24	14.08	11.46	11.55
King 5	9.88	9.86	9.79	10.01
NGC 1245	10.44	10.60	10.32	10.66
King 7	9.96	10.36	10.22	10.54
NGC 1798	12.39	13.05	11.68	12.50
Berkeley 17	10.69	9.79	10.68	11.08
Berkeley 71	11.26	11.26	11.03	11.51
Teutsch 51	11.30	11.78	11.20	11.68
NGC 2158	13.05	12.75	11.70	12.41
NGC 2420	10.25	10.61	10.04	10.25
NGC 2682	8.57	8.62	8.58	8.60

2.4.4 Comparison to Previous Work

A summary of current results in the literature (from studies using high-resolution spectroscopy) is found in Table 2.3. We omit studies that measure a gradient in a region significantly different than that considered in this paper. We can readily compare the APOGEE metallicity gradients to these results.

Table 2.5: OCCAM DR14 Cluster Abundances

Cluster name	[O/Fe] (dex)	[Mg/Fe] (dex)	[Si/Fe] (dex)	[S/Fe] (dex)	[Ca/Fe] (dex)	[V/Fe] (dex)	[Cr/Fe] (dex)	[Mn/Fe] (dex)	[Co/Fe] (dex)	[Ni/Fe] (dex)
NGC 6791	0.07±0.04	0.06±0.06	-0.01±0.05	0.05±0.11	0.02±0.06	-0.01±0.16	-0.11±0.08	-0.00±0.14	0.04±0.27	-0.00±0.04
NGC 6819	-0.02±0.03	0.00±0.02	0.00±0.03	-0.02±0.05	0.01±0.02	0.02±0.07	0.02±0.03	0.03±0.02	0.05±0.08	0.02±0.02
NGC 6811	-0.09±0.04	-0.02±0.02	0.00±0.03	0.05±0.05	-0.00±0.03	-0.05±0.08	0.01±0.04	-0.00±0.02	-0.21±0.12	-0.02±0.02
Berkeley 53	-0.02±0.03	-0.02±0.02	0.01±0.03	0.03±0.06	0.01±0.03	0.00±0.08	-0.03±0.04	-0.01±0.03	-0.31±0.30	-0.02±0.02
NGC 7789	-0.03±0.03	-0.02±0.02	-0.02±0.02	-0.00±0.05	-0.02±0.02	-0.01±0.09	0.00±0.05	-0.01±0.02	-0.07±0.09	-0.03±0.02
FSR 0494	-0.05±0.05	-0.04±0.02	-0.02±0.03	-0.01±0.08	-0.00±0.04	0.12±0.11	0.03±0.06	0.02±0.04	0.05±0.22	0.01±0.03
NGC 188	0.02±0.04	0.05±0.02	0.01±0.02	0.01±0.08	-0.02±0.02	0.03±0.08	-0.01±0.06	0.08±0.03	0.13±0.11	0.04±0.02
IC 166	-0.02±0.07	0.02±0.04	0.07±0.06	0.04±0.14	-0.00±0.04	-0.12±0.27	0.00±0.06	0.00±0.04	-0.41±0.60	-0.02±0.03
Berkeley 66	0.04±0.10	0.06±0.03	0.05±0.03	0.01±0.07	-0.00±0.04	-0.14±0.17	0.01±0.06	-0.05±0.04	-0.01±0.22	-0.03±0.05
King 5	0.00±0.04	-0.02±0.02	0.03±0.03	0.07±0.06	-0.00±0.03	-0.01±0.11	0.04±0.04	-0.03±0.04	-0.00±0.12	-0.01±0.02
NGC 1245	-0.03±0.07	-0.03±0.02	0.03±0.03	0.00±0.07	-0.00±0.03	0.04±0.09	0.01±0.05	-0.01±0.03	-0.17±0.50	-0.04±0.02
King 7	-0.02±0.03	-0.01±0.02	0.04±0.03	0.10±0.07	0.00±0.02	-0.06±0.07	0.03±0.03	0.03±0.03	-0.04±0.07	-0.05±0.02
NGC 1798	0.01±0.06	-0.01±0.02	0.01±0.03	0.01±0.06	0.03±0.03	-0.03±0.11	-0.00±0.05	-0.07±0.03	-0.18±0.25	-0.03±0.02
Berkeley 17	0.03±0.03	0.06±0.02	0.02±0.03	0.06±0.05	0.01±0.03	0.02±0.07	0.03±0.04	-0.01±0.03	0.06±0.07	0.03±0.02
Berkeley 71	0.02±0.09	0.03±0.05	0.06±0.03	0.13±0.08	0.03±0.03	0.03±0.11	0.01±0.07	-0.04±0.04	-0.14±0.23	-0.03±0.02
Teutsch 51	0.08±0.08	0.01±0.03	0.06±0.06	0.01±0.13	0.03±0.05	-0.00±0.13	0.05±0.08	-0.03±0.05	0.09±0.21	-0.01±0.04
NGC 2158	0.00±0.07	0.03±0.02	0.03±0.03	0.10±0.09	-0.00±0.03	-0.15±0.13	-0.07±0.12	-0.05±0.04	-0.07±0.22	-0.01±0.03
NGC 2420	0.05±0.06	0.00±0.03	0.01±0.03	-0.01±0.06	0.03±0.03	-0.09±0.13	-0.04±0.10	-0.04±0.03	-0.18±0.20	-0.02±0.02
NGC 2682	-0.03±0.04	0.01±0.02	-0.03±0.02	-0.02±0.05	-0.02±0.02	-0.08±0.13	-0.02±0.07	0.01±0.02	-0.00±0.09	0.02±0.02

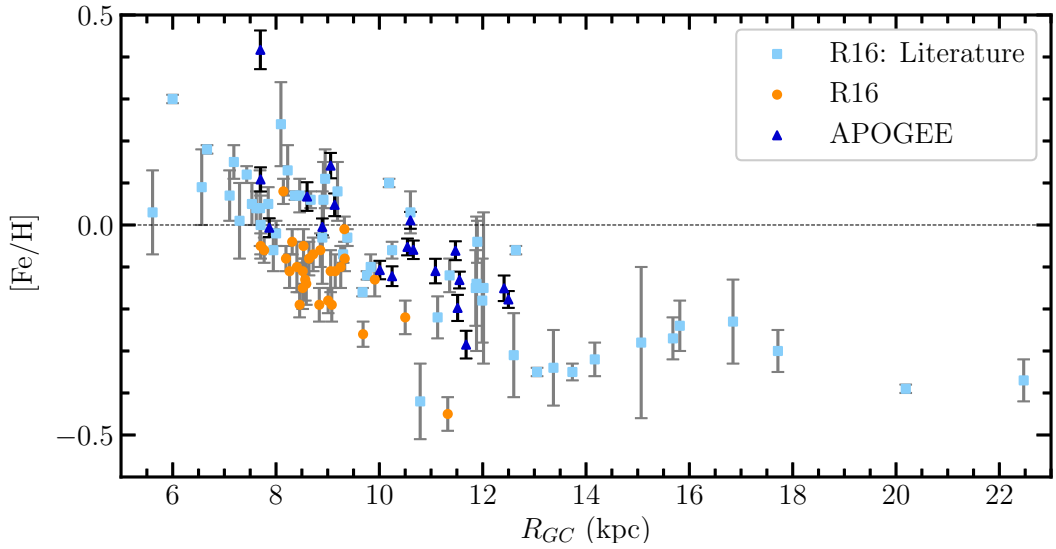

Figure 2.6: The Galactic abundance trend (R_{GC} vs.[Fe/H]) assuming $R_{GC,\odot}$ = 8.0 kpc. Our sample (dark blue triangles) is shown along with a literature sample from Reddy et al. (2016) (light blue points), and clusters analyzed by (Reddy et al. 2012; 2013; 2015; 2016, R16) (orange points).

2.4.4.1 Comparison to APOGEE DR12

We recomputed the metallicity gradient found from APOGEE DR12 (Cunha et al. 2016) using only clusters in common with this work (and excluding NGC 6791) and distances from Dias et al. (2002) and found a gradient of -0.035 ± 0.014. This agrees within the uncertainties with our gradient measured using the Dias catalog. The differences between the metallicity gradients can be explained in terms of improvements in the data reduction of APOGEE spectra, line list, and methodology, detailed in Holtzman et al. (2018).

2.4.4.2 Comparison to the Other Work

We find a metallicity gradient consistent with 4 of the 6 studies in Table 2.3, the 2 discrepent results being Carraro et al. (1998) and Yong et al. (2012), which both quote

particularly steep gradients. We find a relatively close agreement with Friel et al. (2002), Carrera & Pancino (2011), and Reddy et al. (2016). We note that if we instead compare the metallicity gradient computed with NGC 6791, our result is in agreement with Carraro et al. (1998) and Yong et al. (2012), but would no longer be in agreement with Reddy et al. (2016) or Friel et al. (2002). It is worth emphasizing that Reddy et al. (2016) and Friel et al. (2002) both had large uniform samples (24 and 28 open clusters, respectively) in addition to the literature samples included in their studies. Since the Reddy et al. (2016) study is both recent and very large, we compare to it directly. In Figure 2.6, we show the sample uniformly analyzed in Reddy et al. (2016) (orange points) and their literature compiled sample (light blue points), along with the APOGEE results (dark blue triangles).

2.5 Other Elements Beyond [Fe/H]

We compute mean DR14 cluster abundances for reliable α-related elements (O, Ca, Mg, Si, S) and iron peak elements (Cr, Co, Ni, Mn, V) in the same manner as [Fe/H], shown in Table 2.5. The abundances are shown for individual stars in Table 2.6.

Table 2.6: DR14 OCAAM Open Cluster Member Star Abundances

Cluster	2MASS ID	RV (km s^{-1})	[Fe/H] (dex)	[O/Fe] (dex)	[Mg/Fe] (dex)	[Ca/Fe] (dex)	[Si/Fe] (dex)	[S/Fe] (dex)
				[V/Fe] (dex)	[Cr/Fe] (dex)	[Mn/Fe] (dex)	[Co/Fe] (dex)	[Ni/Fe] (dex)
NGC 6819	2M19404803+4008085	2.4 ± 0.1	0.09 ± 0.01	-0.01 ± 0.02	0.02 ± 0.02	0.01 ± 0.02	0.02 ± 0.02	-0.00 ± 0.05
				0.04 ± 0.06	0.02 ± 0.03	0.01 ± 0.02	0.07 ± 0.06	0.01 ± 0.01
NGC 6819	2M19404965+4014313	3.1 ± 0.0	0.12 ± 0.01	0.01 ± 0.03	0.01 ± 0.02	0.02 ± 0.02	0.00 ± 0.02	-0.03 ± 0.05
				0.06 ± 0.07	0.02 ± 0.04	0.03 ± 0.03	0.07 ± 0.08	0.02 ± 0.02
NGC 6819	2M19405020+4013109	4.3 ± 0.0	0.15 ± 0.01	0.00 ± 0.03	0.00 ± 0.02	-0.00 ± 0.02	-0.04 ± 0.02	-0.04 ± 0.05
				-0.02 ± 0.06	-0.02 ± 0.03	0.01 ± 0.02	0.03 ± 0.07	0.02 ± 0.01
NGC 6819	2M19405601+4013395	3.3 ± 0.1	0.09 ± 0.01	0.04 ± 0.04	-0.00 ± 0.02	0.02 ± 0.03	-0.13 ± 0.03	-0.07 ± 0.06
				-0.01 ± 0.09	-0.00 ± 0.05	0.02 ± 0.03	0.10 ± 0.10	0.00 ± 0.02
NGC 6819	2M19405797+4008174	4.5 ± 0.1	0.13 ± 0.01	0.00 ± 0.03	0.02 ± 0.02	0.00 ± 0.02	0.01 ± 0.02	-0.06 ± 0.05
				0.08 ± 0.07	0.03 ± 0.03	0.05 ± 0.02	0.03 ± 0.07	0.00 ± 0.01
NGC 6819	2M19410524+4014042	3.3 ± 0.1	0.14 ± 0.01	-0.03 ± 0.03	-0.01 ± 0.02	0.04 ± 0.02	0.02 ± 0.03	0.03 ± 0.05
				0.02 ± 0.07	0.02 ± 0.04	0.03 ± 0.03	-0.04 ± 0.08	0.04 ± 0.02
NGC 6819	2M19410622+4010532	3.2 ± 0.0	0.12 ± 0.01	0.07 ± 0.04	0.01 ± 0.02	0.02 ± 0.03	0.03 ± 0.03	-0.05 ± 0.06
				0.02 ± 0.08	-0.04 ± 0.04	0.02 ± 0.03	0.03 ± 0.10	0.02 ± 0.02
NGC 6819	2M19410858+4013299	2.3 ± 0.0	0.11 ± 0.01	-0.06 ± 0.03	0.00 ± 0.02	-0.01 ± 0.02	0.03 ± 0.02	-0.03 ± 0.05
				0.03 ± 0.06	0.03 ± 0.03	0.03 ± 0.02	0.08 ± 0.07	0.01 ± 0.01
NGC 6819	2M19410926+4014436	2.3 ± 0.1	0.13 ± 0.01	-0.03 ± 0.03	0.00 ± 0.02	-0.00 ± 0.02	-0.03 ± 0.02	-0.02 ± 0.05
				-0.04 ± 0.06	-0.00 ± 0.03	0.00 ± 0.02	0.01 ± 0.07	-0.02 ± 0.01
NGC 6819	2M19410991+4015495	2.5 ± 0.1	0.07 ± 0.01	-0.03 ± 0.03	-0.00 ± 0.02	0.05 ± 0.02	0.01 ± 0.03	0.02 ± 0.05
				0.13 ± 0.07	0.06 ± 0.04	0.00 ± 0.03	0.13 ± 0.08	0.03 ± 0.02
				.....				

[a] Table 2.1 is published in its entirety in Appendix B

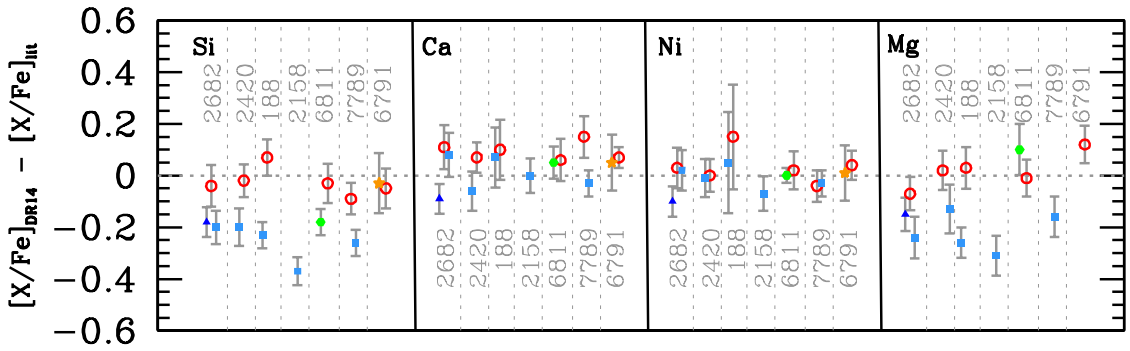

Figure 2.7: Comparison of individual elemental abundances using the APOGEE calibration clusters with available comparison elements in the other literature studies. Clusters are color-coded by analysis group: *dark blue* for Reddy et al. 2013; 2016, *light blue* for Jacobson et al. 2011, *green* for Bragaglia et al. 2001, *orange* for Carraro et al. 2006, and *red* for O'Connell et al. 2018 (submitted).

2.5.1 OCCAM DR14 Calibration Sample

We use the APOGEE calibration cluster set to search for systematics in other available elements (Si, Ca, Ni, Mg). As shown in Figure 2.7 and listed in Table 2.7, there are no significant systematic offsets, with the possible exception of [Mg/Fe] and [Si/Fe]. For all other elements, the offsets are within the uncertainties (see §2.4.1) for nearly every study and cluster. Jönsson et al. (2018) also perform a detailed comparison to the literature for these elements, and find no significant systematic offsets. For [Mg/Fe], the APOGEE data are offset from the Jacobson et al. 2011 clusters, but not from Bragaglia et al. 2001 and Carraro et al. 2006 data. These [Mg/Fe] discrepancies are most likely due to line-list differences and will require further exploration; however, since we are consistent with some clusters and likely the effect is systematic between groups, we apply no offset here.

2.5.2 Galactic Gradients in Other Elements

The full APOGEE DR14 sample allows an exploration of individual abundance gradients for key element groups[3], such as α-related elements and iron peak elements. These elements are key for exploring how Galactic chemical enrichment occurs, as each element is produced in a different manner (e.g., SNe II vs. SNe Ia yield ratios). We find statistically significant *increasing* trends for some of the α elements ([O/Fe], [Mg/Fe], and [Si/Fe]), seen in Figure 2.8. The other α trends (Si, Ca) also show a positive trend, but their large uncertainties make them also consistent with a slope of 0. This behavior is consistent with previous work (e.g., Jacobson et al. 2011), who also found a significant d[O/Fe]/dR trend from a literature compiled cluster sample.

This mild positive [α/Fe] gradient is in agreement with the chemical evolution models of Minchev et al. (2014), who find an [Mg/Fe] gradient (averaged over all age ranges, for $|Z| < 0.25$ kpc) of 0.009 dex kpc^{-1}, although the gradient for younger populations (which may better match our relatively young sample) is steeper, e.g. 0.027 dex kpc^{-1} for age < 2 Gyr. The models of Kubryk et al. (2015) also show a qualitatively similar trend for [O/Fe]. We also see a statistically significant *decreasing* trend for the iron-peak elements [Mn/Fe] and [Ni/Fe] as seen in Figure 2.9. The uncertainties are too large to draw meaningful conclusions for other elements (V, Cr, Co).

[3]While the DR14 APOGEE sample also contains C and N, these elements have strong stellar evolutionary changes along the giant branch. Given the small numbers of stars per cluster, we have excluded these elements from consideration in this paper.

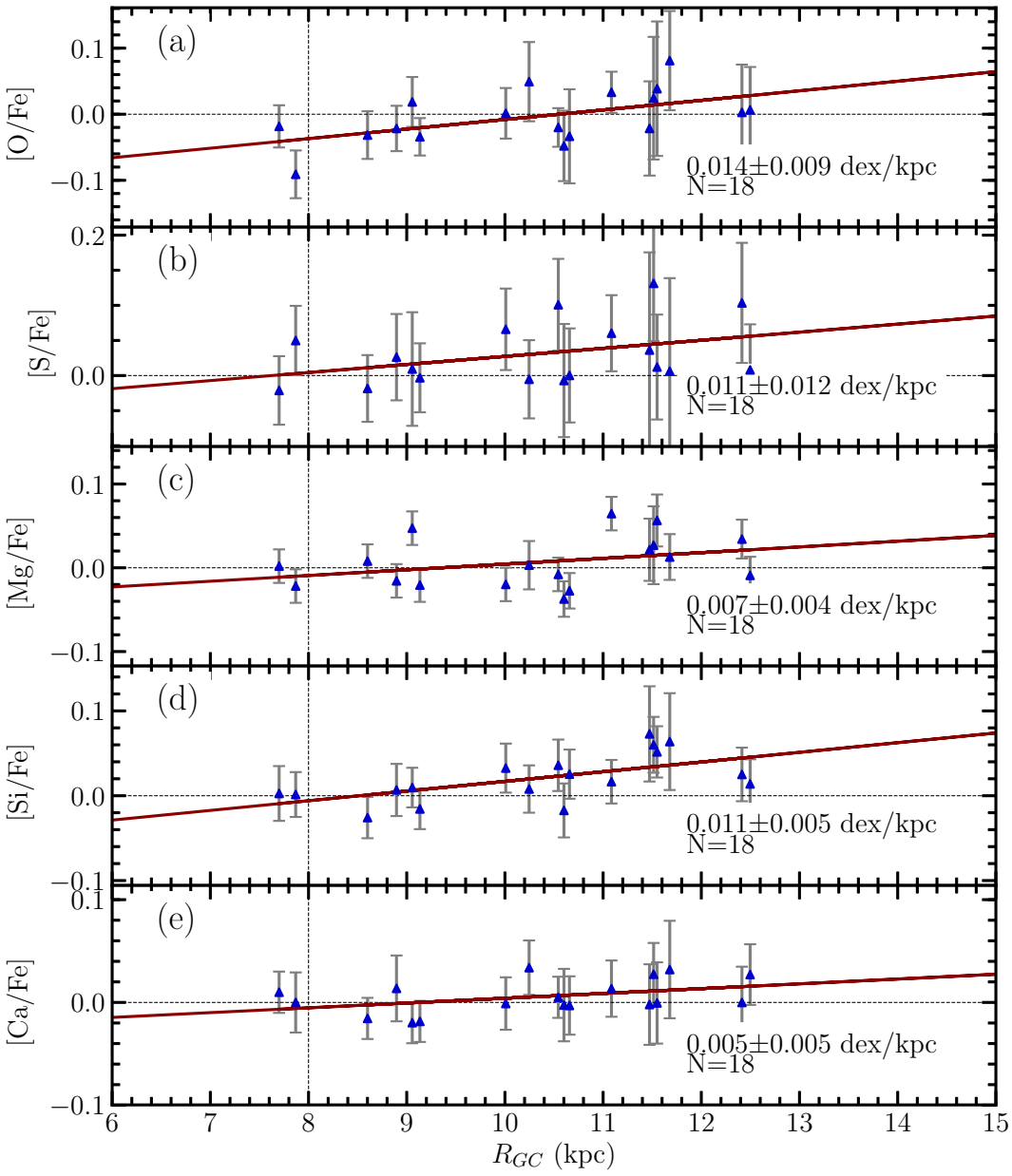

Figure 2.8: Galactic Trend for our sample for the α elements (O, S, Mg, Si, Ca) from DR14.

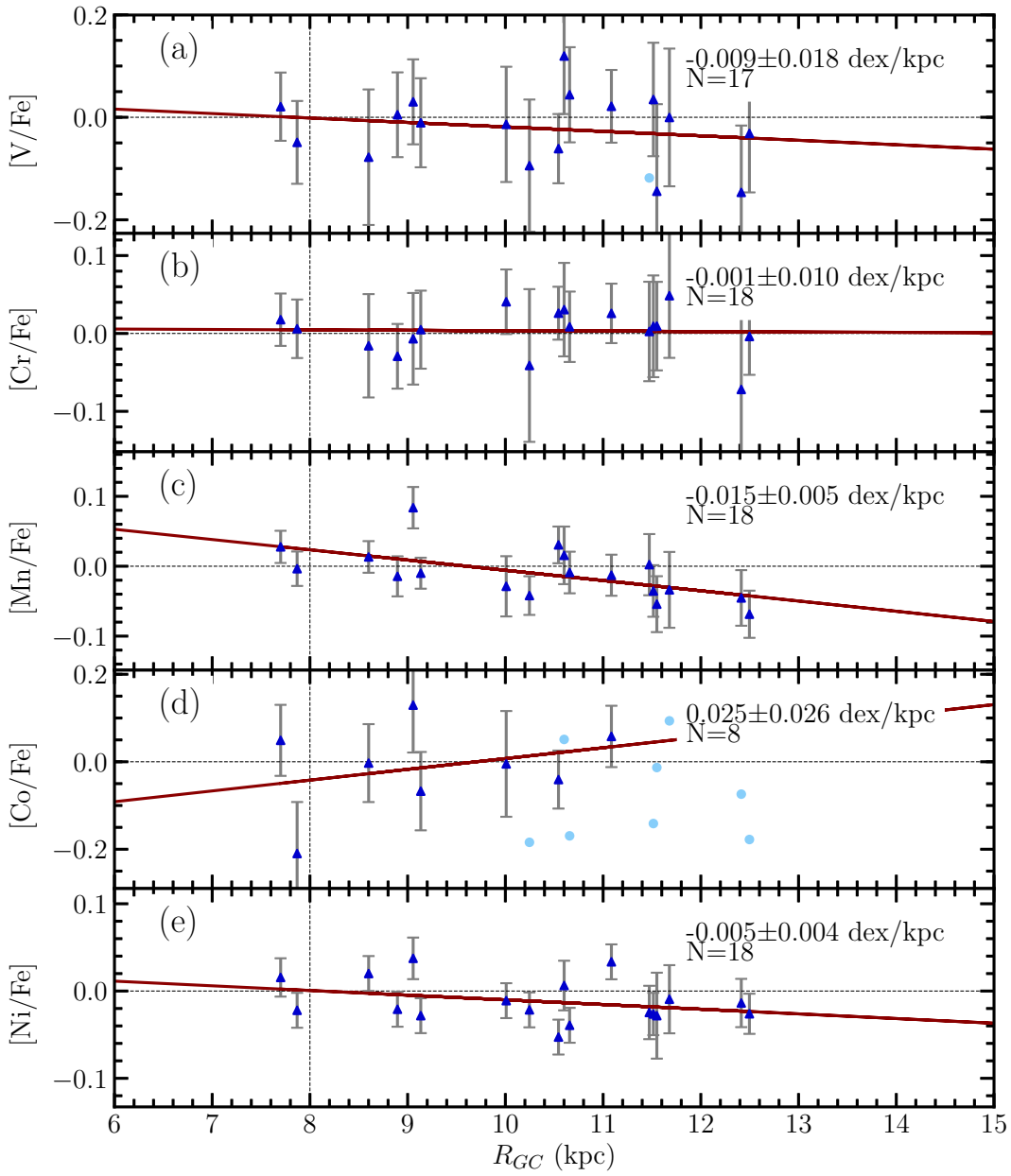

Figure 2.9: Galactic trend for our sample for the iron-peak (V, Co, Mn, Cr, Ni) elements from DR14. Clusters with very large uncertainties are not included in the fit (N reflects only those included in the fit), but are shown for reference as blue dots.

Table 2.7: DR14 OCCAM Abundance Comparison to Literature

Cluster	Abundance Lit. (dex)	# cluster stars Lit.	Abundance DR 14 (dex)	# cluster stars DR14	Δ[X/Fe] (dex)	References
			[Si/Fe]			
NGC 6819	+0.18 ± 0.04	3	+0.00 ± 0.03	36	−0.18 ± 0.05	Bragaglia et al. 2001
NGC 6819	+0.03 ± 0.07	3	+0.00 ± 0.03	36	−0.03 ± 0.08	O'Connell et al. 2018
NGC 6791	+0.02 ± 0.10	10	−0.01 ± 0.06	31	−0.03 ± 0.12	Carraro et al. 2006
NGC 6791	+0.04 ± 0.05	2	−0.01 ± 0.06	31	−0.05 ± 0.08	O'Connell et al. 2018
NGC 2158	+0.39 ± 0.05	15	+0.02 ± 0.02	18	−0.37 ± 0.05	Jacobson et al. 2009
NGC 188	+0.25 ± 0.05	27	+0.02 ± 0.01	13	−0.23 ± 0.05	Jacobson et al. 2011
NGC 188	−0.05 ± 0.07	3	+0.02 ± 0.01	13	+0.07 ± 0.07	O'Connell et al. 2018
NGC 2420	+0.21 ± 0.07	9	+0.01 ± 0.02	15	−0.20 ± 0.07	Jacobson et al. 2011
NGC 2420	+0.03 ± 0.06	6	+0.01 ± 0.02	15	−0.02 ± 0.06	O'Connell et al. 2018
NGC 2682	+0.21 ± 0.05	19	+0.01 ± 0.04	35	−0.20 ± 0.06	Jacobson et al. 2011
NGC 2682	+0.19 ± 0.04	3	+0.01 ± 0.04	35	−0.18 ± 0.06	Reddy et al. 2013
NGC 2682	+0.05 ± 0.07	10	+0.01 ± 0.04	35	−0.04 ± 0.08	O'Connell et al. 2018
NGC 7789	+0.25 ± 0.05	28	−0.01 ± 0.01	17	−0.26 ± 0.05	Jacobson et al. 2011
NGC 7789	+0.08 ± 0.06	5	−0.01 ± 0.01	17	−0.09 ± 0.06	O'Connell et al. 2018
			[Ca/Fe]			
NGC 6819	−0.04 ± 0.06	3	+0.01 ± 0.02	36	+0.05 ± 0.06	Bragaglia et al. 2001
NGC 6819	−0.05 ± 0.08	3	+0.01 ± 0.02	36	+0.06 ± 0.08	O'Connell et al. 2018
NGC 6791	−0.03 ± 0.10	10	+0.02 ± 0.04	31	+0.05 ± 0.11	Carraro et al. 2006
NGC 6791	−0.05 ±—	2	+0.02 ± 0.04	31	+0.07 ± —	O'Connell et al. 2018
NGC 2158	+0.00 ± 0.06	15	+0.00 ± 0.03	18	+0.00 ± 0.07	Jacobson et al. 2009
NGC 188	−0.04 ± 0.06	27	+0.03 ± 0.10	13	+0.07 ± 0.12	Jacobson et al. 2011
NGC 188	−0.07 ± 0.06	3	+0.03 ± 0.10	13	+0.10 ± 0.12	O'Connell et al. 2018
NGC 2420	+0.10 ± 0.07	9	+0.04 ± 0.03	15	−0.06 ± 0.08	Jacobson et al. 2011
NGC 2420	−0.03 ± 0.05	6	+0.04 ± 0.03	15	+0.07 ± 0.06	O'Connell et al. 2018
NGC 2682	−0.11 ± 0.07	19	−0.03 ± 0.05	35	+0.08 ± 0.09	Jacobson et al. 2011
NGC 2682	+0.06 ± 0.03	3	−0.03 ± 0.05	35	−0.09 ± 0.06	Reddy et al. 2013
NGC 2682	−0.14 ± 0.07	10	−0.03 ± 0.05	35	+0.11 ± 0.09	O'Connell et al. 2018
NGC 7789	+0.01 ± 0.05	28	−0.02 ± 0.01	17	−0.03 ± 0.05	Jacobson et al. 2011
NGC 7789	−0.17 ± 0.08	5	−0.02 ± 0.01	17	+0.15 ± 0.08	O'Connell et al. 2018
			[Ni/Fe]			
NGC 6819	+0.01 ± 0.02	3	+0.01 ± 0.02	36	+0.00 ± 0.03	Bragaglia et al. 2001
NGC 6819	−0.01 ± 0.07	3	+0.01 ± 0.02	36	+0.02 ± 0.07	O'Connell et al. 2018
NGC 6791	−0.01 ± 0.10	10	+0.00 ± 0.04	31	+0.01 ± 0.11	Carraro et al. 2006
NGC 6791	−0.04 ± 0.04	2	+0.00 ± 0.04	31	+0.04 ± 0.06	O'Connell et al. 2018
NGC 2158	+0.05 ± 0.06	15	−0.02 ± 0.03	18	−0.07 ± 0.07	Jacobson et al. 2009
NGC 188	+0.08 ± 0.05	27	+0.13 ± 0.19	13	+0.05 ± 0.20	Jacobson et al. 2011
NGC 188	−0.02 ± 0.07	3	+0.13 ± 0.19	13	+0.15 ± 0.20	O'Connell et al. 2018
NGC 2420	−0.01 ± 0.07	9	−0.02 ± 0.02	15	−0.01 ± 0.07	Jacobson et al. 2011
NGC 2420	−0.02 ± 0.06	6	−0.02 ± 0.02	15	−0.00 ± 0.06	O'Connell et al. 2018
NGC 2682	−0.01 ± 0.06	19	+0.01 ± 0.05	35	+0.02 ± 0.08	Jacobson et al. 2011
NGC 2682	+0.11 ± 0.03	3	+0.01 ± 0.05	35	−0.10 ± 0.06	Reddy et al. 2013
NGC 2682	−0.02 ± 0.06	10	+0.01 ± 0.05	35	+0.03 ± 0.08	O'Connell et al. 2018
NGC 7789	+0.00 ± 0.05	28	−0.03 ± 0.01	17	−0.03 ± 0.05	Jacobson et al. 2011

Continued on Next Page...

Table 2.7 – Continued

Cluster	Abundance Lit. (dex)	# cluster stars Lit.	Abundance DR 14 (dex)	# cluster stars DR14	Δ[X/Fe] (dex)	References
NGC 7789	+0.01 ± 0.06	5	−0.03 ± 0.01	17	−0.04 ± 0.06	O'Connell et al. 2018
			[Mg/Fe]			
NGC 6819	−0.12 ± 0.07	3	+0.00 ± 0.01	36	+0.12 ± 0.07	Bragaglia et al. 2001
NGC 6819	+0.01 ± 0.07	3	+0.00 ± 0.01	36	−0.01 ± 0.07	O'Connell et al. 2018
NGC 2158	+0.22 ± 0.07	15	+0.03 ± 0.01	18	−0.19 ± 0.07	Jacobson et al. 2009
NGC 188	+0.26 ± 0.05	27	+0.03 ± 0.04	13	−0.23 ± 0.06	Jacobson et al. 2011
NGC 188	+0.00 ± 0.07	3	+0.03 ± 0.04	13	+0.03 ± 0.08	O'Connell et al. 2018
NGC 2420	+0.11 ± 0.09	9	+0.00 ± 0.03	15	−0.11 ± 0.09	Jacobson et al. 2011
NGC 2420	−0.02 ± 0.07	6	+0.00 ± 0.03	15	+0.02 ± 0.08	O'Connell et al. 2018
NGC 2682	+0.23 ± 0.07	19	−0.03 ± 0.05	35	−0.26 ± 0.09	Jacobson et al. 2011
NGC 2682	+0.12 ± 0.04	3	−0.03 ± 0.05	35	−0.16 ± 0.06	Reddy et al. 2013
NGC 2682	+0.04 ± 0.04	10	−0.03 ± 0.05	35	−0.07 ± 0.06	O'Connell et al. 2018
NGC 7789	+0.14 ± 0.05	28	−0.02 ± 0.01	17	−0.16 ± 0.05	Jacobson et al. 2011
NGC 7789	−0.07 ± 0.04	5	−0.02 ± 0.01	17	+0.05 ± 0.04	O'Connell et al. 2018

Chapter 3

Evolution of Galactic Chemical Trends

In Chapter 2 the methods for membership determination in the OCCAM survey were explained, and abundance gradients for 11 elements available in APOGEE DR14 were measured using a "highly reliable" sample of clusters that were required to have at least 4 APOGEE member stars. In this chapter we significantly expand the OCCAM sample by allowing clusters with any number of member stars to be included, and using the expanded APOGEE DR16, which has many more stars than DR14. This expanded sample is now large enough to separate into age bins to measure the evolution of chemical abundance trends.

3.1 Data

To minimize the impact of calibration differences and other systematic effects, and ensure uniformity, the OCCAM survey uses as much data from as few sources as possible; therefore, the majority of this analysis is based primarily on two large surveys, *Gaia* and SDSS/APOGEE. Our primary source of chemical abundance and RV data is the SDSS data release 16 (DR16) (Jönsson et al., *in press*; Ahumada et al. 2019, Blanton et al. 2017) taken as part of the second, dual hemisphere phase of APOGEE, which is APOGEE 2 (Majewski et al. 2017). APOGEE is a high resolution, near infrared spectroscopic survey currently operating in both hemispheres, at Apache Point Observatory (APO; New Mexico, Gunn et al. 2006) and Las Campanas Observatory (LCO; Chile, Bowen & Vaughan 1973). The APOGEE/DR16 dataset includes about 430,000 stars, collected between August 2011 and August 2018 using the two 300-fiber APOGEE spectrographs (Wilson et al. 2019) and, for the first time, the APOGEE survey has near-complete coverage in Galactic longitude, due to the first release of data from LCO. The APOGEE data reduction pipeline (Nidever et al. 2015, Holtzman et al. 2015; 2018, Jönsson et al., *in press*) provides stellar atmospheric parameters and radial velocity measurements, while elemental abundances are provided from the ASPCAP pipeline (García Pérez et al. 2016, Mészáros et al. 2012, Zamora et al. 2015, Holtzman et al. 2018, Jönsson et al., *in press*). Copper, cerium (Cunha et al. 2017), neodymium (Hasselquist et al. 2016), and ytterbium abundances are reported from ASPCAP for the first time in DR16, although neodymium and ytterbium lines are so weak or blended that these ASPCAP abundances are considered unreliable. Concerning cerium, the APOGEE region contains several Ce

II lines (Cunha et al. 2017), however, the current DR16 results are only based on one Ce II line; future data releases will use the full sample of cerium lines. Therefore we will postpone any discussion of cerium until future data releases.

In the APOGEE DR16 allStar-file, several types of abundances are reported for every star and element: firstly the abundance reported by the analysis pipeline is supplied in the FELEM-array. Secondly, these abundances have been calibrated with a zero-point shift to ensure solar metallicity stars in the solar neighborhood have [X/M]=0; in practice these shifts are small, < 0.05 dex, except for Al, K, V, and Mn. Finally, these calibrated abundances have been culled for particular uncertain values by the ASPCAP-team (e.g., for [Y/Fe] or [Nd/Fe]). These final, "cleaned" and calibrated abundances are supplied in the "named tags"; FE_H, MG_FE, CE_FE, etc. More information, including what zero-point shifts have been applied, is provided in Jönsson et al., *in press*. In this paper, we use the abundances of the "named tags" as is recommended in Jönsson et al., *in press*.

Targeting for APOGEE relied on input from two all-sky surveys: 2MASS (Cutri et al. 2003) and WISE (Wright et al. 2010). More details specifically about open cluster targeting are provided in Chapter 2, and details about APOGEE targeting generally can be found in Zasowski et al. (2013; 2017).

Our secondary source of data is *Gaia* DR2 (Gaia Collaboration et al. 2016; 2018, Lindegren et al. 2018); we use photometric and astrometric data for 1,365,376 *Gaia* stars, radial velocity measurements for 16,084 stars, and parallax values for 886 stars in common with APOGEE. We use cluster coordinates and radii from Dias et al. (2002). For this study, we use the uniform distance determination from Kharchenko et al. (2013, generally referred to as the Milky Way Star Cluster, MWSC, catalog) when measuring

galactic trends; however, we briefly compare to other uniform distance catalogs (e.g., Cantat-Gaudin et al. 2018, Bailer-Jones et al. 2018) in §3.4.1.

Table 3.1: OCCAM DR16 Sample - Basic Parameters

Cluster name	Qual flag	l deg	b deg	R (')	Age Gyr	R_{GC} (kpc)	μ_α (mas yr^{-1})	μ_δ (mas yr^{-1})	RV (km s^{-1})	[Fe/H] (dex)	Num stars
High Quality Clusters											
Ruprecht 147	1	21.0089	−12.7301	30.0	2.14	7.72	−0.87 ± 0.10	−26.72 ± 0.10	+42.4 ± 1.5	+0.12 ± 0.03	27
NGC 6705	1	27.2873	−2.7594	9.0	0.32	5.94	−1.56 ± 0.08	−4.17 ± 0.07	+35.4 ± 1.0	+0.12 ± 0.04	12
Berkeley 43	1	45.6843	−0.1391	6.3	0.61	5.73	−0.92 ± 0.08	−3.27 ± 0.07	+30.0 ± 0.1	+0.03 ± 0.01	1
Berkeley 44	1	53.2093	+3.3443	6.3	1.41	6.50	−0.17 ± 0.05	−3.17 ± 0.05	+23.0 ± 0.1	−0.00 ± 0.01	1
NGC 6791	2	69.9658	+10.9080	6.3	4.42	7.71	−0.44 ± 0.03	−2.25 ± 0.03	−46.9 ± 1.3	+0.35 ± 0.04	36
NGC 6819	2	73.9834	+8.4882	6.9	1.62	7.70	−2.96 ± 0.03	−3.87 ± 0.03	+2.7 ± 1.7	+0.05 ± 0.03	37
NGC 6811	2	79.2233	+12.0047	7.2	0.64	7.87	−3.44 ± 0.06	−8.73 ± 0.04	+8.0 ± 0.3	−0.05 ± 0.02	4
NGC 6866	1	79.5648	+6.8354	5.1	0.44	7.87	−1.18 ± 0.04	−5.91 ± 0.08	+14.2 ± 0.4	+0.01 ± 0.01	2
IC 1369	1	89.6019	−0.4154	5.1	0.35	8.70	−4.68 ± 0.05	−5.55 ± 0.04	−48.5 ± 0.1	−0.08 ± 0.03	3
NGC 7062	1	89.9667	−2.7397	3.6	0.69	8.34	−1.84 ± 0.04	−4.08 ± 0.04	−22.0 ± 0.1	+0.01 ± 0.01	1
.....											

Table 2.1 is published in its entirety in Appendix C

[1] Radius from Dias et al. (2002)

[2] Calculated using or taken from MWSC Catalog.

[3] μ_α and μ_δ and their 1σ uncertainties are those of the 2D Gaussian fit, as in 2.

Table 3.2: OCCAM DR16 Sample - Detailed Chemistry

Cluster name	[Fe/H] (dex)	[O/Fe] (dex)	[Na/Fe] (dex)	[Mg/Fe] (dex)	[Al/Fe] (dex)	[Si/Fe] (dex)	[S/Fe] (dex)	[K/Fe] (dex)
	[Ca/Fe] (dex)	[Ti/Fe] (dex)	[V/Fe] (dex)	[Cr/Fe] (dex)	[Mn/Fe] (dex)	[Co/Fe] (dex)	[Ni/Fe] (dex)	[Cu/Fe] (dex)
High Quality Clusters								
Ruprecht 147	0.12 ± 0.03	-0.05 ± 0.03	0.11 ± 0.03	-0.01 ± 0.02	0.02 ± 0.04	-0.00 ± 0.05	0.02 ± 0.06	0.04 ± 0.08
	-0.01 ± 0.04	-0.07 ± 0.09	0.01 ± 0.07	0.02 ± 0.09	0.04 ± 0.03	0.14 ± 0.20	0.01 ± 0.02	-0.09 ± 0.20
NGC 6705	0.12 ± 0.04	-0.05 ± 0.02	0.23 ± 0.04	-0.07 ± 0.02	-0.13 ± 0.03	0.01 ± 0.01	0.07 ± 0.02	-0.16 ± 0.06
	-0.03 ± 0.02	-0.00 ± 0.02	-0.01 ± 0.04	-0.03 ± 0.04	0.11 ± 0.02	0.04 ± 0.03	0.03 ± 0.01	0.17 ± 0.07
Berkeley 43	0.03 ± 0.01	-0.05 ± 0.01	0.15 ± 0.03	-0.08 ± 0.01	-0.22 ± 0.02	0.03 ± 0.01	0.13 ± 0.02	-0.18 ± 0.03
	-0.05 ± 0.01	-0.01 ± 0.01	-0.02 ± 0.04	-0.08 ± 0.03	0.12 ± 0.01	0.01 ± 0.03	0.02 ± 0.01	-0.26 ± 0.03
Berkeley 44	-0.00 ± 0.01	0.04 ± 0.01	-0.16 ± 0.03	-0.02 ± 0.01	-0.30 ± 0.02	0.01 ± 0.01	0.02 ± 0.03	-0.15 ± 0.03
	-0.14 ± 0.01	-0.13 ± 0.01	-0.29 ± 0.04	-0.17 ± 0.03	0.06 ± 0.01	0.05 ± 0.03	-0.03 ± 0.01	0.04 ± 0.03
NGC 6791	0.35 ± 0.04	0.04 ± 0.03	0.08 ± 0.06	0.11 ± 0.03	0.01 ± 0.07	0.01 ± 0.03	-0.02 ± 0.05	0.03 ± 0.10
	-0.02 ± 0.03	0.09 ± 0.05	-0.06 ± 0.30	-0.02 ± 0.09	0.01 ± 0.13	0.11 ± 0.08	0.01 ± 0.04	0.14 ± 0.07
NGC 6819	0.05 ± 0.03	-0.01 ± 0.03	0.07 ± 0.09	-0.01 ± 0.01	-0.04 ± 0.03	0.00 ± 0.03	0.00 ± 0.03	-0.04 ± 0.07
	0.01 ± 0.02	0.01 ± 0.03	0.04 ± 0.13	0.01 ± 0.03	0.05 ± 0.03	0.02 ± 0.06	0.02 ± 0.02	0.04 ± 0.06
NGC 6811	-0.05 ± 0.02	-0.04 ± 0.02	0.06 ± 0.07	-0.04 ± 0.01	-0.07 ± 0.03	-0.02 ± 0.01	0.05 ± 0.04	-0.06 ± 0.05
	0.02 ± 0.01	0.00 ± 0.02	—	0.05 ± 0.03	0.01 ± 0.02	-0.16 ± 0.12	-0.03 ± 0.01	-0.06 ± 0.10
NGC 6866	0.01 ± 0.01	—	-0.00 ± 0.04	-0.05 ± 0.01	-0.04 ± 0.02	-0.04 ± 0.01	0.04 ± 0.03	-0.06 ± 0.03
	0.01 ± 0.02	0.01 ± 0.02	—	0.03 ± 0.05	0.02 ± 0.01	-0.14 ± 0.08	-0.03 ± 0.01	0.02 ± 0.03
IC 1369	-0.08 ± 0.03	-0.08 ± 0.02	0.08 ± 0.10	-0.04 ± 0.02	-0.11 ± 0.02	-0.01 ± 0.01	0.09 ± 0.07	0.02 ± 0.03
	0.01 ± 0.04	-0.08 ± 0.02	—	0.01 ± 0.04	0.04 ± 0.03	-0.04 ± 0.04	-0.06 ± 0.01	0.09 ± 0.04
NGC 7062	0.01 ± 0.01	—	0.17 ± 0.04	-0.07 ± 0.01	-0.05 ± 0.02	-0.01 ± 0.01	0.00 ± 0.03	-0.05 ± 0.03
	-0.00 ± 0.01	-0.02 ± 0.02	—	-0.08 ± 0.03	-0.00 ± 0.01	0.01 ± 0.04	-0.02 ± 0.01	-0.04 ± 0.03
.....								

Table 2.1 is published in its entirety in Appendix D

3.2 Methods

3.2.1 Membership Analysis

The selection of cluster member stars utilizes the stellar radial velocities, proper motions (PM), spatial location, and derived metallicities as membership discriminators. For this study, we use the membership procedure, fully described in Chapter 2 with some minor improvements. The method of Chapter 2 first performs a PM analysis using *Gaia* DR2 to isolate likely cluster members (§2.2.2.1). If multiple APOGEE stars are selected for the same cluster that have very different RVs, there is an inherent ambiguity and a "correct" systemic cluster velocity cannot be chosen. We now leverage the RV measurements from *Gaia* , when available, for stars identified as likely PM members to significantly increase the number of RV measurements in a cluster and more reliably determine the cluster system velocity. To be included as a cluster member, a star must fall within 3σ of the cluster mean as established by the kernel convolution (described in Chapter 2) in *all three* spaces considered (RV, [Fe/H], and PM).

3.2.2 Visual Quality Check

A visual inspection of each cluster's PM-cleaned color-magnitude diagram (CMD) was performed by multiple of the authors. Figure 3.1 shows five example CMDs. The visual assessment is meant to evaluate whether stars that pass the combined RV, proper motion and metallicity criteria also lie in a sensible position in the observed cluster CMD, considering their spectroscopically determined log(g). This is an easy case when, for example, one or more APOGEE OCCAM candidates with high log(g) ($log(g) \geq 3.7$) are found

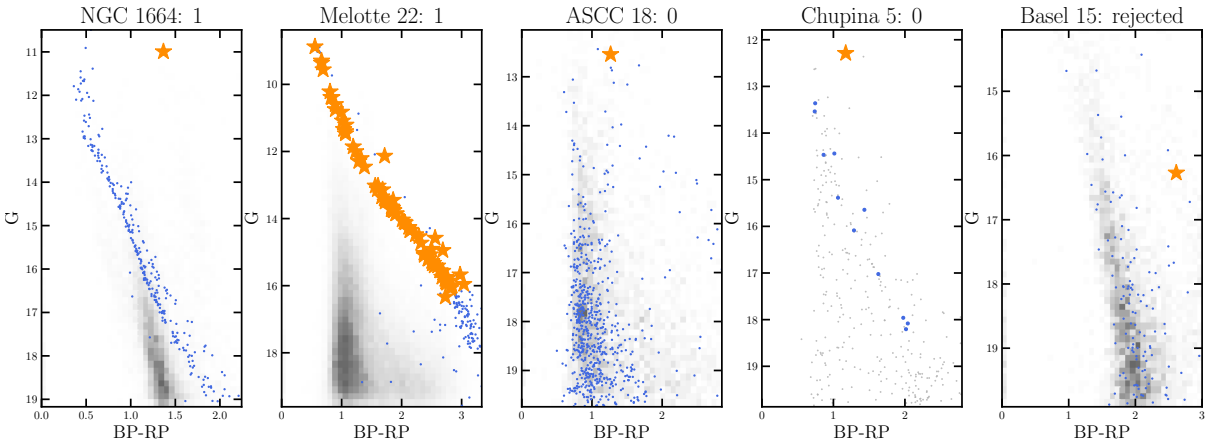

Figure 3.1: Five example color-magnitude diagrams of open clusters analyzed in the study, with cluster name and quality designation from Table 3.1 . *Gaia* stars within twice the cluster radius are shown; stars identified as PM members and inside the cluster radius are blue. Non-member stars are shown as a Hess diagram in grey except for Chupina 5 where actual stars are shown. The OCCAM pipeline-identified APOGEE members are shown as orange stars.

to lie along an easily discernible photometric main sequence in the CMD (e.g., Melotte 22), thus providing a joint affirmation that the star is likely a main sequence member of the cluster. These clusters are flagged as "1" or "high quality". However, most of the OCCAM stars from APOGEE turn out to be evolved stars — subgiants, giants and red clump stars, with $log(g) < 3.7$. In this case, the star is still considered a member if the star lies along the subgiant/giant branch of the cluster, which, however, must generally be projected from the location of the main sequence and its turn-off, given that the subgiant/giant sequences in most clusters are typically very poorly populated (e.g., NGC 1664). These clusters are also flagged as "1", indicating they are "high quality". The latter process becomes more challenging when the main sequence is also poorly populated (e.g., Chupina 5), or when the field star contamination becomes so dominant as to obscure the cluster main sequence (e.g., ASCC 18). These clusters are flagged as "0" or "potentially unreliable". Clusters where the APOGEE OCCAM candidate is not a part

of any discernable sequence or where there is no discernable sequence (e.g., Basel 15) are rejected. We note that all clusters from Chapter 2 satisfy the "high quality" criteria, but as they have been checked even more thoroughly, and are additionally required to have 4 or more members, they are flagged as "2", which has the additional benefit of quickly identifying the previous sample. Thus, clusters considered "high quality" in this sample can be easily identified as quality > 0. These quality flags are included in the full version of Tables 3.1 and 3.2 (available online), and in the value added catalog, described below.

3.2.3 Data Access - SDSS Value Added Catalog

The data this analysis uses are also available as a Value Added Catalog (VAC) that was released along with SDSS-IV DR16. The VAC consists of two tables. The first is a combination of Table 3.1 and Table 3.2, showing bulk cluster parameters derived here including PM, and RV, but also including abundances for all[1] elements reported in DR16. We note that cluster ages are not included in the VAC as only ages from the MWSC catalog are used in this work.

Five measurements of R_{GC} are also included. We calculate R_{GC} using catalog distances from Dias et al. (2002)[2], Kharchenko et al. (2013, MWSC), and Cantat-Gaudin et al. (2018). We also calculate R_{GC} based on median parallax from member stars and median distance for member stars from Bailer-Jones et al. (2018), as in 2. In §3.4.1 we discuss differences in these distance measurements.

[1]Elements such as Rb and Y that do not have calibrated values reported in DR16 are not included.

[2]We acknowledge an error in our pipeline that populated R_{GC} for some clusters where no distance is reported by Dias et al. (2002). "R_GC_DIAS" values for the clusters ASCC 16, Chupina 3, 4, & 5, Collinder 95, FSR 0687, L 1241s, NGC 358, and Platais 4 should be disregarded

The second table in the VAC shows all of the APOGEE stars considered in this analysis (all the stars that fall within $2 \times Radius_{Dias}$ of the cluster center). For each star, we reproduce relevant parameters (RV, [Fe/H], and proper motion) and provide our membership probability estimate based on each parameter. For convenience, we also provide the membership determination from Cantat-Gaudin et al. (2018) (when provided). All columns available in the VAC are presented in Table 3. The catalog is available from sdss.org here [3].

Both tables are also available for exploration using Filtergraph (Burger et al. 2013) at `https://filtergraph.com/sdss_apogee_occam/`.

Table 3.3: A summary of the individual star data included in the DR16 OCCAM VAC

Label	Description
CLUSTER	The associated open cluster
2MASS ID	star ID from 2MASS survey
LOCATION_ID[1]	from APOGEE DR16
GLAT	Galactic latitude
GLON	Galactic longitude
FE_H[1]	[Fe/H]
FE_H_ERR[1]	uncertainty in FE_H
VHELIO_AVG[1]	heliocentric radial velocity
VSCATTER[1]	scatter in APOGEE RV measurements
PMRA[2]	proper motion in right ascension
PMDEC[2]	proper motion in declination
PMRA_ERR[2]	uncertainty in PMRA
PMDEC_ERR[2]	uncertainty in PMDEC
RV_PROB	membership probability based on RV (This study)
FEH_PROB	membership probability based on FE_H (This study)
PM_PROB	membership probability based on PM (This study)
CG_PROB	membership probability from Cantat-Gaudin et al. (2018)

[1] Taken directly from APOGEE DR16

[2] From *Gaia* DR2

[3]The full url is `https://www.sdss.org/dr16/data_access/value-added-catalogs/?vac_id=open-cluster-chemical-abundances-and-mapping-catalog`

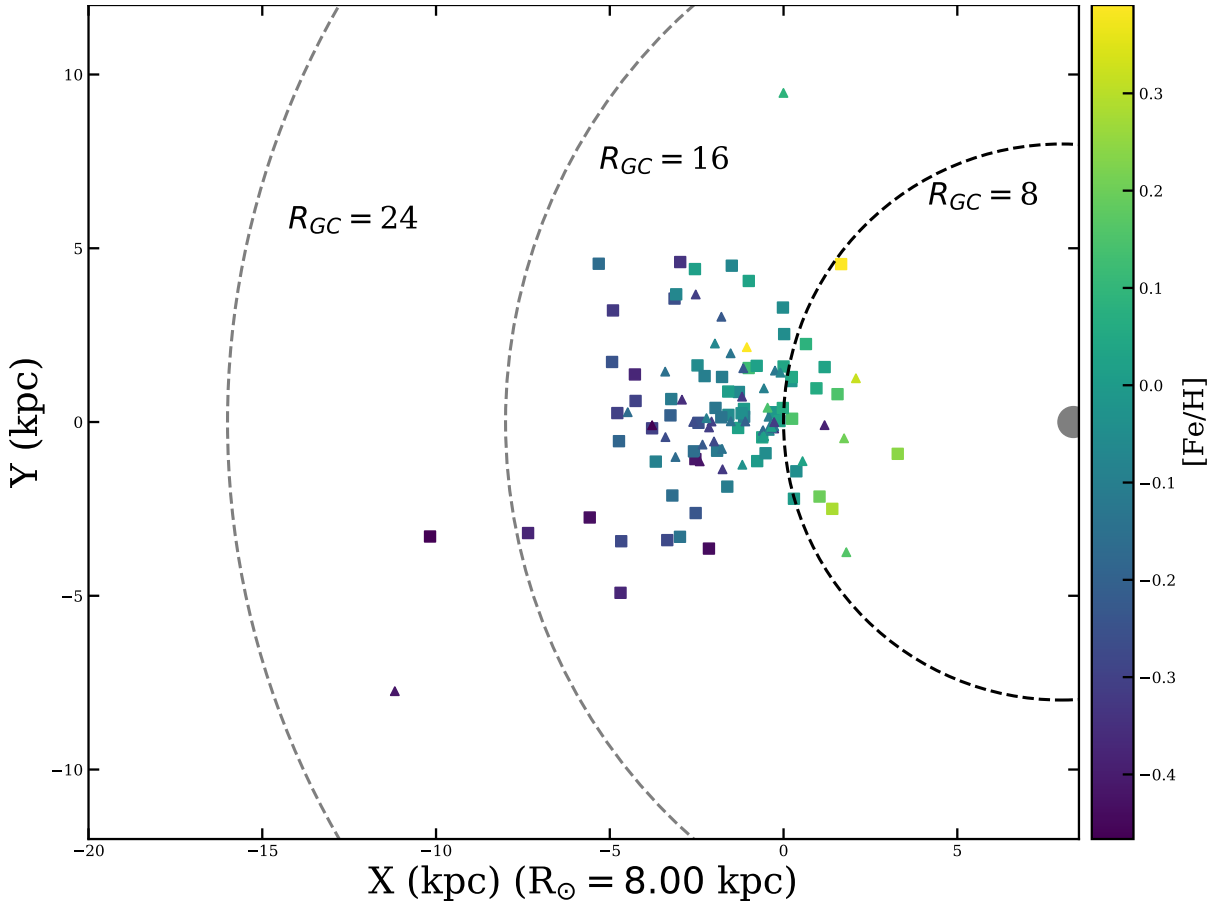

Figure 3.2: The full OCCAM DR16 sample plotted in the Galactic plane. Square points are "high quality" clusters, triangles are the lower quality clusters. The colorbar shows [Fe/H]. The concentric circles show R_{GC} = 8, 16, & 24 kpc

3.3 The OCCAM DR16 Sample

Our final sample in this study consists of 128 open clusters with 914 member stars, out of 10,191 stars near cluster fields considered in the analysis. Of those 128 clusters, 83 clusters were designated as "high quality" based on a visual CMD inspection. For the Galactic abundance analysis in this study, we will only use those clusters flagged as high quality, as presented in Table 3.1. The other clusters with questionable quality, e.g., those that did not pass visual checks (§3.2), are also presented in Table 3.1.

The Galactic spatial distribution of the OCCAM DR16 sample is shown in Figure 3.2. The majority of the OCCAM DR16 open clusters fall between $6 \leq R_{GC} \leq 14$ kpc, with good R_{GC} coverage in that range. Two high quality clusters fall outside of this range: Berkeley 20 at $R_{GC} \approx 15.5$ kpc and Berkeley 29 at $R_{GC} \approx 18.5$ kpc[4]. Using age estimates from the MWSC catalog, our sample spans a range in age from ~ 5 Myr to ~ 6 Gyr[5], with nearly half under 1 Gyr.

3.3.1 Modifications to the High Quality Sample

We have further excluded 12 clusters (ASCC 16, ASCC 19, ASCC 21, Briceno 1, Chupina 1, Chupina 3, Collinder 69, Collinder 70, IC 348, NGC 1980, NGC 1981, NGC 2264) that would otherwise be considered "high quality" because they are reported to be very young (< 50 Myr) (Kharchenko et al. 2013) and previous studies of young stars in APOGEE suggest the pipeline results may be unreliable (e.g., Kounkel et al. 2018). Thus the final sample used for analysis consists of 71 clusters.

There are additional affects within clusters that may result in unreliable abundance determinations. Souto et al. (2018; 2019) showed that abundances in dwarf and giant stars in the old cluster NGC 2682 differed significantly due to atomic diffusion. For this reason, the dwarf stars in NGC 2682 are excluded from our abundance analysis. NGC 752 is also relatively old and may suffer from diffusion effects, we therefore exclude the dwarfs in this cluster from abundance analysis as well. As a result, for both NGC 752 & NGC 2682 we only use the giant stars to determine the cluster abundances.

[4]We note Dias et al. (2002) find Be 29 to be significantly further away at $R_{GC} \approx 22.5$ kpc, but for consistency we are using distances from the MWSC catalog for all clusters.

[5]We note some studies of NGC 6791 (e.g. Brogaard et al. 2012) find it to be significantly older, however in the interest of a uniform analysis we rely only on ages from the MWSC catalog

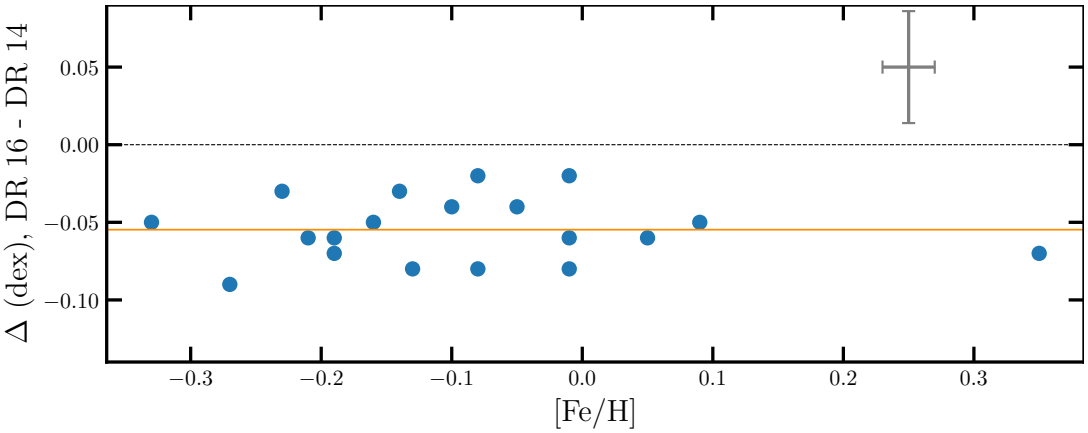

Figure 3.3: The difference in reported [Fe/H] from DR14 to DR16 for the 19 clusters from 2. A characteristic error-bar is shown.

3.3.2 Comparison to previous work

3.3.2.1 APOGEE DR14 – Chapter 2

For the 19 open clusters studied in Chapter 2, we plot Δ[Fe/H] vs DR16 [Fe/H] in Figure 3.3. Figure 3.3 shows that the mean [Fe/H] for OCCAM clusters changed between APOGEE DR14 and DR16; this is mostly due to changes in the DR16 line list (Smith et al. *in prep*). There is a clear offset for all clusters, with a mean difference of 0.05 dex. In Chapter 2, it was shown that APOGEE DR14 [Fe/H] values for six well studied open clusters were on average approximately 0.05 dex more metal-rich than the results in the literature. If we repeat the same literature comparison using our DR16 values, we find a mean offset of [Fe/H] = 0.004. All of these offsets are within their measured 1σ dispersions.

Figure 3.4 shows a similar plot for other elements. Beyond the quoted uncertainties in each case, there are no obvious systematic trends for any of these elements.

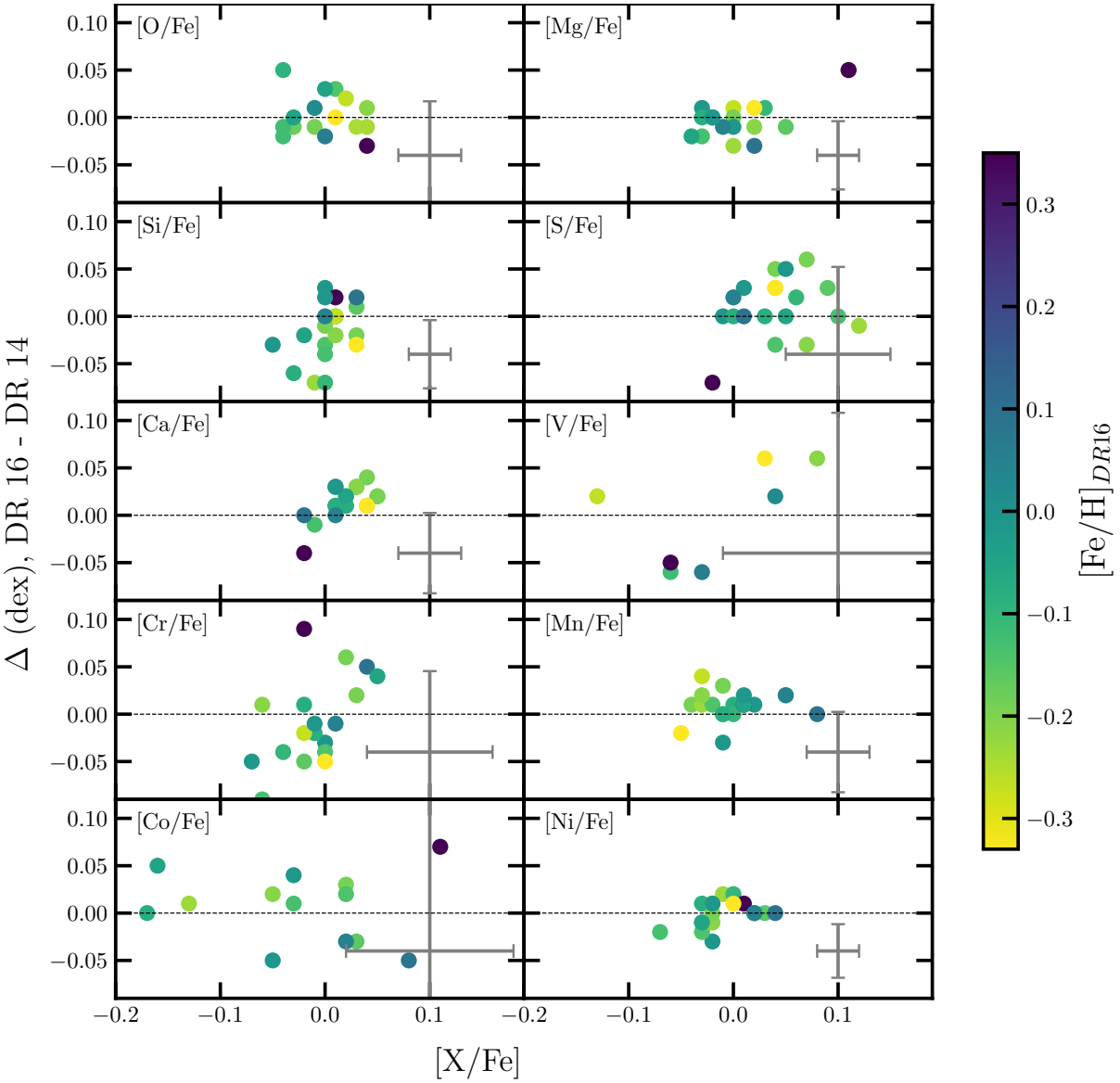

Figure 3.4: Similar to Figure 3.3 but for other elements. Characteristic error bars are shown. Datapoints are colored by their [Fe/H] as reported in APOGEE DR16

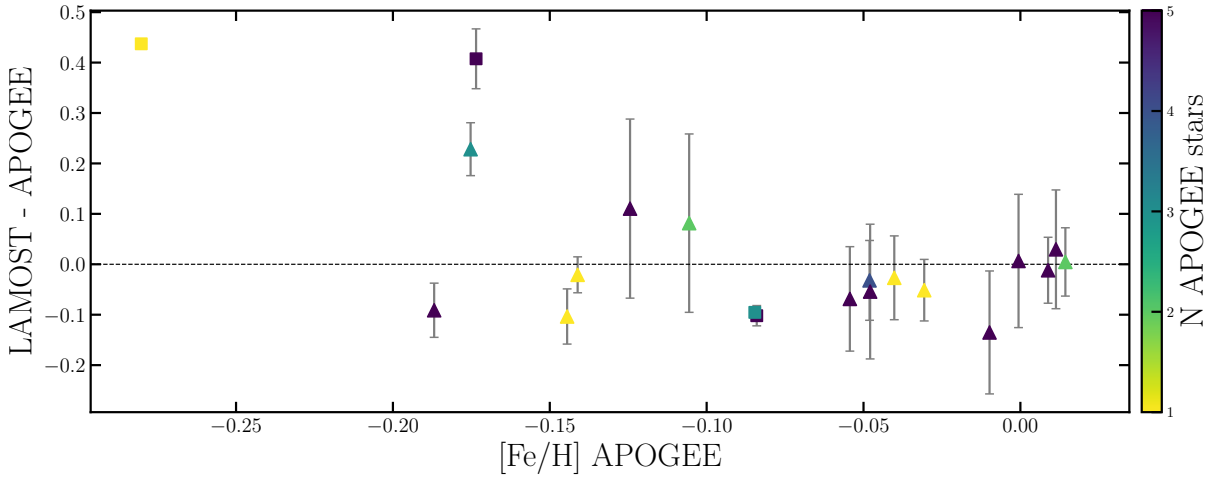

Figure 3.5: The difference between the metallicities in the LAMOST (from Zhang et al. 2019) and APOGEE surveys for open clusters in common. The color bar indicates the number of APOGEE stars in the cluster (saturating at 5). The square symbols denote clusters with a single star in Zhang et al. (2019).

3.3.2.2 Open Clusters Observed by the LAMOST Survey

Zhang et al. (2019) published mean abundances for open clusters using results from the LAMOST survey (Luo et al. 2015). Our sample includes 22 open clusters in common with Zhang et al. (2019) and we find a median offset in [Fe/H] (in the sense LAMOST - APOGEE) of -0.01 dex; however we note some significant outliers. Figure 3.5 shows the difference in [Fe/H] between Zhang et al. (2019) and this work ($[Fe/H]_{LAMOST}$ - $[Fe/H]_{APOGEE}$). There is fairly good agreement near solar metallicity, but towards lower metallicities (as measured by APOGEE), there are some clusters with highly discrepant results. The three clusters with the most discrepant metallicities, $\gtrsim 0.2$ dex, are Czernik 23, ASCC 21, and NGC 2264 (in increasing order by their APOGEE [Fe/H]). The two clusters off by ~ 0.4 dex (Czernik 23 and NGC 2264) have only one star in the Zhang et al. (2019) analysis, and Czernik 23 has only one star in APOGEE as well. NGC 2264 and ASCC 21 are among the young clusters which were excluded from our high quality

sample. Removing these three most discrepant clusters, the LAMOST values are much more consistent with APOGEE.

A previous comparison of APOGEE DR14 to LAMOST found an offset in [Fe/H] of 0.06 with a scatter of 0.13 (Anguiano et al. 2018). Given the analysis in §3.3.2.1, it is not surprising that APOGEE DR16 appears to be in better agreement with LAMOST.

3.4 Measuring Galactic Trends

3.4.1 Choosing a Distance Catalog

In Chapter 2, Galactocentric distances to open clusters were calculated using the average distance for member stars from Bailer-Jones et al. (2018). However, due to the application of a geometric prior to each star individually, this may not be an optimal solution for clusters (Bailer-Jones et al. 2018). Another uniform source of distances is therefore desired.

Distances to open clusters are frequently recomputed by many groups. Some form of isochrone fitting has been used by a number of studies (e.g., von Hippel et al. 2006, Kharchenko et al. 2013), however, only Kharchenko et al. (2013, MWSC) have produced a catalog using a uniform isochrone fitting method to measure distances for a very large (over 1000) set of open clusters. Recently, the *Gaia* survey has made it possible to create large catalogs of cluster distances based on parallax (e.g., Cantat-Gaudin et al. 2018). Of the two large catalogs, the MWSC catalog covers significantly more of our sample, but still, two clusters in our high quality sample (BH 211 and Teutsch 12) are not included.

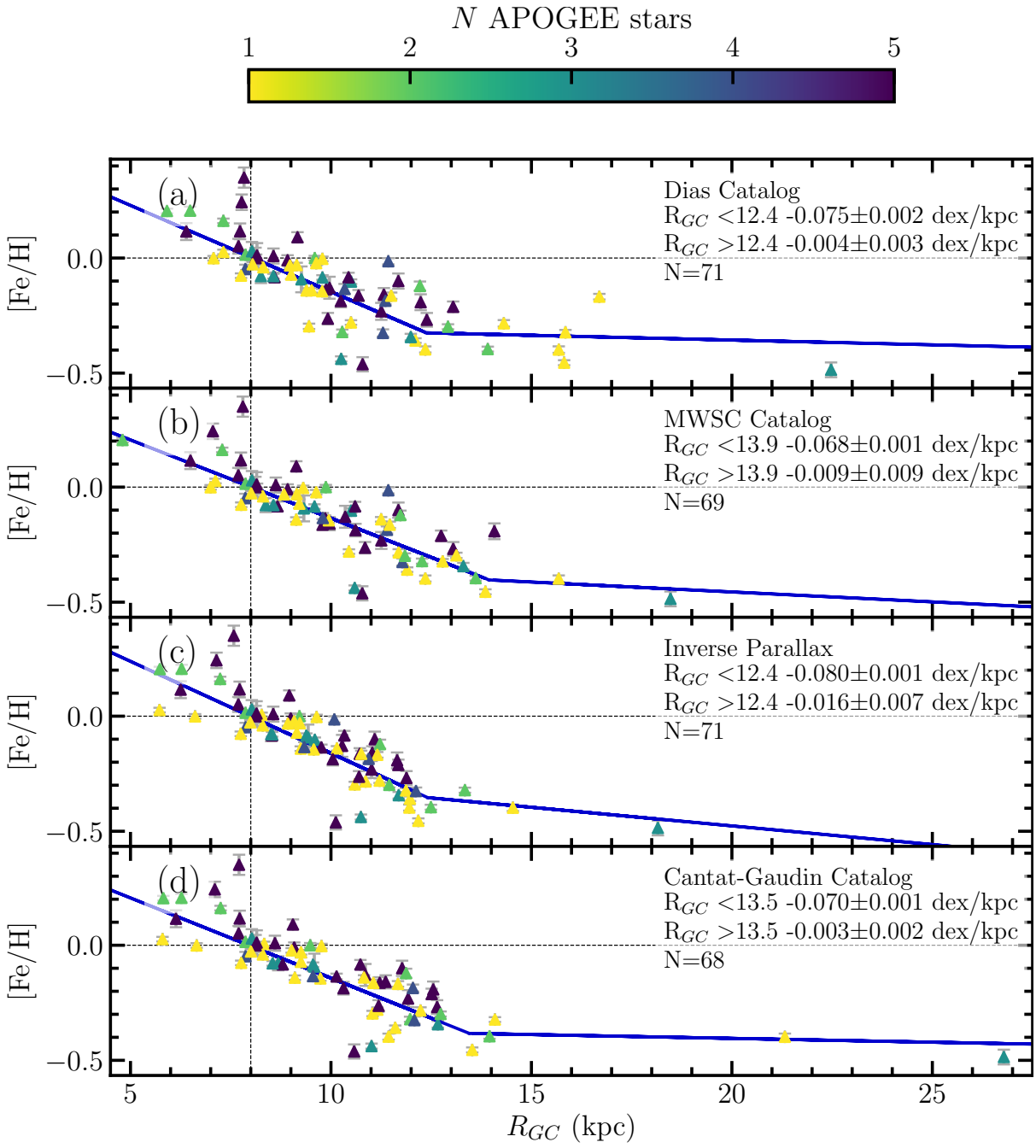

Figure 3.6: [Fe/H] vs R_{GC} trends measured using different distance determinations. This is similar to an analysis performed in 2, but we have added measurements from Cantat-Gaudin et al. (2018) where available. The colorbar shows the number of APOGEE stars per cluster, saturating at 5.

For these clusters, we rely on stellar parallaxes from *Gaia* DR2. Since the MWSC catalog does not include distance uncertainties, we assume an uncertainty of 10% of the distance.

For completeness, and to highlight the significant influence that choosing a particular distance catalog can have on the measured gradient, the basic analysis of §3.5 is repeated using three other distance catalogs (the catalogs of Dias et al. (2002) and Cantat-Gaudin et al. (2018), as well as inverse parallax as discussed in Chapter 2). These fits are shown in Figure 3.6. The difference in the measured gradients is much less severe than in Chapter 2 (where it was ∼40%), but it is still significant, potentially as large as ∼15%.

3.4.2 Fitting Galactic Abundance Gradients

It has become common in the literature, when measuring Galactic metallicity gradients, to divide the sample somewhere between $R_{GC} \approx 10$ kpc and $R_{GC} \approx 13$ kpc and fit two separate lines to the data (e.g., Twarog et al. 1997, Sestito et al. 2008, Friel et al. 2010, Jacobson et al. 2011, Carrera & Pancino 2011, Yong et al. 2012, Frinchaboy et al. 2013, Reddy et al. 2016, Magrini et al. 2017), with a much shallower trend in the outer galaxy than in the inner galaxy. Since the OCCAM sample includes open clusters as far away as $R_{GC} \approx 19$ kpc, we can investigate if the Galactic metallicity gradient becomes significantly shallower at a given R_{GC}.

In this study, we fit two separate lines to the data, and impose the additional constraint that both must meet at some "knee", although the location of the knee is allowed to vary. Using the standard notation of m as the slope of a line, b as the y-intercept, and letting k be the x-coordinate of the knee, the equation describing the fit line is then:

$$y = \begin{cases} m_1 \cdot x + b_1 & x \leq k \\ \\ m_2 \cdot (x - k) + (m_1 \cdot k + b_1) & x > k \end{cases} \tag{3.1}$$

We estimate the values of m_1, b_1, m_2, and k using maximum likelihood estimation. Uncertainties in each parameter are estimated using the *emcee* package (Foreman-Mackey et al. 2013). For trends which do not appear to have multiple components (e.g., [α/Fe] vs R_{GC} trends), we perform a maximum likelihood fit and *emcee* error estimation for a single line.

3.5 The Galactic Metallicity Gradient

Fitting to the overall [Fe/H] versus R_{GC} gradient using open clusters as probes is common in many Galactic studies (see e.g., Table 2.3). We fit the overall [Fe/H] vs R_{GC} trend using our high quality sample of 71 open clusters, with a 2 line function fit (Figure 3.7). We find an inner ($R_{GC} < 13.9$ kpc) gradient of -0.068 ± 0.004 dex/kpc and an outer ($R_{GC} > 13.9$ kpc) gradient of -0.009 ± 0.011 dex/kpc. The "corner plot" showing correlations between the fit parameters is shown in Figure 3.8

A consensus on the apparent location of the "knee" has nearly been reached in the literature, with values converging around $R_{GC} \approx 12$ kpc. However, this location does not appear to have been rigorously tested ; that is, the position of the "knee" has never been included as a free parameter in the fit. We find the location of the break in the Galactic [Fe/H] vs R_{GC} trend to be at $R_{GC} = 13.9$ kpc. To our knowledge this is the first study to fit the "knee" as a free parameter. However, as shown in Figure 3.6, this

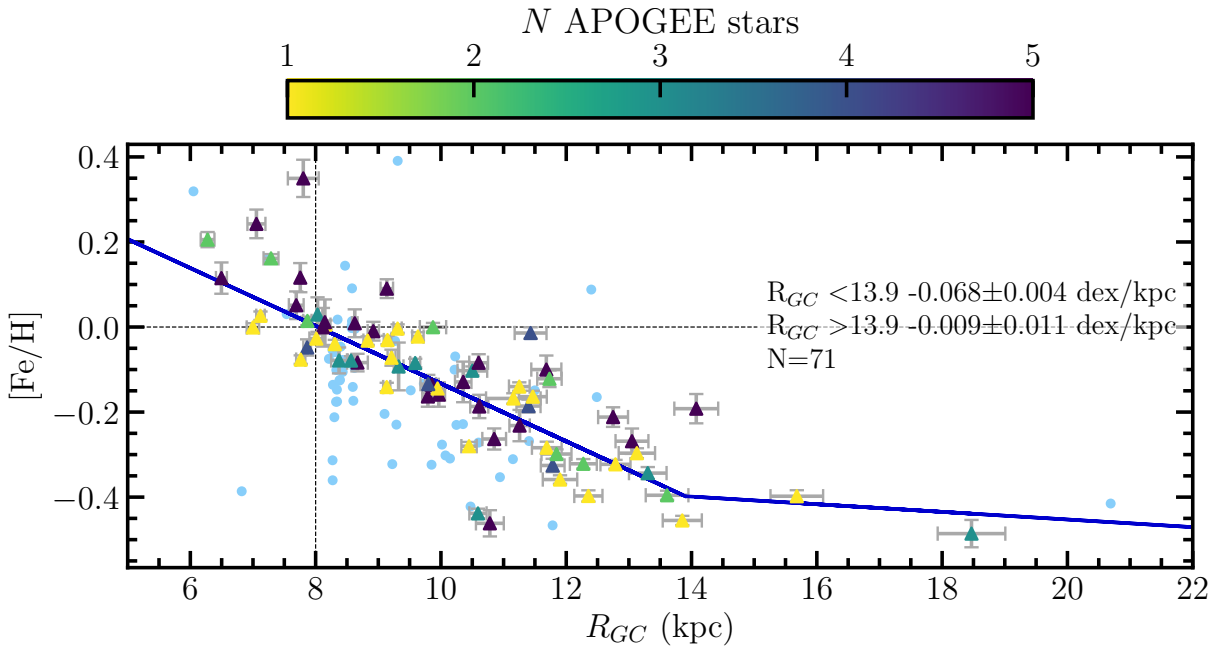

Figure 3.7: The full high quality sample Galactic [Fe/H] versus R_{GC} trend, with a 2-line fit (described by Eq. 3.1). Clusters flagged with quality "0" are shown as light blue circles. The color bar indicates the number of member stars per cluster, saturating at 5.

is dependent on the distance catalog adopted, and we recognize the poor coverage of our sample in the region $R_{GC} > 14$ kpc and the effect this may have on the determination of this parameter. Additional open clusters in this R_{GC} range have been targeted as part of APOGEE 2 and should be observed soon.

If we consider only the 19 open clusters studied in Chapter 2 and fit a single line as in that previous study, we find a gradient of -0.047 ± 0.005 dex/kpc if we include NGC 6791 and -0.041 ± 0.005 dex/kpc if we do not include NGC 6791. OCCAM II found a gradient of -0.044 ± 0.003 dex/kpc using distances from the MWSC catalog and excluding NGC 6791. We emphasize that although we find a global offset of 0.05 dex in [Fe/H] between DR14 and DR16, this is not expected to have an effect on the slope of the [Fe/H] versus R_{GC} trend as the offset should be roughly similar at any given [Fe/H]. Given the comparison between gradients derived from DR14 and DR16 results,

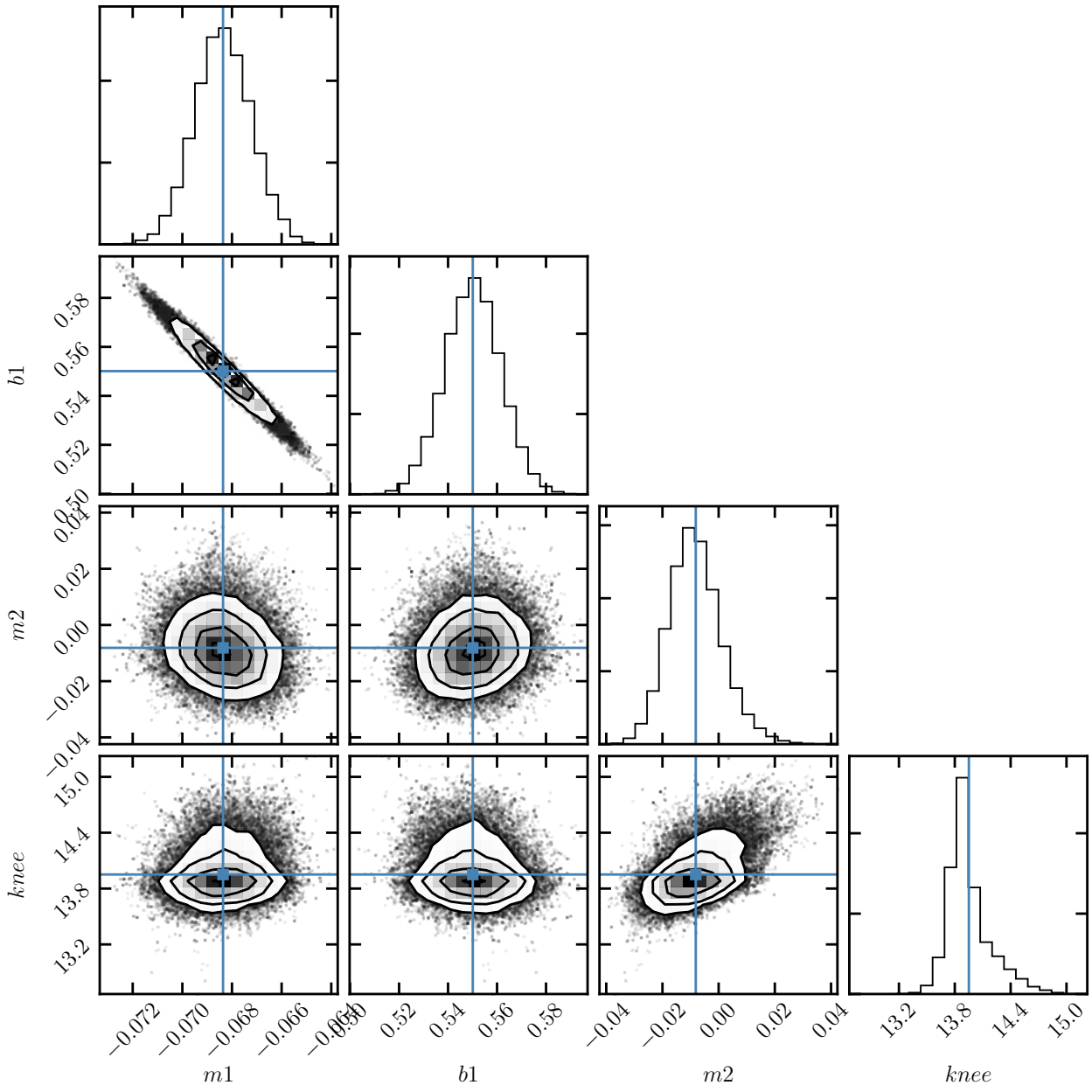

Figure 3.8: The "corner plot" showing correlations between the 4 free parameters of the 2-line abundance gradient fit shown in Figure 3.7

this appears to be the case. Table 2.3 summarized recent measurements of the Galactic metallicity gradient from the literature in the distance range considered of $6 \lesssim R_{GC} \lesssim 14$ kpc, and revealed a range of gradients between -0.052 dex/kpc to -0.085 dex/kpc. The result in this study of -0.068 dex/kpc sits neatly in the middle of this range.

We can compare in more detail to the recent results from Carrera et al. (2019), which also used APOGEE data (from DR14). The authors chose to split their sample at $R_{GC} = 11$ kpc, and find an inner gradient of -0.077 ± 0.007 dex/kpc. This is nearly in agreement with our result. We note the authors used distances from Cantat-Gaudin et al. (2018); in Figure 3.6d we measure the metallacity gradient using the same distances and find a slope of -0.070 ± 0.001 dex/kpc, in good agreement with their result.

3.6 Galactic Trends for Other Elements

3.6.1 Galactic Trends for α-Elements

Figure 3.9 shows Galactic trends versus Fe for six α-elements (O, Mg, S, Si, Ca, and Ti). Since we find a break in the [Fe/H] vs R_{GC} trend at $R_{GC} \approx 14$ kpc, we limit the sample to $R_{GC} < 14$ kpc and measure trends for the inner clusters. For all α elements studied here, except for silicon and titanium, there is a statistically significant slight positive trend from the inner galaxy to the outer galaxy and the gradients in [α/Fe] are consistent overall. However, for silicon and titanium we find a flat gradient. We note there is significant scatter for [S/Fe], and very little scatter for [Ca/Fe].

Our results are consistent with Yong et al. (2012) who measured mild positive gradients for [O/Fe], [Si/Fe], and [Ca/Fe], of the order of 0.01 dex kpc^{-1}, but a flat trend for [Mg/Fe], although the uncertainties on all four trends are nearly as large as their measured gradients. Casamiquela et al. (2019) report slight positive gradients for [Si/Fe] (0.022 ± 0.007) and [Mg/Fe] (0.011 ± 0.01) in their uniform sample of open clusters in the range $6 \leq R_{GC} \leq 11$ kpc, although both slopes are much shallower when they include more clusters from the literature. Carrera & Pancino (2011) and Reddy et al. (2016) report [α/Fe] vs R_{GC} gradients of 0.004 ± 0.001 dex kpc^{-1} and 0.014 ± 0.005 dex kpc^{-1}, respectively. Our results are therefore in good agreement with the literature, except perhaps for Si which appears to be almost completely flat in our case.

Recent work using APOGEE data showed a possible temperature effect for silicon abundances (Zasowski et al. 2019): cooler stars show lower abundances than warmer ones. The stars in more distant clusters tend to be cooler since only brighter, more evolved stars are detectable farther away. Thus the flat [Si/Fe] trend may partly reflect this effect in APOGEE data.

3.6.2 Galactic Trends for Iron-Peak Elements

APOGEE DR16 reports abundances for six elements that are classified as "iron-peak" elements: vanadium, chromium, manganese, cobalt, nickel, and copper. Figure 3.10 shows Galactic abundance trends for each of these elements. The [Ni/Fe] vs R_{GC} trend is completely flat; the abundances stay very near solar with small scatter for the Galactic radii explored. Statistically significant slightly positive trends are measured for [V/Fe],

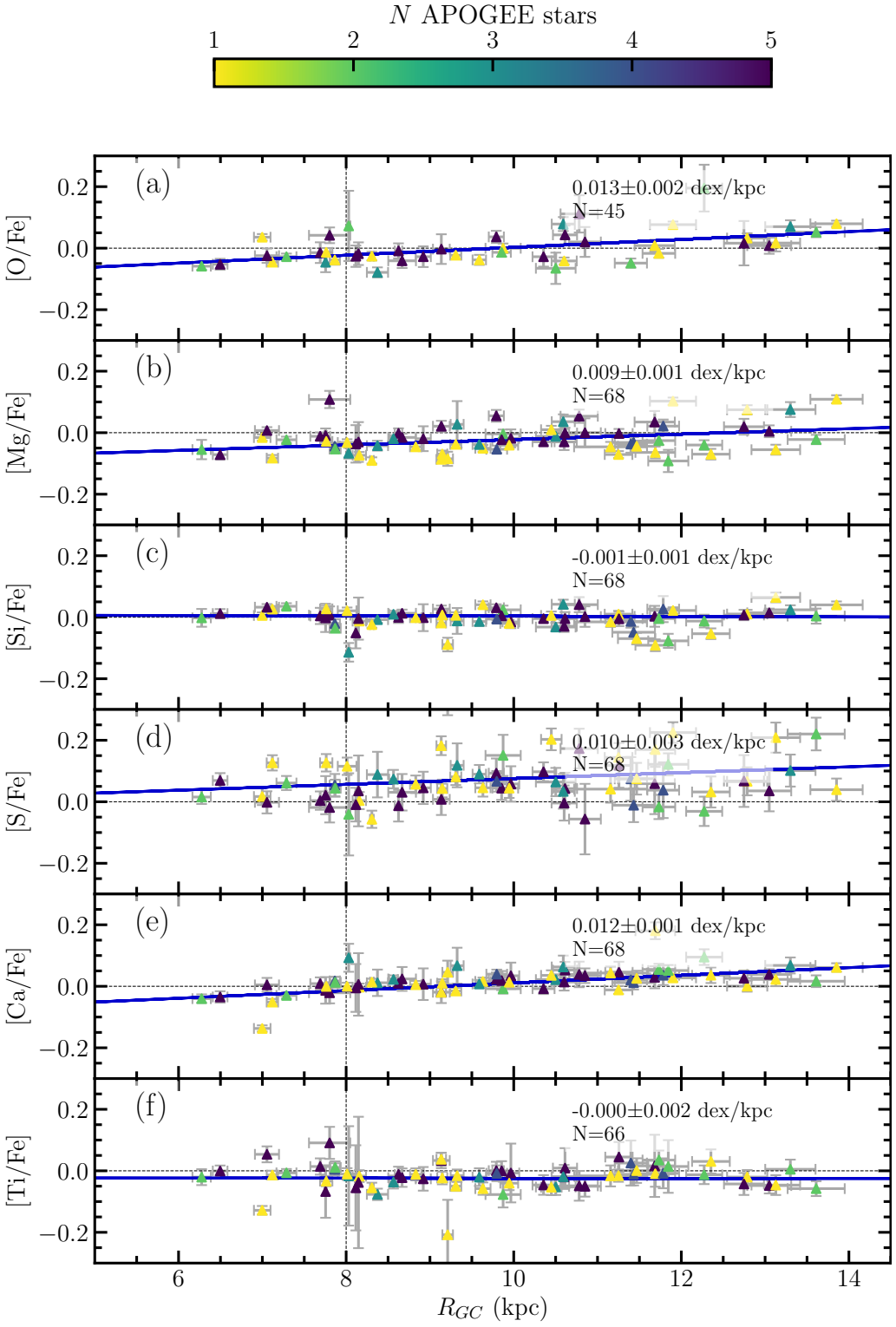

Figure 3.9: The [X/Fe] vs R_{GC} trend for α elements. As before the color bar indicates number of member stars, saturating at 5.

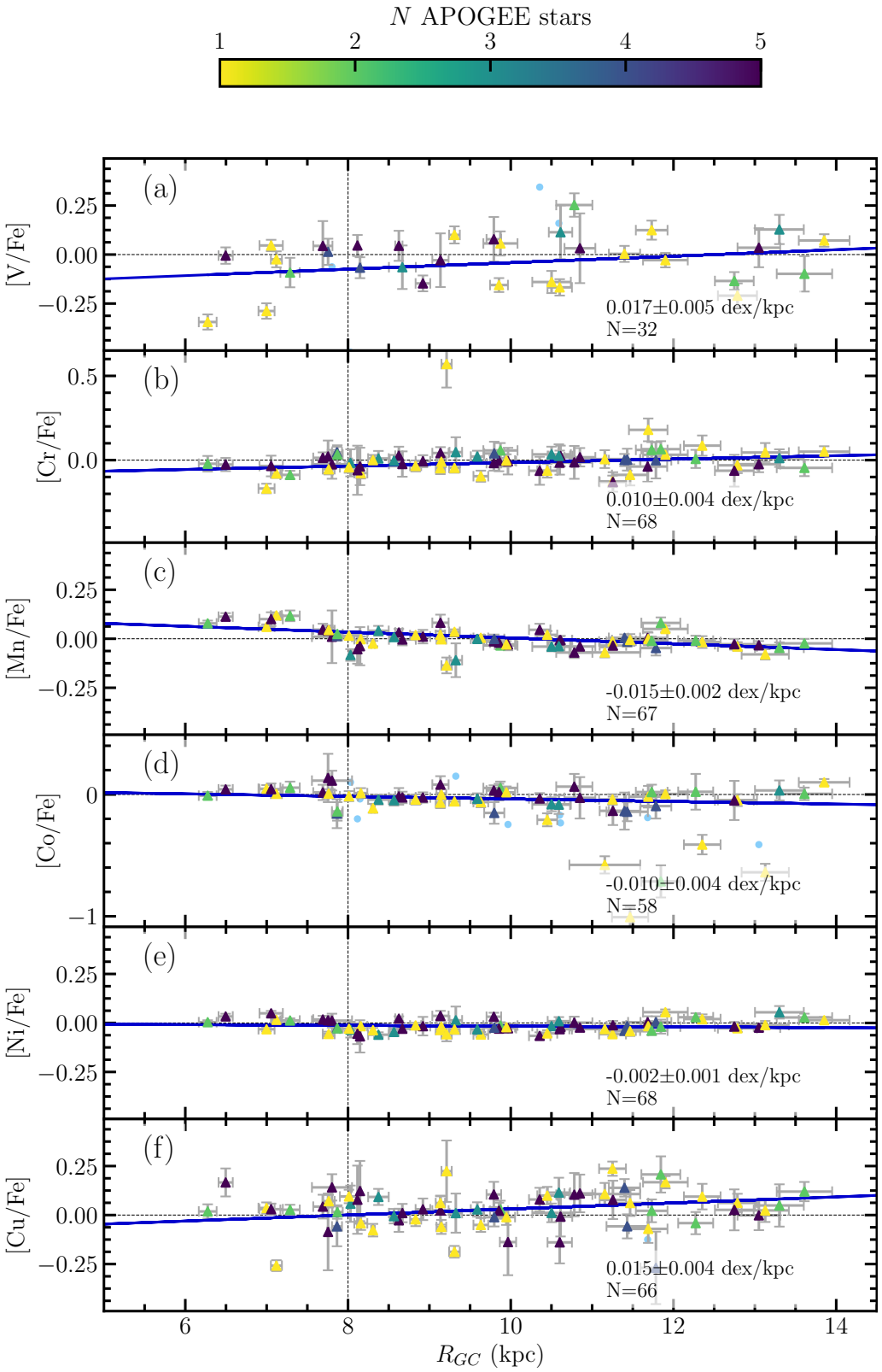

Figure 3.10: The [X/Fe] vs R_{GC} trend for iron-peak elements. Light blue circles are clusters that have an [X/Fe] abundance reported but σ [X/Fe] ≥ 0.2 dex.

[Cr/Fe], and [Cu/Fe], however there are some significant outliers for [Cr/Fe] (Czernik 18 having a single star with [Cr/Fe] = +0.57) and [Cu/Fe] (Chupina 1 having a single star with [Cu/Fe] = −0.58). There is a statistically significant, slightly negative trend measured for [Co/Fe], however a number of outliers to this trend are present between $11 \lessapprox R_{GC} \lessapprox 13$ kpc. Interestingly, Casamiquela et al. (2019) find a mildly significant *negative* trend for [V/Fe]. For [Cr/Fe] they find conflicting trends depending on which sample they use. This suggests a need for more observational data to better constrain the gradients in these elements.

For [Mn/Fe], a significant negative trend of -0.015 ± 0.002 is found. We note this is consistent with the trend first presented in Chapter 2. Yong et al. (2012) find a [Mn/Fe] gradient of -0.06 ± 0.01 in the region $R_{GC} < 13$ kpc, but this measurement is made using only ~ 8 open clusters. Since this trend is not well studied, little discussion of it exists in the literature. A relatively simple explanation may be that higher [Mn/Fe] abundances in the inner Galaxy are the result of larger contributions to chemical enrichment from type Ia supernovae (SNe Ia) (Nomoto et al. 2013), perhaps suggesting less recent star formation towards the inner galaxy or higher SNe Ia efficiency in the inner Galaxy.

3.6.3 "Odd-z" Gradients

There are three other APOGEE elements that do not readily fall into the above categories: sodium, aluminum, and potassium , often referred to as "odd-z" elements. We note that while [P/Fe] abundances are reported in DR16, there are serious doubts about the reliability of the abundances for this element (see Jönsson et al. *in press*). Figure 3.11

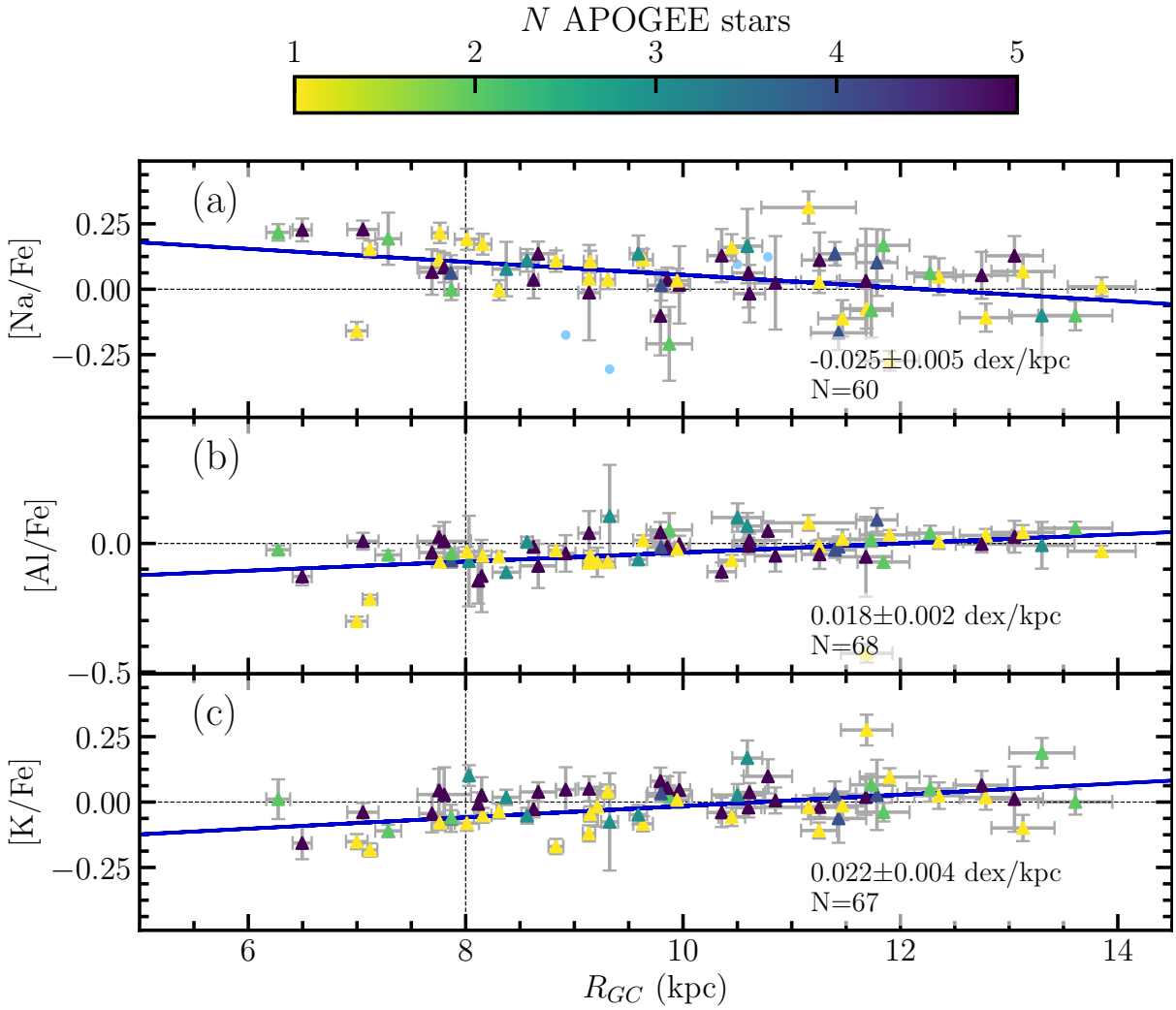

Figure 3.11: The [X/Fe] vs R_{GC} trend for the "odd-z" elements reported in APOGEE DR16. As before, the color bar indicates number of members and light blue circles are clusters with very high uncertainty in that element.

shows the Galactic trends for [Na/Fe], [Al/Fe], and [K/Fe]. [Al/Fe] and [K/Fe] show nearly identical significant positive gradients, while [Na/Fe] shows a significant negative gradient. All three trends have at least one significant outlier, but the trends nevertheless appear fairly robust. Yong et al. (2012) find a similar trend for [Al/Fe] of 0.03 ± 0.01 dex/kpc; for [Na/Fe], however, they find a flat trend with significant scatter.

3.7 The Evolution of Galactic Abundance Gradients

Minchev et al. (2019) discuss the effect that sample selection can have on measured abundance gradients, in particular the bias introduced by most samples containing a majority of young clusters. To more accurately compare to previous work, and provide more meaningful comparisons for galactic evolution models, we compare mono-age samples in this section.

3.7.1 Iron

Our sample is large enough that it can be split into four age bins, which we divide at 400 Myr, 800 Myr, and 2 Gyr, with all bins being reasonably well populated. Figure 3.12 shows the [Fe/H] versus R_{GC} trend for clusters separated in age bins. We use ages from the MWSC catalog because they are derived in a uniform fashion, and should certainly be reliable enough to place clusters in the coarse bins we have chosen.

The evolution of the [Fe/H] vs R_{GC} trend has been studied extensively in the literature (e.g. Carraro et al. 1998, Friel et al. 2002, Jacobson et al. 2011, Carrera & Pancino 2011, Yong et al. 2012). A summary of results from the literature is provided in Figure 3.13. Here we plot the measured metallicity gradient for clusters in a given age range vs the middle of that age range (for example the middles of our age bins are 0.2, 0.6, 1.4, 4 Gyr). It is important to note that the majority of clusters from all four studies in Figure 3.13 fall in the range $R_{GC} < 14$ kpc, with the exception of a few clusters from Carraro et al. (1998). Figure 3.13 shows a consistent trend of steeper metallicity gradients for older populations. There is one point in disagreement with this trend: the oldest clusters

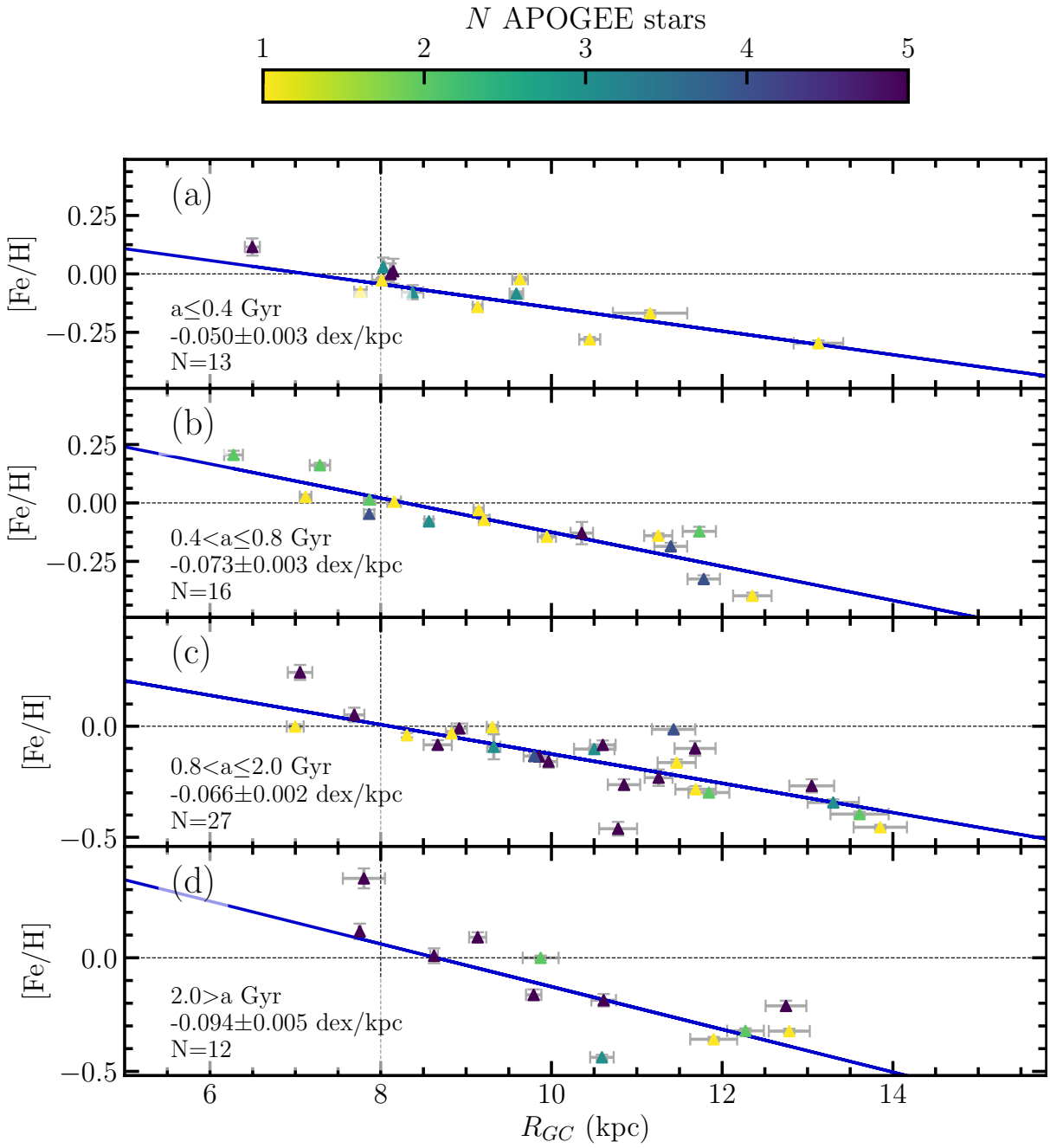

Figure 3.12: The Galactic [Fe/H] vs R_{GC} trend in 4 age bins, showing the general decrease in steepness over time.

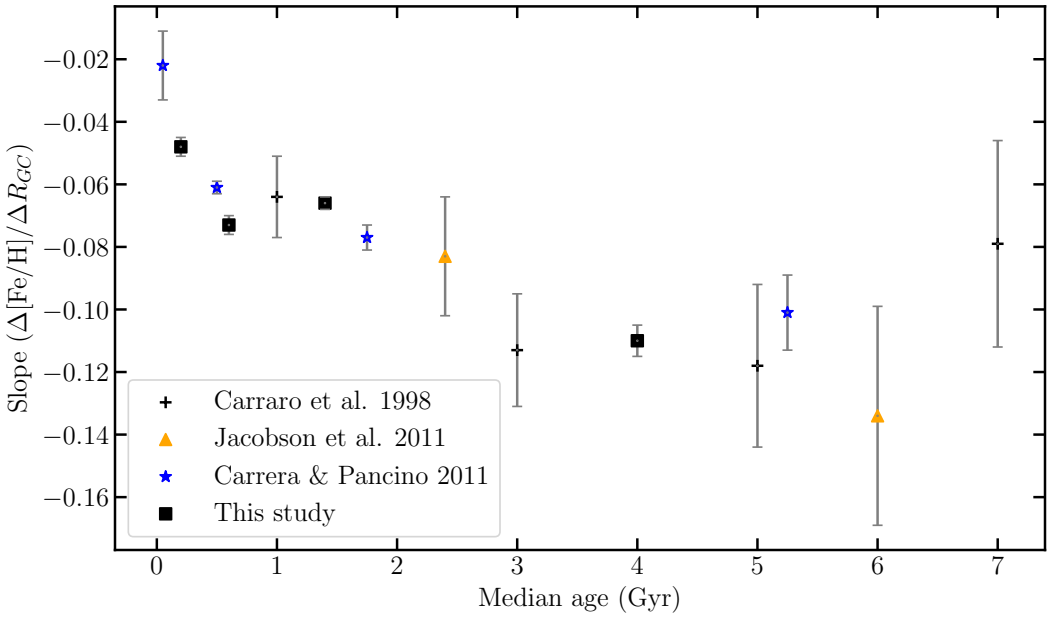

Figure 3.13: A summary of Galactic metallicity gradients measured in mono-age populations from the literature.

from Carraro et al. (1998) appear to reverse this trend. This may be due to the inclusion of some clusters near $R_{GC} \approx 15$ in their oldest bin. If we consider the large uncertainties on the two oldest measurements, it is possible the trend levels out after 4 Gyr.

It should be mentioned that the trend found here is opposite that seen for field stars (e.g., Anders et al. 2017), where the oldest populations show a shallower gradient. Radial migration is expected to cause this flattening of the metallicity gradient on a long enough time scale (e.g., Minchev et al. 2018). To explain the absence of this phenomenon in open clusters Anders et al. (2017) suggest that clusters that do not migrate or clusters that migrate towards the inner Galaxy preferentially break up.

In Figure 3.14, we show our sample sample plotted with the pure chemical evolution model of Chiappini (2009) and the chemo-dynamical simulation of Minchev et al. (2013;

2014, MCM), divided in the same age bins as Figure 3.12. There is good agreement between the models and our sample in the younger three bins. In the oldest bin the effects of radial migration are clearly seen in the MCM points. Also in the oldest bin, there is a noticeable lack of clusters towards the inner galaxy, and a clear steepening of the gradient, which could be due to migration of inner old clusters towards outer regions. This is consistent with the suggestion from Anders et al. (2017) that clusters migrating inward preferentially break up. Elsewhere, the clusters are roughly consistent with the MCM model.

3.7.2 Other Elements

Age trends in elements other than iron also provide insight into the chemical evolution of the Galaxy. The top panel of Figure 3.15 provides a summary of abundance gradients for each element presented previously as a function of cluster age, measured in the same four age bins as for iron (Figure 3.12). The top panel of Figure 3.15 shows an overall similar behavior for all elements: the gradient for the oldest population (open clusters older than ~ 2 Gyr) is the steepest; this is reminiscent of what was observed for [Fe/H]. For [Na/H], [Ti/H], [Cr/H], and [Mn/H] we cannot distinguish between the gradients measured for the intermediate-age and young populations. For [O/H], [Mg/H], [Si/H], [S/H], [K/H], [V/H], [Co/H], [Fe/H], and [Ni/H] the youngest population shows a distinctly flatter gradient, but the two intermediate-age populations are indistinguishable within the uncertainties. Relatively flat α-element abundance gradients have also been found for young B stars (e.g., Daflon & Cunha 2004) and H II regions (e.g., Esteban et al. 2015). We note that for

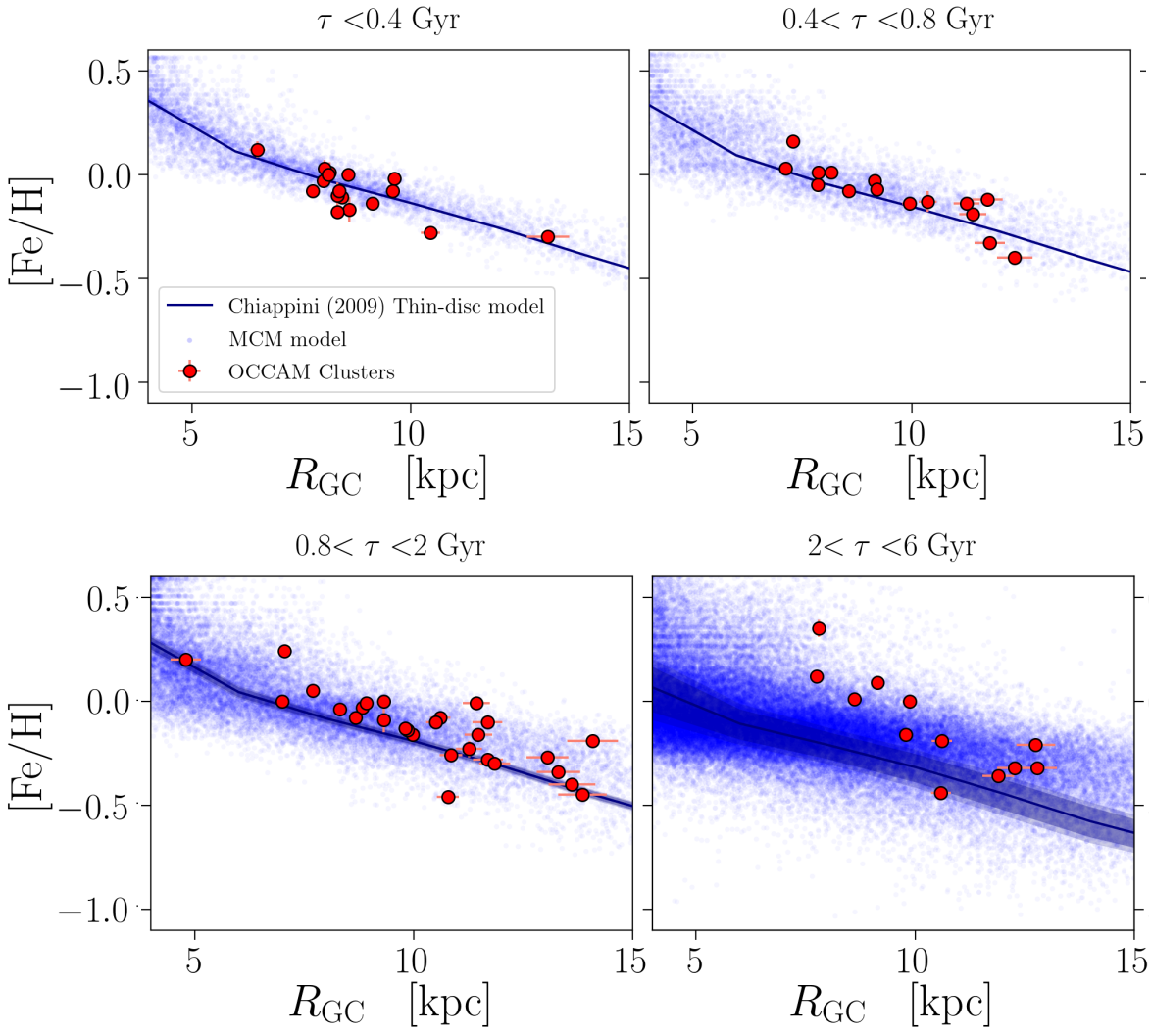

Figure 3.14: OCCAM IV clusters (red) plotted with the pure chemical evolution model of Chiappini (2009) (blue line) and the MCM chemo-dynamical simulation (Minchev et al. 2013; 2014), seperated into the age bins used previously.

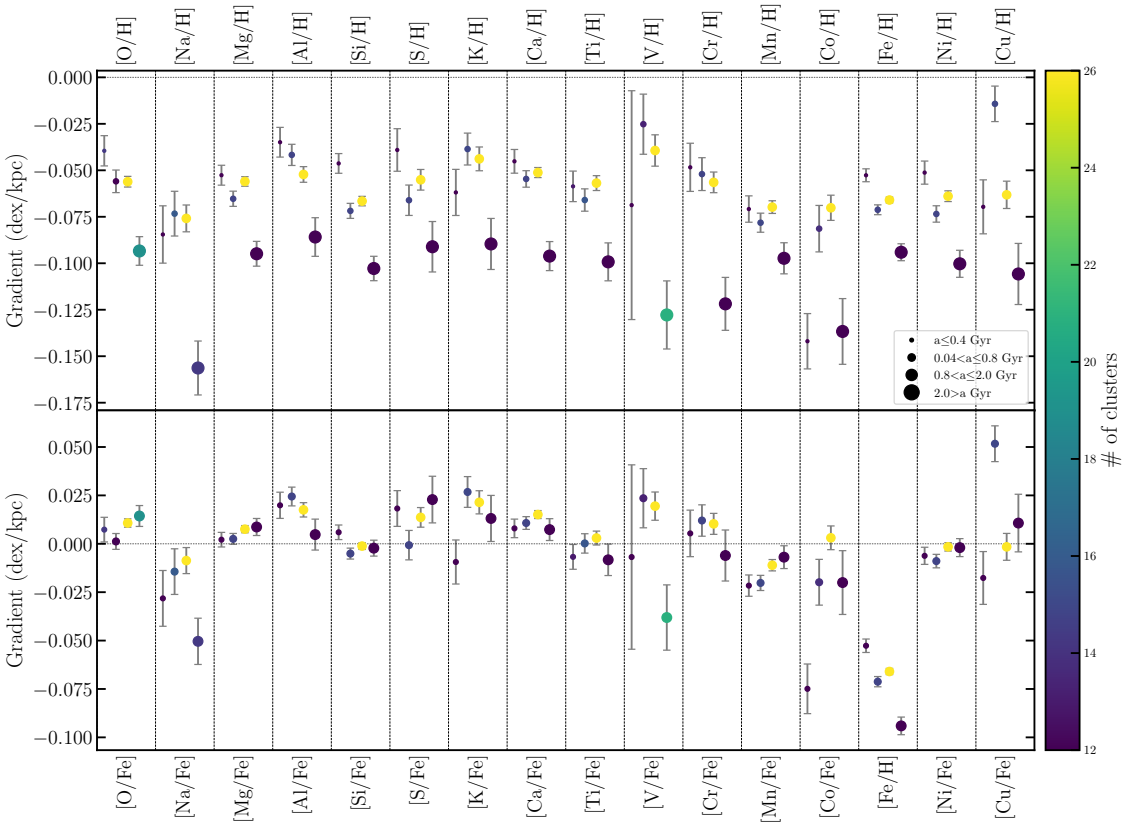

Figure 3.15: Gradients measured in four age bins as for Figure 3.12 are plotted for each element. The points increase in size from youngest to oldest; the color indicates number of clusters used to measure each gradient.

[V/H] the youngest bin is populated with only five clusters, while for [Co/H] the gradient in the youngest population is heavily influenced by a single very [Co/H]-poor cluster.

3.7.3 The Evolution of [X/Fe] Gradients

To understand the differences in the evolution of elemental abundances better, it is also informative to study the evolution of [X/Fe] gradients over time. The bottom panel of figure 3.15 is similar to the top panel but now we show the evolution of [X/Fe] trends. A variety of trends can be seen; some elements show a stable trend over time (e.g., [Ni/Fe],

[Si/Fe]), some show an increasingly positive trend (e.g., [Al/Fe]), and [Mn/Fe] shows an increasingly negative trend. All of these trends are worth discussing and we do so below. We do not consider [V/Fe], [Cr/Fe], [Co/Fe], or [Cu/Fe] in detail, either because the uncertainties are larger than the trends or because one or more age bins are poorly populated for that element. We do not discuss [Ni/Fe] further because, as stated in §3.6.2, Ni appears to track Fe closely.

The results in Figure 3.15 show no clear evidence of evolution in the [α/Fe] gradients within the time spanned by this open cluster sample. It could be argued that there are mild trends with age for the [O/Fe], [Mg/Fe], and [Ca/Fe] gradients, but the changes between different aged populations are on the order of the uncertainties. For [Si/Fe], [S/Fe], and [Ti/Fe] there are more variations, but also larger uncertainties and it is more appropriate to consider the gradients as roughly constant for different aged populations. It was shown in Figure 3.9 that nearly all of the [α/Fe] abundances exhibit mildly increasing radial trends and Figure 3.15 indicates that such trends appear to be fairly stable within the time spanned by our cluster sample. The flattening of the abundance gradients in recent times suggests more recent chemical enrichment in the outer Galaxy, but, taken together with the stability of the increasing [α/Fe] gradient, we might deduce that the enrichment in the outer Galaxy had a more significant contribution from core-collapse supernovae. This is consistent with the conclusions from §3.6.2 and the discussion below, that supernovae Ia dominated recent enrichment in the inner Galaxy.

For [Na/Fe] and [Al/Fe], the gradients for the oldest clusters are clearly set apart, even considering the sizeable uncertainty. For [Al/Fe], in particular, there appears to be a clear trend where we see the younger populations showing an increasingly positive slope.

Significantly larger Na and Al yields are expected from core collapse supernovae than SNe Ia (Nomoto et al. 2013), so a flattening of the [Na/Fe] gradient and an increasingly positive [Al/Fe] gradient are both consistent with either more recent star formation in the outer Galaxy than the inner Galaxy or higher SNe Ia efficiency in the inner Galaxy. This is also consistent with the explanation for the [Mn/Fe] gradient in §3.6.2.

Figure 3.15 shows that the [Mn/Fe] gradient becomes more negative for younger cluster populations. Yamaguchi et al. (2015) showed that SNe Ia yields of manganese are strongly dependent on progenitor metallicity; higher metallicity progenitors will yield significantly more manganese. So as metals build up in the inner Galaxy, a higher [Mn/Fe] abundance is expected. This may explain the evolution of the [Mn/Fe] gradient in general terms.

Chapter 4

Characterizing Open Cluster Radial Migration

4.1 Deriving Birth Radius from a Model

Chen & Zhao 2020, hereafter C20 used a novel method for approximating the birth radius of an open cluster. The authors relied on the Galactic chemical evolution model derived by Minchev et al. 2018, hereafter M18. The M18 model utilizes a simple assumption that birth radius (R_{Birth}) for a star can be uniquely determined given the stars age and [Fe/H]. Using this simple assumption, they derive the Galactic metallicity gradient (Δ[Fe/H] / ΔR_{GC}) and [Fe/H] at solar radius ($R_{\odot} = 8$ kpc) as a function of look-back time. Given these distributions, one can estimate the metallicity of the Inter-Stellar Medium (ISM), from which stars and star clusters form, for a given R_{GC} and age.

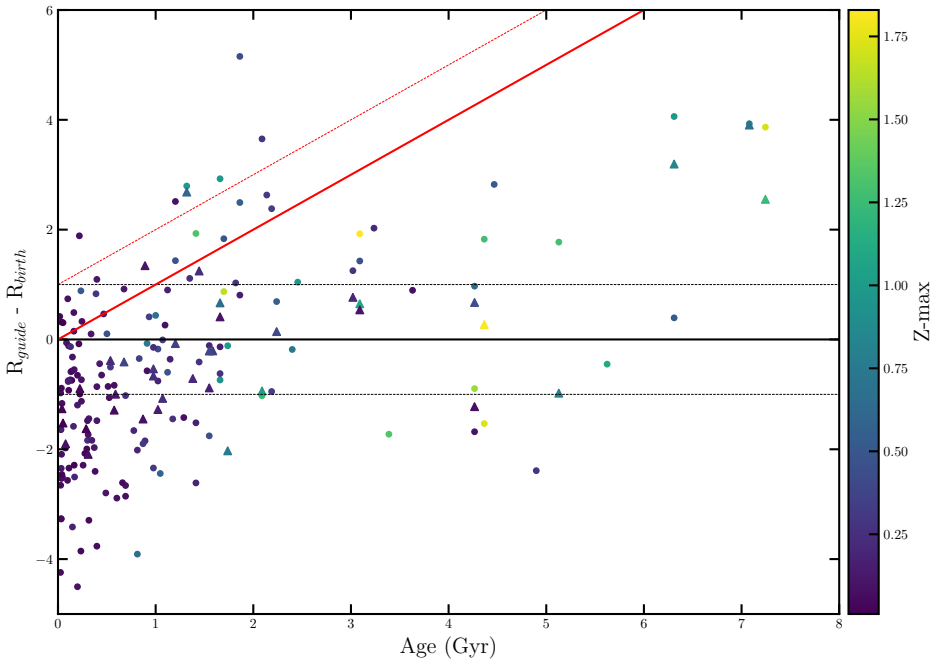

Figure 4.1: A reproduction of Figure 11 from C20, but with updated distances and ages from Cantat-Gaudin et al. (2020). We also color the points by their computed Z-max; the maximum distance a cluster will move away from the Galactic plane during its orbit.

C20 used the M18 model to estimate R_{Birth} for a large sample of open clusters, using [Fe/H] and age from Netopil et al. (2016). They further determine guiding radius (R_{guide}; defined to be the radius of a circular orbit having the same angular momentum) for each cluster in their sample using kinematic data from Soubiran et al. (2018) and the `galpy` (Bovy 2015) package to compute orbital parameters. In Figure 11 of C20, they show $R_{guide} - R_{birth}$ vs age for this sample, presenting a view of migration rate for open clusters. Figure 4.1 is a recreation of this figure, but using improved distances and ages from Cantat-Gaudin et al. (2020). The black line indicates no migration, while the solid red line shows a migration rate of 1 kpc/Gyr. The dashed lines indicate an uncertainty of 1 kpc, which C20 estimate as the uncertainty in birth radius using their technique.

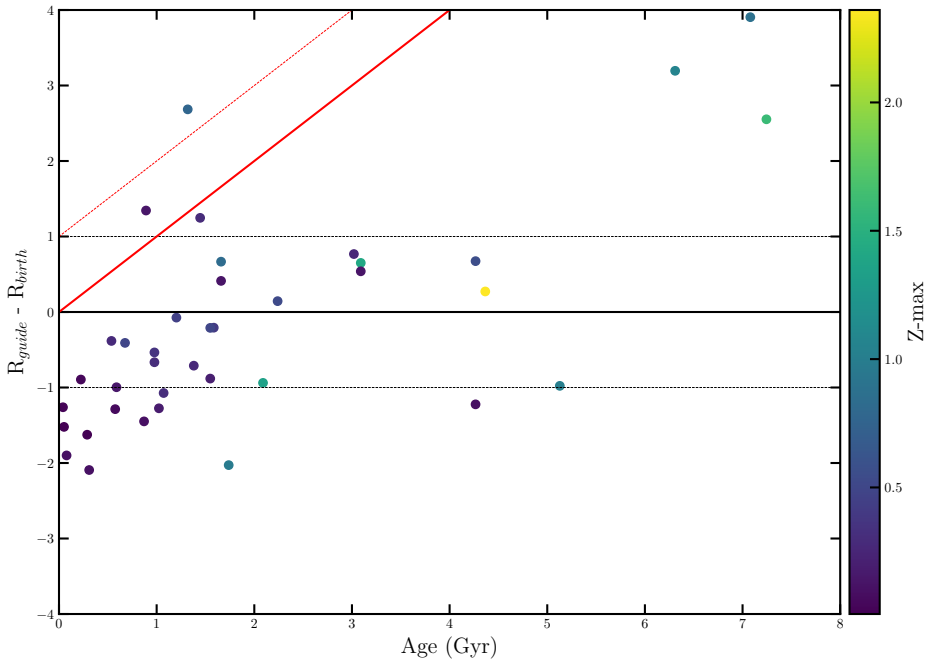

Figure 4.2: Similar to Figure 4.1 but using the OCCAM high-quality sample.

Neglecting the youngest clusters, their sample shows that more clusters tend to migrate outwards, as expected from §3.7.1 and Anders et al. (2017). The authors further make the point that a few clusters seem to move much faster than the migration rate of 1 kpc/Gyr presented in Quillen et al. (2018), seen above the 1 kpc/Gyr line. Figure 4.1 is colored by Z–max (the maximum distance a cluster will move away from the Galactic plane during it's orbit), revealing a general trend: clusters that migrate further out generally move farther from the plane during their orbits. This is consistent with the expectation that clusters migrating outward will transfer energy to the vertical direction (Sellwood 2014).

The authors are unfortunately somewhat dismissive of the large clump of young (< 500 Myr) clusters with very high negative migration distances. They cite the theoretical

work of Fujii & Baba (2012), who showed that some particles in an N-body simulation could migrate as much as a few kpc in less than 1 Gyr, in certain circumstances. If significant inward migration is common though, we would not expect abundance gradients for young clusters and cepheids ($\lessapprox$ 100 Myr) to agree with abundance gradients for star forming regions ($\lessapprox$ 5 Myr). Observations however show that, at least in the solar neighborhood ($6 \leq R_{GC} \leq 9$ kpc), the abundance gradients for young clusters and star forming regions are nearly identical (Spina et al. 2017). The cepheids, while noisy, are also in rough agreement (Genovali et al. 2014).

The migration of the young clusters in the C20 can be characterized briefly. There are 67 clusters younger than 400 Myr and they have migrated, on average, -1.32 kpc, but the standard deviation of that mean is 1.36 kpc. This very large spread in migration distance is clearly seen in Figure 4.1. There are a further 16 clusters falling in the range $400 < age \leq 800$ Myr, and they have migrated an average of -1.21 kpc, again with a large standard deviation of 1.20 kpc. If these migration rates are to be believed, drastic smearing effects to abundance gradients measured using clusters in these age bins are expected, as some clusters migrate 3 kpc inward and others don't move at all. The observational evidence shows exactly the opposite. Indeed, we have shown in Figure 3.12 that the abundance gradients for clusters in these bins are well defined and close to a single trend. Figure 3.12 also shows that the trend is noisier for older clusters, which we expect to have experienced more migration. Thus it appears there is no strong evidence that the C20 predictions for migration in these young clusters are accurate.

4.2 Implications from the Model

The general trends seen in Figure 4.1 may still be valid for older (age $\gtrsim 1-2$ Gyr). As stated previously, the general result that more clusters migrate outwards, and few clusters migrate inwards (neglecting the very young clusters), is supported. We have repeated the C20 analysis for the OCCAM high-quality sample, using APOGEE metallicities, with age and distance also taken from Cantat-Gaudin et al. (2020), shown in Figure 4.2. With the exception of the young clusters, the results for the APOGEE sample are consistent with the findings of C20. A majority of clusters are between the dashed black lines, meaning they must be considered consistent with little or no migration. A single cluster (IC 166) falls above the red dashed line, and only barely.

Table 4.1: Comparison of Netopil et al. (2016) and APOGEE migration results

Name	Age (Gyr)	R_{guide} (kpc)	Netopil R_{birth} (kpc)	Netopil [Fe/H] (dex)	APOGEE R_{birth} (kpc)	APOGEE [Fe/H] (dex)
Berkeley 17	7.2	10.51	6.81	-0.06	7.95	-0.16
IC 166	1.3	12.93	11.20	-0.17	10.25	-0.10
NGC 188	7.1	9.12	4.99	0.11	5.22	0.09
NGC 6791	6.3	5.78	1.77	0.42	2.58	0.35

Interestingly, the 3 old clusters with large migration distances in the APOGEE sample are the same 3 old clusters with large migration distances in the Netopil et al. (2016) sample used by C20. In Table 4.1, we directly compare results using these two different sources for metallicity for the four clusters that appear to have migrated significantly in the APOGEE sample (the three old clusters and IC 166). Table 4.1 shows both the metallicity of each cluster and the resulting birth radius from the C20 model, for the two different samples. R_{birth} is within the 1 kpc uncertainty for the C20 model for all clusters except Berkeley 17, where it is not far off. It appears then the APOGEE results are in good agreement with the C20 results; we find similar general trends for cluster migration (neglecting the youngest clusters).

Chapter 5

Conclusions

We describe the technique used by the OCCAM survey for targeting likely open cluster members, and another technique for determining the likelihood of their membership in a cluster. Using the determined likely cluster giant members, in Chapter 2 we present the first multi-element data from the OCCAM collaboration's exploration of the SDSS/APOGEE open cluster data presented in DR14.

We present abundance measurements of 11 elements for 19 open clusters, and find no systematic offsets from previous work in the literature. Using distance measurements from Bailer-Jones et al. (2018), we make measurements of the Galactic abundance gradient for all 11 elements.

In Chapter 2, using this smaller sample, we find an [Fe/H] gradient of -0.061 ± 0.004 dex kpc^{-1}, derived from clusters spanning $7 < R_{GC} < 13$ kpc. This is in agreement with previous studies, though we emphasize Figure 2.6, which shows the tight correlation in the uniform OCCAM sample superimposed on the disjoint literature + R16 sample.

In Chapter 2, we further measure a mild [α/Fe] gradient, including [O/Fe], [Mg/Fe], and [Si/Fe], in agreement with some previous work (e.g., Jacobson et al. 2011), and loosely in agreement with chemical evolution models (e.g., Minchev et al. 2014, Kubryk et al. 2015). We also measure a mild negative gradient for the iron peak element [Mn/Fe] and very mild negative gradient for [Ni/Fe]. Yong et al. (2012) found a much steeper negative gradient for [Mn/Fe] but using many fewer clusters.

In Chapter 3, we present an expanded sample of 128 open clusters, 71 of which we designate "high quality", using APOGEE DR16. We demonstrate that DR16 cluster abundances are in good agreement with those of other high resolution abundance studies. Using the high quality sample, we measure Galactic abundance gradients in 16 chemical elements, and we measure how those gradients change for different age samples.

We find an overall Galactic [Fe/H] vs R_{GC} gradient of -0.068 ± 0.004 dex kpc^{-1} for $R_{GC} < 13.9$ kpc, but we re-emphasize the point of Chapter 2 that this result can vary significantly depending on which catalog of distances is used. Especially considering this catalog effect, this result is consistent with the literature, though we emphasize the warning of Minchev et al. (2019) that gradients measured for a cluster sample spanning a wide age range are prone to large uncertainties, leading to a careful investigation of mono-age populations.

For the first time, we fit the knee in the Galactic abundance gradient as a free parameter at $R_{GC} = 13.9$ kpc. This is roughly consistent with the literature, though most studies place the break further inward. We recognize a need for more clusters beyond this break to more reliably constrain the fit.

We find general agreement with the literature for gradients in α elements measured using the expanded sample, as in Chapter 2. We present further evidence for the negative [Mn/Fe] vs R_{GC} trend first seen in Chapter 2. We find significant Galactic trends in vanadium, chromium, and copper, although we are unable to suggest a strong explanation for these trends. We discuss other measurements of some of these trends in Casamiquela et al. (2019), but as there results are also fairly inclusive, we find more work is needed to constrain these trends. We find very significant trends in sodium, aluminum, and potassium; so-called "odd-Z" elements. We recognize a need for further study of trends in these elements as they are not well reported in the literature.

With the warning of Minchev et al. (2019) in mind, we divide our sample into four age bins and investigate changes in 16 elements over time. We show that [X/H] abundance gradients for all 16 elements follow the same general trend, becoming more shallow over time, as has consistently been found for iron. We find general agreement with previous work studying the evolution of the [Fe/H] vs R_{GC} gradient. With this age divided sample, we are able to compare explicitly to the MCM chemical evolution model. We find good agreement with the model for younger clusters, but increasing uncertainty for the older clusters. We agree with the suggestion from Anders et al. (2017), who found similar discrepancies, that this may be due to clusters preferentially migrating outward, or inward migrating clusters being disrupted.

We further investigate age trends in [X/Fe] for 15 elements. A number of these trends seem to support a similar conclusion: either increased SNe Ia efficiency towards the inner Galaxy or less recent star formation in the inner Galaxy compared to the outer Galaxy. We also discuss the complication that SNe Ia yields for Mn are metallicity dependent

(Yamaguchi et al. 2015), which may explain the observed evolution in the [Mn/Fe] trend on its own.

In Chapter 4, we investigate a model of cluster radial migration. We find that while it is unreliable for young clusters, the predictions for older clusters are in agreement with our finding in Chapter 3, which was in agreement with Anders et al. (2017). Namely: clusters appear to be more likely to migrate away from the Galactic center, and older clusters are expected to undergo more migration on average.

Appendix A

Table 2.1: OCCAM sample from APOGEE data used for membership analysis – Full Version

Table A.1: OCCAM sample from APOGEE data used for membership analysis (Full)

Cluster name	2MASS ID	RV (km s^{-1})	[Fe/H] (dex)	μ_α (mas yr^{-1})	μ_δ (mas yr^{-1})	RV Prob	[Fe/H] Prob	PM Prob	Memb
NGC 6791	2M19200622+3753403	-5.8 ± 0.0	0.28 ± 0.01	-5.05 ± 0.04	-9.41 ± 0.04	0.00	0.00	0.00	NM
NGC 6791	2M19201118+3749482	-73.7 ± 0.0	0.17 ± 0.01	-0.47 ± 0.02	0.65 ± 0.03	0.00	0.00	0.00	NM
NGC 6791	2M19201348+3744095	-45.8 ± 0.0	-0.02 ± 0.01	-2.13 ± 0.04	-2.61 ± 0.04	0.00	0.00	0.00	NM
NGC 6791	2M19201973+3746549	-43.7 ± 3.6	0.40 ± 0.01	-0.49 ± 0.04	-2.29 ± 0.04	0.00	0.00	0.97	NM
NGC 6791	2M19202244+3751414	-58.9 ± 0.2	-0.04 ± 0.01	-3.83 ± 0.05	-7.19 ± 0.05	0.00	0.00	0.00	NM
NGC 6791	2M19202341+3749231	-7.4 ± 0.0	-0.10 ± 0.01	-3.24 ± 0.04	13.59 ± 0.04	0.00	0.00	0.00	NM
NGC 6791	2M19202354+3751229	-48.1 ± 0.1	0.15 ± 0.01	-0.43 ± 0.03	-2.37 ± 0.03	0.00	0.00	0.95	NM
NGC 6791	2M19202816+3741194	-21.5 ± 0.0	0.00 ± 0.01	-4.63 ± 0.05	-12.44 ± 0.05	0.00	0.00	0.00	NM
NGC 6791	2M19202870+3743169	-48.3 ± 0.4	0.46 ± 0.01	-0.51 ± 0.05	-2.24 ± 0.05	0.91	0.66	0.93	GM
NGC 6791	2M19203005+3750191	-47.5 ± 0.0	0.43 ± 0.01	-0.40 ± 0.03	-2.10 ± 0.03	1.00	0.99	0.83	GM
NGC 6791	2M19203092+3748450	-5.8 ± 0.0	0.23 ± 0.01	-2.11 ± 0.03	-1.71 ± 0.03	0.00	0.00	0.00	NM
NGC 6791	2M19203326+3750123	-194.5 ± 0.4	-0.89 ± 0.01	-5.68 ± 0.03	-5.32 ± 0.03	0.00	0.00	0.00	NM
NGC 6791	2M19203485+3746298	-47.1 ± 0.1	0.44 ± 0.01	-0.44 ± 0.03	-2.30 ± 0.03	0.97	0.92	1.00	GM
NGC 6791	2M19203519+3748579	-48.3 ± 0.0	0.35 ± 0.01	-0.34 ± 0.03	-2.31 ± 0.03	0.92	0.19	0.93	GM
NGC 6791	2M19203784+3745249	-48.6 ± 0.1	0.42 ± 0.01	-0.40 ± 0.04	-2.33 ± 0.04	0.85	1.00	0.98	GM
NGC 6791	2M19203934+3748048	-46.8 ± 0.0	0.40 ± 0.01	-0.46 ± 0.03	-2.23 ± 0.03	0.94	0.92	0.97	GM
NGC 6791	2M19204102+3743025	-47.9 ± 0.1	0.47 ± 0.01	-0.51 ± 0.05	-2.32 ± 0.05	0.98	0.52	0.94	GM
NGC 6791	2M19204273+3751073	-48.9 ± 0.1	0.25 ± 0.01	-0.45 ± 0.03	-2.26 ± 0.04	0.78	0.00	0.99	NM

Continued on next page

Table A.1 – Continued

Cluster name	2MASS ID	RV (km s^{-1})	[Fe/H] (dex)	μ_α (mas yr^{-1})	μ_δ (mas yr^{-1})	RV Prob	[Fe/H] Prob	PM Prob	Memb
NGC 6791	2M19204377+3749075	-33.0 ± 1.2	-0.04 ± 0.01	1.06 ± 0.04	2.23 ± 0.05	0.00	-1.00	0.00	NM
NGC 6791	2M19204485+3746215	-44.9 ± 0.1	0.38 ± 0.01	-0.48 ± 0.03	-2.38 ± 0.03	0.41	0.57	0.91	GM
NGC 6791	2M19204517+3744339	-48.4 ± 0.1	0.41 ± 0.01	-0.44 ± 0.03	-2.27 ± 0.04	0.90	0.98	1.00	GM
NGC 6791	2M19204557+3739509	-46.1 ± 0.2	0.50 ± 0.01	-0.41 ± 0.03	-2.22 ± 0.03	0.00	0.00	0.98	NM
NGC 6791	2M19204624+3749105	-46.1 ± 0.0	0.43 ± 0.01	-0.35 ± 0.04	-2.22 ± 0.05	0.77	0.94	0.94	GM
NGC 6791	2M19204635+3750228	-45.3 ± 0.0	0.37 ± 0.01	-0.36 ± 0.05	-2.36 ± 0.06	0.53	0.48	0.93	GM
NGC 6791	2M19204765+3747322	-64.9 ± 1.6	0.44 ± 0.01	-0.46 ± 0.03	-2.29 ± 0.04	0.00	0.88	0.99	NM
NGC 6791	2M19204971+3743426	-47.4 ± 0.2	0.32 ± 0.01	-0.34 ± 0.12	-2.16 ± 0.12	1.00	0.04	0.87	GM
NGC 6791	2M19205003+3747282	-59.3 ± 1.1	0.13 ± 0.01	-6.07 ± 0.05	-5.04 ± 0.06	0.00	0.00	0.00	NM
NGC 6791	2M19205038+3743335	-43.9 ± 5.6	0.37 ± 0.01	-0.42 ± 0.09	-2.26 ± 0.09	0.17	0.46	1.00	GM
NGC 6791	2M19205160+3739408	16.6 ± 0.0	-0.32 ± 0.01	-6.41 ± 0.05	-5.21 ± 0.05	0.00	0.00	0.00	NM
NGC 6791	2M19205259+3744281	-45.4 ± 0.0	0.38 ± 0.01	-0.45 ± 0.03	-2.18 ± 0.04	0.55	0.65	0.94	GM
NGC 6791	2M19205287+3745331	-46.0 ± 0.0	0.42 ± 0.01	-0.37 ± 0.03	-1.92 ± 0.04	0.74	1.00	0.46	GM
NGC 6791	2M19205338+3748282	-48.4 ± 0.1	0.44 ± 0.01	-0.48 ± 0.04	-2.23 ± 0.05	0.90	0.85	0.96	GM
NGC 6791	2M19205368+3750236	-48.5 ± 0.1	0.46 ± 0.01	-0.35 ± 0.03	-2.10 ± 0.04	0.87	0.62	0.79	GM
NGC 6791	2M19205510+3747162	-48.2 ± 0.0	0.37 ± 0.01	-0.37 ± 0.05	-2.29 ± 0.06	0.93	0.44	0.98	GM
NGC 6791	2M19205530+3743152	-47.9 ± 0.1	0.48 ± 0.01	-0.48 ± 0.03	-2.34 ± 0.04	0.97	0.30	0.95	GM
NGC 6791	2M19205620+3752185	-48.4 ± 0.1	-0.06 ± 0.01	0.38 ± 0.91	-6.43 ± 1.03	0.90	-1.00	0.00	NM
NGC 6791	2M19205629+3744334	-49.0 ± 0.0	0.45 ± 0.01	-0.39 ± 0.03	-2.15 ± 0.04	0.74	0.68	0.90	GM
NGC 6791	2M19205784+3747067	-46.9 ± 0.9	0.42 ± 0.01	-0.42 ± 0.05	-2.24 ± 0.06	0.95	1.00	0.99	GM
NGC 6791	2M19205862+3747404	-13.2 ± 0.1	0.19 ± 0.01	-6.49 ± 0.22	-15.00 ± 0.25	0.00	0.00	0.00	NM
NGC 6791	2M19205958+3748108	-47.2 ± 0.2	0.54 ± 0.01	-0.43 ± 0.04	-2.41 ± 0.06	0.99	0.01	0.91	GM
NGC 6791	2M19210052+3750188	-46.7 ± 0.0	0.33 ± 0.01	-0.44 ± 0.03	-2.34 ± 0.04	0.92	0.09	0.98	GM
NGC 6791	2M19210086+3745339	-45.8 ± 0.1	0.46 ± 0.01	-0.53 ± 0.04	-2.27 ± 0.05	0.67	0.62	0.91	GM
NGC 6791	2M19210112+3742134	-47.6 ± 0.1	0.43 ± 0.01	-0.83 ± 0.04	-2.02 ± 0.05	1.00	0.93	0.17	GM
NGC 6791	2M19210286+3737297	-8.9 ± 0.1	-0.18 ± 0.01	-6.03 ± 0.04	-10.75 ± 0.05	0.00	0.00	0.00	NM
NGC 6791	2M19210326+3741190	-84.0 ± 0.0	-0.19 ± 0.01	-3.02 ± 0.03	-5.32 ± 0.04	0.00	0.00	0.00	NM
NGC 6791	2M19210426+3747187	-46.8 ± 0.1	0.41 ± 0.01	-0.41 ± 0.03	-2.25 ± 0.03	0.94	0.95	0.99	GM
NGC 6791	2M19210483+3741036	-50.1 ± 0.0	0.43 ± 0.01	-0.44 ± 0.03	-2.37 ± 0.04	0.40	0.94	0.94	GM
NGC 6791	2M19210604+3752049	-48.0 ± 0.1	0.39 ± 0.01	-0.43 ± 0.04	-2.17 ± 0.05	0.97	0.75	0.94	GM
NGC 6791	2M19210629+3744596	-45.3 ± 0.1	0.44 ± 0.01	-0.55 ± 0.04	-2.33 ± 0.04	0.54	0.85	0.87	GM
NGC 6791	2M19211002+3758518	-12.0 ± 0.0	-0.02 ± 0.01	30.36 ± 0.03	-0.74 ± 0.04	0.00	-1.00	0.00	NM
NGC 6791	2M19211007+3750008	-48.9 ± 0.1	0.38 ± 0.01	-0.42 ± 0.03	-2.36 ± 0.04	0.77	0.62	0.96	GM
NGC 6791	2M19211041+3734464	30.7 ± 0.0	-0.07 ± 0.01	-5.90 ± 0.04	-16.11 ± 0.05	0.00	0.00	0.00	NM
NGC 6791	2M19211052+3740310	-10.8 ± 0.4	0.00 ± 0.01	0.85 ± 0.05	0.86 ± 0.06	0.00	0.00	0.00	NM
NGC 6791	2M19211116+3744581	-25.7 ± 0.1	0.25 ± 0.01	-14.83 ± 0.03	-15.71 ± 0.04	0.00	-1.00	0.00	NM
NGC 6791	2M19211300+3743005	-48.1 ± 0.2	0.45 ± 0.01	-0.38 ± 0.04	-2.27 ± 0.05	0.95	0.70	0.99	GM
NGC 6791	2M19211415+3746578	-3.4 ± 0.0	0.36 ± 0.01	-1.25 ± 0.04	-0.58 ± 0.05	0.00	0.29	0.00	NM
NGC 6791	2M19211542+3756528	-48.3 ± 0.1	0.35 ± 0.01	-0.50 ± 0.03	-2.21 ± 0.03	0.00	0.00	0.93	NM
NGC 6791	2M19211632+3752154	-11.6 ± 0.1	-0.25 ± 0.01	-0.72 ± 0.03	-4.98 ± 0.04	0.00	0.00	0.00	NM
NGC 6791	2M19211713+3748039	-3.3 ± 0.0	-0.18 ± 0.01	3.52 ± 0.04	-2.14 ± 0.05	0.00	0.00	0.00	NM
NGC 6791	2M19211888+3743232	-36.4 ± 0.3	0.05 ± 0.01	-3.44 ± 0.03	0.66 ± 0.03	0.00	-1.00	0.00	NM
NGC 6791	2M19213390+3750202	-46.9 ± 0.1	0.36 ± 0.01	-0.32 ± 0.04	-2.16 ± 0.05	0.00	0.00	0.85	NM
NGC 6791	2M19214099+3751064	-10.7 ± 0.0	-0.02 ± 0.01	25.28 ± 0.03	-30.71 ± 0.04	0.00	-1.00	0.00	NM
NGC 6791	2M19215339+3743039	-12.6 ± 0.0	-0.30 ± 0.01	-4.99 ± 0.04	-8.58 ± 0.04	0.00	0.00	0.00	NM
NGC 6819	2M19401402+4016306	-56.4 ± 0.0	0.06 ± 0.01	-5.85 ± 0.03	-9.04 ± 0.03	0.00	0.00	0.00	NM
NGC 6819	2M19401466+4004598	-18.9 ± 0.0	-0.03 ± 0.01	50.96 ± 0.04	99.82 ± 0.04	0.00	-1.00	0.00	NM
NGC 6819	2M19401937+4015495	-52.3 ± 0.2	-0.35 ± 0.01	-5.93 ± 0.03	-6.26 ± 0.03	0.00	0.00	0.00	NM
NGC 6819	2M19402284+4006008	-50.3 ± 0.1	-0.34 ± 0.01	-1.60 ± 0.03	-2.91 ± 0.03	0.00	0.00	0.00	NM
NGC 6819	2M19403569+4005038	2.7 ± 0.1	-0.45 ± 0.01	-3.76 ± 0.03	-3.46 ± 0.03	0.00	0.00	0.00	NM
NGC 6819	2M19403684+4015172	2.1 ± 0.0	0.15 ± 0.01	-3.00 ± 0.03	-3.66 ± 0.03	0.00	0.00	0.54	NM
NGC 6819	2M19404262+4003043	-35.2 ± 0.1	0.07 ± 0.01	-4.36 ± 0.04	-19.13 ± 0.04	0.00	0.00	0.00	NM
NGC 6819	2M19404341+4020235	-11.8 ± 16.3	-0.01 ± 0.01	0.65 ± 0.09	-3.89 ± 0.09	0.00	-1.00	0.00	NM
NGC 6819	2M19404803+4008085	2.4 ± 0.1	0.09 ± 0.01	-2.98 ± 0.04	-3.83 ± 0.04	1.00	0.82	0.94	GM
NGC 6819	2M19404965+4014313	3.1 ± 0.0	0.12 ± 0.01	-2.84 ± 0.03	-3.72 ± 0.03	0.95	0.94	0.69	GM
NGC 6819	2M19405020+4013109	4.3 ± 0.0	0.15 ± 0.01	-3.03 ± 0.04	-3.84 ± 0.04	0.66	0.59	0.85	GM
NGC 6819	2M19405420+4018159	-31.6 ± 0.0	0.29 ± 0.01	-7.54 ± 0.04	1.76 ± 0.04	0.00	0.00	0.00	NM
NGC 6819	2M19405560+4006292	2.3 ± 0.0	0.20 ± 0.01	-0.21 ± 0.04	-5.14 ± 0.04	1.00	0.03	0.00	NM
NGC 6819	2M19405601+4013395	3.3 ± 0.1	0.09 ± 0.01	-2.86 ± 0.03	-3.74 ± 0.03	0.92	0.76	0.78	GM
NGC 6819	2M19405704+4010068	-14.8 ± 8.9	0.13 ± 0.01	-2.79 ± 0.04	-3.79 ± 0.04	0.00	0.80	0.72	NM
NGC 6819	2M19405797+4008174	4.5 ± 0.1	0.13 ± 0.01	-2.73 ± 0.04	-3.77 ± 0.04	0.61	0.84	0.52	GM
NGC 6819	2M19410203+4006280	2.8 ± 0.2	-0.08 ± 0.01	-0.68 ± 0.04	-4.74 ± 0.04	0.99	0.00	0.00	NM
NGC 6819	2M19410301+4009409	-84.6 ± 0.2	-0.38 ± 0.01	-2.35 ± 0.05	-2.80 ± 0.04	0.00	0.00	0.00	NM

Continued on next page

Table A.1 – Continued

Cluster name	2MASS ID	RV (km s^{-1})	[Fe/H] (dex)	μ_α (mas yr^{-1})	μ_δ (mas yr^{-1})	RV Prob	[Fe/H] Prob	PM Prob	Memb
NGC 6819	2M19410524+4014042	3.3 ± 0.1	0.14 ± 0.01	-2.74 ± 0.04	-3.86 ± 0.04	0.93	0.64	0.60	GM
NGC 6819	2M19410622+4010532	3.2 ± 0.0	0.12 ± 0.01	-3.00 ± 0.03	-4.08 ± 0.03	0.93	0.95	0.49	GM
NGC 6819	2M19410819+4015085	0.1 ± 0.1	0.06 ± 0.01	0.40 ± 0.67	-2.47 ± 0.63	0.48	0.33	0.00	NM
NGC 6819	2M19410822+4019319	2.5 ± 0.3	-0.08 ± 0.01	-2.91 ± 0.07	-3.49 ± 0.06	0.00	0.00	0.17	NM
NGC 6819	2M19410858+4013299	2.3 ± 0.0	0.11 ± 0.01	-2.90 ± 0.04	-4.00 ± 0.04	1.00	1.00	0.77	GM
NGC 6819	2M19410926+4014436	2.3 ± 0.1	0.13 ± 0.01	-2.76 ± 0.04	-3.91 ± 0.04	1.00	0.89	0.65	GM
NGC 6819	2M19410991+4015495	2.5 ± 0.1	0.07 ± 0.01	-2.74 ± 0.04	-3.90 ± 0.04	1.00	0.45	0.61	GM
NGC 6819	2M19410994+4009056	2.9 ± 3.1	0.02 ± 0.01	-3.02 ± 0.03	-3.80 ± 0.03	0.98	0.02	0.83	GM
NGC 6819	2M19411085+4023048	-43.6 ± 0.0	0.30 ± 0.01	0.04 ± 0.04	2.36 ± 0.05	0.00	0.00	0.00	NM
NGC 6819	2M19411102+4011116	3.0 ± 0.0	0.10 ± 0.01	-3.07 ± 0.04	-3.81 ± 0.04	0.97	0.92	0.68	GM
NGC 6819	2M19411115+4011422	4.6 ± 0.0	0.14 ± 0.01	-3.03 ± 0.04	-3.91 ± 0.04	0.56	0.67	0.83	GM
NGC 6819	2M19411184+4013301	-38.5 ± 0.2	-0.52 ± 0.01	-5.44 ± 0.06	-3.22 ± 0.09	0.00	0.00	0.00	NM
NGC 6819	2M19411215+4018560	-22.2 ± 0.1	0.29 ± 0.01	-5.63 ± 0.04	-8.60 ± 0.05	0.00	0.00	0.00	NM
NGC 6819	2M19411279+4012238	2.8 ± 0.0	0.12 ± 0.01	-2.98 ± 0.05	-3.78 ± 0.04	0.99	0.98	0.87	GM
NGC 6819	2M19411318+4006417	11.6 ± 0.0	0.09 ± 0.01	-2.56 ± 0.03	-4.40 ± 0.02	0.00	0.81	0.00	NM
NGC 6819	2M19411319+4014567	-1.8 ± 0.1	0.10 ± 0.01	-3.03 ± 0.03	-4.14 ± 0.04	0.10	0.96	0.32	GM
NGC 6819	2M19411355+4012205	2.6 ± 0.1	0.09 ± 0.01	-2.88 ± 0.04	-3.78 ± 0.04	1.00	0.82	0.89	GM
NGC 6819	2M19411367+4003382	2.8 ± 0.0	0.07 ± 0.01	-3.03 ± 0.02	-3.90 ± 0.02	0.00	0.00	0.82	NM
NGC 6819	2M19411476+4011008	1.0 ± 0.2	0.15 ± 0.01	-3.09 ± 0.05	-3.83 ± 0.06	0.76	0.53	0.66	GM
NGC 6819	2M19411564+4010105	1.6 ± 0.1	0.15 ± 0.01	-2.90 ± 0.03	-3.93 ± 0.04	0.91	0.55	0.93	GM
NGC 6819	2M19411593+4011114	5.2 ± 0.1	0.11 ± 0.01	-2.68 ± 0.04	-3.97 ± 0.04	0.40	1.00	0.36	GM
NGC 6819	2M19411631+4005508	-1.0 ± 0.0	0.08 ± 0.01	-2.66 ± 0.04	-4.20 ± 0.05	0.20	0.59	0.08	GM
NGC 6819	2M19411705+4010517	1.4 ± 0.1	0.07 ± 0.01	-2.93 ± 0.04	-3.68 ± 0.05	0.85	0.41	0.65	GM
NGC 6819	2M19411776+4009158	-1.0 ± 0.5	0.12 ± 0.01	-3.20 ± 0.04	-4.05 ± 0.04	0.20	0.98	0.20	GM
NGC 6819	2M19411893+4011408	1.0 ± 0.1	0.10 ± 0.01	-2.99 ± 0.03	-3.73 ± 0.04	0.75	0.97	0.75	GM
NGC 6819	2M19411971+4023362	1.4 ± 0.0	0.06 ± 0.01	-3.14 ± 0.05	-3.75 ± 0.07	0.00	0.00	0.41	NM
NGC 6819	2M19412133+4011572	6.8 ± 0.0	0.12 ± 0.01	-2.32 ± 0.04	-4.06 ± 0.05	0.09	0.97	0.00	NM
NGC 6819	2M19412136+4011002	1.9 ± 0.0	0.11 ± 0.01	-3.11 ± 0.04	-3.92 ± 0.05	0.96	1.00	0.56	GM
NGC 6819	2M19412147+4013573	1.5 ± 0.0	0.13 ± 0.01	-3.00 ± 0.03	-3.87 ± 0.04	0.88	0.85	0.91	GM
NGC 6819	2M19412176+4012111	0.6 ± 0.2	0.14 ± 0.01	-2.87 ± 0.04	-3.79 ± 0.04	0.64	0.68	0.90	GM
NGC 6819	2M19412222+4016442	2.7 ± 0.1	0.12 ± 0.01	-2.96 ± 0.03	-3.87 ± 0.04	1.00	0.97	0.98	GM
NGC 6819	2M19412369+4012355	3.7 ± 0.0	0.08 ± 0.01	-3.45 ± 0.04	-3.81 ± 0.04	0.83	0.62	0.02	GM
NGC 6819	2M19412386+4021444	2.1 ± 0.0	0.12 ± 0.01	-2.93 ± 0.04	-3.86 ± 0.05	0.00	0.00	1.00	NM
NGC 6819	2M19412463+4003196	7.9 ± 0.0	-0.22 ± 0.01	-1.77 ± 0.04	-14.02 ± 0.05	0.00	0.00	0.00	NM
NGC 6819	2M19412491+4007440	-37.1 ± 0.2	-0.46 ± 0.01	-3.12 ± 0.04	-5.67 ± 0.04	0.00	0.00	0.00	NM
NGC 6819	2M19412658+4011418	2.2 ± 0.0	0.09 ± 0.01	-2.78 ± 0.04	-3.81 ± 0.04	0.99	0.81	0.73	GM
NGC 6819	2M19412707+4012283	0.8 ± 0.1	0.09 ± 0.01	-2.97 ± 0.04	-3.83 ± 0.04	0.70	0.78	0.96	GM
NGC 6819	2M19412730+4004548	1.2 ± 0.0	0.13 ± 0.01	-2.90 ± 0.03	-4.70 ± 0.03	0.00	0.00	0.00	NM
NGC 6819	2M19412915+4013040	1.4 ± 0.0	0.11 ± 0.01	-3.04 ± 0.04	-3.94 ± 0.04	0.85	1.00	0.76	GM
NGC 6819	2M19412942+4014199	3.5 ± 0.0	0.11 ± 0.01	-2.97 ± 0.04	-3.69 ± 0.04	0.88	0.99	0.64	GM
NGC 6819	2M19412953+4012210	2.9 ± 0.2	0.15 ± 0.01	-2.84 ± 0.04	-3.92 ± 0.05	0.98	0.47	0.87	GM
NGC 6819	2M19413027+4015218	2.1 ± 0.0	0.12 ± 0.01	-3.00 ± 0.04	-4.02 ± 0.05	0.98	0.95	0.67	GM
NGC 6819	2M19413031+4009005	6.2 ± 0.1	0.09 ± 0.01	-2.70 ± 0.04	-3.43 ± 0.04	0.17	0.86	0.04	GM
NGC 6819	2M19413330+4012349	4.3 ± 0.0	0.07 ± 0.01	-2.79 ± 0.04	-4.07 ± 0.04	0.67	0.55	0.44	GM
NGC 6819	2M19413439+4017482	2.6 ± 0.0	0.13 ± 0.01	-2.83 ± 0.04	-3.80 ± 0.04	0.00	0.00	0.83	NM
NGC 6819	2M19413683+4009031	38.9 ± 0.0	0.06 ± 0.01	-0.27 ± 0.04	-4.36 ± 0.05	0.00	0.33	0.00	NM
NGC 6819	2M19414006+4023060	20.0 ± 0.1	-0.28 ± 0.01	-2.63 ± 0.04	-4.80 ± 0.04	0.00	0.00	0.00	NM
NGC 6819	2M19414095+4013260	-6.5 ± 0.1	-0.06 ± 0.01	-0.98 ± 0.04	-2.22 ± 0.04	0.00	0.00	0.00	NM
NGC 6819	2M19414162+4017128	-26.9 ± 0.2	-0.02 ± 0.01	-3.54 ± 0.04	-5.58 ± 0.04	0.00	0.00	0.00	NM
NGC 6819	2M19414427+4005527	3.8 ± 0.1	0.09 ± 0.01	-2.83 ± 0.04	-3.86 ± 0.05	0.00	0.00	0.88	NM
NGC 6819	2M19414807+4019455	-36.0 ± 0.1	0.19 ± 0.01	-0.63 ± 0.03	-3.23 ± 0.03	0.00	0.00	0.00	NM
NGC 6819	2M19414825+4010323	-17.6 ± 3.4	0.09 ± 0.01	-5.41 ± 0.28	-8.24 ± 0.33	0.00	-1.00	0.00	NM
NGC 6819	2M19415064+4016010	4.4 ± 0.0	0.18 ± 0.01	-2.96 ± 0.03	-3.81 ± 0.03	0.00	0.00	0.94	NM
NGC 6819	2M19415437+4002097	3.9 ± 0.2	0.07 ± 0.01	-2.86 ± 0.05	-3.54 ± 0.05	0.00	0.00	0.24	NM
NGC 6819	2M19415538+4004348	11.0 ± 0.0	0.16 ± 0.01	-3.62 ± 0.04	-9.79 ± 0.05	0.00	0.00	0.00	NM
NGC 6819	2M19415566+4015526	17.3 ± 0.0	-0.35 ± 0.01	-2.44 ± 0.03	-8.87 ± 0.03	0.00	0.00	0.00	NM
NGC 6819	2M19421683+4008114	-54.0 ± 0.7	0.14 ± 0.01	4.56 ± 0.04	7.90 ± 0.05	0.00	0.00	0.00	NM
NGC 6819	2M19421943+4016074	-3.8 ± 0.1	-0.24 ± 0.01	1.43 ± 0.04	-1.19 ± 0.04	0.00	0.00	0.00	NM
NGC 6811	2M19361068+4627380	-18.1 ± 0.1	0.02 ± 0.01	6.09 ± 0.03	20.13 ± 0.04	0.00	-1.00	0.00	NM
NGC 6811	2M19361498+4631091	-10.3 ± 0.0	-0.08 ± 0.01	1.03 ± 0.06	-10.81 ± 0.06	0.00	0.00	0.00	NM
NGC 6811	2M19363005+4614500	-96.7 ± 0.0	-0.37 ± 0.01	-5.87 ± 0.04	-9.46 ± 0.04	0.00	0.00	0.00	NM
NGC 6811	2M19363103+4629507	-8.9 ± 0.1	-0.07 ± 0.01	6.07 ± 0.04	-16.76 ± 0.04	0.00	-1.00	0.00	NM
NGC 6811	2M19363131+4612460	-23.9 ± 0.0	-0.12 ± 0.01	-1.95 ± 0.05	2.06 ± 0.04	0.00	0.00	0.00	NM

Continued on next page

Table A.1 – Continued

Cluster name	2MASS ID	RV (km s^{-1})	[Fe/H] (dex)	μ_α (mas yr^{-1})	μ_δ (mas yr^{-1})	RV Prob	[Fe/H] Prob	PM Prob	Memb
NGC 6811	2M19363688+4618348	9.4 ± 1.2	-0.08 ± 0.01	-3.33 ± 0.08	-8.76 ± 0.06	0.00	-1.00	0.94	NM
NGC 6811	2M19364603+4622415	5.6 ± 5.5	-0.10 ± 0.01	-3.34 ± 0.05	-8.74 ± 0.05	0.88	-1.00	0.95	DM
NGC 6811	2M19365036+4628479	-17.5 ± 0.2	0.06 ± 0.01	-3.30 ± 0.91	-13.71 ± 1.04	0.00	-1.00	0.00	NM
NGC 6811	2M19365179+4624301	5.6 ± 0.0	-0.19 ± 0.01	-6.40 ± 0.05	-6.01 ± 0.06	0.88	0.00	0.00	NM
NGC 6811	2M19365518+4625345	-35.4 ± 0.0	-0.13 ± 0.01	-2.82 ± 0.05	-7.32 ± 0.06	0.00	0.00	0.00	NM
NGC 6811	2M19365580+4627376	7.4 ± 0.1	-0.02 ± 0.01	-3.24 ± 0.04	-8.69 ± 0.05	0.98	0.80	0.64	GM
NGC 6811	2M19365712+4622425	7.9 ± 0.0	-0.03 ± 0.01	-3.33 ± 0.04	-8.73 ± 0.06	0.91	0.47	0.91	GM
NGC 6811	2M19365957+4632505	10.4 ± 0.0	-0.13 ± 0.01	-0.88 ± 0.04	-3.92 ± 0.04	0.00	0.00	0.00	NM
NGC 6811	2M19370267+4623130	8.1 ± 0.0	0.01 ± 0.01	-3.55 ± 0.05	-8.73 ± 0.06	0.87	0.81	0.63	GM
NGC 6811	2M19370579+4620590	-66.2 ± 0.0	-0.13 ± 0.01	-7.15 ± 0.03	2.93 ± 0.04	0.00	0.00	0.00	NM
NGC 6811	2M19370580+4611080	-61.7 ± 5.2	0.12 ± 0.01	15.83 ± 0.05	4.99 ± 0.05	0.00	-1.00	0.00	NM
NGC 6811	2M19372208+4632505	7.1 ± 0.0	0.00 ± 0.01	-3.42 ± 0.04	-8.77 ± 0.04	0.00	0.00	0.98	NM
NGC 6811	2M19372426+4617048	-19.1 ± 0.0	0.23 ± 0.01	-13.10 ± 0.05	-9.07 ± 0.05	0.00	-1.00	0.00	NM
NGC 6811	2M19372604+4624339	5.9 ± 0.1	-0.01 ± 0.01	0.29 ± 0.05	-2.31 ± 0.06	0.93	0.93	0.00	NM
NGC 6811	2M19372671+4623561	-19.6 ± 0.0	0.02 ± 0.01	-2.77 ± 0.03	-1.99 ± 0.03	0.00	0.71	0.00	NM
NGC 6811	2M19373232+4609282	-61.3 ± 0.4	-0.59 ± 0.01	-3.57 ± 0.07	4.42 ± 0.08	0.00	0.00	0.00	NM
NGC 6811	2M19373233+4620099	-45.9 ± 0.4	0.01 ± 0.01	10.16 ± 0.07	4.07 ± 0.10	0.00	-1.00	0.00	NM
NGC 6811	2M19373462+4624098	7.7 ± 0.0	0.02 ± 0.01	-3.54 ± 0.04	-8.79 ± 0.05	0.95	0.64	0.69	GM
NGC 6811	2M19373578+4619574	-96.7 ± 0.1	-0.31 ± 0.01	-2.21 ± 0.04	-6.92 ± 0.05	0.00	0.00	0.00	NM
NGC 6811	2M19373759+4624347	12.0 ± 0.0	-0.39 ± 0.01	2.41 ± 0.04	-1.22 ± 0.05	0.11	0.00	0.00	NM
NGC 6811	2M19374258+4614203	-57.8 ± 0.0	0.41 ± 0.01	-5.05 ± 0.05	-7.68 ± 0.05	0.00	0.00	0.00	NM
NGC 6811	2M19374795+4614570	-32.3 ± 0.0	-0.21 ± 0.01	-1.71 ± 0.11	-4.97 ± 0.12	0.00	0.00	0.00	NM
NGC 6811	2M19375204+4624559	-50.9 ± 0.1	-0.02 ± 0.01	10.41 ± 0.04	9.42 ± 0.04	0.00	0.75	0.00	NM
NGC 6811	2M19375291+4630095	-40.4 ± 0.0	0.01 ± 0.01	-5.73 ± 0.04	-2.58 ± 0.04	0.00	0.00	0.00	NM
NGC 6811	2M19375505+4633279	-22.9 ± 0.0	0.09 ± 0.01	3.02 ± 0.04	2.80 ± 0.05	0.00	0.00	0.00	NM
NGC 6811	2M19380290+4635575	-79.4 ± 0.0	0.14 ± 0.01	-3.13 ± 0.04	-2.51 ± 0.04	0.00	0.00	0.00	NM
NGC 6811	2M19380324+4627206	-12.6 ± 0.0	0.04 ± 0.01	-2.25 ± 0.04	-2.16 ± 0.04	0.00	0.00	0.00	NM
NGC 6811	2M19380489+4624422	-40.1 ± 0.0	-0.06 ± 0.01	-18.68 ± 0.04	-34.77 ± 0.05	0.00	0.00	0.00	NM
NGC 6811	2M19380947+4617411	-24.6 ± 0.4	0.18 ± 0.01	-6.43 ± 0.05	-8.80 ± 0.06	0.00	-1.00	0.00	NM
NGC 6811	2M19381492+4627414	-42.0 ± 0.0	-0.16 ± 0.01	-0.09 ± 0.04	-16.45 ± 0.04	0.00	0.00	0.00	NM
NGC 6811	2M19382280+4619389	-14.0 ± 0.1	0.14 ± 0.01	-6.75 ± 0.03	-10.65 ± 0.02	0.00	0.00	0.00	NM
NGC 6811	2M19382526+4632508	-23.4 ± 0.1	0.11 ± 0.01	-4.55 ± 0.04	-19.01 ± 0.04	0.00	0.00	0.00	NM
NGC 6811	2M19383160+4630328	-11.2 ± 0.0	0.18 ± 0.01	-4.84 ± 0.04	-8.24 ± 0.04	0.00	0.00	0.00	NM
NGC 6811	2M19383572+4624093	-13.6 ± 0.0	0.07 ± 0.01	-3.73 ± 0.02	-6.67 ± 0.02	0.00	0.00	0.00	NM
Berkeley 53	2M20542838+5104228	-26.8 ± 0.2	-0.59 ± 0.01	-3.22 ± 0.22	-2.79 ± 0.21	0.00	0.00	0.00	NM
Berkeley 53	2M20543359+5108309	-27.5 ± 0.1	-0.30 ± 0.01	-0.88 ± 0.11	-2.09 ± 0.11	0.00	0.00	0.00	NM
Berkeley 53	2M20545763+5053012	-81.1 ± 0.1	-0.24 ± 0.01	-3.30 ± 0.33	-2.07 ± 0.34	0.00	0.00	0.00	NM
Berkeley 53	2M20551286+5057186	-62.9 ± 0.1	-0.29 ± 0.01	-4.39 ± 0.12	-5.16 ± 0.11	0.00	0.00	0.06	NM
Berkeley 53	2M20551461+5059152	-55.6 ± 0.0	0.03 ± 0.01	1.42 ± 0.09	-2.63 ± 0.09	0.00	0.00	0.00	NM
Berkeley 53	2M20551721+5100097	-21.5 ± 0.1	-0.11 ± 0.01	-1.89 ± 0.19	-5.57 ± 0.19	0.00	0.00	0.00	NM
Berkeley 53	2M20553052+5103087	-84.9 ± 0.1	-0.31 ± 0.01	-2.14 ± 0.19	-2.64 ± 0.19	0.00	0.00	0.00	NM
Berkeley 53	2M20553095+5051062	-6.7 ± 0.0	0.09 ± 0.01	-5.13 ± 0.05	-1.13 ± 0.05	0.00	0.00	0.00	NM
Berkeley 53	2M20553347+5059087	11.4 ± 0.0	-0.03 ± 0.01	-1.52 ± 0.12	-2.01 ± 0.13	0.00	0.35	0.00	NM
Berkeley 53	2M20554232+5106153	-35.6 ± 0.0	-0.01 ± 0.01	-4.11 ± 0.10	-5.65 ± 0.10	1.00	0.94	0.66	GM
Berkeley 53	2M20554417+5117478	-16.8 ± 1.8	-0.18 ± 0.01	-3.13 ± 0.20	-4.22 ± 0.17	0.00	0.00	0.00	NM
Berkeley 53	2M20554430+5112252	-45.2 ± 0.1	0.07 ± 0.01	-3.91 ± 0.12	-4.75 ± 0.11	0.00	0.00	0.03	NM
Berkeley 53	2M20554697+5058402	-66.2 ± 0.0	0.08 ± 0.01	-3.34 ± 0.09	-3.68 ± 0.09	0.00	0.00	0.00	NM
Berkeley 53	2M20554821+5105211	-99.2 ± 0.2	-0.29 ± 0.01	-2.97 ± 0.14	-2.64 ± 0.13	0.00	0.00	0.00	NM
Berkeley 53	2M20554936+5106545	-36.9 ± 0.1	0.01 ± 0.01	-3.82 ± 0.08	-5.59 ± 0.07	0.77	0.71	0.95	GM
Berkeley 53	2M20554976+5103438	-51.1 ± 1.1	-0.36 ± 0.01	-4.67 ± 0.10	-7.34 ± 0.09	0.00	0.00	0.00	NM
Berkeley 53	2M20554992+5112540	-50.7 ± 0.0	0.02 ± 0.01	-3.35 ± 0.14	-2.79 ± 0.12	0.00	0.00	0.00	NM
Berkeley 53	2M20554998+5102175	-36.1 ± 0.0	-0.00 ± 0.01	-3.88 ± 0.10	-5.65 ± 0.09	0.95	1.00	0.95	GM
Berkeley 53	2M20555090+5109495	-35.9 ± 0.0	-0.06 ± 0.01	-4.42 ± 0.09	-7.16 ± 0.08	0.98	0.03	0.00	NM
Berkeley 53	2M20555552+5111166	-45.7 ± 0.1	-0.05 ± 0.01	-2.24 ± 0.15	-4.05 ± 0.16	0.00	0.00	0.00	NM
Berkeley 53	2M20555767+5103206	-34.2 ± 0.1	-0.07 ± 0.01	-3.75 ± 0.09	-5.60 ± 0.09	0.82	0.00	0.97	NM
Berkeley 53	2M20555947+5105436	-34.7 ± 0.0	-0.00 ± 0.01	-2.31 ± 0.23	-5.69 ± 0.20	0.93	1.00	0.00	NM
Berkeley 53	2M20555959+5100466	-36.7 ± 0.0	-0.03 ± 0.01	-3.37 ± 0.13	-6.00 ± 0.15	0.82	0.33	0.33	GM
Berkeley 53	2M20560374+5058123	-68.6 ± 0.0	-0.27 ± 0.01	-3.24 ± 0.10	-4.97 ± 0.10	0.00	0.00	0.07	NM
Berkeley 53	2M20560675+5109042	-92.4 ± 0.1	-0.09 ± 0.01	-3.52 ± 0.14	-3.59 ± 0.12	0.00	0.00	0.00	NM
Berkeley 53	2M20560728+5107047	-11.7 ± 0.1	-0.10 ± 0.01	-3.28 ± 0.17	-2.48 ± 0.16	0.00	0.00	0.00	NM
Berkeley 53	2M20561018+5102389	-36.3 ± 0.2	0.01 ± 0.01	-3.87 ± 0.10	-5.91 ± 0.10	0.92	0.77	0.82	GM
Berkeley 53	2M20561021+5112460	-24.5 ± 0.1	0.11 ± 0.01	-3.54 ± 0.07	-4.37 ± 0.07	0.00	0.00	0.00	NM
Berkeley 53	2M20561531+5113537	-126.6 ± 0.8	-0.24 ± 0.01	-2.52 ± 0.11	-3.07 ± 0.10	0.00	0.00	0.00	NM

Continued on next page

Table A.1 – Continued

Cluster name	2MASS ID	RV (km s^{-1})	[Fe/H] (dex)	μ_α (mas yr^{-1})	μ_δ (mas yr^{-1})	RV Prob	[Fe/H] Prob	PM Prob	Memb
Berkeley 53	2M20561671+5110193	-51.1 ± 0.1	-0.18 ± 0.01	-4.09 ± 0.15	-2.75 ± 0.12	0.00	0.00	0.00	NM
Berkeley 53	2M20562042+5107238	-76.9 ± 0.3	-0.65 ± 0.01	-2.39 ± 0.09	-2.85 ± 0.08	0.00	-1.00	0.00	NM
Berkeley 53	2M20563100+5106356	-96.9 ± 0.2	-0.37 ± 0.01	-1.99 ± 0.23	-2.91 ± 0.20	0.00	0.00	0.00	NM
Berkeley 53	2M20563163+5112590	-28.3 ± 5.6	0.36 ± 0.01	-3.01 ± 0.15	-1.76 ± 0.13	0.00	0.00	0.00	NM
Berkeley 53	2M20563698+5101435	-74.7 ± 0.0	-0.03 ± 0.01	0.43 ± 0.08	-3.95 ± 0.07	0.00	0.53	0.00	NM
Berkeley 53	2M20564102+5053169	-120.9 ± 0.1	-0.50 ± 0.01	-2.64 ± 0.18	-2.24 ± 0.19	0.00	0.00	0.00	NM
Berkeley 53	2M20564361+5100448	-12.6 ± 0.0	0.14 ± 0.01	-7.12 ± 0.05	-13.93 ± 0.05	0.00	0.00	0.00	NM
Berkeley 53	2M20565199+5057103	-19.1 ± 0.0	0.10 ± 0.01	-2.08 ± 0.12	-5.03 ± 0.11	0.00	0.00	0.00	NM
Berkeley 53	2M20570324+5107109	-38.8 ± 0.1	0.15 ± 0.01	-2.04 ± 0.13	-1.99 ± 0.12	0.00	0.00	0.00	NM
Berkeley 53	2M20570367+5056406	-64.8 ± 0.1	-0.21 ± 0.01	-3.01 ± 0.24	-3.84 ± 0.23	0.00	0.00	0.00	NM
NGC 7789	2M23542762+5647131	17.9 ± 0.1	-0.18 ± 0.01	-0.49 ± 0.03	-4.79 ± 0.02	0.00	0.00	0.00	NM
NGC 7789	2M23543657+5650099	-52.4 ± 0.0	-0.06 ± 0.01	-4.22 ± 0.03	-1.42 ± 0.03	0.00	0.00	0.00	NM
NGC 7789	2M23543872+5645090	-174.8 ± 0.1	-0.17 ± 0.01	-1.97 ± 0.03	-1.43 ± 0.02	0.00	0.00	0.00	NM
NGC 7789	2M23544116+5641326	-10.3 ± 0.2	-0.04 ± 0.01	14.27 ± 0.02	3.46 ± 0.02	0.00	-1.00	0.00	NM
NGC 7789	2M23544735+5638483	-85.6 ± 0.1	0.07 ± 0.01	-3.43 ± 0.03	-1.20 ± 0.03	0.00	0.00	0.00	NM
NGC 7789	2M23544743+5647164	-74.1 ± 0.1	0.27 ± 0.01	-5.45 ± 0.04	0.89 ± 0.04	0.00	0.00	0.00	NM
NGC 7789	2M23545286+5624311	-114.2 ± 0.1	-0.40 ± 0.01	-1.56 ± 0.03	-0.23 ± 0.03	0.00	0.00	0.00	NM
NGC 7789	2M23545349+5623577	-0.3 ± 0.2	0.11 ± 0.01	0.05 ± 0.03	7.30 ± 0.02	0.00	-1.00	0.00	NM
NGC 7789	2M23545921+5644288	-57.0 ± 0.1	-0.23 ± 0.01	-1.35 ± 0.03	-1.27 ± 0.03	0.00	0.00	0.00	NM
NGC 7789	2M23551199+5656246	-62.2 ± 0.0	0.01 ± 0.01	-4.14 ± 0.04	-0.29 ± 0.03	0.00	0.00	0.00	NM
NGC 7789	2M23551266+5638476	-110.9 ± 0.1	-0.23 ± 0.01	-1.36 ± 0.03	-3.77 ± 0.02	0.00	0.00	0.00	NM
NGC 7789	2M23551799+5646223	-64.7 ± 0.1	-0.14 ± 0.01	-3.20 ± 0.03	-0.32 ± 0.02	0.00	0.00	0.00	NM
NGC 7789	2M23554031+5702426	-109.6 ± 0.3	-0.45 ± 0.01	-2.04 ± 0.07	-1.47 ± 0.05	0.00	0.00	0.00	NM
NGC 7789	2M23554838+5704029	-63.2 ± 0.1	0.39 ± 0.01	-1.98 ± 0.04	-1.63 ± 0.04	0.00	0.00	0.00	NM
NGC 7789	2M23554966+5639180	-56.9 ± 0.1	0.09 ± 0.01	-0.91 ± 0.04	-1.79 ± 0.04	0.46	0.36	0.74	GM
NGC 7789	2M23555111+5631370	-22.3 ± 0.3	0.13 ± 0.01	-0.27 ± 0.04	0.00 ± 0.03	0.00	0.00	0.00	NM
NGC 7789	2M23555809+5702517	-119.9 ± 0.0	-0.12 ± 0.01	-1.84 ± 0.04	-1.11 ± 0.04	0.00	0.00	0.00	NM
NGC 7789	2M23560553+5655198	8.4 ± 0.0	0.08 ± 0.01	1.81 ± 0.03	0.26 ± 0.02	0.00	0.00	0.00	NM
NGC 7789	2M23561297+5620359	-18.5 ± 0.3	-0.10 ± 0.01	4.58 ± 0.03	-1.50 ± 0.02	0.00	-1.00	0.00	NM
NGC 7789	2M23561563+5637097	-33.1 ± 0.3	-0.15 ± 0.01	-4.24 ± 0.03	-1.71 ± 0.02	0.00	-1.00	0.00	NM
NGC 7789	2M23562433+5659554	-99.0 ± 0.1	0.17 ± 0.01	-4.19 ± 0.03	-0.61 ± 0.03	0.00	0.00	0.00	NM
NGC 7789	2M23562469+5655480	-44.7 ± 0.0	-0.36 ± 0.01	-2.25 ± 0.05	4.15 ± 0.05	0.00	0.00	0.00	NM
NGC 7789	2M23562953+5648399	-55.4 ± 0.0	-0.01 ± 0.01	-1.02 ± 0.04	-2.00 ± 0.04	0.91	0.10	0.83	GM
NGC 7789	2M23563279+5704466	-36.4 ± 0.1	-0.43 ± 0.01	-4.17 ± 0.04	-0.51 ± 0.04	0.00	0.00	0.00	NM
NGC 7789	2M23563464+5653548	4.7 ± 0.1	0.12 ± 0.01	-2.47 ± 0.03	17.58 ± 0.03	0.00	-1.00	0.00	NM
NGC 7789	2M23563632+5645024	-54.4 ± 0.0	-0.06 ± 0.01	-0.93 ± 0.03	-1.74 ± 0.03	0.99	0.00	0.59	NM
NGC 7789	2M23563732+5707153	-48.7 ± 0.0	0.00 ± 0.01	-1.70 ± 0.03	-1.86 ± 0.02	0.00	0.00	0.00	NM
NGC 7789	2M23563748+5706276	-75.9 ± 28.4	-0.15 ± 0.01	-1.73 ± 0.04	-2.02 ± 0.05	0.00	0.00	0.00	NM
NGC 7789	2M23563768+5654165	-89.2 ± 0.0	0.04 ± 0.01	-3.99 ± 0.03	-1.12 ± 0.03	0.00	0.94	0.00	NM
NGC 7789	2M23563930+5645242	-55.1 ± 0.1	0.04 ± 0.01	-1.07 ± 0.04	-1.97 ± 0.04	0.97	0.97	0.76	GM
NGC 7789	2M23564206+5615465	-67.5 ± 0.1	0.22 ± 0.01	-1.92 ± 0.03	-0.97 ± 0.03	0.00	0.00	0.00	NM
NGC 7789	2M23564304+5650477	-53.4 ± 0.0	0.06 ± 0.01	-0.80 ± 0.05	-1.95 ± 0.04	0.79	0.94	0.82	GM
NGC 7789	2M23564466+5625293	-54.3 ± 0.0	0.03 ± 0.01	-0.91 ± 0.04	-2.00 ± 0.03	0.00	0.00	0.94	NM
NGC 7789	2M23564690+5616205	-85.6 ± 0.5	-0.27 ± 0.01	-1.93 ± 0.03	-0.34 ± 0.03	0.00	0.00	0.00	NM
NGC 7789	2M23564703+5658124	-54.1 ± 1.0	-0.19 ± 0.01	-0.79 ± 0.03	-1.82 ± 0.03	0.00	-1.00	0.65	NM
NGC 7789	2M23564982+5657593	-20.5 ± 0.0	0.21 ± 0.01	31.61 ± 0.05	-14.69 ± 0.04	0.00	-1.00	0.00	NM
NGC 7789	2M23565053+5649208	-50.6 ± 0.0	0.01 ± 0.01	-0.68 ± 0.05	-1.96 ± 0.04	0.09	0.40	0.47	GM
NGC 7789	2M23565251+5643298	-16.9 ± 0.3	-0.43 ± 0.01	-1.55 ± 0.05	1.68 ± 0.04	0.00	0.00	0.00	NM
NGC 7789	2M23565527+5638268	-55.4 ± 0.1	-0.07 ± 0.01	-0.06 ± 0.79	-3.36 ± 0.95	0.92	0.00	0.00	NM
NGC 7789	2M23565751+5645272	-55.2 ± 0.0	0.06 ± 0.01	-0.78 ± 0.04	-1.91 ± 0.04	0.96	0.95	0.74	GM
NGC 7789	2M23570895+5648504	-54.7 ± 0.0	0.08 ± 0.01	-0.93 ± 0.05	-1.84 ± 0.05	1.00	0.62	0.88	GM
NGC 7789	2M23571400+5640586	-53.9 ± 0.2	0.07 ± 0.01	-0.95 ± 0.05	-2.13 ± 0.04	0.92	0.76	0.57	GM
NGC 7789	2M23571604+5702432	1.2 ± 0.1	-0.26 ± 0.01	-4.06 ± 0.03	-1.19 ± 0.02	0.00	0.00	0.00	NM
NGC 7789	2M23571728+5645333	-55.1 ± 0.1	0.04 ± 0.01	-1.14 ± 0.04	-2.03 ± 0.04	0.97	0.96	0.47	GM
NGC 7789	2M23571729+5636481	-88.8 ± 0.0	-0.34 ± 0.01	-2.16 ± 0.03	0.00 ± 0.03	0.00	0.00	0.00	NM
NGC 7789	2M23571847+5650271	-55.5 ± 0.1	0.01 ± 0.01	-1.14 ± 0.05	-1.86 ± 0.05	0.88	0.49	0.54	GM
NGC 7789	2M23571885+5659355	-59.4 ± 0.2	-0.49 ± 0.01	-6.87 ± 0.03	-4.69 ± 0.03	0.00	-1.00	0.00	NM
NGC 7789	2M23572242+5641459	-54.9 ± 0.1	0.06 ± 0.01	-1.02 ± 0.05	-1.55 ± 0.04	0.99	0.92	0.13	GM
NGC 7789	2M23572545+5639376	-82.7 ± 3.7	-0.07 ± 0.01	4.86 ± 0.05	-23.10 ± 0.05	0.00	0.00	0.00	NM
NGC 7789	2M23573126+5635167	-19.6 ± 0.0	0.20 ± 0.01	15.37 ± 0.05	-19.30 ± 0.04	0.00	-1.00	0.00	NM
NGC 7789	2M23573184+5641221	-55.8 ± 0.1	0.05 ± 0.01	-0.99 ± 0.07	-1.95 ± 0.06	0.82	0.99	0.95	GM
NGC 7789	2M23573563+5640000	-54.7 ± 0.1	0.08 ± 0.01	-0.94 ± 0.05	-1.79 ± 0.04	1.00	0.60	0.74	GM
NGC 7789	2M23573895+5638370	-54.6 ± 0.6	-0.27 ± 0.01	-1.01 ± 0.03	-1.72 ± 0.03	1.00	-1.00	0.50	DM

Continued on next page

Table A.1 – Continued

Cluster name	2MASS ID	RV (km s^{-1})	[Fe/H] (dex)	μ_α (mas yr^{-1})	μ_δ (mas yr^{-1})	RV Prob	[Fe/H] Prob	PM Prob	Memb
NGC 7789	2M23574745+5650095	-51.2 ± 0.1	0.15 ± 0.01	-0.84 ± 0.03	-2.04 ± 0.02	0.17	0.00	0.78	NM
NGC 7789	2M23575066+5657272	-35.0 ± 0.0	-0.13 ± 0.01	-2.67 ± 0.05	-2.32 ± 0.04	0.00	0.00	0.00	NM
NGC 7789	2M23575198+5616414	-16.6 ± 2.8	0.05 ± 0.01	3.55 ± 0.04	0.12 ± 0.04	0.00	0.00	0.00	NM
NGC 7789	2M23575438+5647439	-53.6 ± 0.1	0.04 ± 0.01	-0.55 ± 0.09	-1.59 ± 0.07	0.85	0.90	0.03	GM
NGC 7789	2M23575458+5656165	-38.2 ± 0.0	0.04 ± 0.01	-5.04 ± 0.04	-2.77 ± 0.04	0.00	0.90	0.00	NM
NGC 7789	2M23580015+5650125	-54.5 ± 0.1	0.02 ± 0.01	-0.97 ± 0.05	-1.86 ± 0.04	1.00	0.64	0.92	GM
NGC 7789	2M23580275+5647208	-54.4 ± 0.0	0.04 ± 0.01	-0.85 ± 0.04	-1.97 ± 0.04	0.99	0.98	0.92	GM
NGC 7789	2M23580564+5649404	-71.9 ± 0.1	-0.43 ± 0.01	-3.31 ± 0.04	-1.21 ± 0.03	0.00	0.00	0.00	NM
NGC 7789	2M23581471+5651466	-56.1 ± 0.0	0.06 ± 0.01	-0.85 ± 0.05	-1.78 ± 0.04	0.73	0.94	0.66	GM
NGC 7789	2M23583199+5657304	-44.6 ± 0.1	-0.21 ± 0.01	-3.77 ± 0.03	-0.87 ± 0.03	0.00	0.00	0.00	NM
NGC 7789	2M23583343+5635047	-55.0 ± 0.1	-0.12 ± 0.01	-1.08 ± 0.05	-1.92 ± 0.05	0.98	0.00	0.74	NM
NGC 7789	2M23584180+5651146	-33.2 ± 0.1	-0.32 ± 0.01	-1.70 ± 0.04	0.04 ± 0.03	0.00	0.00	0.00	NM
NGC 7789	2M23584368+5707550	-87.2 ± 0.2	-0.09 ± 0.01	-2.01 ± 0.04	-3.34 ± 0.03	0.00	0.00	0.00	NM
NGC 7789	2M23584648+5638183	-93.8 ± 0.0	-0.44 ± 0.01	-1.16 ± 0.04	0.63 ± 0.04	0.00	0.00	0.00	NM
NGC 7789	2M23585296+5659204	-55.5 ± 0.0	-0.02 ± 0.01	-6.57 ± 0.04	-1.30 ± 0.04	0.00	0.00	0.00	NM
NGC 7789	2M23585468+5700306	-64.8 ± 0.1	-0.12 ± 0.01	-2.12 ± 0.03	-1.45 ± 0.03	0.00	0.00	0.00	NM
NGC 7789	2M23585484+5622588	-82.9 ± 0.1	-0.08 ± 0.01	-3.37 ± 0.03	-1.72 ± 0.03	0.00	0.00	0.00	NM
NGC 7789	2M23585820+5624317	-117.7 ± 0.4	-0.28 ± 0.01	-1.06 ± 0.05	-1.52 ± 0.04	0.00	0.00	0.09	NM
NGC 7789	2M23585861+5702009	-84.3 ± 0.0	-0.30 ± 0.01	-2.47 ± 0.05	-1.43 ± 0.04	0.00	0.00	0.00	NM
NGC 7789	2M23590085+5621116	-87.0 ± 0.3	-0.05 ± 0.01	-3.42 ± 0.03	-0.48 ± 0.03	0.00	0.00	0.00	NM
NGC 7789	2M23590494+5630245	-104.5 ± 0.1	0.07 ± 0.01	-2.24 ± 0.04	-1.45 ± 0.03	0.00	0.00	0.00	NM
NGC 7789	2M23590685+5703369	-39.8 ± 23.3	-0.21 ± 0.01	-4.92 ± 0.04	-4.35 ± 0.03	0.00	0.00	0.00	NM
NGC 7789	2M23591253+5633484	-56.7 ± 0.2	-0.54 ± 0.01	2.32 ± 0.03	3.60 ± 0.03	0.00	0.00	0.00	NM
NGC 7789	2M23591965+5648504	-50.4 ± 0.1	-0.17 ± 0.01	-9.95 ± 0.05	-1.52 ± 0.04	0.00	0.00	0.00	NM
NGC 7789	2M23592385+5703106	-60.0 ± 0.0	-0.58 ± 0.01	3.46 ± 0.04	-0.78 ± 0.03	0.00	0.00	0.00	NM
NGC 7789	2M23594182+5637552	-27.4 ± 0.0	0.07 ± 0.01	0.63 ± 0.05	-2.70 ± 0.04	0.00	0.00	0.00	NM
NGC 7789	2M23595837+5700444	-70.4 ± 0.1	-0.41 ± 0.01	-3.28 ± 0.04	-0.76 ± 0.04	0.00	0.00	0.00	NM
FSR 0494	2M00244088+6341178	-56.2 ± 0.0	0.31 ± 0.01	-3.97 ± 0.04	-0.63 ± 0.04	0.00	0.00	0.01	NM
FSR 0494	2M00244149+6344347	-55.1 ± 0.3	-0.38 ± 0.01	-2.80 ± 0.11	0.44 ± 0.08	0.00	0.00	0.05	NM
FSR 0494	2M00244484+6353233	-5.9 ± 0.0	-0.19 ± 0.01	8.49 ± 0.04	-3.11 ± 0.04	0.00	0.00	0.00	NM
FSR 0494	2M00245394+6340553	-83.7 ± 0.1	-0.13 ± 0.01	-3.96 ± 0.04	-0.29 ± 0.04	0.00	0.00	0.00	NM
FSR 0494	2M00250743+6352480	-37.9 ± 0.0	-0.20 ± 0.01	-5.34 ± 0.03	-1.91 ± 0.03	0.00	0.00	0.00	NM
FSR 0494	2M00250773+6341202	-74.1 ± 0.2	-0.23 ± 0.01	-2.08 ± 0.10	-0.04 ± 0.08	0.00	0.00	0.33	NM
FSR 0494	2M00251367+6348591	-62.9 ± 0.0	-0.07 ± 0.01	-1.60 ± 0.06	-1.12 ± 0.05	1.00	0.00	0.13	NM
FSR 0494	2M00251373+6345437	-60.2 ± 0.1	-0.08 ± 0.01	-2.54 ± 0.06	0.82 ± 0.04	0.48	0.00	0.01	NM
FSR 0494	2M00251423+6338077	-48.8 ± 0.2	-0.13 ± 0.01	-2.17 ± 0.04	-0.80 ± 0.03	0.00	0.00	0.80	NM
FSR 0494	2M00251609+6346352	-94.8 ± 0.1	0.13 ± 0.01	-0.74 ± 0.06	0.36 ± 0.04	0.00	0.00	0.00	NM
FSR 0494	2M00252183+6350478	-33.7 ± 0.1	-0.03 ± 0.01	5.73 ± 0.05	-5.39 ± 0.04	0.00	0.00	0.00	NM
FSR 0494	2M00252192+6337541	-113.5 ± 0.0	-0.42 ± 0.01	-4.33 ± 0.05	-0.77 ± 0.04	0.00	0.00	0.00	NM
FSR 0494	2M00253373+6345239	-64.2 ± 0.0	0.03 ± 0.01	-2.62 ± 0.05	-0.90 ± 0.04	0.88	0.64	0.82	GM
FSR 0494	2M00253400+6346574	-64.3 ± 0.1	0.02 ± 0.01	-2.46 ± 0.06	-0.72 ± 0.05	0.87	1.00	0.99	GM
FSR 0494	2M00253826+6344101	-63.5 ± 0.1	0.01 ± 0.01	-2.51 ± 0.06	-0.87 ± 0.05	0.98	0.98	0.89	GM
FSR 0494	2M00253997+6340595	-0.2 ± 0.1	0.18 ± 0.01	0.37 ± 0.05	-1.72 ± 0.04	0.00	0.00	0.00	NM
FSR 0494	2M00254447+6345058	-79.3 ± 2.7	-0.02 ± 0.01	-2.57 ± 0.04	-0.90 ± 0.04	0.00	0.05	0.84	NM
FSR 0494	2M00255011+6343565	-60.4 ± 0.1	0.01 ± 0.01	-2.57 ± 0.06	-0.92 ± 0.05	0.53	0.96	0.83	GM
FSR 0494	2M00260027+6343287	-63.9 ± 0.1	-0.02 ± 0.01	-2.53 ± 0.06	-0.85 ± 0.05	0.93	0.08	0.91	GM
FSR 0494	2M00260429+6343040	-38.6 ± 0.1	0.02 ± 0.01	-0.93 ± 0.08	0.45 ± 0.06	0.00	0.85	0.00	NM
FSR 0494	2M00260492+6339353	-83.6 ± 0.1	-0.12 ± 0.01	-1.59 ± 0.06	0.22 ± 0.05	0.00	0.00	0.04	NM
FSR 0494	2M00260720+6352354	-50.5 ± 0.0	-0.03 ± 0.01	-6.38 ± 0.04	-2.47 ± 0.03	0.00	0.00	0.00	NM
FSR 0494	2M00261895+6352376	-82.3 ± 0.1	0.05 ± 0.01	0.47 ± 0.22	-1.02 ± 0.17	0.00	0.00	0.00	NM
FSR 0494	2M00262464+6354460	-78.1 ± 0.2	-0.25 ± 0.01	-2.40 ± 0.06	0.67 ± 0.05	0.00	0.00	0.02	NM
FSR 0494	2M00264227+6345059	-85.4 ± 0.0	-0.04 ± 0.01	-3.36 ± 0.04	-0.12 ± 0.05	0.00	0.00	0.09	NM
FSR 0494	2M00265230+6337184	-51.8 ± 0.1	0.10 ± 0.01	12.57 ± 0.03	2.07 ± 0.03	0.00	-1.00	0.00	NM
FSR 0494	2M00265251+6351059	-106.8 ± 0.0	0.06 ± 0.01	-2.05 ± 0.06	-1.12 ± 0.06	0.00	0.00	0.44	NM
NGC 188	2M00214840+8521385	9.9 ± 2.5	-0.18 ± 0.01	15.50 ± 0.29	1.37 ± 0.23	0.00	-1.00	0.00	NM
NGC 188	2M00220828+8527196	25.4 ± 0.1	0.27 ± 0.01	60.51 ± 0.03	6.19 ± 0.02	0.00	-1.00	0.00	NM
NGC 188	2M00234604+8507158	-75.6 ± 0.1	0.17 ± 0.01	5.51 ± 0.04	3.65 ± 0.03	0.00	-1.00	0.00	NM
NGC 188	2M00243191+8509159	-54.4 ± 0.0	-0.00 ± 0.01	-6.47 ± 0.04	7.34 ± 0.03	0.00	0.00	0.00	NM
NGC 188	2M00250337+8520037	-45.4 ± 0.0	-0.38 ± 0.01	13.60 ± 0.03	45.65 ± 0.02	0.00	-1.00	0.00	NM
NGC 188	2M00260624+8532326	8.8 ± 0.2	-0.31 ± 0.01	29.56 ± 1.73	-32.73 ± 1.99	0.00	-1.00	0.00	NM
NGC 188	2M00261005+8506091	-62.3 ± 0.1	-0.14 ± 0.01	-9.05 ± 0.28	4.88 ± 0.27	0.00	-1.00	0.00	NM
NGC 188	2M00265017+8538319	7.8 ± 0.1	-0.21 ± 0.01	7.64 ± 0.05	5.98 ± 0.04	0.00	-1.00	0.00	NM
NGC 188	2M00271909+8518135	-41.5 ± 0.2	0.17 ± 0.01	-2.32 ± 0.04	-1.21 ± 0.04	0.00	0.00	0.30	NM

Continued on next page

Table A.1 – Continued

Cluster name	2MASS ID	RV (km s^{-1})	[Fe/H] (dex)	μ_α (mas yr^{-1})	μ_δ (mas yr^{-1})	RV Prob	[Fe/H] Prob	PM Prob	Memb
NGC 188	2M00274728+8449362	-64.2 ± 0.1	-0.13 ± 0.01	-0.68 ± 0.05	0.78 ± 0.04	0.00	0.00	0.00	NM
NGC 188	2M00280841+8522089	-20.4 ± 0.1	-0.15 ± 0.01	15.09 ± 0.03	1.45 ± 0.03	0.00	-1.00	0.00	NM
NGC 188	2M00281957+8528084	-92.9 ± 0.2	-0.66 ± 0.01	-1.98 ± 0.04	2.95 ± 0.04	0.00	0.00	0.00	NM
NGC 188	2M00282391+8513282	-43.0 ± 0.2	-0.32 ± 0.01	1.55 ± 0.03	-5.26 ± 0.03	0.00	-1.00	0.00	NM
NGC 188	2M00283971+8530377	-48.9 ± 0.2	0.08 ± 0.01	-2.86 ± 0.03	1.61 ± 0.03	0.00	0.00	0.00	NM
NGC 188	2M00285616+8458283	-12.5 ± 0.1	-0.22 ± 0.01	-1.00 ± 0.03	1.16 ± 0.03	0.00	0.00	0.00	NM
NGC 188	2M00290883+8538194	-55.8 ± 0.1	-0.43 ± 0.01	5.56 ± 0.03	-3.56 ± 0.03	0.00	-1.00	0.00	NM
NGC 188	2M00293513+8453101	-6.0 ± 0.0	0.08 ± 0.01	15.36 ± 0.04	12.22 ± 0.03	0.00	-1.00	0.00	NM
NGC 188	2M00302055+8538318	-37.9 ± 2.5	0.40 ± 0.01	8.17 ± 0.03	9.71 ± 0.03	0.00	-1.00	0.00	NM
NGC 188	2M00302772+8505006	-18.5 ± 0.1	0.25 ± 0.01	2.72 ± 0.03	-0.39 ± 0.03	0.00	-1.00	0.00	NM
NGC 188	2M00304683+8506596	-44.0 ± 0.1	-0.38 ± 0.01	-1.18 ± 0.02	-0.95 ± 0.03	0.00	0.00	0.00	NM
NGC 188	2M00310678+8508494	-12.3 ± 0.4	0.04 ± 0.01	23.69 ± 0.04	-5.87 ± 0.05	0.00	-1.00	0.00	NM
NGC 188	2M00311352+8448490	5.5 ± 0.1	-0.19 ± 0.01	12.54 ± 0.05	-16.47 ± 0.04	0.00	-1.00	0.00	NM
NGC 188	2M00320079+8511465	-42.3 ± 0.0	0.17 ± 0.01	-2.34 ± 0.04	-1.11 ± 0.04	0.00	0.00	0.64	NM
NGC 188	2M00320426+8522568	-63.4 ± 0.7	-0.61 ± 0.01	-1.36 ± 0.04	1.69 ± 0.05	0.00	0.00	0.00	NM
NGC 188	2M00320949+8502263	-44.3 ± 0.1	0.07 ± 0.01	-1.82 ± 0.11	5.26 ± 0.09	0.00	-1.00	0.00	NM
NGC 188	2M00321775+8519580	-16.9 ± 0.1	0.25 ± 0.01	6.87 ± 0.03	1.65 ± 0.03	0.00	-1.00	0.00	NM
NGC 188	2M00322120+8518390	-51.8 ± 32.5	-0.01 ± 0.01	-2.28 ± 0.04	-1.09 ± 0.03	0.00	0.00	0.74	NM
NGC 188	2M00322263+8526069	-41.1 ± 0.4	-0.53 ± 0.01	-2.17 ± 0.04	4.70 ± 0.04	0.00	-1.00	0.00	NM
NGC 188	2M00325164+8445517	-24.0 ± 0.0	-0.03 ± 0.01	-0.93 ± 0.03	1.04 ± 0.03	0.00	0.00	0.00	NM
NGC 188	2M00325807+8512069	-61.0 ± 0.1	-0.04 ± 0.01	-0.38 ± 0.04	-0.12 ± 0.04	0.00	0.00	0.00	NM
NGC 188	2M00330093+8454150	-4.5 ± 0.2	0.00 ± 0.01	-10.38 ± 0.04	-7.76 ± 0.04	0.00	-1.00	0.00	NM
NGC 188	2M00332038+8454103	-3.4 ± 0.1	0.25 ± 0.01	22.69 ± 0.05	10.41 ± 0.05	0.00	-1.00	0.00	NM
NGC 188	2M00332074+8510002	-1.0 ± 0.1	0.44 ± 0.01	11.05 ± 0.04	-0.26 ± 0.04	0.00	0.00	0.00	NM
NGC 188	2M00332817+8451593	-73.5 ± 0.0	-0.00 ± 0.01	-14.57 ± 0.31	-5.05 ± 0.24	0.00	-1.00	0.00	NM
NGC 188	2M00334320+8523017	-68.7 ± 1.2	-0.18 ± 0.01	0.67 ± 0.03	3.71 ± 0.03	0.00	-1.00	0.00	NM
NGC 188	2M00334975+8448198	-59.2 ± 0.1	-0.27 ± 0.01	-0.44 ± 0.04	-0.91 ± 0.04	0.00	0.00	0.00	NM
NGC 188	2M00341150+8526111	-41.9 ± 0.2	-0.53 ± 0.01	-2.14 ± 0.04	-2.84 ± 0.04	0.00	0.00	0.00	NM
NGC 188	2M00343487+8452069	-37.2 ± 63.7	-0.15 ± 0.01	-11.91 ± 0.06	0.62 ± 0.04	0.00	-1.00	0.00	NM
NGC 188	2M00344509+8512058	-38.8 ± 6.8	0.07 ± 0.01	-2.34 ± 0.04	-1.11 ± 0.04	0.26	0.06	0.62	GM
NGC 188	2M00345382+8532431	-8.8 ± 0.0	-0.01 ± 0.01	16.01 ± 0.03	6.54 ± 0.03	0.00	-1.00	0.00	NM
NGC 188	2M00345967+8524489	-26.0 ± 0.2	-0.36 ± 0.01	3.94 ± 0.04	5.43 ± 0.04	0.00	-1.00	0.00	NM
NGC 188	2M00350324+8452103	-43.0 ± 0.1	-0.25 ± 0.01	-7.30 ± 0.07	1.65 ± 0.05	0.00	0.00	0.00	NM
NGC 188	2M00360773+8534155	-58.0 ± 0.6	0.12 ± 0.01	15.49 ± 0.04	4.09 ± 0.04	0.00	-1.00	0.00	NM
NGC 188	2M00362011+8445432	4.3 ± 0.2	0.18 ± 0.01	24.06 ± 0.03	0.36 ± 0.03	0.00	-1.00	0.00	NM
NGC 188	2M00363416+8529046	-42.9 ± 49.1	-0.17 ± 0.01	-7.29 ± 0.04	3.07 ± 0.04	0.00	-1.00	0.00	NM
NGC 188	2M00364556+8454157	7.9 ± 0.2	-0.01 ± 0.01	14.98 ± 0.05	0.37 ± 0.03	0.00	-1.00	0.00	NM
NGC 188	2M00365177+8451529	-29.2 ± 0.0	-0.21 ± 0.01	5.49 ± 0.18	1.60 ± 0.13	0.00	-1.00	0.00	NM
NGC 188	2M00370172+8455256	-38.5 ± 0.5	-0.62 ± 0.01	-0.11 ± 0.04	-8.94 ± 0.03	0.00	-1.00	0.00	NM
NGC 188	2M00370540+8506214	-36.2 ± 0.2	0.16 ± 0.01	4.77 ± 0.03	3.54 ± 0.03	0.01	-1.00	0.00	NM
NGC 188	2M00370650+8507344	3.9 ± 0.1	-0.16 ± 0.01	4.40 ± 0.04	-0.86 ± 0.04	0.00	0.00	0.00	NM
NGC 188	2M00373960+8457317	-17.8 ± 0.4	0.01 ± 0.01	-11.39 ± 0.03	3.77 ± 0.03	0.00	-1.00	0.00	NM
NGC 188	2M00383864+8523453	-26.9 ± 0.2	0.02 ± 0.01	0.13 ± 0.04	2.11 ± 0.03	0.00	-1.00	0.00	NM
NGC 188	2M00383985+8500218	-15.4 ± 0.0	-0.16 ± 0.01	1.01 ± 0.04	1.67 ± 0.03	0.00	0.00	0.00	NM
NGC 188	2M00392911+8443569	-15.4 ± 0.1	0.33 ± 0.01	47.02 ± 0.05	19.91 ± 0.04	0.00	-1.00	0.00	NM
NGC 188	2M00392934+8500595	-47.9 ± 0.7	-0.31 ± 0.01	44.61 ± 0.03	-13.93 ± 0.02	0.01	-1.00	0.00	NM
NGC 188	2M00394524+8449597	-42.1 ± 0.2	0.01 ± 0.01	-2.25 ± 0.05	-0.94 ± 0.03	0.00	0.00	0.93	NM
NGC 188	2M00395193+8520363	-0.2 ± 0.0	0.02 ± 0.01	19.00 ± 0.04	-2.30 ± 0.04	0.00	-1.00	0.00	NM
NGC 188	2M00401683+8531380	-22.0 ± 0.3	0.20 ± 0.01	4.22 ± 0.03	-4.24 ± 0.03	0.00	-1.00	0.00	NM
NGC 188	2M00404318+8510373	-8.3 ± 0.6	-0.35 ± 0.01	2.77 ± 0.04	-1.51 ± 0.03	0.00	-1.00	0.00	NM
NGC 188	2M00404570+8514568	-9.8 ± 0.0	0.26 ± 0.01	9.51 ± 0.03	6.37 ± 0.02	0.00	-1.00	0.00	NM
NGC 188	2M00405390+8527104	-42.4 ± 0.0	-0.04 ± 0.01	-2.88 ± 0.02	2.50 ± 0.02	0.97	0.00	0.00	NM
NGC 188	2M00410020+8511328	-24.4 ± 0.1	0.18 ± 0.01	-9.19 ± 0.04	4.72 ± 0.04	0.00	0.42	0.00	NM
NGC 188	2M00410552+8448262	-14.9 ± 0.1	-0.03 ± 0.01	-5.43 ± 0.06	10.68 ± 0.04	0.00	-1.00	0.00	NM
NGC 188	2M00413078+8502123	-13.8 ± 0.1	-0.68 ± 0.01	19.81 ± 0.04	-6.78 ± 0.03	0.00	0.00	0.00	NM
NGC 188	2M00414022+8545581	-23.9 ± 0.1	0.08 ± 0.01	0.32 ± 0.03	1.60 ± 0.03	0.00	0.00	0.00	NM
NGC 188	2M00414928+8505299	-23.5 ± 0.1	0.17 ± 0.01	30.40 ± 0.03	-0.53 ± 0.02	0.00	-1.00	0.00	NM
NGC 188	2M00415197+8527070	-42.6 ± 0.1	0.17 ± 0.01	-2.20 ± 0.04	-1.01 ± 0.04	0.94	0.70	0.82	GM
NGC 188	2M00420347+8522520	-80.4 ± 0.1	-0.19 ± 0.01	-0.75 ± 0.05	1.92 ± 0.04	0.00	0.00	0.00	NM
NGC 188	2M00420349+8501088	-34.0 ± 0.1	0.06 ± 0.01	52.92 ± 0.05	24.38 ± 0.04	0.00	-1.00	0.00	NM
NGC 188	2M00421194+8454240	-72.5 ± 0.1	-0.47 ± 0.01	-13.54 ± 0.05	17.93 ± 0.04	0.00	-1.00	0.00	NM
NGC 188	2M00421653+8544323	-23.1 ± 0.2	0.01 ± 0.01	0.33 ± 0.03	1.15 ± 0.03	0.00	-1.00	0.00	NM
NGC 188	2M00422570+8516219	-40.3 ± 0.0	0.14 ± 0.01	-2.03 ± 0.05	-0.82 ± 0.04	0.70	0.99	0.18	GM

Continued on next page

Table A.1 – Continued

Cluster name	2MASS ID	RV (km s^{-1})	[Fe/H] (dex)	μ_α (mas yr^{-1})	μ_δ (mas yr^{-1})	RV Prob	[Fe/H] Prob	PM Prob	Memb
NGC 188	2M00423766+8450214	-23.4 ± 0.2	-0.36 ± 0.01	2.60 ± 0.06	2.55 ± 0.04	0.00	-1.00	0.00	NM
NGC 188	2M00432328+8448184	-50.9 ± 0.1	0.26 ± 0.01	-4.77 ± 0.03	-0.04 ± 0.03	0.00	-1.00	0.00	NM
NGC 188	2M00434931+8522225	-54.8 ± 0.1	-0.42 ± 0.01	63.07 ± 0.04	-1.50 ± 0.03	0.00	-1.00	0.00	NM
NGC 188	2M00441812+8516024	-36.7 ± 9.5	0.05 ± 0.01	-14.70 ± 0.03	6.63 ± 0.02	0.02	-1.00	0.00	NM
NGC 188	2M00444460+8532163	-42.2 ± 0.1	0.14 ± 0.01	-2.38 ± 0.03	-0.93 ± 0.02	0.99	0.96	0.92	GM
NGC 188	2M00444521+8525347	-45.2 ± 0.1	0.02 ± 0.01	0.48 ± 0.04	2.71 ± 0.03	0.24	-1.00	0.00	NM
NGC 188	2M00445183+8446137	1.6 ± 0.1	0.24 ± 0.01	-13.62 ± 0.05	-3.63 ± 0.04	0.00	-1.00	0.00	NM
NGC 188	2M00454489+8504180	-42.6 ± 0.8	0.12 ± 0.01	-2.16 ± 0.04	-0.96 ± 0.03	0.95	0.80	0.71	GM
NGC 188	2M00454764+8500111	-109.6 ± 0.1	-0.06 ± 0.01	-0.59 ± 0.45	2.88 ± 0.33	0.00	0.00	0.00	NM
NGC 188	2M00454828+8451091	-47.2 ± 0.1	0.11 ± 0.01	-6.10 ± 0.04	-3.83 ± 0.03	0.00	-1.00	0.00	NM
NGC 188	2M00462757+8510261	-17.2 ± 0.0	-0.29 ± 0.01	0.60 ± 0.03	-1.30 ± 0.02	0.00	-1.00	0.00	NM
NGC 188	2M00463232+8449541	-59.2 ± 0.1	0.13 ± 0.01	-3.09 ± 0.04	3.21 ± 0.03	0.00	-1.00	0.00	NM
NGC 188	2M00463676+8541092	-22.4 ± 0.1	0.07 ± 0.01	5.51 ± 0.03	-3.54 ± 0.02	0.00	0.00	0.00	NM
NGC 188	2M00463801+8441448	-52.6 ± 4.7	-0.10 ± 0.01	1.71 ± 0.05	3.56 ± 0.04	0.00	-1.00	0.00	NM
NGC 188	2M00463920+8523336	-41.0 ± 4.9	0.13 ± 0.01	-2.59 ± 0.04	-0.70 ± 0.04	0.87	0.93	0.13	GM
NGC 188	2M00465109+8441110	-46.4 ± 0.2	-0.13 ± 0.01	-2.50 ± 0.03	-0.52 ± 0.02	0.00	0.00	0.03	NM
NGC 188	2M00465194+8459289	4.3 ± 1.7	-0.51 ± 0.01	0.56 ± 0.05	-3.24 ± 0.04	0.00	0.00	0.00	NM
NGC 188	2M00470330+8542522	-104.5 ± 0.1	-0.45 ± 0.01	-0.09 ± 0.03	1.73 ± 0.02	0.00	0.00	0.00	NM
NGC 188	2M00471754+8456301	-65.4 ± 0.2	-0.12 ± 0.01	24.15 ± 0.04	-8.18 ± 0.03	0.00	-1.00	0.00	NM
NGC 188	2M00472975+8524140	-40.9 ± 0.0	0.18 ± 0.01	-2.37 ± 0.05	-0.95 ± 0.04	0.86	0.44	0.95	GM
NGC 188	2M00473059+8528566	-42.2 ± 0.2	0.02 ± 0.01	-2.33 ± 0.04	-1.01 ± 0.04	0.99	0.00	0.94	NM
NGC 188	2M00473076+8454480	-12.4 ± 0.4	-0.06 ± 0.01	12.93 ± 0.30	4.26 ± 0.23	0.00	-1.00	0.00	NM
NGC 188	2M00473246+8448081	-81.8 ± 0.3	-0.48 ± 0.01	24.98 ± 0.04	-3.42 ± 0.03	0.00	-1.00	0.00	NM
NGC 188	2M00475315+8504023	-13.7 ± 0.3	-0.25 ± 0.01	-2.72 ± 0.03	-2.50 ± 0.03	0.00	-1.00	0.00	NM
NGC 188	2M00475858+8458472	-31.0 ± 0.1	0.13 ± 0.01	3.16 ± 0.31	8.02 ± 0.20	0.00	-1.00	0.00	NM
NGC 188	2M00482923+8520326	-43.3 ± 0.1	-0.29 ± 0.01	-10.85 ± 0.03	2.68 ± 0.02	0.78	-1.00	0.00	NM
NGC 188	2M00491917+8440009	-27.1 ± 0.0	0.36 ± 0.01	31.06 ± 0.03	4.36 ± 0.02	0.00	-1.00	0.00	NM
NGC 188	2M00492040+8518388	-67.8 ± 0.0	0.18 ± 0.01	-13.22 ± 0.05	-24.77 ± 0.03	0.00	-1.00	0.00	NM
NGC 188	2M00492985+8538189	-38.6 ± 0.1	0.03 ± 0.01	-7.12 ± 0.03	-7.27 ± 0.02	0.00	-1.00	0.00	NM
NGC 188	2M00493147+8500016	-20.5 ± 0.6	-0.21 ± 0.01	-13.35 ± 0.10	9.36 ± 0.07	0.00	-1.00	0.00	NM
NGC 188	2M00493469+8547296	-27.3 ± 0.2	-0.29 ± 0.01	16.79 ± 0.07	2.10 ± 0.06	0.00	0.00	0.00	NM
NGC 188	2M00493568+8544408	5.6 ± 1.0	-0.38 ± 0.01	-8.24 ± 0.15	-6.33 ± 0.05	0.00	-1.00	0.00	NM
NGC 188	2M00493706+8529330	-6.8 ± 0.1	-0.05 ± 0.01	6.35 ± 0.06	-3.62 ± 0.05	0.00	-1.00	0.00	NM
NGC 188	2M00494354+8454272	-114.2 ± 0.1	-0.49 ± 0.01	-1.37 ± 0.04	0.71 ± 0.03	0.00	0.00	0.00	NM
NGC 188	2M00504066+8453499	25.3 ± 0.1	-0.36 ± 0.01	22.42 ± 0.03	-9.46 ± 0.03	0.00	-1.00	0.00	NM
NGC 188	2M00512176+8512377	-40.2 ± 0.1	0.13 ± 0.01	-2.43 ± 0.03	-0.86 ± 0.02	0.67	0.88	0.72	GM
NGC 188	2M00513648+8443583	-42.9 ± 5.7	0.33 ± 0.01	-10.90 ± 0.04	-0.45 ± 0.04	0.00	-1.00	0.00	NM
NGC 188	2M00520845+8519573	-60.3 ± 0.1	-0.43 ± 0.01	-0.36 ± 0.05	0.55 ± 0.04	0.00	0.00	0.00	NM
NGC 188	2M00520873+8517190	-45.2 ± 0.4	0.07 ± 0.01	22.65 ± 0.05	25.29 ± 0.03	0.23	-1.00	0.00	NM
NGC 188	2M00522777+8444434	-40.3 ± 0.0	0.03 ± 0.01	-2.58 ± 0.04	0.14 ± 0.04	0.00	0.00	0.00	NM
NGC 188	2M00523662+8500184	-19.7 ± 0.2	-0.03 ± 0.01	0.07 ± 0.06	0.99 ± 0.04	0.00	-1.00	0.00	NM
NGC 188	2M00530810+8450348	-29.0 ± 0.1	-0.46 ± 0.01	-0.27 ± 0.04	1.03 ± 0.03	0.00	0.00	0.00	NM
NGC 188	2M00532016+8508553	-22.2 ± 1.0	0.16 ± 0.01	-23.01 ± 0.05	-2.49 ± 0.04	0.00	-1.00	0.00	NM
NGC 188	2M00533497+8511145	-42.1 ± 0.1	0.10 ± 0.01	-2.32 ± 0.03	-0.89 ± 0.02	1.00	0.36	0.93	GM
NGC 188	2M00533572+8520583	-42.7 ± 0.1	0.16 ± 0.01	-2.27 ± 0.04	-0.97 ± 0.04	0.92	0.92	0.97	GM
NGC 188	2M00541152+8515231	-42.1 ± 0.1	0.14 ± 0.01	-2.33 ± 0.05	-0.87 ± 0.04	1.00	1.00	0.88	GM
NGC 188	2M00542287+8455398	-42.6 ± 0.1	0.11 ± 0.01	-2.28 ± 0.03	-0.94 ± 0.03	0.00	0.00	0.97	NM
NGC 188	2M00542989+8450545	-36.4 ± 0.7	-0.14 ± 0.02	-7.34 ± 0.03	1.44 ± 0.02	0.00	-1.00	0.00	NM
NGC 188	2M00543664+8501152	-42.4 ± 0.0	0.16 ± 0.01	-2.30 ± 0.05	-0.91 ± 0.04	0.97	0.85	0.95	GM
NGC 188	2M00551101+8522510	-83.1 ± 3.2	0.01 ± 0.01	2.54 ± 0.08	-14.57 ± 0.06	0.00	-1.00	0.00	NM
NGC 188	2M00552582+8542389	-27.2 ± 0.5	-0.36 ± 0.01	-1.01 ± 0.02	0.03 ± 0.02	0.00	0.00	0.00	NM
NGC 188	2M00554526+8512209	-40.0 ± 0.1	-0.33 ± 0.01	-2.53 ± 0.05	0.22 ± 0.04	0.59	0.00	0.00	NM
NGC 188	2M00554649+8454427	-21.8 ± 0.2	-0.45 ± 0.01	-1.40 ± 0.03	1.18 ± 0.02	0.00	0.00	0.00	NM
NGC 188	2M00561381+8450190	-56.7 ± 0.0	-0.15 ± 0.01	-7.39 ± 0.04	0.58 ± 0.03	0.00	-1.00	0.00	NM
NGC 188	2M00562255+8459582	10.0 ± 0.0	-0.09 ± 0.01	-0.30 ± 0.05	8.95 ± 0.04	0.00	-1.00	0.00	NM
NGC 188	2M00571844+8510288	-42.0 ± 0.0	0.18 ± 0.01	-2.34 ± 0.05	-0.87 ± 0.03	1.00	0.46	0.87	GM
NGC 188	2M00573487+8542430	-49.0 ± 0.3	-0.20 ± 0.01	21.35 ± 0.03	-14.99 ± 0.02	0.00	-1.00	0.00	NM
NGC 188	2M00573719+8452524	-56.0 ± 0.7	0.13 ± 0.01	-17.07 ± 0.03	-2.78 ± 0.02	0.00	-1.00	0.00	NM
NGC 188	2M00574795+8502290	-96.5 ±103.0	-0.87 ± 0.01	-13.08 ± 0.03	7.97 ± 0.03	0.00	0.00	0.00	NM
NGC 188	2M00581608+8528569	-26.0 ± 0.2	0.18 ± 0.01	8.04 ± 0.11	6.84 ± 0.10	0.00	-1.00	0.00	NM
NGC 188	2M00581691+8540183	-42.7 ± 0.1	0.18 ± 0.01	-2.31 ± 0.03	-0.70 ± 0.03	0.00	0.00	0.32	NM
NGC 188	2M00591212+8458279	-210.7 ± 0.1	-0.69 ± 0.01	-1.61 ± 0.03	1.79 ± 0.02	0.00	0.00	0.00	NM
NGC 188	2M00591266+8529340	-1.1 ± 0.1	-0.08 ± 0.01	6.85 ± 0.04	-16.20 ± 0.03	0.00	-1.00	0.00	NM

Continued on next page

Table A.1 – Continued

Cluster name	2MASS ID	RV (km s^{-1})	[Fe/H] (dex)	μ_α (mas yr^{-1})	μ_δ (mas yr^{-1})	RV Prob	[Fe/H] Prob	PM Prob	Memb
NGC 188	2M00593409+8503084	-89.6 ± 0.9	-0.79 ± 0.01	8.24 ± 0.05	-5.65 ± 0.03	0.00	-1.00	0.00	NM
NGC 188	2M00595090+8450392	-3.7 ± 0.0	0.05 ± 0.01	1.11 ± 0.05	-0.51 ± 0.04	0.00	0.00	0.00	NM
NGC 188	2M01000342+8452559	-47.9 ± 0.1	-0.12 ± 0.01	1.33 ± 0.05	0.58 ± 0.04	0.00	0.00	0.00	NM
NGC 188	2M01002279+8535123	-104.8 ± 0.1	-0.42 ± 0.01	-1.13 ± 0.04	0.35 ± 0.03	0.00	0.00	0.00	NM
NGC 188	2M01003483+8503198	-42.0 ± 0.1	0.12 ± 0.01	-2.36 ± 0.04	-0.92 ± 0.03	0.00	0.00	0.95	NM
NGC 188	2M01012824+8456243	-53.3 ± 0.1	0.28 ± 0.01	12.96 ± 0.05	6.92 ± 0.03	0.00	0.00	0.00	NM
NGC 188	2M01013538+8515100	-80.2 ± 0.1	0.10 ± 0.01	-2.95 ± 0.03	-0.09 ± 0.02	0.00	0.30	0.00	NM
NGC 188	2M01013568+8522254	-50.5 ± 7.1	0.16 ± 0.01	-2.39 ± 0.04	-0.80 ± 0.03	0.00	0.00	0.61	NM
NGC 188	2M01014374+8535599	-4.6 ± 0.1	-0.32 ± 0.01	12.35 ± 0.04	-1.44 ± 0.03	0.00	-1.00	0.00	NM
NGC 188	2M01015206+8506329	-42.1 ± 0.0	0.15 ± 0.01	-2.29 ± 0.06	-0.85 ± 0.04	0.00	0.00	0.80	NM
NGC 188	2M01025280+8517563	-42.1 ± 0.1	0.12 ± 0.01	-2.40 ± 0.05	-0.78 ± 0.03	0.00	0.00	0.55	NM
NGC 188	2M01040237+8516593	-14.9 ± 0.1	-0.24 ± 0.01	0.46 ± 0.04	4.13 ± 0.03	0.00	0.00	0.00	NM
NGC 188	2M01044930+8455570	-101.9 ± 0.2	-0.11 ± 0.01	-1.49 ± 0.04	1.25 ± 0.03	0.00	0.00	0.00	NM
NGC 188	2M01045184+8535464	-104.9 ± 4.1	-0.95 ± 0.01	-0.28 ± 0.03	0.18 ± 0.03	0.00	0.00	0.00	NM
NGC 188	2M01051495+8448210	-60.6 ± 0.1	-0.03 ± 0.01	1.71 ± 0.07	2.67 ± 0.08	0.00	0.00	0.00	NM
NGC 188	2M01054356+8514412	-11.3 ± 0.3	0.05 ± 0.01	15.46 ± 0.05	1.92 ± 0.04	0.00	-1.00	0.00	NM
NGC 188	2M01073954+8504072	1.4 ± 1.4	0.03 ± 0.02	1.43 ± 0.05	-4.97 ± 0.04	0.00	-1.00	0.00	NM
NGC 188	2M01082326+8457027	-119.2 ± 0.1	-0.44 ± 0.01	-1.04 ± 0.03	0.49 ± 0.02	0.00	0.00	0.00	NM
NGC 188	2M01083610+8504122	-46.4 ± 0.1	0.13 ± 0.01	-5.60 ± 0.03	2.81 ± 0.02	0.00	0.00	0.00	NM
NGC 188	2M01111089+8517361	-102.6 ± 0.1	-0.09 ± 0.01	5.19 ± 0.03	-1.66 ± 0.02	0.00	0.00	0.00	NM
IC 166	2M01503014+6148068	-68.0 ± 0.3	-0.44 ± 0.01	1.13 ± 0.04	-0.76 ± 0.06	0.00	0.00	0.00	NM
IC 166	2M01512519+6203439	-63.7 ± 1.4	-0.14 ± 0.01	0.08 ± 0.05	0.30 ± 0.07	0.00	0.00	0.00	NM
IC 166	2M01513603+6138099	-94.7 ± 0.1	-0.23 ± 0.01	-0.06 ± 0.04	-0.77 ± 0.06	0.00	0.00	0.00	NM
IC 166	2M01514975+6150556	-39.8 ± 0.4	-0.05 ± 0.01	-1.44 ± 0.06	1.11 ± 0.09	0.96	0.97	1.00	GM
IC 166	2M01515473+6148552	-39.8 ± 0.3	-0.08 ± 0.01	-1.48 ± 0.06	1.17 ± 0.08	0.96	0.79	0.99	GM
IC 166	2M01520006+6153008	-41.2 ± 0.3	0.05 ± 0.01	-1.37 ± 0.06	1.15 ± 0.08	0.94	0.00	0.86	NM
IC 166	2M01520137+6159477	-41.0 ± 0.1	-0.04 ± 0.01	0.26 ± 0.04	-0.17 ± 0.05	0.00	0.00	0.00	NM
IC 166	2M01520209+6147453	-39.8 ± 0.2	-0.01 ± 0.01	-1.54 ± 0.06	1.29 ± 0.08	0.96	0.16	0.81	GM
IC 166	2M01520770+6150058	-40.0 ± 0.4	-0.09 ± 0.01	-1.24 ± 0.06	1.15 ± 0.09	0.97	0.60	0.42	GM
IC 166	2M01521347+6152558	-44.1 ± 0.7	-0.05 ± 0.01	-1.44 ± 0.06	1.29 ± 0.09	0.23	0.97	0.74	GM
IC 166	2M01521509+6151407	-40.2 ± 0.2	-0.05 ± 0.01	-1.46 ± 0.04	1.07 ± 0.06	0.99	0.91	0.96	GM
IC 166	2M01522060+6150364	-37.4 ± 0.1	-0.04 ± 0.01	-1.44 ± 0.05	1.20 ± 0.06	0.37	0.66	0.93	GM
IC 166	2M01522077+6153186	-37.6 ± 0.0	-0.13 ± 0.01	-1.48 ± 0.03	1.12 ± 0.05	0.41	-1.00	0.99	DM
IC 166	2M01522289+6148493	-40.9 ± 0.1	0.02 ± 0.01	-1.48 ± 0.05	1.09 ± 0.07	0.98	0.01	0.95	NM
IC 166	2M01522357+6154011	-40.0 ± 0.2	-0.09 ± 0.01	-1.45 ± 0.04	1.10 ± 0.06	0.98	0.54	0.99	GM
IC 166	2M01522919+6159381	-42.6 ± 0.7	-0.04 ± 0.01	-1.59 ± 0.03	1.38 ± 0.04	0.00	0.00	0.59	NM
IC 166	2M01522953+6151427	-41.3 ± 0.1	-0.04 ± 0.01	-1.46 ± 0.04	1.14 ± 0.05	0.93	0.75	1.00	GM
IC 166	2M01523324+6152050	-42.2 ± 0.1	-0.06 ± 0.01	-1.28 ± 0.04	1.17 ± 0.06	0.73	0.99	0.56	GM
IC 166	2M01523388+6149126	-41.5 ± 0.1	0.05 ± 0.01	-1.53 ± 0.07	1.32 ± 0.09	0.90	0.00	0.76	NM
IC 166	2M01523513+6154318	-39.3 ± 0.1	-0.08 ± 0.01	-1.42 ± 0.04	1.17 ± 0.06	0.86	0.74	0.95	GM
IC 166	2M01524136+6151507	-42.0 ± 0.0	-0.05 ± 0.01	-1.58 ± 0.05	1.21 ± 0.07	0.78	0.96	0.83	GM
IC 166	2M01524515+6153369	-39.9 ± 0.2	-0.08 ± 0.01	-1.40 ± 0.04	1.18 ± 0.06	0.97	0.69	0.90	GM
IC 166	2M01525074+6145411	-39.7 ± 0.1	-0.09 ± 0.01	-1.48 ± 0.04	1.03 ± 0.06	0.94	0.60	0.83	GM
IC 166	2M01525435+6152344	-95.8 ± 7.3	-0.55 ± 0.01	-0.55 ± 0.08	0.37 ± 0.11	0.00	0.00	0.00	NM
IC 166	2M01525543+6148504	-41.7 ± 0.2	-0.07 ± 0.01	-1.41 ± 0.04	1.00 ± 0.06	0.85	0.94	0.85	GM
IC 166	2M01531358+6151269	-92.5 ± 0.0	-0.10 ± 0.01	-2.50 ± 0.04	-0.03 ± 0.06	0.00	0.24	0.00	NM
IC 166	2M01531721+6159383	-128.3 ± 0.0	-0.25 ± 0.01	-0.95 ± 0.05	0.12 ± 0.06	0.00	0.00	0.00	NM
IC 166	2M01533801+6142438	-105.4 ± 0.0	0.22 ± 0.01	-3.08 ± 0.03	1.47 ± 0.05	0.00	0.00	0.00	NM
Berkeley 66	2M03031417+5843004	-55.5 ± 0.0	-0.13 ± 0.01	0.13 ± 0.16	-0.24 ± 0.14	0.00	0.00	0.86	NM
Berkeley 66	2M03040128+5846422	-50.2 ± 0.0	-0.11 ± 0.01	0.06 ± 0.19	-0.15 ± 0.16	1.00	0.81	0.93	GM
Berkeley 66	2M03040371+5844017	-49.8 ± 0.1	-0.14 ± 0.01	-0.18 ± 0.18	-0.10 ± 0.15	0.94	0.89	0.98	GM
Berkeley 66	2M03040715+5847555	-31.0 ± 0.1	-0.24 ± 0.01	-1.55 ± 0.14	-2.23 ± 0.14	0.00	0.00	0.00	NM
Berkeley 66	2M03040784+5846174	-75.3 ± 0.1	-0.01 ± 0.01	-0.32 ± 0.12	0.38 ± 0.10	0.00	0.00	0.84	NM
Berkeley 66	2M03041010+5845484	-50.4 ± 0.0	-0.15 ± 0.01	0.01 ± 0.21	0.26 ± 0.14	0.92	0.55	0.89	GM
Berkeley 66	2M03041054+5847594	-36.4 ± 0.0	-0.11 ± 0.01	-0.85 ± 0.09	-2.03 ± 0.07	0.00	0.00	0.00	NM
Berkeley 66	2M03041368+5843387	-49.9 ± 0.1	-0.14 ± 0.01	-0.22 ± 0.20	0.25 ± 0.16	0.96	0.93	0.94	GM
Berkeley 66	2M03042113+5845433	-50.7 ± 0.0	-0.14 ± 0.01	-0.20 ± 0.16	0.07 ± 0.13	0.80	0.92	0.99	GM
Berkeley 66	2M03042535+5847399	-63.8 ± 0.1	-0.29 ± 0.01	0.39 ± 0.25	0.73 ± 0.20	0.00	0.00	0.36	NM
Berkeley 66	2M03042797+5845042	-49.9 ± 0.1	-0.11 ± 0.01	0.31 ± 0.25	-0.23 ± 0.16	0.96	0.60	0.74	GM
Berkeley 66	2M03042930+5846337	-62.0 ± 1.2	0.04 ± 0.01	0.48 ± 0.15	-1.62 ± 0.12	0.00	0.00	0.04	NM
Berkeley 66	2M03043132+5846570	-17.9 ± 0.1	-0.32 ± 0.01	-0.44 ± 0.16	0.16 ± 0.12	0.00	0.00	0.88	NM
Berkeley 66	2M03043163+5844477	-49.5 ± 0.0	-0.11 ± 0.01	-0.10 ± 0.15	-0.01 ± 0.12	0.00	0.00	1.00	NM
NGC 1245	2M03124208+4720598	-22.6 ± 0.0	-0.19 ± 0.01	-3.01 ± 0.09	-3.37 ± 0.08	0.00	0.00	0.00	NM

Continued on next page

Table A.1 – Continued

Cluster name	2MASS ID	RV (km s^{-1})	[Fe/H] (dex)	μ_α (mas yr^{-1})	μ_δ (mas yr^{-1})	RV Prob	[Fe/H] Prob	PM Prob	Memb
NGC 1245	2M03124729+4707150	-3.9 ± 0.1	-0.02 ± 0.01	-0.22 ± 0.09	-0.76 ± 0.06	0.00	0.00	0.00	NM
NGC 1245	2M03130140+4725188	-57.8 ± 0.0	0.12 ± 0.01	-1.94 ± 0.05	-0.99 ± 0.05	0.00	0.00	0.00	NM
NGC 1245	2M03132374+4730260	-4.4 ± 0.1	-0.30 ± 0.01	13.69 ± 0.07	-6.39 ± 0.06	0.00	0.00	0.00	NM
NGC 1245	2M03132425+4725485	3.3 ± 0.1	-0.19 ± 0.01	19.80 ± 0.05	-25.89 ± 0.05	0.00	-1.00	0.00	NM
NGC 1245	2M03134113+4733169	-40.1 ± 0.1	-0.11 ± 0.01	1.37 ± 0.05	-1.37 ± 0.04	0.00	0.00	0.00	NM
NGC 1245	2M03135098+4722010	-29.3 ± 0.2	-0.00 ± 0.01	0.60 ± 0.05	-1.59 ± 0.04	0.00	0.00	0.92	NM
NGC 1245	2M03135669+4705538	49.6 ± 0.0	-0.09 ± 0.01	7.04 ± 0.09	-7.03 ± 0.06	0.00	0.00	0.00	NM
NGC 1245	2M03135719+4709350	-49.5 ± 0.2	-0.39 ± 0.01	-2.23 ± 0.25	1.51 ± 0.22	0.00	0.00	0.00	NM
NGC 1245	2M03140068+4716181	-15.7 ± 0.1	-0.18 ± 0.01	1.31 ± 0.05	-0.21 ± 0.04	0.00	0.00	0.00	NM
NGC 1245	2M03140338+4726224	-73.7 ± 0.0	-0.04 ± 0.01	-2.60 ± 0.07	-1.09 ± 0.05	0.00	0.00	0.00	NM
NGC 1245	2M03140724+4703122	-19.3 ± 0.1	-0.09 ± 0.01	-0.21 ± 0.09	-0.21 ± 0.06	0.00	0.00	0.00	NM
NGC 1245	2M03140839+4716330	-29.1 ± 0.0	-0.04 ± 0.01	0.50 ± 0.05	-1.64 ± 0.04	0.99	0.51	0.93	GM
NGC 1245	2M03141040+4708453	-46.7 ± 0.0	-0.59 ± 0.01	-0.16 ± 0.05	-0.37 ± 0.04	0.00	0.00	0.00	NM
NGC 1245	2M03141134+4709173	-29.4 ± 0.0	-0.05 ± 0.01	0.47 ± 0.08	-1.61 ± 0.06	1.00	0.82	0.96	GM
NGC 1245	2M03141166+4718037	-13.8 ± 0.1	-0.24 ± 0.01	-0.38 ± 0.07	-0.95 ± 0.04	0.00	0.00	0.00	NM
NGC 1245	2M03141268+4717315	-29.9 ± 0.1	-0.09 ± 0.01	0.42 ± 0.05	-1.58 ± 0.04	0.94	0.17	0.90	GM
NGC 1245	2M03142464+4711327	-29.9 ± 0.2	-0.06 ± 0.01	0.55 ± 0.05	-1.64 ± 0.04	0.95	1.00	0.92	GM
NGC 1245	2M03142472+4720598	5.0 ± 0.3	0.15 ± 0.01	-0.03 ± 0.24	-1.07 ± 0.20	0.00	-1.00	0.00	NM
NGC 1245	2M03142901+4700105	-66.4 ± 1.3	-0.34 ± 0.01	0.10 ± 0.06	-0.11 ± 0.05	0.00	0.00	0.00	NM
NGC 1245	2M03143100+4714204	-30.3 ± 0.0	-0.06 ± 0.01	0.30 ± 0.05	-1.68 ± 0.04	0.83	0.98	0.58	GM
NGC 1245	2M03143256+4716277	-28.2 ± 0.1	-0.07 ± 0.01	0.43 ± 0.06	-1.64 ± 0.04	0.76	0.91	0.87	GM
NGC 1245	2M03143558+4732345	-53.6 ± 0.0	-0.24 ± 0.01	-0.99 ± 0.08	-1.25 ± 0.06	0.00	0.00	0.00	NM
NGC 1245	2M03143819+4720444	-29.2 ± 0.0	-0.04 ± 0.01	0.59 ± 0.04	-1.60 ± 0.03	0.99	0.55	0.93	GM
NGC 1245	2M03143823+4724503	-20.0 ± 0.1	-0.07 ± 0.01	-0.00 ± 0.09	-1.46 ± 0.07	0.00	0.81	0.05	NM
NGC 1245	2M03143888+4718202	-28.3 ± 0.0	-0.08 ± 0.01	0.47 ± 0.05	-1.56 ± 0.04	0.81	0.63	0.98	GM
NGC 1245	2M03143977+4714400	-26.6 ± 0.7	-0.06 ± 0.01	0.49 ± 0.04	-1.69 ± 0.04	0.21	1.00	0.83	GM
NGC 1245	2M03143977+4716488	-18.2 ± 2.7	-0.10 ± 0.01	0.58 ± 0.05	-1.76 ± 0.04	0.00	0.07	0.56	NM
NGC 1245	2M03144021+4715280	-29.9 ± 0.0	-0.05 ± 0.01	0.41 ± 0.04	-1.57 ± 0.03	0.93	0.78	0.89	GM
NGC 1245	2M03144182+4717086	-39.3 ± 1.6	-0.07 ± 0.01	0.51 ± 0.05	-1.64 ± 0.04	0.00	0.84	0.93	NM
NGC 1245	2M03144404+4712251	-44.3 ± 0.4	-0.12 ± 0.01	5.83 ± 0.05	-5.78 ± 0.04	0.00	0.00	0.00	NM
NGC 1245	2M03144576+4723310	-49.9 ± 0.1	-0.36 ± 0.01	-2.02 ± 0.05	-3.09 ± 0.04	0.00	0.00	0.00	NM
NGC 1245	2M03144698+4711579	-30.4 ± 0.1	-0.07 ± 0.01	0.58 ± 0.06	-1.58 ± 0.05	0.80	0.75	0.96	GM
NGC 1245	2M03144911+4734214	-52.1 ± 0.0	-0.23 ± 0.01	-0.13 ± 0.06	0.34 ± 0.05	0.00	0.00	0.00	NM
NGC 1245	2M03145222+4720570	-67.8 ± 2.2	0.05 ± 0.01	-7.57 ± 0.04	-11.07 ± 0.03	0.00	-1.00	0.00	NM
NGC 1245	2M03145260+4704431	-34.2 ± 0.1	-0.04 ± 0.01	0.77 ± 0.07	-0.28 ± 0.05	0.01	0.74	0.00	NM
NGC 1245	2M03145265+4719245	-29.1 ± 0.1	-0.10 ± 0.01	0.36 ± 0.05	-1.64 ± 0.03	0.99	0.06	0.76	GM
NGC 1245	2M03145273+4714033	-29.5 ± 0.1	-0.06 ± 0.01	0.52 ± 0.04	-1.61 ± 0.04	1.00	0.99	0.97	GM
NGC 1245	2M03145518+4712146	-30.2 ± 0.1	-0.03 ± 0.01	0.51 ± 0.05	-1.64 ± 0.04	0.87	0.26	0.92	GM
NGC 1245	2M03145841+4708245	-29.4 ± 0.0	-0.10 ± 0.01	0.55 ± 0.05	-1.60 ± 0.04	1.00	0.10	0.97	GM
NGC 1245	2M03145950+4721138	-29.3 ± 0.1	-0.00 ± 0.01	0.53 ± 0.05	-1.59 ± 0.04	1.00	0.01	0.99	GM
NGC 1245	2M03150229+4713385	-8.7 ± 0.1	-0.08 ± 0.01	-0.83 ± 0.05	0.24 ± 0.04	0.00	0.64	0.00	NM
NGC 1245	2M03150241+4719582	-28.9 ± 0.1	-0.07 ± 0.01	0.59 ± 0.05	-1.67 ± 0.04	0.96	0.83	0.81	GM
NGC 1245	2M03150510+4714411	-30.3 ± 0.0	-0.04 ± 0.01	0.60 ± 0.05	-1.66 ± 0.04	0.84	0.68	0.82	GM
NGC 1245	2M03150591+4704315	19.8 ± 0.2	-0.16 ± 0.01	2.42 ± 0.10	-3.82 ± 0.08	0.00	0.00	0.00	NM
NGC 1245	2M03150614+4716352	-29.1 ± 0.1	-0.06 ± 0.01	0.53 ± 0.04	-1.54 ± 0.04	0.99	0.96	0.99	GM
NGC 1245	2M03151244+4708556	-28.5 ± 0.1	-0.07 ± 0.01	0.45 ± 0.06	-1.62 ± 0.04	0.86	0.88	0.93	GM
NGC 1245	2M03151253+4717291	-29.3 ± 0.1	-0.06 ± 0.01	0.50 ± 0.04	-1.65 ± 0.04	1.00	0.99	0.92	GM
NGC 1245	2M03151260+4721342	-54.3 ± 0.1	-0.04 ± 0.01	-0.91 ± 0.05	-0.43 ± 0.04	0.00	0.56	0.00	NM
NGC 1245	2M03151560+4714338	-30.0 ± 0.1	-0.12 ± 0.01	0.51 ± 0.04	-1.66 ± 0.04	0.92	0.01	0.89	NM
NGC 1245	2M03151881+4712051	-28.4 ± 0.1	-0.06 ± 0.01	0.51 ± 0.04	-1.63 ± 0.04	0.82	0.99	0.95	GM
NGC 1245	2M03151975+4713477	-29.4 ± 0.1	-0.06 ± 0.01	0.61 ± 0.05	-1.66 ± 0.04	1.00	1.00	0.81	GM
NGC 1245	2M03152016+4715253	-88.0 ± 0.1	-0.43 ± 0.01	-1.22 ± 0.06	-0.32 ± 0.05	0.00	0.00	0.00	NM
NGC 1245	2M03152825+4710367	-5.7 ± 0.0	-0.17 ± 0.01	-1.27 ± 0.07	-0.92 ± 0.06	0.00	0.00	0.00	NM
NGC 1245	2M03152826+4713235	-37.5 ± 0.3	0.04 ± 0.01	1.55 ± 0.06	0.99 ± 0.05	0.00	0.00	0.00	NM
NGC 1245	2M03153155+4703269	-39.5 ± 0.2	-0.16 ± 0.01	0.17 ± 0.05	-1.37 ± 0.04	0.00	0.00	0.14	NM
NGC 1245	2M03153331+4715486	-42.8 ± 4.0	-0.44 ± 0.01	-0.91 ± 0.04	-1.24 ± 0.04	0.00	0.00	0.00	NM
NGC 1245	2M03153367+4724292	-13.9 ± 0.2	-0.47 ± 0.01	2.18 ± 0.06	-0.67 ± 0.05	0.00	0.00	0.00	NM
NGC 1245	2M03153878+4700490	-52.4 ± 0.1	0.26 ± 0.01	-0.74 ± 0.07	-1.92 ± 0.06	0.00	0.00	0.00	NM
NGC 1245	2M03154254+4713369	14.4 ± 0.9	-0.35 ± 0.01	1.04 ± 0.05	1.22 ± 0.04	0.00	0.00	0.00	NM
NGC 1245	2M03154477+4713579	6.2 ± 0.5	-0.24 ± 0.01	-0.59 ± 0.04	-0.36 ± 0.04	0.00	0.00	0.00	NM
NGC 1245	2M03154668+4704100	-64.2 ± 0.0	-0.41 ± 0.01	2.27 ± 1.28	-7.06 ± 0.96	0.00	0.00	0.00	NM
NGC 1245	2M03155176+4717426	-57.4 ± 0.1	-0.48 ± 0.01	-1.36 ± 0.07	-1.78 ± 0.08	0.00	0.00	0.00	NM
NGC 1245	2M03155670+4727546	-21.8 ± 0.1	0.03 ± 0.01	-2.15 ± 0.05	-2.96 ± 0.05	0.00	0.00	0.00	NM

Continued on next page

Table A.1 – Continued

Cluster name	2MASS ID	RV (km s^{-1})	[Fe/H] (dex)	μ_α (mas yr^{-1})	μ_δ (mas yr^{-1})	RV Prob	[Fe/H] Prob	PM Prob	Memb
NGC 1245	2M03161086+4711012	-92.3 ± 0.1	-0.39 ± 0.01	-1.69 ± 0.05	0.02 ± 0.04	0.00	0.00	0.00	NM
NGC 1245	2M03161476+4720510	-11.5 ± 0.1	0.04 ± 0.01	2.32 ± 0.05	-3.00 ± 0.04	0.00	0.00	0.00	NM
NGC 1245	2M03162625+4706253	-60.1 ± 0.0	-0.49 ± 0.01	-0.52 ± 0.06	-1.97 ± 0.05	0.00	0.00	0.00	NM
NGC 1245	2M03162869+4728134	-80.1 ± 0.1	-0.38 ± 0.01	-0.30 ± 0.06	-0.01 ± 0.05	0.00	0.00	0.00	NM
NGC 1245	2M03163440+4707595	-24.3 ± 0.2	-0.12 ± 0.01	0.61 ± 0.07	-0.43 ± 0.06	0.00	0.00	0.00	NM
NGC 1245	2M03164598+4718506	7.8 ± 0.1	-0.44 ± 0.01	-1.66 ± 0.06	-2.15 ± 0.06	0.00	0.00	0.00	NM
NGC 1245	2M03164907+4711491	-58.6 ± 0.1	-0.07 ± 0.01	-3.31 ± 0.05	-1.82 ± 0.04	0.00	0.00	0.00	NM
King 7	2M03565231+5139284	-31.7 ± 0.1	-0.06 ± 0.01	0.43 ± 0.19	0.22 ± 0.13	0.00	0.00	0.00	NM
King 7	2M03570238+5148353	-32.4 ± 0.2	-0.25 ± 0.01	0.54 ± 0.33	-1.13 ± 0.23	0.00	0.00	0.61	NM
King 7	2M03570990+5138053	-33.1 ± 0.1	-0.05 ± 0.01	2.45 ± 0.13	-3.19 ± 0.09	0.00	0.00	0.00	NM
King 7	2M03573154+5156051	-36.6 ± 0.2	-0.20 ± 0.01	-0.16 ± 0.04	2.23 ± 0.03	0.00	0.00	0.00	NM
King 7	2M03573428+5131377	-66.7 ± 0.0	-0.09 ± 0.01	0.33 ± 0.13	-0.90 ± 0.10	0.00	0.00	0.29	NM
King 7	2M03574798+5148086	-72.2 ± 0.2	-0.34 ± 0.01	-0.54 ± 0.19	1.20 ± 0.12	0.00	0.00	0.00	NM
King 7	2M03575304+5157524	-47.2 ± 0.1	-0.27 ± 0.01	-0.50 ± 0.19	-1.65 ± 0.16	0.00	0.00	0.01	NM
King 7	2M03582042+5152284	-13.2 ± 0.3	0.02 ± 0.01	0.30 ± 0.06	-12.94 ± 0.05	0.69	-1.00	0.00	NM
King 7	2M03582676+5146556	11.4 ± 0.1	-0.01 ± 0.01	-0.02 ± 0.06	-3.69 ± 0.05	0.00	0.01	0.00	NM
King 7	2M03582679+5156303	-44.1 ± 1.4	-0.20 ± 0.01	-1.04 ± 0.18	0.39 ± 0.16	0.00	0.00	0.00	NM
King 7	2M03582953+5139275	-50.3 ± 0.0	-0.18 ± 0.01	-0.70 ± 0.11	0.95 ± 0.09	0.00	0.00	0.00	NM
King 7	2M03583626+5201252	-0.6 ± 0.2	-0.09 ± 0.01	371.70 ± 0.09	-215.79 ± 0.07	0.00	-1.00	0.00	NM
King 7	2M03584356+5137555	-49.7 ± 0.1	0.12 ± 0.01	3.75 ± 0.07	-1.94 ± 0.05	0.00	0.00	0.00	NM
King 7	2M03584454+5200333	-29.5 ± 0.0	0.09 ± 0.01	1.14 ± 0.06	-1.93 ± 0.05	0.00	0.00	0.22	NM
King 7	2M03584774+5151379	-42.1 ± 0.1	-0.23 ± 0.01	-0.93 ± 0.14	-1.96 ± 0.12	0.00	0.00	0.00	NM
King 7	2M03585117+5148462	-10.9 ± 0.0	0.01 ± 0.01	0.72 ± 0.13	-1.82 ± 0.12	1.00	0.00	0.30	NM
King 7	2M03585279+5155016	3.5 ± 0.8	0.14 ± 0.01	6.80 ± 0.08	-21.96 ± 0.07	0.00	-1.00	0.00	NM
King 7	2M03585815+5133085	-65.9 ± 0.1	-0.38 ± 0.01	-0.34 ± 0.17	2.73 ± 0.13	0.00	0.00	0.00	NM
King 7	2M03585931+5148593	-26.4 ± 0.1	-0.30 ± 0.01	0.51 ± 0.10	-1.99 ± 0.08	0.00	0.00	0.11	NM
King 7	2M03590292+5138021	9.0 ± 0.0	0.03 ± 0.01	6.19 ± 0.07	-4.29 ± 0.05	0.00	0.00	0.00	NM
King 7	2M03590443+5148003	-10.8 ± 0.1	-0.06 ± 0.01	1.23 ± 0.13	-1.18 ± 0.12	1.00	0.98	0.95	GM
King 7	2M03590571+5150002	7.8 ± 0.7	-0.08 ± 0.01	0.67 ± 0.10	-1.73 ± 0.08	0.00	0.14	0.38	NM
King 7	2M03590818+5145215	-15.4 ± 2.5	-0.03 ± 0.01	1.24 ± 0.14	-1.38 ± 0.12	0.27	0.16	0.87	GM
King 7	2M03590908+5158548	-23.6 ± 0.3	0.03 ± 0.01	4.57 ± 0.05	-8.26 ± 0.05	0.00	-1.00	0.00	NM
King 7	2M03590945+5145379	-6.9 ± 0.1	0.03 ± 0.01	0.56 ± 0.10	-1.32 ± 0.09	0.47	0.00	0.64	NM
King 7	2M03591013+5145193	-10.5 ± 0.0	-0.06 ± 0.01	1.17 ± 0.10	-1.34 ± 0.09	1.00	0.88	0.93	GM
King 7	2M03591747+5147014	-10.7 ± 0.0	-0.01 ± 0.01	1.19 ± 0.13	-1.36 ± 0.11	1.00	0.00	0.91	NM
King 7	2M03592828+5148425	-10.9 ± 0.1	-0.06 ± 0.01	0.76 ± 0.14	-1.39 ± 0.13	1.00	0.97	0.79	GM
King 7	2M03593013+5153563	-48.5 ± 0.2	-0.09 ± 0.01	-0.29 ± 0.14	-1.97 ± 0.11	0.00	0.07	0.01	NM
King 7	2M03594961+5136545	17.9 ± 0.1	-0.27 ± 0.01	2.25 ± 0.08	0.78 ± 0.06	0.00	0.00	0.00	NM
King 7	2M03595696+5131152	-25.7 ± 0.3	-0.02 ± 0.01	-3.21 ± 0.17	-0.59 ± 0.13	0.00	0.00	0.00	NM
King 7	2M04000404+5144564	-27.6 ± 0.1	-0.12 ± 0.01	-1.26 ± 0.07	-0.78 ± 0.06	0.00	0.00	0.00	NM
King 7	2M04000424+5150574	-78.1 ± 0.3	-0.20 ± 0.01	0.10 ± 0.30	-1.17 ± 0.21	0.00	0.00	0.20	NM
King 7	2M04000772+5156501	-77.6 ± 0.1	-0.39 ± 0.01	-0.30 ± 0.27	-0.24 ± 0.22	0.00	0.00	0.00	NM
King 7	2M04000879+5141543	-17.4 ± 0.1	-0.05 ± 0.01	-1.73 ± 0.05	-0.64 ± 0.04	0.08	0.94	0.00	NM
King 7	2M04001357+5151196	33.7 ± 2.7	-0.10 ± 0.01	12.92 ± 0.11	-13.08 ± 0.11	0.00	-1.00	0.00	NM
King 7	2M04001419+5204350	11.7 ± 0.1	-0.04 ± 0.01	0.55 ± 0.10	-2.46 ± 0.07	0.00	0.00	0.01	NM
King 7	2M04002015+5144250	8.2 ± 0.2	-0.12 ± 0.01	-4.07 ± 0.10	-5.14 ± 0.10	0.00	0.00	0.00	NM
King 7	2M04003265+5135376	-30.7 ± 0.2	-0.36 ± 0.01	0.25 ± 0.20	0.05 ± 0.14	0.00	0.00	0.00	NM
King 7	2M04003407+5145388	-9.1 ± 0.1	-0.14 ± 0.01	1.81 ± 0.12	-0.85 ± 0.10	0.00	0.00	0.29	NM
King 7	2M04003494+5204047	-80.9 ± 0.2	-0.02 ± 0.01	0.71 ± 0.30	-1.04 ± 0.21	0.00	0.00	0.73	NM
King 7	2M04004107+5134539	-19.8 ± 0.1	-0.39 ± 0.01	1.45 ± 0.16	-0.21 ± 0.11	0.00	0.00	0.05	NM
King 7	2M04005735+5155440	-56.9 ± 0.2	-0.31 ± 0.01	-0.07 ± 0.15	-1.48 ± 0.12	0.00	0.00	0.10	NM
NGC 1798	2M05104038+4744160	-72.4 ± 0.1	-0.34 ± 0.01	0.52 ± 0.07	-0.82 ± 0.06	0.00	0.00	0.16	NM
NGC 1798	2M05104618+4746094	-2.4 ± 1.2	-0.24 ± 0.01	0.81 ± 0.07	-0.37 ± 0.06	0.00	0.00	0.97	NM
NGC 1798	2M05112446+4740027	3.4 ± 0.0	-0.16 ± 0.01	0.82 ± 0.06	-0.25 ± 0.04	0.96	0.71	0.95	GM
NGC 1798	2M05112945+4742298	8.4 ± 2.1	-0.22 ± 0.01	1.67 ± 0.05	-2.22 ± 0.04	0.09	0.50	0.00	NM
NGC 1798	2M05113113+4751040	23.7 ± 0.0	-0.36 ± 0.01	2.40 ± 0.05	0.52 ± 0.04	0.00	0.00	0.00	NM
NGC 1798	2M05113450+4741177	-2.3 ± 1.5	-0.19 ± 0.01	0.98 ± 0.05	-0.26 ± 0.05	0.17	0.98	0.94	GM
NGC 1798	2M05113666+4741482	2.9 ± 0.1	-0.17 ± 0.01	0.93 ± 0.04	-0.33 ± 0.04	1.00	0.86	0.99	GM
NGC 1798	2M05113768+4742329	3.2 ± 0.1	-0.20 ± 0.01	0.76 ± 0.05	-0.29 ± 0.04	0.98	0.84	0.92	GM
NGC 1798	2M05113859+4743446	4.4 ± 0.7	0.20 ± 0.01	0.38 ± 0.05	-5.10 ± 0.04	0.81	0.00	0.00	NM
NGC 1798	2M05114006+4739238	2.4 ± 0.0	-0.17 ± 0.01	1.01 ± 0.04	-0.36 ± 0.04	1.00	0.84	0.93	GM
NGC 1798	2M05114134+4740406	0.8 ± 0.1	-0.17 ± 0.01	0.84 ± 0.05	-0.25 ± 0.05	0.78	0.91	0.95	GM
NGC 1798	2M05114422+4741517	3.3 ± 0.1	-0.16 ± 0.01	0.85 ± 0.06	-0.33 ± 0.05	0.97	0.69	0.99	GM
NGC 1798	2M05114476+4738148	-17.0 ± 0.2	-0.19 ± 0.01	1.51 ± 0.07	-1.63 ± 0.06	0.00	0.96	0.00	NM

Continued on next page

Table A.1 – Continued

Cluster name	2MASS ID	RV (km s^{-1})	[Fe/H] (dex)	μ_α (mas yr^{-1})	μ_δ (mas yr^{-1})	RV Prob	[Fe/H] Prob	PM Prob	Memb
NGC 1798	2M05114484+4751437	-1.2 ± 0.1	-0.39 ± 0.01	0.20 ± 0.07	0.54 ± 0.06	0.00	0.00	0.00	NM
NGC 1798	2M05114626+4743422	1.9 ± 0.0	-0.17 ± 0.01	0.79 ± 0.05	-0.24 ± 0.04	0.96	0.95	0.92	GM
NGC 1798	2M05114795+4740258	1.9 ± 0.0	-0.21 ± 0.01	0.79 ± 0.07	-0.50 ± 0.07	0.96	0.77	0.83	GM
NGC 1798	2M05115945+4751127	7.3 ± 0.0	-0.29 ± 0.01	0.40 ± 0.04	-1.00 ± 0.04	0.00	0.00	0.03	NM
NGC 1798	2M05120369+4748162	-12.0 ± 0.4	-0.10 ± 0.01	1.59 ± 0.06	-0.42 ± 0.05	0.00	0.00	0.10	NM
NGC 1798	2M05120657+4735418	12.7 ± 0.1	-0.36 ± 0.01	0.87 ± 0.06	-1.06 ± 0.06	0.00	0.00	0.06	NM
NGC 1798	2M05121264+4750118	-27.8 ± 0.1	-0.19 ± 0.01	-0.25 ± 0.06	-0.93 ± 0.05	0.00	0.00	0.00	NM
NGC 1798	2M05122202+4740569	-16.5 ± 0.2	-0.46 ± 0.01	-1.15 ± 0.07	-0.36 ± 0.06	0.00	0.00	0.00	NM
NGC 1798	2M05123954+4738401	-34.7 ± 0.1	-0.37 ± 0.01	1.25 ± 0.07	0.47 ± 0.06	0.00	0.00	0.02	NM
Berkeley 17	2M05195385+3035095	-73.9 ± 0.2	-0.03 ± 0.01	2.59 ± 0.07	-0.40 ± 0.05	0.00	0.00	0.96	NM
Berkeley 17	2M05195417+3037252	16.3 ± 0.0	-0.13 ± 0.01	-2.42 ± 0.08	-0.59 ± 0.05	0.00	0.00	0.00	NM
Berkeley 17	2M05202118+3035544	-73.6 ± 0.1	-0.10 ± 0.01	2.69 ± 0.06	-0.28 ± 0.04	0.99	0.96	0.92	GM
Berkeley 17	2M05202386+3037219	-68.7 ± 1.6	-0.12 ± 0.01	2.45 ± 0.06	-0.35 ± 0.04	0.00	0.98	0.96	NM
Berkeley 17	2M05202755+3021384	22.0 ± 0.0	-0.08 ± 0.01	1.73 ± 0.05	-3.56 ± 0.04	0.00	0.00	0.00	NM
Berkeley 17	2M05202905+3032414	-73.5 ± 0.1	-0.13 ± 0.01	2.73 ± 0.09	-0.37 ± 0.06	1.00	0.86	0.90	GM
Berkeley 17	2M05203028+3040200	-2.0 ± 0.0	-0.03 ± 0.01	-1.82 ± 0.05	-1.70 ± 0.03	0.00	0.14	0.00	NM
Berkeley 17	2M05203121+3035067	-73.2 ± 0.1	-0.12 ± 0.01	2.50 ± 0.06	-0.35 ± 0.04	0.98	0.97	0.98	GM
Berkeley 17	2M05203650+3030351	-74.2 ± 0.1	-0.06 ± 0.01	2.70 ± 0.06	-0.34 ± 0.04	0.81	0.47	0.93	GM
Berkeley 17	2M05203799+3034414	-73.1 ± 0.2	-0.08 ± 0.01	2.66 ± 0.05	-0.40 ± 0.04	0.95	0.68	0.94	GM
Berkeley 17	2M05203962+3041419	3.4 ± 0.1	-0.04 ± 0.01	0.58 ± 0.06	-2.15 ± 0.04	0.00	0.23	0.00	NM
Berkeley 17	2M05204143+3036042	-73.1 ± 0.1	-0.14 ± 0.01	2.56 ± 0.07	-0.29 ± 0.05	0.94	0.72	0.99	GM
Berkeley 17	2M05204409+3031576	-45.0 ± 0.0	-0.03 ± 0.01	3.41 ± 0.06	-1.96 ± 0.04	0.00	0.10	0.00	NM
Berkeley 17	2M05204488+3038020	-73.1 ± 0.1	-0.13 ± 0.01	2.82 ± 0.06	-0.48 ± 0.04	0.95	0.84	0.75	GM
Berkeley 17	2M05204975+3034404	-12.4 ± 0.2	-0.05 ± 0.01	1.55 ± 0.06	-1.94 ± 0.04	0.00	0.36	0.00	NM
Berkeley 17	2M05205545+3038339	11.3 ± 0.2	-0.20 ± 0.01	0.41 ± 0.08	-0.13 ± 0.05	0.00	0.08	0.00	NM
Berkeley 71	2M05403528+3215430	-4.4 ± 0.1	-0.07 ± 0.01	2.06 ± 0.12	-2.38 ± 0.10	0.37	0.01	0.00	NM
Berkeley 71	2M05403567+3220477	31.1 ± 0.1	-0.25 ± 0.01	0.20 ± 0.11	1.60 ± 0.08	0.00	0.00	0.00	NM
Berkeley 71	2M05404076+3215219	12.2 ± 0.1	-0.15 ± 0.01	1.87 ± 0.12	-2.60 ± 0.10	0.00	0.48	0.00	NM
Berkeley 71	2M05404312+3217303	-10.0 ± 0.2	-0.21 ± 0.01	0.76 ± 0.08	-1.71 ± 0.06	0.91	0.94	0.97	GM
Berkeley 71	2M05404351+3219171	0.6 ± 0.2	-0.13 ± 0.01	1.02 ± 0.11	-0.35 ± 0.09	0.01	0.23	0.00	NM
Berkeley 71	2M05404432+3213387	-4.1 ± 0.2	-0.31 ± 0.01	0.68 ± 0.11	0.56 ± 0.08	0.31	0.02	0.00	NM
Berkeley 71	2M05404529+3219367	29.8 ± 0.3	-0.25 ± 0.01	3.24 ± 0.11	-5.49 ± 0.08	0.00	0.34	0.00	NM
Berkeley 71	2M05404953+3217001	28.7 ± 0.2	-0.22 ± 0.01	0.75 ± 0.15	-1.22 ± 0.12	0.00	0.84	0.53	NM
Berkeley 71	2M05405157+3220398	-1.9 ± 0.0	-0.40 ± 0.01	0.98 ± 0.20	-0.31 ± 0.15	0.00	0.00	0.00	NM
Berkeley 71	2M05405311+3215557	-9.2 ± 0.1	-0.25 ± 0.01	0.46 ± 0.09	-1.49 ± 0.07	0.98	0.42	0.86	GM
Berkeley 71	2M05405316+3215197	-9.4 ± 0.1	-0.23 ± 0.01	0.70 ± 0.07	-1.77 ± 0.06	0.97	0.72	0.92	GM
Berkeley 71	2M05405442+3217298	-10.1 ± 0.1	-0.17 ± 0.01	0.84 ± 0.11	-1.62 ± 0.09	0.89	0.77	0.93	GM
Berkeley 71	2M05405484+3215567	-9.3 ± 0.1	-0.17 ± 0.01	0.44 ± 0.10	-1.65 ± 0.08	0.97	0.87	0.86	GM
Berkeley 71	2M05405503+3214099	-9.9 ± 0.1	-0.20 ± 0.01	0.67 ± 0.10	-1.68 ± 0.08	0.92	0.99	0.99	GM
Berkeley 71	2M05405901+3211175	27.0 ± 0.0	-0.24 ± 0.01	-0.24 ± 0.12	-1.81 ± 0.09	0.00	0.47	0.08	NM
Berkeley 71	2M05405956+3215182	-3.3 ± 0.4	-0.16 ± 0.01	0.47 ± 0.08	-1.68 ± 0.06	0.20	0.64	0.88	GM
Berkeley 71	2M05410217+3216397	50.2 ± 0.0	-0.15 ± 0.01	0.03 ± 0.07	-0.71 ± 0.06	0.00	0.54	0.03	NM
Berkeley 71	2M05410271+3220441	34.1 ± 0.1	-0.21 ± 0.01	0.23 ± 0.13	-2.35 ± 0.10	0.00	0.00	0.06	NM
Berkeley 71	2M05410828+3216381	30.0 ± 0.0	-0.12 ± 0.01	-0.57 ± 0.18	-1.90 ± 0.15	0.00	0.19	0.01	NM
Berkeley 71	2M05410990+3219148	-20.4 ± 0.0	-0.16 ± 0.01	-0.01 ± 0.10	-2.35 ± 0.08	0.00	0.75	0.03	NM
Berkeley 71	2M05411239+3215304	5.8 ± 0.0	-0.10 ± 0.01	0.66 ± 0.14	-1.46 ± 0.10	0.00	0.06	0.91	NM
Berkeley 71	2M05411690+3217021	32.7 ± 0.2	0.08 ± 0.01	3.00 ± 0.09	-10.14 ± 0.07	0.00	-1.00	0.00	NM
Berkeley 71	2M05412682+3216315	23.9 ± 0.0	0.02 ± 0.01	-0.05 ± 0.14	-3.74 ± 0.10	0.00	0.00	0.00	NM
Teutsch 51	2M05533556+2649202	8.2 ± 0.1	-0.34 ± 0.01	-0.10 ± 0.13	-1.38 ± 0.10	0.00	0.00	0.00	NM
Teutsch 51	2M05534263+2652119	5.6 ± 0.1	-0.10 ± 0.01	-4.47 ± 0.05	-1.03 ± 0.04	0.00	0.00	0.00	NM
Teutsch 51	2M05534332+2649595	17.5 ± 0.1	-0.28 ± 0.01	0.66 ± 0.11	0.04 ± 0.09	0.99	0.95	0.47	GM
Teutsch 51	2M05534495+2650052	14.7 ± 1.2	-0.14 ± 0.01	0.31 ± 0.38	-1.47 ± 0.30	0.65	-1.00	0.00	NM
Teutsch 51	2M05534659+2651366	14.4 ± 0.1	-0.25 ± 0.01	0.55 ± 0.10	-0.29 ± 0.08	0.60	0.84	0.99	GM
Teutsch 51	2M05534689+2648234	17.1 ± 0.0	-0.25 ± 0.01	0.61 ± 0.15	-0.37 ± 0.12	1.00	0.84	0.98	GM
Teutsch 51	2M05535153+2649515	20.9 ± 0.5	-0.21 ± 0.01	-0.81 ± 0.17	-0.01 ± 0.15	0.42	0.31	0.00	NM
Teutsch 51	2M05535170+2649417	5.7 ± 0.2	-0.34 ± 0.01	0.52 ± 0.11	-0.11 ± 0.09	0.00	0.22	0.79	NM
Teutsch 51	2M05535387+2654101	7.2 ± 0.1	-0.18 ± 0.01	0.82 ± 0.06	-1.91 ± 0.05	0.00	0.00	0.00	NM
Teutsch 51	2M05535631+2648351	17.8 ± 0.2	-0.32 ± 0.01	0.63 ± 0.13	-0.27 ± 0.11	0.98	0.50	0.94	GM
Teutsch 51	2M05535681+2653029	38.3 ± 0.2	-0.44 ± 0.01	0.64 ± 0.09	-1.12 ± 0.07	0.00	0.00	0.06	NM
Teutsch 51	2M05535767+2649296	18.2 ± 0.1	-0.32 ± 0.01	0.34 ± 0.11	-0.31 ± 0.09	0.94	0.41	0.77	GM
Teutsch 51	2M05535784+2649525	31.4 ± 0.1	-0.03 ± 0.01	3.00 ± 0.10	-1.87 ± 0.08	0.00	0.00	0.00	NM
King 5	2M03131520+5246343	-49.0 ± 0.1	-0.04 ± 0.01	1.14 ± 0.29	-0.03 ± 0.24	0.00	0.00	0.00	NM
King 5	2M03132577+5236244	-80.8 ± 0.2	-0.39 ± 0.01	0.32 ± 0.10	-0.10 ± 0.10	0.00	0.00	0.00	NM

Continued on next page

Table A.1 – Continued

Cluster name	2MASS ID	RV (km s^{-1})	[Fe/H] (dex)	μ_α (mas yr^{-1})	μ_δ (mas yr^{-1})	RV Prob	[Fe/H] Prob	PM Prob	Memb
King 5	2M03140245+5234396	-39.0 ± 0.1	-0.16 ± 0.01	1.66 ± 0.08	0.27 ± 0.07	0.00	0.00	0.00	NM
King 5	2M03140441+5244263	-44.6 ± 0.0	-0.13 ± 0.01	0.02 ± 0.06	1.32 ± 0.06	1.00	0.92	0.00	NM
King 5	2M03140915+5237511	-42.6 ± 0.1	-0.12 ± 0.01	-0.49 ± 0.05	-0.91 ± 0.05	0.73	1.00	0.49	GM
King 5	2M03141169+5243476	-37.3 ± 0.1	0.15 ± 0.01	-0.34 ± 0.05	-0.76 ± 0.04	0.01	0.00	0.36	NM
King 5	2M03141752+5245394	-70.9 ± 0.1	-0.29 ± 0.01	0.44 ± 0.07	-0.38 ± 0.07	0.00	0.00	0.00	NM
King 5	2M03142157+5250144	-98.4 ± 0.2	-0.60 ± 0.01	-0.27 ± 0.10	0.67 ± 0.09	0.00	0.00	0.00	NM
King 5	2M03142548+5247355	-43.5 ± 0.1	-0.07 ± 0.01	-0.27 ± 0.08	-1.44 ± 0.09	0.90	0.16	0.61	GM
King 5	2M03142663+5245499	-32.1 ± 1.8	-0.02 ± 0.01	-0.14 ± 0.07	-0.42 ± 0.06	0.00	0.00	0.03	NM
King 5	2M03142784+5242408	-45.0 ± 0.1	-0.12 ± 0.01	0.04 ± 0.05	-1.37 ± 0.04	0.99	0.98	0.43	GM
King 5	2M03143688+5243034	20.0 ± 0.0	-0.18 ± 0.01	3.70 ± 0.05	-2.81 ± 0.04	0.00	0.13	0.00	NM
King 5	2M03144335+5242143	-47.0 ± 1.8	-0.10 ± 0.01	0.16 ± 0.05	-1.45 ± 0.04	0.61	0.66	0.20	GM
King 5	2M03150947+5232148	-32.9 ± 0.0	0.24 ± 0.01	-0.92 ± 0.04	0.53 ± 0.04	0.00	0.00	0.00	NM
King 5	2M03151237+5235181	-109.3 ± 0.2	-0.56 ± 0.01	-0.62 ± 0.08	0.08 ± 0.07	0.00	0.00	0.00	NM
King 5	2M03151256+5248354	-56.3 ± 0.1	0.09 ± 0.01	2.15 ± 0.10	-2.99 ± 0.11	0.00	0.00	0.00	NM
King 5	2M03153205+5248038	-22.8 ± 0.1	-0.09 ± 0.01	-0.07 ± 0.09	-0.41 ± 0.07	0.00	0.00	0.03	NM
King 5	2M03154012+5242565	-43.6 ± 0.2	-0.13 ± 0.01	-0.29 ± 0.07	-1.33 ± 0.06	0.93	0.94	0.82	GM
King 5	2M03154067+5246068	-11.1 ± 0.1	-0.19 ± 0.01	0.50 ± 0.14	-0.36 ± 0.10	0.00	0.00	0.00	NM
King 5	2M03154508+5241191	-27.6 ± 0.3	-0.13 ± 0.01	3.88 ± 0.10	-4.23 ± 0.09	0.00	0.00	0.00	NM
NGC 2158	2M06065513+2406594	30.9 ± 0.1	-0.04 ± 0.01	-1.23 ± 0.05	-1.57 ± 0.04	0.48	0.00	0.00	NM
NGC 2158	2M06065552+2405309	32.2 ± 0.1	0.02 ± 0.01	-0.05 ± 0.06	-3.23 ± 0.05	0.23	0.00	0.00	NM
NGC 2158	2M06070155+2401470	27.9 ± 0.1	-0.16 ± 0.01	-0.16 ± 0.08	-2.20 ± 0.07	1.00	0.90	0.79	GM
NGC 2158	2M06070387+2413277	-9.6 ± 4.0	-0.17 ± 0.01	2.82 ± 0.05	-3.09 ± 0.04	0.00	-1.00	0.00	NM
NGC 2158	2M06070415+2409180	26.0 ± 0.1	-0.12 ± 0.01	-0.22 ± 0.06	-2.02 ± 0.05	0.82	0.57	0.99	GM
NGC 2158	2M06070703+2418045	-6.3 ± 1.7	-0.11 ± 0.01	2.25 ± 0.05	-2.99 ± 0.04	0.00	-1.00	0.00	NM
NGC 2158	2M06071494+2407517	26.8 ± 0.1	-0.15 ± 0.01	-0.30 ± 0.05	-1.99 ± 0.04	0.96	1.00	0.92	GM
NGC 2158	2M06071579+2349116	38.2 ± 0.1	-0.56 ± 0.01	-0.54 ± 0.10	-1.83 ± 0.09	0.00	0.00	0.45	NM
NGC 2158	2M06071696+2402007	25.6 ± 0.1	-0.13 ± 0.01	-0.24 ± 0.06	-1.85 ± 0.05	0.74	0.83	0.84	GM
NGC 2158	2M06071764+2410276	25.8 ± 0.1	-0.22 ± 0.01	-0.31 ± 0.05	-2.09 ± 0.04	0.79	0.08	0.84	GM
NGC 2158	2M06071787+2405542	29.1 ± 0.0	-0.09 ± 0.01	-0.27 ± 0.05	-1.88 ± 0.04	0.86	0.21	0.87	GM
NGC 2158	2M06071913+2400148	28.5 ± 0.2	-0.16 ± 0.01	-0.52 ± 0.06	-1.94 ± 0.05	0.95	0.95	0.52	GM
NGC 2158	2M06072041+2407463	28.6 ± 0.2	-0.18 ± 0.01	-0.11 ± 0.06	-2.00 ± 0.05	0.94	0.64	0.97	GM
NGC 2158	2M06072443+2400524	28.5 ± 0.1	-0.16 ± 0.01	-0.26 ± 0.07	-1.98 ± 0.06	0.94	0.96	0.96	GM
NGC 2158	2M06072624+2409568	25.1 ± 0.0	-0.17 ± 0.01	-0.25 ± 0.05	-1.88 ± 0.05	0.63	0.84	0.88	GM
NGC 2158	2M06072907+2402151	27.9 ± 0.1	-0.12 ± 0.01	-0.26 ± 0.06	-1.99 ± 0.05	0.99	0.56	0.96	GM
NGC 2158	2M06072918+2408185	29.2 ± 0.1	-0.15 ± 0.01	-0.14 ± 0.10	-1.91 ± 0.08	0.85	1.00	0.90	GM
NGC 2158	2M06073636+2405001	29.1 ± 0.1	-0.13 ± 0.01	-0.07 ± 0.06	-2.00 ± 0.05	0.85	0.82	0.93	GM
NGC 2158	2M06073901+2416594	37.6 ± 8.7	-0.14 ± 0.01	0.88 ± 1.07	-5.18 ± 0.92	0.00	-1.00	0.00	NM
NGC 2158	2M06073917+2409098	29.5 ± 0.1	-0.11 ± 0.01	-0.17 ± 0.05	-2.07 ± 0.05	0.78	0.42	0.98	GM
NGC 2158	2M06073998+2403546	29.0 ± 0.0	-0.17 ± 0.01	-0.16 ± 0.06	-2.14 ± 0.05	0.88	0.80	0.89	GM
NGC 2158	2M06074162+2405540	26.6 ± 0.1	-0.14 ± 0.01	-0.46 ± 0.07	-2.13 ± 0.06	0.92	0.97	0.52	GM
NGC 2158	2M06074272+2402514	25.0 ± 0.1	-0.19 ± 0.01	-0.24 ± 0.06	-1.91 ± 0.05	0.62	0.42	0.93	GM
NGC 2158	2M06075243+2403561	25.9 ± 0.1	-0.15 ± 0.01	-0.19 ± 0.06	-2.07 ± 0.05	0.81	0.99	0.98	GM
NGC 2158	2M06083074+2402181	0.3 ± 0.1	0.10 ± 0.01	-2.01 ± 0.08	0.44 ± 0.07	0.00	0.00	0.00	NM
NGC 2420	2M07372731+2134182	8.1 ± 0.0	0.07 ± 0.01	1.35 ± 0.11	-0.05 ± 0.07	0.00	0.00	0.00	NM
NGC 2420	2M07374517+2140545	-12.7 ± 0.1	-0.10 ± 0.01	3.18 ± 0.08	-1.53 ± 0.07	0.00	0.00	0.00	NM
NGC 2420	2M07375511+2121153	27.2 ± 0.1	-0.02 ± 0.01	0.57 ± 0.08	-2.86 ± 0.06	0.00	0.00	0.00	NM
NGC 2420	2M07375926+2134154	-9.3 ± 0.2	0.01 ± 0.01	-1.12 ± 0.07	-2.28 ± 0.06	0.00	0.00	0.69	NM
NGC 2420	2M07380093+2138364	47.8 ± 2.6	-0.34 ± 0.01	-23.15 ± 0.09	-31.39 ± 0.07	0.00	-1.00	0.00	NM
NGC 2420	2M07380545+2136507	73.3 ± 0.5	-0.14 ± 0.01	-1.06 ± 0.07	-2.22 ± 0.06	0.85	0.96	0.76	GM
NGC 2420	2M07380599+2133071	75.1 ± 0.2	-0.13 ± 0.01	-1.14 ± 0.06	-2.07 ± 0.05	0.86	1.00	0.93	GM
NGC 2420	2M07380627+2136542	73.8 ± 0.1	-0.14 ± 0.01	-1.11 ± 0.08	-2.15 ± 0.06	0.97	0.86	0.93	GM
NGC 2420	2M07381036+2137497	52.9 ± 0.1	0.28 ± 0.01	-3.49 ± 0.07	-4.50 ± 0.05	0.00	0.00	0.00	NM
NGC 2420	2M07381507+2134589	74.3 ± 0.1	-0.14 ± 0.01	-1.36 ± 0.11	-2.23 ± 0.09	1.00	0.94	0.58	GM
NGC 2420	2M07381549+2138015	74.6 ± 0.1	-0.14 ± 0.01	-1.10 ± 0.07	-2.12 ± 0.06	0.97	0.96	0.91	GM
NGC 2420	2M07381562+2142173	53.8 ± 12.3	-0.56 ± 0.01	0.29 ± 0.06	-0.34 ± 0.05	0.00	0.00	0.00	NM
NGC 2420	2M07381972+2136522	74.6 ± 0.1	-0.12 ± 0.01	-1.10 ± 0.06	-2.12 ± 0.05	0.97	0.94	0.90	GM
NGC 2420	2M07382114+2131418	74.3 ± 0.0	-0.09 ± 0.01	-1.13 ± 0.08	-2.11 ± 0.06	1.00	0.38	0.95	GM
NGC 2420	2M07382148+2135050	74.3 ± 0.0	-0.10 ± 0.01	-1.12 ± 0.07	-2.09 ± 0.05	1.00	0.53	0.91	GM
NGC 2420	2M07382195+2135508	73.5 ± 0.2	-0.09 ± 0.01	-1.19 ± 0.07	-2.20 ± 0.06	0.91	0.24	0.92	GM
NGC 2420	2M07382325+2142409	49.0 ± 0.5	-0.48 ± 0.01	-4.47 ± 0.10	-21.39 ± 0.07	0.00	-1.00	0.00	NM
NGC 2420	2M07382327+2132569	73.5 ± 0.2	-0.16 ± 0.01	-1.15 ± 0.06	-2.19 ± 0.05	0.90	0.61	0.93	GM
NGC 2420	2M07382347+2124448	74.1 ± 0.1	-0.16 ± 0.01	-1.44 ± 0.06	-2.21 ± 0.05	0.00	0.00	0.42	NM
NGC 2420	2M07382501+2133283	74.4 ± 0.2	-0.12 ± 0.01	-1.23 ± 0.05	-2.01 ± 0.04	0.99	0.87	0.81	GM

Continued on next page

Table A.1 – Continued

Cluster name	2MASS ID	RV (km s^{-1})	[Fe/H] (dex)	μ_α (mas yr^{-1})	μ_δ (mas yr^{-1})	RV Prob	[Fe/H] Prob	PM Prob	Memb
NGC 2420	2M07382539+2131123	13.0 ± 0.3	0.07 ± 0.01	-12.16 ± 0.06	-9.38 ± 0.04	0.00	-1.00	0.00	NM
NGC 2420	2M07382670+2128514	74.5 ± 0.1	-0.07 ± 0.01	-1.19 ± 0.07	-2.02 ± 0.06	0.98	0.06	0.85	GM
NGC 2420	2M07382696+2138244	73.9 ± 0.1	-0.11 ± 0.01	-1.28 ± 0.07	-2.08 ± 0.06	0.97	0.81	0.90	GM
NGC 2420	2M07382745+2141499	38.6 ± 0.1	-0.26 ± 0.01	0.28 ± 0.07	-0.38 ± 0.05	0.00	0.00	0.00	NM
NGC 2420	2M07382939+2128469	-26.7 ± 0.0	-0.30 ± 0.01	-1.68 ± 0.10	-0.28 ± 0.08	0.00	0.00	0.00	NM
NGC 2420	2M07382984+2134509	75.1 ± 0.2	-0.13 ± 0.01	-1.03 ± 0.13	-1.92 ± 0.08	0.83	1.00	0.38	GM
NGC 2420	2M07383034+2131593	-7.9 ± 1.3	-0.00 ± 0.01	-43.37 ± 0.15	-11.71 ± 0.12	0.00	-1.00	0.00	NM
NGC 2420	2M07383116+2130254	-37.0 ± 0.3	0.22 ± 0.01	20.11 ± 0.08	-13.60 ± 0.07	0.00	-1.00	0.00	NM
NGC 2420	2M07383200+2125301	59.0 ± 0.5	-0.22 ± 0.01	-2.43 ± 0.06	-0.02 ± 0.05	0.00	0.00	0.00	NM
NGC 2420	2M07383449+2124088	61.4 ± 0.2	-0.01 ± 0.01	0.17 ± 0.07	0.51 ± 0.05	0.00	0.00	0.00	NM
NGC 2420	2M07383625+2128409	21.2 ± 0.2	0.06 ± 0.01	-4.98 ± 0.21	-29.29 ± 0.17	0.00	-1.00	0.00	NM
NGC 2420	2M07383760+2134119	73.9 ± 0.0	-0.15 ± 0.01	-1.23 ± 0.07	-2.00 ± 0.06	0.98	0.79	0.81	GM
NGC 2420	2M07384226+2131021	81.5 ± 2.8	-0.48 ± 0.01	-2.96 ± 0.08	-0.09 ± 0.07	0.00	0.00	0.00	NM
NGC 2420	2M07384367+2139557	-30.4 ± 0.1	-0.03 ± 0.01	-0.57 ± 0.08	-5.70 ± 0.07	0.00	0.00	0.00	NM
NGC 2420	2M07384370+2142362	-0.4 ± 0.6	-1.49 ± 0.01	2.75 ± 0.07	-2.13 ± 0.06	0.00	0.00	0.00	NM
NGC 2420	2M07384636+2129320	-30.4 ± 0.3	0.15 ± 0.01	-0.56 ± 0.06	-6.79 ± 0.06	0.00	-1.00	0.00	NM
NGC 2420	2M07384958+2141260	1.6 ± 0.1	0.09 ± 0.01	-12.50 ± 0.08	-14.32 ± 0.07	0.00	-1.00	0.00	NM
NGC 2420	2M07385109+2132052	-9.6 ± 0.3	0.22 ± 0.01	7.92 ± 0.12	-0.20 ± 0.11	0.00	-1.00	0.00	NM
NGC 2420	2M07385123+2145432	-24.5 ± 0.0	-0.01 ± 0.01	1.58 ± 0.08	-2.41 ± 0.06	0.00	0.00	0.00	NM
NGC 2420	2M07385724+2139461	-18.3 ± 0.5	-0.37 ± 0.01	-23.31 ± 0.08	-4.86 ± 0.07	0.00	-1.00	0.00	NM
NGC 2420	2M07385807+2134121	81.7 ± 1.0	-0.23 ± 0.01	-19.20 ± 0.91	-2.76 ± 0.81	0.00	-1.00	0.00	NM
NGC 2420	2M07385992+2132060	64.4 ± 0.2	-0.10 ± 0.01	-0.59 ± 0.05	-2.34 ± 0.05	0.00	0.00	0.02	NM
NGC 2420	2M07390472+2133277	69.3 ± 0.1	-0.49 ± 0.01	0.20 ± 0.05	-0.97 ± 0.04	0.00	0.00	0.00	NM
NGC 2420	2M07390789+2133056	-22.7 ± 0.0	-0.20 ± 0.01	10.18 ± 0.08	-4.27 ± 0.07	0.00	0.00	0.00	NM
NGC 2420	2M07391721+2129358	8.3 ± 0.0	-0.01 ± 0.01	0.20 ± 0.08	-3.39 ± 0.08	0.00	0.00	0.00	NM
NGC 2682	2M08465424+1147146	28.9 ± 0.2	0.07 ± 0.01	-13.48 ± 0.06	-12.12 ± 0.04	0.00	-1.00	0.00	NM
NGC 2682	2M08465797+1144036	-21.2 ± 0.2	0.05 ± 0.01	12.14 ± 0.07	-28.65 ± 0.05	0.00	-1.00	0.00	NM
NGC 2682	2M08465835+1142474	51.9 ± 0.2	-0.30 ± 0.01	-2.85 ± 0.07	-3.04 ± 0.05	0.00	0.00	0.00	NM
NGC 2682	2M08470047+1200251	3.7 ± 0.1	0.34 ± 0.01	4.59 ± 0.07	-11.07 ± 0.04	0.00	-1.00	0.00	NM
NGC 2682	2M08470209+1139026	20.7 ± 0.1	0.08 ± 0.01	-3.43 ± 0.13	-1.22 ± 0.11	0.00	0.00	0.00	NM
NGC 2682	2M08470616+1137340	-4.6 ± 0.1	0.22 ± 0.01	-43.06 ± 0.09	-73.82 ± 0.08	0.00	-1.00	0.00	NM
NGC 2682	2M08470659+1134580	8.1 ± 28.0	-0.25 ± 0.01	-27.18 ± 0.07	2.97 ± 0.06	0.00	0.00	0.00	NM
NGC 2682	2M08471039+1144260	10.2 ± 0.4	-0.20 ± 0.01	-1.10 ± 0.08	-22.17 ± 0.06	0.00	-1.00	0.00	NM
NGC 2682	2M08471287+1156591	44.7 ± 0.4	-0.15 ± 0.01	-9.71 ± 0.08	8.13 ± 0.05	0.00	-1.00	0.00	NM
NGC 2682	2M08471677+1153594	-35.4 ± 0.1	-0.44 ± 0.01	8.54 ± 0.06	-8.09 ± 0.04	0.00	0.00	0.00	NM
NGC 2682	2M08471940+1147513	8.7 ± 0.0	0.17 ± 0.01	-23.42 ± 0.06	-13.87 ± 0.04	0.00	-1.00	0.00	NM
NGC 2682	2M08471960+1200558	70.1 ± 0.4	-0.34 ± 0.01	-1.70 ± 0.08	-0.45 ± 0.05	0.00	0.00	0.00	NM
NGC 2682	2M08472719+1207438	67.8 ± 0.2	-0.21 ± 0.01	-8.53 ± 0.07	-0.16 ± 0.05	0.00	0.00	0.00	NM
NGC 2682	2M08472830+1122142	18.5 ± 0.1	0.18 ± 0.01	-4.84 ± 0.08	-3.03 ± 0.07	0.00	0.00	0.00	NM
NGC 2682	2M08473204+1117387	-13.5 ± 0.2	0.08 ± 0.01	3.29 ± 0.06	-8.51 ± 0.06	0.00	-1.00	0.00	NM
NGC 2682	2M08473407+1146061	14.4 ± 0.1	0.05 ± 0.01	-17.89 ± 0.06	0.17 ± 0.03	0.00	-1.00	0.00	NM
NGC 2682	2M08473625+1216354	-3.9 ± 0.1	-0.23 ± 0.01	2.46 ± 0.08	2.26 ± 0.05	0.00	0.00	0.00	NM
NGC 2682	2M08474075+1214417	-11.3 ± 0.3	0.25 ± 0.01	13.29 ± 0.09	-33.25 ± 0.05	0.00	-1.00	0.00	NM
NGC 2682	2M08474187+1214007	71.3 ± 0.1	-0.15 ± 0.01	-3.67 ± 0.05	-9.63 ± 0.03	0.00	0.00	0.00	NM
NGC 2682	2M08474335+1148349	66.7 ± 0.4	-0.79 ± 0.01	-0.01 ± 0.08	-0.13 ± 0.05	0.00	0.00	0.00	NM
NGC 2682	2M08474422+1147248	35.6 ± 0.3	-0.46 ± 0.01	-1.17 ± 0.05	-2.77 ± 0.03	0.00	0.00	0.00	NM
NGC 2682	2M08474835+1216307	36.9 ± 0.1	-0.20 ± 0.01	-33.62 ± 0.05	-53.49 ± 0.03	0.00	-1.00	0.00	NM
NGC 2682	2M08474835+1213249	76.4 ± 0.1	-0.07 ± 0.01	-4.93 ± 0.05	-4.09 ± 0.03	0.00	0.00	0.00	NM
NGC 2682	2M08474967+1209048	-13.2 ± 0.2	-0.25 ± 0.01	-10.09 ± 0.09	-6.60 ± 0.06	0.00	-1.00	0.00	NM
NGC 2682	2M08475131+1147500	23.4 ± 0.3	0.02 ± 0.01	-9.19 ± 0.09	-6.54 ± 0.06	0.00	-1.00	0.00	NM
NGC 2682	2M08475214+1226481	50.0 ± 0.2	0.26 ± 0.01	-3.53 ± 0.25	-4.23 ± 0.15	0.00	0.00	0.00	NM
NGC 2682	2M08475226+1138067	44.0 ± 0.4	0.42 ± 0.01	-14.75 ± 0.08	-3.54 ± 0.06	0.00	-1.00	0.00	NM
NGC 2682	2M08475362+1155177	12.5 ± 0.3	-0.75 ± 0.01	11.60 ± 0.08	-7.37 ± 0.05	0.00	0.00	0.00	NM
NGC 2682	2M08475364+1213548	-46.9 ± 0.0	-0.10 ± 0.01	1.21 ± 1.12	-29.99 ± 0.74	0.00	-1.00	0.00	NM
NGC 2682	2M08475570+1217389	8.2 ± 0.3	0.24 ± 0.01	-0.05 ± 0.07	-4.42 ± 0.04	0.00	-1.00	0.00	NM
NGC 2682	2M08475659+1143557	81.8 ± 0.5	-0.42 ± 0.01	-11.61 ± 0.26	-4.19 ± 0.16	0.00	-1.00	0.00	NM
NGC 2682	2M08475698+1154467	70.2 ± 0.5	-0.33 ± 0.01	-2.60 ± 0.08	-56.93 ± 0.05	0.00	-1.00	0.00	NM
NGC 2682	2M08475900+1209234	17.9 ± 0.1	-0.02 ± 0.01	-4.72 ± 0.07	-0.17 ± 0.04	0.00	0.00	0.00	NM
NGC 2682	2M08480048+1224225	121.2 ± 0.3	-0.72 ± 0.01	1.67 ± 0.07	-4.37 ± 0.04	0.00	0.00	0.00	NM
NGC 2682	2M08480285+1157534	-13.0 ± 13.9	0.07 ± 0.01	2.08 ± 0.08	-19.28 ± 0.05	0.00	-1.00	0.00	NM
NGC 2682	2M08480371+1137211	55.9 ± 0.2	-0.26 ± 0.01	-29.16 ± 0.07	0.02 ± 0.05	0.00	-1.00	0.00	NM
NGC 2682	2M08480413+1204155	60.3 ± 0.1	-0.04 ± 0.01	-25.13 ± 0.70	-13.16 ± 0.45	0.00	-1.00	0.00	NM
NGC 2682	2M08480433+1118214	13.3 ± 10.3	-0.04 ± 0.01	0.18 ± 0.10	0.63 ± 0.08	0.00	-1.00	0.00	NM

Continued on next page

Table A.1 – Continued

Cluster name	2MASS ID	RV (km s^{-1})	[Fe/H] (dex)	μ_α (mas yr^{-1})	μ_δ (mas yr^{-1})	RV Prob	[Fe/H] Prob	PM Prob	Memb
NGC 2682	2M08480433+1210049	104.7 ± 0.1	-0.85 ± 0.01	-2.68 ± 0.07	-7.07 ± 0.04	0.00	0.00	0.00	NM
NGC 2682	2M08480651+1129404	16.0 ± 0.2	0.21 ± 0.01	-12.16 ± 0.06	2.88 ± 0.04	0.00	-1.00	0.00	NM
NGC 2682	2M08480751+1211126	59.6 ± 0.1	0.15 ± 0.01	1.85 ± 0.07	-4.19 ± 0.05	0.00	0.00	0.00	NM
NGC 2682	2M08480807+1209316	57.1 ± 0.4	-1.12 ± 0.01	1.01 ± 0.08	-3.38 ± 0.05	0.00	0.00	0.00	NM
NGC 2682	2M08480981+1202496	38.6 ± 0.3	0.04 ± 0.01	-9.90 ± 0.06	-6.02 ± 0.04	0.00	-1.00	0.00	NM
NGC 2682	2M08481206+1209193	16.3 ± 0.1	-0.30 ± 0.01	-3.09 ± 0.07	-3.15 ± 0.05	0.00	0.00	0.00	NM
NGC 2682	2M08481209+1228556	78.0 ± 0.1	-0.12 ± 0.01	-1.40 ± 0.04	-2.32 ± 0.03	0.00	0.00	0.00	NM
NGC 2682	2M08481249+1219218	34.0 ± 0.1	0.12 ± 0.01	-2.49 ± 0.08	-20.65 ± 0.05	0.00	-1.00	0.00	NM
NGC 2682	2M08481310+1121317	-10.8 ± 0.3	0.06 ± 0.01	17.24 ± 0.08	-31.91 ± 0.05	0.00	-1.00	0.00	NM
NGC 2682	2M08481407+1133318	-11.1 ± 6.3	-0.21 ± 0.01	-1.70 ± 0.04	-1.22 ± 0.03	0.00	0.00	0.00	NM
NGC 2682	2M08481428+1235172	-4.7 ± 0.3	-0.02 ± 0.01	15.58 ± 0.07	-7.22 ± 0.04	0.00	-1.00	0.00	NM
NGC 2682	2M08481532+1208430	-12.9 ± 0.0	-0.35 ± 0.01	1.27 ± 0.07	-3.67 ± 0.05	0.00	0.00	0.00	NM
NGC 2682	2M08481784+1222097	33.8 ± 0.1	0.02 ± 0.01	-10.86 ± 0.07	-2.98 ± 0.04	0.00	-1.00	0.90	NM
NGC 2682	2M08481832+1153154	28.6 ± 0.2	0.02 ± 0.01	-1.42 ± 0.07	-9.83 ± 0.04	0.00	-1.00	0.00	NM
NGC 2682	2M08481950+1146414	32.0 ± 0.1	0.18 ± 0.01	-7.03 ± 0.07	-13.62 ± 0.05	0.00	0.00	0.00	NM
NGC 2682	2M08482003+1114207	-22.8 ± 0.0	0.05 ± 0.01	-1.48 ± 0.06	-34.42 ± 0.04	0.00	-1.00	0.00	NM
NGC 2682	2M08482033+1100455	35.4 ± 4.1	-0.44 ± 0.01	-2.79 ± 0.08	-17.45 ± 0.05	0.00	-1.00	0.00	NM
NGC 2682	2M08482099+1200564	-8.3 ± 0.2	0.26 ± 0.01	9.20 ± 0.06	-17.00 ± 0.03	0.00	-1.00	0.00	NM
NGC 2682	2M08482212+1119472	216.0 ± 0.3	-1.46 ± 0.01	-1.78 ± 0.08	-5.37 ± 0.05	0.00	0.00	0.00	NM
NGC 2682	2M08482220+1231423	14.5 ± 0.3	0.02 ± 0.01	-2.92 ± 0.13	-6.33 ± 0.08	0.00	-1.00	0.00	NM
NGC 2682	2M08482232+1118172	23.8 ± 0.1	0.09 ± 0.01	-2.87 ± 0.07	-2.50 ± 0.04	0.00	0.00	0.00	NM
NGC 2682	2M08482410+1124358	22.9 ± 0.3	-0.55 ± 0.01	-5.71 ± 0.09	-0.40 ± 0.06	0.00	0.00	0.00	NM
NGC 2682	2M08482506+1142272	-3.0 ± 0.1	-0.04 ± 0.01	5.66 ± 0.08	2.16 ± 0.05	0.00	-1.00	0.00	NM
NGC 2682	2M08482568+1230130	95.4 ± 0.8	-1.75 ± 0.02	1.12 ± 0.06	-3.91 ± 0.04	0.00	0.00	0.00	NM
NGC 2682	2M08482629+1146050	-31.1 ± 0.2	-0.28 ± 0.01	-1.20 ± 0.07	-7.67 ± 0.05	0.00	-1.00	0.00	NM
NGC 2682	2M08482637+1112374	49.9 ± 0.3	0.29 ± 0.01	-4.65 ± 0.05	-1.16 ± 0.03	0.00	0.00	0.00	NM
NGC 2682	2M08482768+1118034	6.9 ± 0.1	-0.03 ± 0.01	5.14 ± 0.06	-0.33 ± 0.04	0.00	-1.00	0.00	NM
NGC 2682	2M08482786+1136249	-11.1 ± 0.1	-0.22 ± 0.01	0.96 ± 0.07	5.74 ± 0.05	0.00	-1.00	0.00	NM
NGC 2682	2M08482936+1206353	34.5 ± 0.1	0.06 ± 0.01	-10.92 ± 0.05	-2.84 ± 0.03	0.00	-1.00	0.88	NM
NGC 2682	2M08482936+1202283	-34.2 ± 0.2	-0.35 ± 0.01	7.64 ± 0.05	-8.07 ± 0.03	0.00	-1.00	0.00	NM
NGC 2682	2M08482947+1222197	51.5 ± 0.5	-0.41 ± 0.01	-13.21 ± 0.06	-66.17 ± 0.04	0.00	-1.00	0.00	NM
NGC 2682	2M08482983+1127196	45.6 ± 0.2	-0.24 ± 0.01	-6.41 ± 0.05	3.41 ± 0.03	0.00	-1.00	0.00	NM
NGC 2682	2M08483014+1123564	13.8 ± 0.0	0.41 ± 0.01	9.17 ± 0.04	-17.36 ± 0.03	0.00	-1.00	0.00	NM
NGC 2682	2M08483131+1238069	15.7 ± 0.3	0.28 ± 0.01	-21.90 ± 0.08	-8.68 ± 0.05	0.00	-1.00	0.00	NM
NGC 2682	2M08483339+1139065	-4.1 ± 0.4	0.25 ± 0.01	6.30 ± 0.07	-2.26 ± 0.04	0.00	-1.00	0.00	NM
NGC 2682	2M08483429+1225079	-2.3 ± 2.3	-0.05 ± 0.01	-0.39 ± 0.06	-5.02 ± 0.04	0.00	-1.00	0.00	NM
NGC 2682	2M08483499+1236448	-22.4 ± 10.4	-0.12 ± 0.01	-13.10 ± 0.11	-22.36 ± 0.08	0.00	-1.00	0.00	NM
NGC 2682	2M08483588+1107245	-17.4 ± 0.1	-0.32 ± 0.01	0.76 ± 0.06	-0.59 ± 0.04	0.00	0.00	0.00	NM
NGC 2682	2M08483718+1126251	45.3 ± 0.0	-0.34 ± 0.01	-19.70 ± 0.08	-7.12 ± 0.05	0.00	0.00	0.00	NM
NGC 2682	2M08483794+1239523	70.8 ± 0.1	0.00 ± 0.01	-14.70 ± 0.07	-8.83 ± 0.05	0.00	0.00	0.00	NM
NGC 2682	2M08483845+1236048	20.6 ± 0.0	0.11 ± 0.01	-2.78 ± 0.05	-20.62 ± 0.03	0.00	-1.00	0.00	NM
NGC 2682	2M08483849+1147175	42.9 ± 0.1	-0.12 ± 0.01	-28.95 ± 0.05	22.69 ± 0.03	0.00	-1.00	0.00	NM
NGC 2682	2M08484041+1116361	23.7 ± 0.3	-0.10 ± 0.01	-7.57 ± 0.08	7.73 ± 0.05	0.00	-1.00	0.00	NM
NGC 2682	2M08484473+1131207	24.1 ± 0.0	0.26 ± 0.01	-0.75 ± 0.07	-3.43 ± 0.04	0.00	-1.00	0.00	NM
NGC 2682	2M08484622+1153404	104.5 ± 0.3	-0.50 ± 0.01	-0.54 ± 0.06	-2.17 ± 0.04	0.00	0.00	0.00	NM
NGC 2682	2M08484650+1103478	9.2 ± 0.5	-0.02 ± 0.01	-6.53 ± 0.09	-14.38 ± 0.06	0.00	-1.00	0.00	NM
NGC 2682	2M08484721+1101020	22.1 ± 0.1	-0.11 ± 0.01	-1.46 ± 0.05	-4.70 ± 0.03	0.00	0.00	0.00	NM
NGC 2682	2M08484748+1147431	19.8 ± 0.1	-0.32 ± 0.01	-7.92 ± 0.12	0.70 ± 0.07	0.00	0.00	0.00	NM
NGC 2682	2M08484901+1158336	81.0 ± 0.1	0.25 ± 0.01	-5.27 ± 0.05	-7.44 ± 0.03	0.00	-1.00	0.00	NM
NGC 2682	2M08484974+1207475	19.2 ± 0.1	-0.00 ± 0.01	-51.92 ± 0.07	-0.93 ± 0.04	0.00	-1.00	0.00	NM
NGC 2682	2M08485043+1142106	17.6 ± 0.2	0.01 ± 0.01	18.44 ± 0.07	-24.96 ± 0.04	0.00	-1.00	0.00	NM
NGC 2682	2M08485045+1212575	-18.4 ± 0.1	-0.00 ± 0.01	-16.85 ± 0.06	-19.11 ± 0.04	0.00	-1.00	0.00	NM
NGC 2682	2M08485051+1134020	31.0 ± 13.3	0.03 ± 0.01	-17.56 ± 0.08	0.43 ± 0.05	0.00	-1.00	0.00	NM
NGC 2682	2M08485082+1055422	29.0 ± 0.2	0.19 ± 0.01	-20.50 ± 0.04	-3.95 ± 0.03	0.00	-1.00	0.00	NM
NGC 2682	2M08485299+1149360	2.0 ± 0.0	-0.14 ± 0.01	-5.00 ± 0.06	-3.90 ± 0.04	0.00	0.00	0.00	NM
NGC 2682	2M08485369+1129360	321.8 ± 0.7	-1.49 ± 0.01	-5.17 ± 0.07	-12.71 ± 0.04	0.00	0.00	0.00	NM
NGC 2682	2M08485396+1144228	16.7 ± 0.2	-0.12 ± 0.01	-2.59 ± 0.04	-0.04 ± 0.03	0.00	0.00	0.00	NM
NGC 2682	2M08485429+1100232	-37.3 ± 0.3	0.10 ± 0.01	-4.19 ± 0.07	-16.28 ± 0.05	0.00	-1.00	0.00	NM
NGC 2682	2M08485445+1131061	-70.4 ± 0.1	0.06 ± 0.01	0.09 ± 0.06	-27.20 ± 0.04	0.00	-1.00	0.00	NM
NGC 2682	2M08485590+1209429	33.4 ± 51.1	-0.08 ± 0.01	-10.99 ± 0.06	-2.89 ± 0.04	0.00	-1.00	0.96	NM
NGC 2682	2M08485678+1124111	-8.2 ± 0.2	-0.10 ± 0.01	38.59 ± 0.08	-49.51 ± 0.05	0.00	-1.00	0.00	NM
NGC 2682	2M08485930+1117220	29.1 ± 0.1	-0.21 ± 0.01	-16.32 ± 0.08	0.97 ± 0.05	0.00	0.00	0.00	NM
NGC 2682	2M08485953+1237144	19.4 ± 0.0	0.20 ± 0.01	2.78 ± 0.05	0.29 ± 0.04	0.00	0.00	0.00	NM

Continued on next page

Table A.1 – Continued

Cluster name	2MASS ID	RV (km s^{-1})	[Fe/H] (dex)	μ_α (mas yr^{-1})	μ_δ (mas yr^{-1})	RV Prob	[Fe/H] Prob	PM Prob	Memb
NGC 2682	2M08485981+1241435	40.4 ± 0.2	0.18 ± 0.01	-3.23 ± 0.14	0.12 ± 0.12	0.00	-1.00	0.00	NM
NGC 2682	2M08490048+1106352	28.4 ± 0.1	0.15 ± 0.01	-10.60 ± 0.06	-8.05 ± 0.04	0.00	0.00	0.00	NM
NGC 2682	2M08490142+1124548	14.8 ± 0.1	-0.26 ± 0.01	0.21 ± 0.09	-2.32 ± 0.05	0.00	0.00	0.00	NM
NGC 2682	2M08490606+1108577	66.6 ± 0.3	-0.61 ± 0.01	0.24 ± 0.08	-0.02 ± 0.05	0.00	0.00	0.00	NM
NGC 2682	2M08490674+1129529	33.5 ± 0.0	0.03 ± 0.01	-2.39 ± 0.08	-3.07 ± 0.05	0.00	0.00	0.00	NM
NGC 2682	2M08490883+1122497	-8.5 ± 0.1	-0.10 ± 0.01	38.46 ± 0.08	-49.49 ± 0.05	0.00	-1.00	0.00	NM
NGC 2682	2M08490965+1148267	18.6 ± 6.0	0.13 ± 0.01	-10.89 ± 0.06	-2.82 ± 0.04	0.00	-1.00	0.80	NM
NGC 2682	2M08491100+1058342	-3.9 ± 0.6	-0.23 ± 0.01	5.66 ± 0.08	-2.47 ± 0.07	0.00	-1.00	0.00	NM
NGC 2682	2M08491149+1211177	18.8 ± 0.1	-0.22 ± 0.01	-2.66 ± 0.08	-1.94 ± 0.05	0.00	0.00	0.00	NM
NGC 2682	2M08491294+1241252	0.6 ± 0.1	0.00 ± 0.01	-15.73 ± 0.08	9.90 ± 0.05	0.00	-1.00	0.00	NM
NGC 2682	2M08491444+1106562	48.6 ± 0.0	-0.05 ± 0.01	-30.49 ± 0.05	-28.66 ± 0.03	0.00	-1.00	0.00	NM
NGC 2682	2M08491562+1201501	73.7 ± 0.1	0.42 ± 0.01	-4.34 ± 0.05	-0.60 ± 0.03	0.00	-1.00	0.00	NM
NGC 2682	2M08491593+1146055	33.5 ± 0.2	-0.01 ± 0.01	-10.01 ± 0.07	-3.41 ± 0.05	0.97	-1.00	0.00	NM
NGC 2682	2M08491878+1226439	-0.2 ± 0.1	-0.15 ± 0.01	1.59 ± 0.07	-11.22 ± 0.06	0.00	0.00	0.00	NM
NGC 2682	2M08492247+1117282	130.6 ± 0.1	0.12 ± 0.01	0.21 ± 0.08	-4.01 ± 0.05	0.00	0.00	0.00	NM
NGC 2682	2M08492286+1218563	33.5 ± 0.4	-0.01 ± 0.01	-11.11 ± 0.08	-1.93 ± 0.06	0.00	-1.00	0.00	NM
NGC 2682	2M08492355+1103338	56.6 ± 0.2	-0.01 ± 0.01	-42.58 ± 0.04	-27.07 ± 0.03	0.00	-1.00	0.00	NM
NGC 2682	2M08492385+1206143	30.3 ± 1.5	-0.21 ± 0.01	-10.70 ± 0.81	-13.25 ± 0.59	0.00	-1.00	0.00	NM
NGC 2682	2M08492491+1144057	35.1 ± 1.5	0.11 ± 0.01	-11.06 ± 0.07	-2.87 ± 0.05	0.66	0.60	0.87	GM
NGC 2682	2M08492547+1235297	3.0 ± 0.1	0.18 ± 0.01	3.29 ± 0.05	-115.77 ± 0.04	0.00	-1.00	0.00	NM
NGC 2682	2M08492553+1116449	22.1 ± 1.2	0.14 ± 0.01	-22.67 ± 0.08	-7.71 ± 0.06	0.00	-1.00	0.00	NM
NGC 2682	2M08492689+1154417	21.1 ± 0.0	0.23 ± 0.01	0.26 ± 0.78	2.17 ± 0.66	0.00	0.00	0.00	NM
NGC 2682	2M08492956+1211043	33.8 ± 0.2	-0.09 ± 0.01	-11.19 ± 0.06	-2.37 ± 0.05	0.00	-1.00	0.03	NM
NGC 2682	2M08492977+1237329	21.0 ± 0.3	0.12 ± 0.01	-0.80 ± 0.14	-6.24 ± 0.10	0.00	-1.00	0.00	NM
NGC 2682	2M08493024+1135358	-34.5 ± 0.1	-0.09 ± 0.01	-7.58 ± 0.16	-17.60 ± 0.10	0.00	-1.00	0.00	NM
NGC 2682	2M08493081+1221077	-20.0 ± 0.1	-0.18 ± 0.01	-1.88 ± 0.04	-3.40 ± 0.04	0.00	0.00	0.00	NM
NGC 2682	2M08493120+1112548	52.7 ± 0.0	0.08 ± 0.01	-4.19 ± 0.08	-4.45 ± 0.05	0.00	0.00	0.00	NM
NGC 2682	2M08493261+1144551	-27.9 ± 0.1	-0.57 ± 0.01	-19.91 ± 0.06	-44.01 ± 0.04	0.00	0.00	0.00	NM
NGC 2682	2M08493387+1210146	-11.2 ± 0.5	-0.04 ± 0.01	-38.78 ± 0.09	22.15 ± 0.07	0.00	-1.00	0.00	NM
NGC 2682	2M08493465+1151256	34.0 ± 0.1	-0.14 ± 0.01	-10.98 ± 0.06	-2.92 ± 0.04	1.00	0.00	0.99	NM
NGC 2682	2M08493512+1210395	91.1 ± 0.1	-0.23 ± 0.01	-9.96 ± 0.07	1.98 ± 0.05	0.00	0.00	0.00	NM
NGC 2682	2M08493684+1153221	-0.2 ± 0.1	0.18 ± 0.01	3.33 ± 0.06	0.40 ± 0.04	0.00	0.01	0.00	NM
NGC 2682	2M08493790+1126043	0.5 ± 0.2	0.02 ± 0.01	-19.80 ± 0.06	-17.88 ± 0.04	0.00	-1.00	0.00	NM
NGC 2682	2M08493814+1049542	-9.2 ± 0.0	0.22 ± 0.01	28.67 ± 0.06	-30.36 ± 0.04	0.00	-1.00	0.00	NM
NGC 2682	2M08493910+1100161	54.9 ± 0.1	0.32 ± 0.01	-29.20 ± 0.06	-11.20 ± 0.04	0.00	-1.00	0.00	NM
NGC 2682	2M08493956+1205067	25.3 ± 0.2	0.23 ± 0.01	-16.60 ± 0.05	-6.28 ± 0.03	0.00	-1.00	0.00	NM
NGC 2682	2M08494091+1217243	18.4 ± 0.8	-0.17 ± 0.01	1.24 ± 0.08	-4.66 ± 0.07	0.00	0.00	0.00	NM
NGC 2682	2M08494111+1239292	-14.1 ± 0.3	0.05 ± 0.01	10.21 ± 0.22	-21.80 ± 0.13	0.00	-1.00	0.00	NM
NGC 2682	2M08494289+1143088	35.6 ± 0.1	0.01 ± 0.01	-10.30 ± 0.06	-3.09 ± 0.04	0.42	-1.00	0.02	DM
NGC 2682	2M08494351+1241268	15.6 ± 0.2	0.17 ± 0.01	-3.18 ± 0.06	-22.28 ± 0.04	0.00	-1.00	0.00	NM
NGC 2682	2M08494430+1135327	-13.0 ± 0.2	0.00 ± 0.01	-3.85 ± 0.06	-26.99 ± 0.04	0.00	-1.00	0.00	NM
NGC 2682	2M08494490+1141562	35.1 ± 3.3	0.07 ± 0.01	-10.91 ± 0.07	-2.79 ± 0.04	0.65	-1.00	0.78	DM
NGC 2682	2M08494540+1056467	103.3 ± 0.5	0.02 ± 0.01	-27.01 ± 0.08	3.99 ± 0.05	0.00	-1.00	0.00	NM
NGC 2682	2M08494576+1108005	17.1 ± 0.2	-0.30 ± 0.01	0.46 ± 0.06	-2.55 ± 0.04	0.00	0.00	0.00	NM
NGC 2682	2M08494611+1150351	58.4 ± 0.1	-0.34 ± 0.01	-8.75 ± 0.06	5.25 ± 0.04	0.00	0.00	0.00	NM
NGC 2682	2M08494707+1226116	33.5 ± 7.6	-0.27 ± 0.01	-8.83 ± 0.09	-1.58 ± 0.08	0.00	-1.00	0.00	NM
NGC 2682	2M08494779+1158506	35.0 ± 0.0	0.06 ± 0.01	-10.93 ± 0.04	-3.23 ± 0.03	0.69	-1.00	0.51	DM
NGC 2682	2M08494848+1122299	35.0 ± 0.1	0.08 ± 0.01	-8.65 ± 0.05	-5.48 ± 0.03	0.00	-1.00	0.00	NM
NGC 2682	2M08495254+1133065	-12.1 ± 0.1	0.12 ± 0.01	24.09 ± 0.17	-45.78 ± 0.13	0.00	-1.00	0.00	NM
NGC 2682	2M08495268+1100195	-13.4 ± 0.0	0.20 ± 0.01	5.88 ± 0.06	-8.02 ± 0.04	0.00	-1.00	0.00	NM
NGC 2682	2M08495304+1203599	20.8 ± 0.1	-0.26 ± 0.01	-43.11 ± 0.16	49.63 ± 0.11	0.00	-1.00	0.00	NM
NGC 2682	2M08495333+1103040	-13.1 ± 0.1	0.17 ± 0.01	6.11 ± 0.05	-8.14 ± 0.03	0.00	-1.00	0.00	NM
NGC 2682	2M08495368+1211092	-4.1 ± 0.0	-0.09 ± 0.01	0.39 ± 0.08	15.32 ± 0.06	0.00	-1.00	0.00	NM
NGC 2682	2M08495563+1152518	16.7 ± 0.2	-0.05 ± 0.01	-1.99 ± 0.41	-3.31 ± 0.17	0.00	-1.00	0.00	NM
NGC 2682	2M08495642+1114087	24.6 ± 0.2	0.35 ± 0.01	16.96 ± 0.07	-55.37 ± 0.06	0.00	-1.00	0.00	NM
NGC 2682	2M08495682+1218315	37.8 ± 0.2	0.03 ± 0.01	-126.91 ± 0.09	-37.19 ± 0.06	0.00	-1.00	0.00	NM
NGC 2682	2M08495752+1046205	76.9 ± 0.1	0.05 ± 0.01	-7.28 ± 0.04	5.51 ± 0.03	0.00	0.00	0.00	NM
NGC 2682	2M08495783+1144307	0.8 ± 0.3	-0.23 ± 0.01	-5.09 ± 0.05	-4.39 ± 0.03	0.00	-1.00	0.00	NM
NGC 2682	2M08495920+1128416	33.1 ± 0.3	0.06 ± 0.01	-10.74 ± 0.05	-2.32 ± 0.03	0.86	-1.00	0.02	DM
NGC 2682	2M08500003+1156481	33.4 ± 0.0	0.02 ± 0.01	-10.63 ± 0.04	-2.96 ± 0.03	0.94	-1.00	0.37	DM
NGC 2682	2M08500005+1114327	20.6 ± 5.3	-0.32 ± 0.01	-12.91 ± 0.07	4.79 ± 0.05	0.00	-1.00	0.00	NM
NGC 2682	2M08500047+1105226	24.0 ± 0.1	0.16 ± 0.01	-3.28 ± 0.08	-3.08 ± 0.05	0.00	0.00	0.00	NM
NGC 2682	2M08500058+1143578	0.4 ± 0.1	-0.29 ± 0.01	-5.18 ± 0.10	-3.74 ± 0.07	0.00	0.00	0.00	NM

Continued on next page

Table A.1 – Continued

Cluster name	2MASS ID	RV (km s^{-1})	[Fe/H] (dex)	μ_α (mas yr^{-1})	μ_δ (mas yr^{-1})	RV Prob	[Fe/H] Prob	PM Prob	Memb
NGC 2682	2M08500106+1111017	61.5 ± 0.1	-0.11 ± 0.01	-6.36 ± 0.08	0.16 ± 0.05	0.00	0.00	0.00	NM
NGC 2682	2M08500111+1237590	-11.9 ± 0.4	-0.05 ± 0.01	22.65 ± 0.05	-17.42 ± 0.04	0.00	-1.00	0.00	NM
NGC 2682	2M08500135+1107080	61.9 ± 0.1	0.36 ± 0.01	-52.91 ± 0.06	22.54 ± 0.04	0.00	-1.00	0.00	NM
NGC 2682	2M08500139+1142241	-7.7 ± 0.5	0.12 ± 0.01	-2.11 ± 0.06	-3.53 ± 0.04	0.00	-1.00	0.00	NM
NGC 2682	2M08500243+1138034	7.0 ± 0.1	-0.02 ± 0.01	-4.35 ± 0.05	-8.86 ± 0.03	0.00	-1.00	0.00	NM
NGC 2682	2M08500587+1157508	7.5 ± 0.6	-0.12 ± 0.01	-13.97 ± 0.06	-8.87 ± 0.05	0.00	0.00	0.00	NM
NGC 2682	2M08500821+1243252	57.9 ± 0.1	-0.32 ± 0.01	-9.17 ± 0.09	-4.17 ± 0.05	0.00	0.00	0.00	NM
NGC 2682	2M08500822+1139155	65.6 ± 0.3	-0.79 ± 0.01	0.01 ± 0.08	-0.17 ± 0.05	0.00	0.00	0.00	NM
NGC 2682	2M08501044+1239515	17.6 ± 0.2	0.29 ± 0.01	-16.18 ± 0.07	-2.11 ± 0.05	0.00	-1.00	0.00	NM
NGC 2682	2M08501057+1127257	31.0 ± 0.8	-0.07 ± 0.01	-4.37 ± 0.07	-1.44 ± 0.05	0.09	-1.00	0.00	NM
NGC 2682	2M08501154+1119405	33.8 ± 0.1	0.03 ± 0.01	-11.01 ± 0.06	-3.08 ± 0.04	0.00	-1.00	0.85	NM
NGC 2682	2M08501171+1132251	35.2 ± 0.2	-0.03 ± 0.01	3.26 ± 0.05	-3.05 ± 0.03	0.62	-1.00	0.00	NM
NGC 2682	2M08501230+1151246	32.7 ± 0.0	0.02 ± 0.01	-10.79 ± 0.08	-3.25 ± 0.06	0.66	0.32	0.34	GM
NGC 2682	2M08501301+1150224	-21.0 ± 0.5	-0.63 ± 0.01	12.35 ± 0.21	-26.54 ± 0.15	0.00	-1.00	0.00	NM
NGC 2682	2M08501512+1100464	144.5 ± 0.1	-0.92 ± 0.01	-4.16 ± 0.09	-14.88 ± 0.05	0.00	0.00	0.00	NM
NGC 2682	2M08501545+1142249	52.4 ± 0.3	-0.38 ± 0.01	-3.33 ± 0.05	-2.13 ± 0.04	0.00	0.00	0.00	NM
NGC 2682	2M08501629+1153480	33.8 ± 0.2	0.02 ± 0.01	-11.15 ± 0.07	-2.58 ± 0.06	1.00	-1.00	0.21	DM
NGC 2682	2M08501827+1155212	45.1 ± 0.0	-0.07 ± 0.01	-12.25 ± 0.07	-4.27 ± 0.06	0.00	0.00	0.00	NM
NGC 2682	2M08501854+1231163	70.2 ± 0.4	-0.11 ± 0.01	-41.42 ± 0.08	-32.38 ± 0.05	0.00	-1.00	0.00	NM
NGC 2682	2M08501918+1056436	25.6 ± 0.1	-0.41 ± 0.01	-171.96 ± 0.11	-64.66 ± 0.07	0.00	-1.00	0.00	NM
NGC 2682	2M08501963+1247028	-15.0 ± 0.0	-0.27 ± 0.01	-1.18 ± 0.07	2.25 ± 0.05	0.00	0.00	0.00	NM
NGC 2682	2M08502145+1122265	11.5 ± 0.1	-0.38 ± 0.01	0.34 ± 0.07	-0.83 ± 0.04	0.00	0.00	0.00	NM
NGC 2682	2M08502250+1134206	69.4 ± 0.2	0.11 ± 0.01	-9.55 ± 0.20	-18.70 ± 0.14	0.00	-1.00	0.00	NM
NGC 2682	2M08502330+1111101	25.8 ± 0.1	0.21 ± 0.01	-5.72 ± 0.06	2.28 ± 0.04	0.00	-1.00	0.00	NM
NGC 2682	2M08502417+1139580	7.0 ± 0.1	-0.18 ± 0.01	1.15 ± 0.05	-15.42 ± 0.03	0.00	-1.00	0.00	NM
NGC 2682	2M08502698+1148313	18.7 ± 27.8	0.04 ± 0.01	-11.08 ± 0.04	-3.14 ± 0.04	0.00	-1.00	0.66	NM
NGC 2682	2M08502713+1110571	12.2 ± 55.7	0.21 ± 0.01	3.43 ± 0.07	-11.93 ± 0.04	0.00	-1.00	0.00	NM
NGC 2682	2M08502805+1154505	35.0 ± 0.2	-0.07 ± 0.01	-10.55 ± 0.04	-2.41 ± 0.03	0.72	-1.00	0.02	DM
NGC 2682	2M08502833+1142097	33.8 ± 0.4	-0.03 ± 0.01	-10.85 ± 0.07	-2.83 ± 0.05	1.00	-1.00	0.77	DM
NGC 2682	2M08502988+1208070	33.3 ± 0.1	-0.04 ± 0.01	-11.05 ± 0.07	-2.98 ± 0.05	0.92	-1.00	0.94	DM
NGC 2682	2M08503142+1206565	105.8 ± 0.2	-0.48 ± 0.01	-1.91 ± 0.05	1.11 ± 0.04	0.00	0.00	0.00	NM
NGC 2682	2M08503181+1054192	6.2 ± 0.3	-1.49 ± 0.01	5.43 ± 0.08	-9.43 ± 0.05	0.00	0.00	0.00	NM
NGC 2682	2M08503296+1208239	12.8 ± 3.0	0.20 ± 0.01	-22.52 ± 0.14	-130.59 ± 0.09	0.00	-1.00	0.00	NM
NGC 2682	2M08503390+1205498	-7.7 ± 0.0	0.08 ± 0.01	-40.04 ± 0.05	-4.85 ± 0.04	0.00	-1.00	0.00	NM
NGC 2682	2M08503392+1146272	33.8 ± 0.1	0.00 ± 0.01	-10.97 ± 0.08	-3.05 ± 0.06	1.00	-1.00	0.91	DM
NGC 2682	2M08503402+1129241	-14.9 ± 0.3	0.21 ± 0.01	-5.58 ± 0.06	-5.12 ± 0.04	0.00	-1.00	0.00	NM
NGC 2682	2M08503438+1139566	33.8 ± 0.2	0.05 ± 0.01	-10.79 ± 0.07	-2.94 ± 0.05	1.00	-1.00	0.75	DM
NGC 2682	2M08503613+1202254	12.7 ± 0.0	0.02 ± 0.01	-6.52 ± 0.05	5.18 ± 0.04	0.00	0.27	0.00	NM
NGC 2682	2M08503613+1143180	34.3 ± 0.1	0.02 ± 0.01	-11.06 ± 0.07	-2.74 ± 0.06	0.95	0.31	0.62	GM
NGC 2682	2M08503667+1148553	35.4 ± 0.2	-0.09 ± 0.01	-11.43 ± 0.06	-3.11 ± 0.04	0.54	-1.00	0.12	DM
NGC 2682	2M08503677+1239197	-24.4 ± 0.2	-0.03 ± 0.01	12.02 ± 0.06	-14.39 ± 0.03	0.00	-1.00	0.00	NM
NGC 2682	2M08503700+1154047	35.2 ± 2.0	0.06 ± 0.01	-11.01 ± 0.05	-2.98 ± 0.04	0.60	-1.00	0.97	DM
NGC 2682	2M08503788+1252295	32.4 ± 0.3	0.11 ± 0.01	-11.83 ± 0.07	-3.44 ± 0.05	0.00	-1.00	0.00	NM
NGC 2682	2M08503940+1202338	-38.5 ± 0.0	-0.28 ± 0.01	139.22 ± 0.06	-36.25 ± 0.05	0.00	-1.00	0.00	NM
NGC 2682	2M08504048+1142115	33.4 ± 0.2	-0.03 ± 0.01	-10.99 ± 0.05	-3.16 ± 0.04	0.93	-1.00	0.67	DM
NGC 2682	2M08504075+1125097	48.1 ± 0.1	-0.43 ± 0.01	-3.73 ± 0.04	-1.47 ± 0.03	0.00	0.00	0.00	NM
NGC 2682	2M08504079+1147462	34.6 ± 0.1	-0.07 ± 0.01	-10.89 ± 0.07	-3.08 ± 0.05	0.87	-1.00	0.82	DM
NGC 2682	2M08504198+1136525	34.5 ± 0.1	-0.01 ± 0.01	-11.12 ± 0.07	-3.10 ± 0.05	0.91	-1.00	0.66	DM
NGC 2682	2M08504222+1232433	31.9 ± 0.1	0.29 ± 0.01	-21.83 ± 0.04	-13.97 ± 0.03	0.00	-1.00	0.00	NM
NGC 2682	2M08504250+1139493	33.1 ± 0.1	0.03 ± 0.01	-10.93 ± 0.05	-2.96 ± 0.04	0.83	-1.00	0.99	DM
NGC 2682	2M08504255+1056355	65.4 ± 0.3	-0.43 ± 0.01	-1.22 ± 0.08	-0.62 ± 0.05	0.00	0.00	0.00	NM
NGC 2682	2M08504284+1211372	13.7 ± 8.6	0.15 ± 0.01	-0.59 ± 0.07	-7.12 ± 0.04	0.00	0.12	0.00	NM
NGC 2682	2M08504383+1118455	35.0 ± 15.2	-0.06 ± 0.01	-10.95 ± 0.11	-2.95 ± 0.08	0.69	-1.00	1.00	DM
NGC 2682	2M08504389+1144311	-28.0 ± 0.2	-0.26 ± 0.01	-11.12 ± 0.05	-5.91 ± 0.03	0.00	-1.00	0.00	NM
NGC 2682	2M08504511+1136023	31.1 ± 13.3	0.09 ± 0.01	-10.81 ± 0.08	-2.70 ± 0.07	0.13	-1.00	0.46	DM
NGC 2682	2M08504558+1210398	34.4 ± 0.1	0.11 ± 0.01	-10.95 ± 0.06	-3.05 ± 0.03	0.93	-1.00	0.92	DM
NGC 2682	2M08504590+1152022	15.4 ± 0.1	-0.08 ± 0.01	1.86 ± 0.11	-21.15 ± 0.09	0.00	-1.00	0.00	NM
NGC 2682	2M08504609+1143082	30.7 ± 10.7	0.01 ± 0.01	-10.97 ± 0.06	-2.84 ± 0.04	0.06	-1.00	0.89	DM
NGC 2682	2M08504634+1154310	33.2 ± 0.1	-0.00 ± 0.01	-10.86 ± 0.04	-2.91 ± 0.03	0.90	-1.00	0.89	DM
NGC 2682	2M08504639+1152167	34.3 ± 0.9	-0.26 ± 0.01	-11.07 ± 0.06	-2.63 ± 0.05	0.95	-1.00	0.36	DM
NGC 2682	2M08504704+1210128	33.1 ± 0.0	0.05 ± 0.01	-11.04 ± 0.07	-3.00 ± 0.04	0.85	-1.00	0.94	DM
NGC 2682	2M08504712+1142547	34.1 ± 0.2	0.03 ± 0.01	-11.17 ± 0.05	-3.10 ± 0.03	0.99	-1.00	0.56	DM
NGC 2682	2M08504787+1213058	-0.4 ± 0.2	-0.10 ± 0.01	-5.63 ± 0.06	-21.37 ± 0.04	0.00	-1.00	0.00	NM

Continued on next page

Table A.1 – Continued

Cluster name	2MASS ID	RV (km s^{-1})	[Fe/H] (dex)	μ_α (mas yr^{-1})	μ_δ (mas yr^{-1})	RV Prob	[Fe/H] Prob	PM Prob	Memb
NGC 2682	2M08504811+1154476	33.3 ± 0.2	0.09 ± 0.01	-10.82 ± 0.05	-3.01 ± 0.04	0.92	-1.00	0.80	DM
NGC 2682	2M08504964+1135089	34.9 ± 0.1	0.09 ± 0.01	-10.96 ± 0.08	-2.96 ± 0.06	0.73	0.93	1.00	GM
NGC 2682	2M08504994+1149127	33.8 ± 0.1	0.01 ± 0.01	-10.83 ± 0.07	-3.27 ± 0.05	1.00	0.17	0.33	GM
NGC 2682	2M08505104+1133112	76.5 ± 0.1	0.28 ± 0.01	-11.76 ± 0.05	-6.38 ± 0.04	0.00	-1.00	0.00	NM
NGC 2682	2M08505171+1148102	47.0 ± 0.3	-0.14 ± 0.01	-17.26 ± 0.63	12.58 ± 0.47	0.00	-1.00	0.00	NM
NGC 2682	2M08505177+1200247	33.7 ± 0.2	0.02 ± 0.01	-11.22 ± 0.05	-2.85 ± 0.05	0.99	-1.00	0.53	DM
NGC 2682	2M08505182+1156559	29.8 ± 5.6	-0.03 ± 0.01	-11.44 ± 0.07	-2.96 ± 0.05	0.01	-1.00	0.13	DM
NGC 2682	2M08505236+1113263	24.9 ± 4.6	-0.32 ± 0.01	-0.50 ± 0.06	-2.76 ± 0.04	0.00	0.00	0.00	NM
NGC 2682	2M08505273+1115332	-28.0 ± 0.4	-0.25 ± 0.01	-3.23 ± 0.06	-0.41 ± 0.04	0.00	0.00	0.00	NM
NGC 2682	2M08505306+1131201	46.2 ± 3.0	0.02 ± 0.01	-11.00 ± 0.05	-3.16 ± 0.04	0.00	-1.00	0.68	NM
NGC 2682	2M08505316+1147341	29.3 ± 0.4	0.01 ± 0.01	-11.29 ± 0.05	-3.77 ± 0.04	0.00	-1.00	0.00	NM
NGC 2682	2M08505319+1237116	61.0 ± 0.1	-0.49 ± 0.01	-2.74 ± 0.09	0.77 ± 0.06	0.00	0.00	0.00	NM
NGC 2682	2M08505334+1143399	32.7 ± 0.3	-0.05 ± 0.01	-10.89 ± 0.05	-3.92 ± 0.04	0.69	-1.00	0.00	NM
NGC 2682	2M08505344+1144346	33.7 ± 0.1	0.02 ± 0.01	-10.97 ± 0.05	-2.93 ± 0.03	0.99	-1.00	1.00	DM
NGC 2682	2M08505389+1156464	-24.6 ± 0.1	-0.01 ± 0.01	-59.26 ± 0.05	-36.15 ± 0.04	0.00	-1.00	0.00	NM
NGC 2682	2M08505439+1156290	33.7 ± 0.1	-0.02 ± 0.01	-10.74 ± 0.07	-3.19 ± 0.05	0.99	-1.00	0.39	DM
NGC 2682	2M08505498+1156503	-15.0 ± 20.6	-0.41 ± 0.01	-10.82 ± 0.07	-2.81 ± 0.05	0.00	0.00	0.69	NM
NGC 2682	2M08505526+1117352	36.1 ± 0.0	-0.08 ± 0.01	-9.47 ± 0.06	-2.56 ± 0.05	0.24	0.00	0.00	NM
NGC 2682	2M08505552+1150014	89.9 ± 0.6	-0.82 ± 0.01	-0.65 ± 0.10	0.06 ± 0.07	0.00	0.00	0.00	NM
NGC 2682	2M08505567+1135354	34.1 ± 0.1	-0.02 ± 0.01	-10.83 ± 0.05	-2.63 ± 0.04	0.99	-1.00	0.34	DM
NGC 2682	2M08505569+1152146	34.1 ± 0.1	-0.02 ± 0.01	-11.01 ± 0.18	-2.84 ± 0.13	0.99	-1.00	0.87	DM
NGC 2682	2M08505581+1128447	37.8 ± 0.3	0.24 ± 0.01	-6.16 ± 0.08	-20.99 ± 0.06	0.01	-1.00	0.00	NM
NGC 2682	2M08505604+1209288	34.5 ± 0.5	-0.10 ± 0.01	-10.86 ± 0.04	-2.91 ± 0.03	0.89	-1.00	0.88	DM
NGC 2682	2M08505632+1151292	33.5 ± 0.2	-0.02 ± 0.01	-10.99 ± 0.05	-3.33 ± 0.04	0.96	-1.00	0.28	DM
NGC 2682	2M08505653+1138081	33.6 ± 0.3	0.03 ± 0.01	-10.85 ± 0.05	-2.90 ± 0.03	0.98	-1.00	0.87	DM
NGC 2682	2M08505702+1159158	34.0 ± 0.2	-0.03 ± 0.01	-11.06 ± 0.05	-3.72 ± 0.03	1.00	-1.00	0.01	NM
NGC 2682	2M08505726+1209078	7.9 ± 0.0	0.09 ± 0.01	-28.18 ± 0.05	-24.57 ± 0.03	0.00	-1.00	0.00	NM
NGC 2682	2M08505732+1237201	26.3 ± 0.1	0.05 ± 0.01	-52.20 ± 0.07	-8.53 ± 0.05	0.00	-1.00	0.00	NM
NGC 2682	2M08505762+1155147	33.1 ± 0.2	-0.02 ± 0.01	-10.71 ± 0.04	-2.85 ± 0.03	0.84	-1.00	0.51	DM
NGC 2682	2M08505769+1200406	33.5 ± 0.4	0.13 ± 0.01	-10.96 ± 0.08	-3.06 ± 0.06	0.97	-1.00	0.90	DM
NGC 2682	2M08505798+1218321	33.2 ± 0.0	-0.03 ± 0.01	-10.99 ± 0.07	-3.24 ± 0.04	0.90	-1.00	0.49	DM
NGC 2682	2M08505816+1152223	34.0 ± 0.1	0.08 ± 0.01	-11.13 ± 0.08	-2.86 ± 0.05	0.99	1.00	0.74	GM
NGC 2682	2M08505816+1117302	47.4 ± 0.2	-0.48 ± 0.01	1.85 ± 0.07	-13.12 ± 0.05	0.00	0.00	0.00	NM
NGC 2682	2M08505862+1229517	14.2 ± 0.2	-0.44 ± 0.01	12.52 ± 0.13	-83.34 ± 0.09	0.00	-1.00	0.00	NM
NGC 2682	2M08505923+1146129	32.0 ± 1.8	-0.04 ± 0.01	-10.90 ± 0.05	-2.84 ± 0.03	0.37	-1.00	0.85	DM
NGC 2682	2M08505923+1156368	36.1 ± 1.4	-0.08 ± 0.01	-10.78 ± 0.07	-2.75 ± 0.04	0.24	-1.00	0.50	DM
NGC 2682	2M08505973+1139524	33.2 ± 0.2	-0.03 ± 0.01	-10.62 ± 0.07	-2.74 ± 0.05	0.88	-1.00	0.23	DM
NGC 2682	2M08505976+1139222	-18.8 ± 0.1	0.05 ± 0.01	-9.80 ± 0.07	-9.12 ± 0.05	0.00	-1.00	0.00	NM
NGC 2682	2M08505983+1130493	-167.1 ± 0.1	-2.14 ± 0.01	-229.06 ± 0.15	11.51 ± 0.13	0.00	-1.00	0.00	NM
NGC 2682	2M08510018+1154321	34.0 ± 0.1	0.10 ± 0.01	-5.31 ± 0.55	-5.53 ± 0.46	0.99	-1.00	0.00	NM
NGC 2682	2M08510076+1153115	34.1 ± 0.3	0.01 ± 0.01	-10.76 ± 0.06	-2.93 ± 0.05	0.99	-1.00	0.67	DM
NGC 2682	2M08510082+1139375	29.6 ± 0.0	0.29 ± 0.01	-5.87 ± 0.07	3.68 ± 0.05	0.01	-1.00	0.00	NM
NGC 2682	2M08510103+1118354	69.8 ± 0.1	-0.13 ± 0.01	-0.35 ± 0.06	-3.47 ± 0.05	0.00	0.00	0.00	NM
NGC 2682	2M08510106+1150108	32.9 ± 0.1	-0.02 ± 0.01	-10.79 ± 0.09	-2.93 ± 0.06	0.77	-1.00	0.75	DM
NGC 2682	2M08510131+1141587	32.1 ± 10.6	-0.16 ± 0.01	-11.04 ± 0.04	-2.81 ± 0.03	0.40	-1.00	0.80	DM
NGC 2682	2M08510155+1149342	35.0 ± 1.0	0.00 ± 0.01	-10.60 ± 0.08	-4.11 ± 0.07	0.69	-1.00	0.00	NM
NGC 2682	2M08510156+1147501	32.9 ± 0.2	-0.01 ± 0.01	-10.89 ± 0.05	-3.60 ± 0.04	0.78	-1.00	0.02	DM
NGC 2682	2M08510186+1139591	25.4 ± 0.3	-0.33 ± 0.01	-3.05 ± 0.07	23.84 ± 0.05	0.00	-1.00	0.00	NM
NGC 2682	2M08510212+1149012	24.4 ± 51.1	-0.14 ± 0.01	-11.05 ± 0.11	-2.49 ± 0.09	0.00	-1.00	0.14	NM
NGC 2682	2M08510246+1155221	34.3 ± 0.3	0.15 ± 0.01	-10.83 ± 0.08	-3.04 ± 0.06	0.95	-1.00	0.80	DM
NGC 2682	2M08510263+1134469	58.3 ± 0.1	-0.16 ± 0.01	-2.68 ± 0.06	-1.91 ± 0.04	0.00	0.00	0.00	NM
NGC 2682	2M08510279+1151254	99.6 ± 0.3	-0.22 ± 0.01	-8.18 ± 0.06	-1.36 ± 0.05	0.00	0.00	0.00	NM
NGC 2682	2M08510291+1200214	38.6 ± 0.1	0.19 ± 0.01	-12.01 ± 0.05	7.34 ± 0.04	0.00	-1.00	0.00	NM
NGC 2682	2M08510294+1133254	33.4 ± 0.3	0.11 ± 0.01	-11.00 ± 0.10	-3.19 ± 0.08	0.95	-1.00	0.59	DM
NGC 2682	2M08510300+1207560	14.0 ± 0.1	0.05 ± 0.01	-7.84 ± 0.04	9.85 ± 0.03	0.00	-1.00	0.00	NM
NGC 2682	2M08510325+1145473	35.1 ± 0.2	0.04 ± 0.01	-11.07 ± 0.08	-2.91 ± 0.06	0.65	-1.00	0.90	DM
NGC 2682	2M08510365+1140309	28.7 ± 3.3	-0.05 ± 0.01	-11.39 ± 0.06	-3.03 ± 0.04	0.00	-1.00	0.19	NM
NGC 2682	2M08510439+1208246	33.7 ± 0.0	0.16 ± 0.01	-10.96 ± 0.04	-2.89 ± 0.03	0.99	-1.00	0.96	DM
NGC 2682	2M08510470+1204193	32.9 ± 0.2	0.07 ± 0.01	-10.94 ± 0.04	-2.97 ± 0.03	0.76	-1.00	0.99	DM
NGC 2682	2M08510473+1149359	101.2 ± 0.4	-0.39 ± 0.01	0.28 ± 0.08	0.48 ± 0.07	0.00	0.00	0.00	NM
NGC 2682	2M08510576+1143469	38.3 ± 6.6	0.07 ± 0.01	-10.96 ± 0.05	-2.59 ± 0.04	0.00	-1.00	0.31	NM
NGC 2682	2M08510783+1159354	35.8 ± 0.4	0.06 ± 0.01	-10.95 ± 0.08	-2.84 ± 0.06	0.36	-1.00	0.89	DM
NGC 2682	2M08510811+1201065	33.8 ± 0.2	-0.13 ± 0.01	-11.70 ± 0.04	-3.02 ± 0.03	1.00	-1.00	0.01	NM

Continued on next page

Table A.1 – Continued

Cluster name	2MASS ID	RV (km s^{-1})	[Fe/H] (dex)	μ_α (mas yr^{-1})	μ_δ (mas yr^{-1})	RV Prob	[Fe/H] Prob	PM Prob	Memb
NGC 2682	2M08510824+1126272	-2.3 ± 0.0	-0.08 ± 0.01	-11.16 ± 0.05	-7.11 ± 0.05	0.00	-1.00	0.00	NM
NGC 2682	2M08510839+1147121	33.5 ± 0.2	0.08 ± 0.01	-10.91 ± 0.08	-2.93 ± 0.06	0.97	0.98	0.96	GM
NGC 2682	2M08510864+1146117	34.4 ± 7.8	-0.08 ± 0.01	-10.79 ± 0.05	-3.15 ± 0.04	0.91	-1.00	0.53	DM
NGC 2682	2M08510890+1148377	73.1 ± 8.9	-0.06 ± 0.01	-10.58 ± 0.05	6.58 ± 0.04	0.00	-1.00	0.00	NM
NGC 2682	2M08510925+1148206	32.6 ± 0.0	-0.04 ± 0.01	-9.93 ± 0.05	-3.24 ± 0.04	0.63	-1.00	0.00	NM
NGC 2682	2M08510951+1141449	32.4 ± 0.1	0.07 ± 0.01	-10.33 ± 0.07	-3.11 ± 0.06	0.53	-1.00	0.02	DM
NGC 2682	2M08510969+1159096	34.0 ± 7.3	-0.08 ± 0.01	-10.79 ± 0.04	-2.93 ± 0.03	1.00	-1.00	0.75	DM
NGC 2682	2M08510970+1159136	36.8 ± 1.4	0.00 ± 0.01	-9.60 ± 0.06	-2.93 ± 0.04	0.09	-1.00	0.00	NM
NGC 2682	2M08511130+1157212	34.7 ± 0.3	0.08 ± 0.01	-10.87 ± 0.08	-3.11 ± 0.06	0.82	-1.00	0.73	DM
NGC 2682	2M08511176+1150018	33.5 ± 0.3	0.03 ± 0.01	-11.02 ± 0.08	-3.20 ± 0.05	0.97	-1.00	0.57	DM
NGC 2682	2M08511229+1154230	35.1 ± 0.3	0.05 ± 0.01	-10.81 ± 0.05	-2.87 ± 0.03	0.64	-1.00	0.75	DM
NGC 2682	2M08511229+1146212	31.5 ± 0.3	-0.02 ± 0.01	-10.93 ± 0.05	-3.04 ± 0.04	0.21	-1.00	0.92	DM
NGC 2682	2M08511269+1152423	34.3 ± 0.1	0.08 ± 0.01	-10.95 ± 0.06	-2.98 ± 0.04	0.94	0.98	0.99	GM
NGC 2682	2M08511292+1234492	37.8 ± 0.4	0.15 ± 0.01	-8.11 ± 0.08	1.70 ± 0.04	0.00	-1.00	0.00	NM
NGC 2682	2M08511335+1151401	40.0 ± 10.3	-0.13 ± 0.01	-11.02 ± 0.04	-2.85 ± 0.03	0.00	0.00	0.89	NM
NGC 2682	2M08511339+1139375	35.2 ± 0.3	-0.00 ± 0.01	-10.57 ± 0.42	-4.02 ± 0.32	0.61	-1.00	0.00	NM
NGC 2682	2M08511389+1235484	-1.8 ± 0.5	-0.09 ± 0.01	17.19 ± 0.22	-1.69 ± 0.14	0.00	-1.00	0.00	NM
NGC 2682	2M08511405+1133306	34.8 ± 0.2	-0.03 ± 0.01	-11.02 ± 0.04	-2.87 ± 0.03	0.80	-1.00	0.92	DM
NGC 2682	2M08511428+1208493	-31.9 ± 0.4	-0.51 ± 0.01	6.98 ± 0.17	-14.03 ± 0.12	0.00	-1.00	0.00	NM
NGC 2682	2M08511446+1144409	33.7 ± 0.3	0.11 ± 0.01	-11.27 ± 0.10	-2.73 ± 0.07	1.00	-1.00	0.29	DM
NGC 2682	2M08511476+1147238	34.9 ± 0.2	-0.00 ± 0.01	-10.87 ± 0.08	-2.98 ± 0.06	0.75	-1.00	0.91	DM
NGC 2682	2M08511476+1130088	51.7 ± 0.0	-0.27 ± 0.01	35.43 ± 0.07	-164.15 ± 0.05	0.00	-1.00	0.00	NM
NGC 2682	2M08511515+1126426	33.4 ± 0.1	0.03 ± 0.01	-10.94 ± 0.06	-2.83 ± 0.05	0.94	-1.00	0.88	DM
NGC 2682	2M08511564+1150561	34.0 ± 0.0	0.05 ± 0.01	-10.73 ± 0.07	-2.78 ± 0.05	0.99	-1.00	0.47	DM
NGC 2682	2M08511576+1152587	35.8 ± 0.1	0.01 ± 0.01	-11.96 ± 0.07	-2.03 ± 0.05	0.34	-1.00	0.00	NM
NGC 2682	2M08511588+1127245	1.3 ± 0.3	-0.03 ± 0.01	4.47 ± 0.06	-11.68 ± 0.04	0.00	-1.00	0.00	NM
NGC 2682	2M08511628+1144328	29.2 ± 10.8	-0.07 ± 0.01	-11.01 ± 0.06	-2.95 ± 0.04	0.00	-1.00	0.98	NM
NGC 2682	2M08511670+1145293	35.5 ± 0.2	-0.06 ± 0.01	-11.26 ± 0.13	-2.41 ± 0.09	0.48	-1.00	0.03	DM
NGC 2682	2M08511679+1150389	32.6 ± 0.1	-0.03 ± 0.01	-10.71 ± 0.05	-3.11 ± 0.04	0.64	-1.00	0.44	DM
NGC 2682	2M08511698+1150093	30.3 ± 0.6	0.07 ± 0.01	-9.97 ± 0.06	-4.75 ± 0.04	0.03	-1.00	0.00	NM
NGC 2682	2M08511704+1150464	33.6 ± 0.1	0.05 ± 0.01	-11.16 ± 0.07	-3.32 ± 0.05	0.98	0.79	0.23	GM
NGC 2682	2M08511710+1148160	33.6 ± 0.0	0.10 ± 0.01	-11.43 ± 0.08	-3.29 ± 0.05	0.99	0.75	0.05	GM
NGC 2682	2M08511759+1139359	13.4 ± 14.2	-0.01 ± 0.01	-8.31 ± 0.05	-0.87 ± 0.04	0.00	-1.00	0.00	NM
NGC 2682	2M08511790+1239518	20.9 ± 0.1	0.13 ± 0.01	8.50 ± 0.06	-45.12 ± 0.04	0.00	-1.00	0.00	NM
NGC 2682	2M08511799+1145541	18.5 ± 12.1	-0.08 ± 0.01	-3.19 ± 0.88	-9.21 ± 0.82	0.00	-1.00	0.00	NM
NGC 2682	2M08511805+1126290	33.5 ± 0.2	0.02 ± 0.01	-11.09 ± 0.04	-3.14 ± 0.03	0.97	-1.00	0.63	DM
NGC 2682	2M08511810+1142547	33.9 ± 0.1	0.02 ± 0.01	-10.96 ± 0.05	-2.89 ± 0.04	1.00	-1.00	0.96	DM
NGC 2682	2M08511826+1150196	34.3 ± 4.2	-0.18 ± 0.01	-10.89 ± 0.06	-2.59 ± 0.04	0.95	-1.00	0.29	DM
NGC 2682	2M08511827+1141296	33.9 ± 0.4	0.08 ± 0.01	-10.98 ± 0.11	-3.42 ± 0.08	1.00	-1.00	0.14	DM
NGC 2682	2M08511833+1143251	33.7 ± 0.1	0.00 ± 0.01	-11.34 ± 0.05	-3.11 ± 0.04	0.99	-1.00	0.23	DM
NGC 2682	2M08511854+1149214	34.4 ± 0.1	0.01 ± 0.01	-11.15 ± 0.07	-2.82 ± 0.05	0.94	-1.00	0.64	DM
NGC 2682	2M08511868+1147026	78.7 ± 1.0	-0.21 ± 0.01	-10.63 ± 0.07	-2.94 ± 0.05	0.00	0.00	0.37	NM
NGC 2682	2M08511872+1155497	34.7 ± 0.2	-0.05 ± 0.01	-10.87 ± 0.05	-3.06 ± 0.03	0.83	-1.00	0.82	DM
NGC 2682	2M08511877+1151186	34.1 ± 0.1	0.10 ± 0.01	-10.98 ± 0.07	-2.74 ± 0.05	0.99	-1.00	0.66	DM
NGC 2682	2M08511886+1135177	33.8 ± 0.3	0.11 ± 0.01	-11.00 ± 0.10	-2.64 ± 0.08	1.00	-1.00	0.42	DM
NGC 2682	2M08511897+1158110	34.0 ± 0.1	0.05 ± 0.01	-11.08 ± 0.06	-3.09 ± 0.04	0.99	0.81	0.76	GM
NGC 2682	2M08511901+1150057	-28.2 ± 0.0	-0.48 ± 0.01	-10.95 ± 0.07	-3.08 ± 0.05	0.00	-1.00	0.87	NM
NGC 2682	2M08511960+1045305	100.9 ± 0.3	-0.56 ± 0.01	-1.38 ± 0.05	-2.81 ± 0.03	0.00	0.00	0.00	NM
NGC 2682	2M08511963+1232465	4.7 ± 1.7	0.10 ± 0.01	-16.25 ± 0.08	-5.11 ± 0.04	0.00	-1.00	0.00	NM
NGC 2682	2M08511982+1221332	34.4 ± 0.1	0.26 ± 0.01	-13.42 ± 0.06	-16.98 ± 0.04	0.92	-1.00	0.00	NM
NGC 2682	2M08512003+1151016	35.0 ± 0.3	0.05 ± 0.01	-10.63 ± 0.05	-2.90 ± 0.04	0.68	-1.00	0.35	DM
NGC 2682	2M08512012+1146416	34.3 ± 0.1	-0.03 ± 0.01	-10.88 ± 0.08	-2.75 ± 0.05	0.96	-1.00	0.65	DM
NGC 2682	2M08512033+1145523	33.7 ± 0.3	-0.02 ± 0.01	-10.89 ± 0.06	-2.96 ± 0.04	0.99	-1.00	0.95	DM
NGC 2682	2M08512055+1146047	34.3 ± 0.2	0.05 ± 0.01	-11.24 ± 0.06	-3.26 ± 0.04	0.94	-1.00	0.22	DM
NGC 2682	2M08512080+1145024	33.8 ± 0.1	-0.02 ± 0.01	-10.51 ± 0.06	-3.81 ± 0.04	1.00	-1.00	0.00	NM
NGC 2682	2M08512122+1145526	33.5 ± 0.7	-0.01 ± 0.01	-11.74 ± 0.09	-2.47 ± 0.06	0.96	-1.00	0.00	NM
NGC 2682	2M08512140+1240008	63.7 ± 0.3	0.42 ± 0.01	-13.40 ± 0.07	-16.43 ± 0.05	0.00	-1.00	0.00	NM
NGC 2682	2M08512150+1159048	32.2 ± 0.2	0.07 ± 0.01	-11.95 ± 0.05	-1.88 ± 0.03	0.45	-1.00	0.00	NM
NGC 2682	2M08512156+1146061	34.9 ± 0.1	0.12 ± 0.01	-11.10 ± 0.08	-2.66 ± 0.05	0.76	0.53	0.40	GM
NGC 2682	2M08512175+1152378	34.9 ± 0.0	-0.10 ± 0.01	-10.12 ± 0.10	-1.98 ± 0.08	0.75	-1.00	0.00	NM
NGC 2682	2M08512176+1144050	32.8 ± 0.5	-0.00 ± 0.01	-11.28 ± 0.05	-3.12 ± 0.04	0.72	-1.00	0.34	DM
NGC 2682	2M08512194+1153089	34.5 ± 0.2	0.08 ± 0.01	-10.88 ± 0.09	-2.83 ± 0.05	0.91	-1.00	0.82	DM
NGC 2682	2M08512205+1146409	34.4 ± 0.0	0.02 ± 0.01	-11.01 ± 0.05	-3.05 ± 0.03	0.91	-1.00	0.91	DM

Continued on next page

Table A.1 – Continued

Cluster name	2MASS ID	RV (km s^{-1})	[Fe/H] (dex)	μ_α (mas yr^{-1})	μ_δ (mas yr^{-1})	RV Prob	[Fe/H] Prob	PM Prob	Memb
NGC 2682	2M08512214+1148278	33.0 ± 1.0	-0.18 ± 0.01	-11.07 ± 0.09	-3.22 ± 0.06	0.80	-1.00	0.49	DM
NGC 2682	2M08512239+1200182	3.5 ± 0.4	-0.55 ± 0.02	28.42 ± 0.11	-53.62 ± 0.08	0.00	-1.00	0.00	NM
NGC 2682	2M08512240+1151291	33.4 ± 0.2	-0.08 ± 0.01	-10.94 ± 0.05	-2.96 ± 0.04	0.95	-1.00	0.99	DM
NGC 2682	2M08512280+1148016	33.8 ± 0.0	0.12 ± 0.01	-11.05 ± 0.07	-2.93 ± 0.06	1.00	0.51	0.94	GM
NGC 2682	2M08512314+1154049	33.6 ± 0.3	0.03 ± 0.01	-10.83 ± 0.05	-2.76 ± 0.03	0.98	-1.00	0.60	DM
NGC 2682	2M08512377+1149493	38.2 ± 3.9	0.02 ± 0.01	-11.30 ± 0.14	-2.98 ± 0.08	0.01	0.34	0.37	NM
NGC 2682	2M08512380+1147160	30.2 ± 1.6	0.03 ± 0.01	-10.10 ± 0.07	-3.35 ± 0.05	0.02	-1.00	0.00	NM
NGC 2682	2M08512386+1138521	34.6 ± 0.4	0.02 ± 0.01	-11.04 ± 0.06	-2.81 ± 0.05	0.86	-1.00	0.79	DM
NGC 2682	2M08512395+1124494	35.2 ± 11.4	-0.03 ± 0.01	-10.95 ± 0.04	-2.81 ± 0.03	0.61	-1.00	0.83	DM
NGC 2682	2M08512408+1148218	23.3 ± 6.7	0.03 ± 0.01	-11.07 ± 0.08	-3.03 ± 0.06	0.00	-1.00	0.85	NM
NGC 2682	2M08512428+1123173	33.9 ± 0.1	0.02 ± 0.01	-11.05 ± 0.05	-2.74 ± 0.03	1.00	-1.00	0.64	DM
NGC 2682	2M08512467+1143061	32.0 ± 0.3	0.08 ± 0.01	-10.88 ± 0.07	-2.18 ± 0.05	0.38	-1.00	0.00	NM
NGC 2682	2M08512515+1214495	56.1 ± 22.6	-0.37 ± 0.01	-20.62 ± 0.04	-4.70 ± 0.03	0.00	-1.00	0.00	NM
NGC 2682	2M08512535+1103554	54.0 ± 0.2	0.35 ± 0.01	-27.93 ± 0.06	-14.54 ± 0.04	0.00	-1.00	0.00	NM
NGC 2682	2M08512536+1147342	34.4 ± 0.2	-0.03 ± 0.01	-11.80 ± 0.08	-1.32 ± 0.05	0.93	-1.00	0.00	NM
NGC 2682	2M08512593+1133001	34.9 ± 0.2	-0.01 ± 0.01	-10.89 ± 0.09	-3.07 ± 0.06	0.76	-1.00	0.85	DM
NGC 2682	2M08512604+1149555	32.9 ± 0.3	-0.10 ± 0.01	-11.76 ± 0.06	-3.28 ± 0.04	0.77	-1.00	0.00	NM
NGC 2682	2M08512618+1153520	34.2 ± 0.0	0.07 ± 0.01	-11.00 ± 0.07	-2.88 ± 0.05	0.98	0.99	0.95	GM
NGC 2682	2M08512643+1140125	43.7 ± 0.1	-0.02 ± 0.01	-36.47 ± 0.05	4.03 ± 0.03	0.00	-1.00	0.00	NM
NGC 2682	2M08512655+1157092	-0.9 ± 0.1	-0.14 ± 0.01	-2.40 ± 0.08	-6.88 ± 0.06	0.00	-1.00	0.00	NM
NGC 2682	2M08512734+1207406	19.5 ± 1.6	-0.28 ± 0.01	-19.62 ± 0.14	-31.20 ± 0.10	0.00	-1.00	0.00	NM
NGC 2682	2M08512742+1153265	34.3 ± 0.2	-0.01 ± 0.01	-10.87 ± 0.06	-3.09 ± 0.04	0.95	-1.00	0.79	DM
NGC 2682	2M08512742+1213432	39.5 ± 0.1	-0.12 ± 0.01	-8.05 ± 0.06	14.84 ± 0.04	0.00	-1.00	0.00	NM
NGC 2682	2M08512788+1155409	36.1 ± 0.2	0.02 ± 0.01	-11.13 ± 0.04	-2.40 ± 0.03	0.26	-1.00	0.05	DM
NGC 2682	2M08512839+1203162	18.9 ± 0.2	-0.20 ± 0.01	-14.63 ± 0.06	11.33 ± 0.05	0.00	-1.00	0.00	NM
NGC 2682	2M08512861+1138314	37.1 ± 12.2	-0.03 ± 0.01	-11.11 ± 0.06	-3.12 ± 0.04	0.05	-1.00	0.65	DM
NGC 2682	2M08512879+1151599	33.6 ± 0.1	-0.09 ± 0.01	-10.91 ± 0.07	-3.04 ± 0.05	0.98	-1.00	0.91	DM
NGC 2682	2M08512898+1150330	33.5 ± 0.0	0.08 ± 0.01	-11.14 ± 0.08	-3.22 ± 0.05	0.95	0.97	0.41	GM
NGC 2682	2M08512935+1145275	33.1 ± 0.1	0.04 ± 0.01	-10.74 ± 0.07	-2.98 ± 0.04	0.86	0.66	0.62	GM
NGC 2682	2M08512950+1106515	-0.8 ± 0.2	0.04 ± 0.01	-3.75 ± 0.06	0.19 ± 0.05	0.00	-1.00	0.00	NM
NGC 2682	2M08512990+1147168	36.3 ± 0.0	-0.05 ± 0.01	-11.27 ± 0.09	-3.73 ± 0.05	0.20	0.00	0.00	NM
NGC 2682	2M08512993+1135112	34.4 ± 0.1	-0.05 ± 0.01	-11.20 ± 0.07	-2.72 ± 0.05	0.93	-1.00	0.39	DM
NGC 2682	2M08512996+1151090	34.8 ± 0.2	0.01 ± 0.01	-11.07 ± 0.05	-3.08 ± 0.03	0.78	-1.00	0.79	DM
NGC 2682	2M08513012+1143498	33.5 ± 0.2	-0.08 ± 0.01	-11.11 ± 0.09	-3.09 ± 0.06	0.97	-1.00	0.71	DM
NGC 2682	2M08513044+1148582	30.1 ± 6.1	0.09 ± 0.01	-11.18 ± 0.07	-3.18 ± 0.05	0.02	0.91	0.42	GM
NGC 2682	2M08513057+1149131	30.3 ± 0.1	0.07 ± 0.01	-10.99 ± 0.07	-3.16 ± 0.04	0.03	-1.00	0.67	DM
NGC 2682	2M08513119+1153179	34.2 ± 0.3	-0.01 ± 0.01	-10.82 ± 0.04	-2.98 ± 0.03	0.98	-1.00	0.81	DM
NGC 2682	2M08513194+1153117	32.4 ± 0.1	-0.01 ± 0.01	-11.15 ± 0.06	-3.19 ± 0.04	0.56	-1.00	0.45	DM
NGC 2682	2M08513206+1155085	39.2 ± 3.3	-0.01 ± 0.01	-10.94 ± 0.04	-2.72 ± 0.03	0.00	-1.00	0.61	NM
NGC 2682	2M08513215+1136126	34.3 ± 0.4	-0.02 ± 0.01	-11.22 ± 0.04	-2.83 ± 0.03	0.94	-1.00	0.49	DM
NGC 2682	2M08513240+1148011	33.2 ± 0.7	0.02 ± 0.01	-11.25 ± 0.08	-2.79 ± 0.05	0.89	-1.00	0.38	DM
NGC 2682	2M08513244+1147523	32.8 ± 0.1	-0.05 ± 0.01	-11.62 ± 0.08	-2.77 ± 0.06	0.72	-1.00	0.02	DM
NGC 2682	2M08513322+1148513	35.1 ± 0.1	-0.10 ± 0.01	-11.50 ± 0.07	-2.65 ± 0.05	0.68	-1.00	0.04	DM
NGC 2682	2M08513365+1138336	89.6 ± 1.0	-0.35 ± 0.01	-15.01 ± 0.10	2.48 ± 0.07	0.00	-1.00	0.00	NM
NGC 2682	2M08513381+1122511	33.5 ± 0.1	-0.00 ± 0.01	-11.15 ± 0.07	-2.89 ± 0.05	0.96	-1.00	0.73	DM
NGC 2682	2M08513424+1145535	34.2 ± 0.5	0.19 ± 0.01	-10.83 ± 0.07	-2.81 ± 0.05	0.97	-1.00	0.70	DM
NGC 2682	2M08513444+1137574	34.0 ± 0.1	0.03 ± 0.01	-10.78 ± 0.04	-2.66 ± 0.03	0.99	-1.00	0.35	DM
NGC 2682	2M08513455+1149068	33.5 ± 0.4	0.07 ± 0.01	-11.05 ± 0.08	-3.20 ± 0.05	0.97	-1.00	0.55	DM
NGC 2682	2M08513540+1157564	33.4 ± 0.0	0.01 ± 0.01	-11.10 ± 0.07	-3.01 ± 0.04	0.94	-1.00	0.84	DM
NGC 2682	2M08513553+1139469	42.1 ± 8.9	-0.17 ± 0.01	-11.12 ± 0.05	-1.70 ± 0.04	0.00	-1.00	0.00	NM
NGC 2682	2M08513572+1209273	-11.4 ± 0.3	0.07 ± 0.01	2.41 ± 0.07	-16.68 ± 0.04	0.00	-1.00	0.00	NM
NGC 2682	2M08513577+1153347	34.0 ± 0.1	0.08 ± 0.01	-11.06 ± 0.06	-2.93 ± 0.04	0.99	1.00	0.92	GM
NGC 2682	2M08513673+1149590	34.1 ± 0.3	0.12 ± 0.01	-11.08 ± 0.08	-2.99 ± 0.05	0.99	-1.00	0.89	DM
NGC 2682	2M08513701+1136516	33.2 ± 0.7	0.10 ± 0.01	-10.80 ± 0.06	-3.31 ± 0.04	0.88	-1.00	0.25	DM
NGC 2682	2M08513710+1154599	34.9 ± 0.0	-0.04 ± 0.01	-10.85 ± 0.04	-2.95 ± 0.03	0.76	-1.00	0.87	DM
NGC 2682	2M08513724+1146557	44.4 ± 11.6	0.03 ± 0.01	-11.44 ± 0.05	-2.96 ± 0.03	0.00	-1.00	0.13	NM
NGC 2682	2M08513757+1156445	34.2 ± 0.1	0.09 ± 0.01	-11.25 ± 0.05	-3.06 ± 0.04	0.96	-1.00	0.45	DM
NGC 2682	2M08513795+1158491	35.5 ± 0.0	0.21 ± 0.01	-38.70 ± 0.06	-7.95 ± 0.04	0.48	-1.00	0.00	NM
NGC 2682	2M08513806+1201243	32.1 ± 0.1	0.01 ± 0.01	-11.03 ± 0.06	-3.40 ± 0.04	0.43	-1.00	0.17	DM
NGC 2682	2M08513862+1220141	33.7 ± 0.1	0.04 ± 0.01	-10.95 ± 0.08	-3.00 ± 0.05	1.00	0.66	0.98	GM
NGC 2682	2M08513873+1142373	33.1 ± 0.2	-0.06 ± 0.01	-11.12 ± 0.05	-2.77 ± 0.03	0.83	-1.00	0.61	DM
NGC 2682	2M08513904+1147553	33.5 ± 0.0	0.00 ± 0.01	-10.75 ± 0.04	-3.14 ± 0.03	0.96	-1.00	0.49	DM
NGC 2682	2M08513938+1151456	34.0 ± 0.1	0.05 ± 0.01	-11.10 ± 0.07	-3.12 ± 0.04	1.00	0.83	0.67	GM

Continued on next page

Table A.1 – Continued

Cluster name	2MASS ID	RV (km s^{-1})	[Fe/H] (dex)	μ_α (mas yr^{-1})	μ_δ (mas yr^{-1})	RV Prob	[Fe/H] Prob	PM Prob	Memb
NGC 2682	2M08514042+1201501	69.8 ± 0.1	-0.45 ± 0.01	-10.10 ± 0.06	1.31 ± 0.04	0.00	-1.00	0.00	NM
NGC 2682	2M08514089+1157443	32.7 ± 0.8	0.04 ± 0.01	-10.31 ± 0.09	-2.42 ± 0.06	0.67	-1.00	0.00	NM
NGC 2682	2M08514107+1211319	1.0 ± 0.3	0.17 ± 0.01	0.25 ± 0.07	-3.35 ± 0.05	0.00	0.04	0.00	NM
NGC 2682	2M08514122+1154290	33.6 ± 0.2	-0.01 ± 0.01	-11.15 ± 0.07	-3.06 ± 0.05	0.98	-1.00	0.67	DM
NGC 2682	2M08514189+1149376	35.9 ± 0.3	0.09 ± 0.01	-11.02 ± 0.06	-2.92 ± 0.04	0.32	-1.00	0.97	DM
NGC 2682	2M08514194+1143371	30.0 ± 17.8	-0.10 ± 0.01	-10.95 ± 0.07	-2.88 ± 0.05	0.01	-1.00	0.95	DM
NGC 2682	2M08514234+1150076	34.3 ± 0.0	0.09 ± 0.01	-11.02 ± 0.07	-2.80 ± 0.05	0.96	0.96	0.80	GM
NGC 2682	2M08514235+1151230	33.5 ± 0.1	0.07 ± 0.01	-10.79 ± 0.06	-2.97 ± 0.04	0.97	1.00	0.76	GM
NGC 2682	2M08514236+1132069	33.4 ± 0.1	0.00 ± 0.01	-10.96 ± 0.05	-3.14 ± 0.04	0.93	-1.00	0.73	DM
NGC 2682	2M08514255+1145588	58.4 ± 0.2	0.06 ± 0.01	-3.59 ± 0.08	-1.88 ± 0.05	0.00	0.89	0.00	NM
NGC 2682	2M08514259+1156050	34.2 ± 0.3	0.09 ± 0.01	-11.09 ± 0.09	-3.21 ± 0.06	0.98	-1.00	0.49	DM
NGC 2682	2M08514268+1146365	152.8 ± 0.1	-0.62 ± 0.01	-7.56 ± 0.07	-10.77 ± 0.04	0.00	-1.00	0.00	NM
NGC 2682	2M08514277+1238418	44.4 ± 0.1	-0.46 ± 0.01	-2.44 ± 0.05	-0.29 ± 0.03	0.00	0.00	0.00	NM
NGC 2682	2M08514336+1206484	35.6 ± 0.8	-0.02 ± 0.01	-11.08 ± 0.09	-4.04 ± 0.06	0.42	-1.00	0.00	NM
NGC 2682	2M08514355+1144264	27.8 ± 0.1	0.13 ± 0.01	-10.37 ± 0.07	-2.04 ± 0.04	0.00	0.38	0.00	NM
NGC 2682	2M08514375+1145148	32.4 ± 0.2	-0.09 ± 0.01	-11.22 ± 0.06	-2.94 ± 0.04	0.55	-1.00	0.55	DM
NGC 2682	2M08514388+1156425	32.9 ± 0.0	0.07 ± 0.01	-11.18 ± 0.11	-3.16 ± 0.07	0.78	0.97	0.46	GM
NGC 2682	2M08514401+1146245	33.1 ± 0.1	0.01 ± 0.01	-11.10 ± 0.07	-2.89 ± 0.05	0.85	-1.00	0.82	DM
NGC 2682	2M08514465+1141510	32.9 ± 0.3	-0.01 ± 0.01	-11.33 ± 0.04	-2.95 ± 0.03	0.79	-1.00	0.31	DM
NGC 2682	2M08514474+1146460	33.1 ± 0.1	0.01 ± 0.01	-11.06 ± 0.07	-3.12 ± 0.04	0.85	0.19	0.71	GM
NGC 2682	2M08514475+1145012	34.9 ± 0.2	-0.06 ± 0.01	-10.87 ± 0.04	-2.81 ± 0.03	0.75	-1.00	0.77	DM
NGC 2682	2M08514507+1147459	33.0 ± 0.0	0.10 ± 0.01	-11.05 ± 0.07	-3.03 ± 0.04	0.80	0.74	0.89	GM
NGC 2682	2M08514577+1217052	50.2 ± 0.2	-0.25 ± 0.01	-2.59 ± 0.08	-3.42 ± 0.05	0.00	0.00	0.00	NM
NGC 2682	2M08514597+1144093	32.8 ± 0.1	0.01 ± 0.01	-11.00 ± 0.04	-2.99 ± 0.03	0.72	-1.00	0.98	DM
NGC 2682	2M08514632+1200553	127.2 ± 0.5	-0.39 ± 0.01	-10.11 ± 0.06	0.69 ± 0.04	0.00	-1.00	0.00	NM
NGC 2682	2M08514641+1146267	33.6 ± 0.1	0.02 ± 0.01	-11.01 ± 0.05	-3.21 ± 0.03	0.98	-1.00	0.54	DM
NGC 2682	2M08514742+1147096	31.4 ± 6.0	-0.02 ± 0.01	-11.11 ± 0.05	-3.09 ± 0.03	0.19	-1.00	0.70	DM
NGC 2682	2M08514814+1159313	23.7 ± 28.2	-0.07 ± 0.01	-10.80 ± 0.06	-3.17 ± 0.04	0.00	-1.00	0.51	NM
NGC 2682	2M08514832+1151118	38.2 ± 0.9	-0.08 ± 0.01	-10.89 ± 0.08	-3.13 ± 0.05	0.01	-1.00	0.70	NM
NGC 2682	2M08514879+1158197	-42.9 ± 0.5	-0.43 ± 0.01	6.54 ± 0.46	-9.28 ± 0.31	0.00	-1.00	0.00	NM
NGC 2682	2M08514883+1156511	34.3 ± 0.1	0.01 ± 0.01	-10.96 ± 0.08	-3.26 ± 0.05	0.94	0.16	0.42	GM
NGC 2682	2M08514898+1143398	34.2 ± 0.5	0.12 ± 0.01	-10.86 ± 0.07	-2.79 ± 0.05	0.97	-1.00	0.71	DM
NGC 2682	2M08514960+1206575	21.4 ± 0.4	-1.21 ± 0.01	16.89 ± 0.05	-17.56 ± 0.03	0.00	0.00	0.00	NM
NGC 2682	2M08514992+1133184	33.1 ± 0.2	0.02 ± 0.01	-11.25 ± 0.07	-2.95 ± 0.05	0.84	-1.00	0.50	DM
NGC 2682	2M08514994+1149311	33.3 ± 0.1	-0.02 ± 0.01	-11.35 ± 0.07	-3.10 ± 0.04	0.92	-1.00	0.22	DM
NGC 2682	2M08515020+1146069	37.3 ± 0.4	0.07 ± 0.01	-11.24 ± 0.07	-2.93 ± 0.04	0.03	0.99	0.51	GM
NGC 2682	2M08515094+1128486	33.9 ± 0.1	0.14 ± 0.01	-40.87 ± 0.06	-10.51 ± 0.05	1.00	-1.00	0.00	NM
NGC 2682	2M08515104+1137025	66.9 ± 0.3	-0.70 ± 0.01	-18.26 ± 0.05	5.43 ± 0.03	0.00	-1.00	0.00	NM
NGC 2682	2M08515145+1157497	33.2 ± 0.5	-0.01 ± 0.01	-10.85 ± 0.08	-3.23 ± 0.06	0.89	-1.00	0.44	DM
NGC 2682	2M08515174+1204467	34.2 ± 0.1	0.15 ± 0.01	-10.75 ± 0.04	-3.07 ± 0.03	0.97	-1.00	0.59	DM
NGC 2682	2M08515251+1104256	-31.7 ± 0.4	-0.06 ± 0.01	9.29 ± 0.06	-15.96 ± 0.05	0.00	-1.00	0.00	NM
NGC 2682	2M08515281+1204189	32.5 ± 0.0	-0.04 ± 0.01	-10.98 ± 0.06	-2.85 ± 0.05	0.58	-1.00	0.90	DM
NGC 2682	2M08515290+1146358	34.0 ± 0.5	0.03 ± 0.01	-11.09 ± 0.09	-2.78 ± 0.05	1.00	-1.00	0.68	DM
NGC 2682	2M08515309+1140536	21.5 ± 22.7	-0.26 ± 0.01	-11.27 ± 0.04	-2.95 ± 0.03	0.00	-1.00	0.44	NM
NGC 2682	2M08515335+1148208	34.3 ± 0.0	-0.05 ± 0.01	-11.44 ± 0.07	-2.94 ± 0.04	0.95	-1.00	0.14	DM
NGC 2682	2M08515383+1131072	87.2 ± 0.2	-0.38 ± 0.01	-4.25 ± 0.04	-5.05 ± 0.03	0.00	0.00	0.00	NM
NGC 2682	2M08515515+1139401	35.6 ± 0.4	0.01 ± 0.01	-10.99 ± 0.05	-2.94 ± 0.03	0.41	-1.00	0.99	DM
NGC 2682	2M08515566+1143392	34.4 ± 0.3	-0.02 ± 0.01	-11.27 ± 0.28	-4.20 ± 0.18	0.92	-1.00	0.00	NM
NGC 2682	2M08515567+1217573	33.5 ± 0.1	0.01 ± 0.01	-10.99 ± 0.08	-2.86 ± 0.06	0.97	0.20	0.92	GM
NGC 2682	2M08515586+1109312	31.1 ± 0.9	0.00 ± 0.01	-11.81 ± 0.07	-6.17 ± 0.05	0.00	-1.00	0.00	NM
NGC 2682	2M08515611+1150147	34.7 ± 0.0	0.13 ± 0.01	-11.13 ± 0.08	-3.89 ± 0.05	0.83	0.26	0.00	NM
NGC 2682	2M08515613+1139041	34.3 ± 0.1	0.06 ± 0.01	-11.25 ± 0.05	-3.07 ± 0.03	0.95	-1.00	0.44	DM
NGC 2682	2M08515787+1145459	37.8 ± 2.4	-0.07 ± 0.01	-10.52 ± 0.12	-3.07 ± 0.07	0.01	-1.00	0.15	DM
NGC 2682	2M08515809+1148160	33.2 ± 0.9	0.00 ± 0.02	-11.40 ± 0.10	-3.40 ± 0.06	0.89	-1.00	0.03	DM
NGC 2682	2M08515852+1146529	40.8 ± 0.7	-0.38 ± 0.01	-16.84 ± 0.07	7.17 ± 0.05	0.00	-1.00	0.00	NM
NGC 2682	2M08515877+1201555	34.0 ± 0.4	0.02 ± 0.01	-11.11 ± 0.07	-2.66 ± 0.05	1.00	-1.00	0.40	DM
NGC 2682	2M08515877+1150024	37.0 ± 0.2	-0.07 ± 0.01	-10.51 ± 0.06	-2.89 ± 0.04	0.06	-1.00	0.15	DM
NGC 2682	2M08515893+1159560	33.4 ± 0.2	0.06 ± 0.01	-10.93 ± 0.08	-2.75 ± 0.05	0.94	-1.00	0.68	DM
NGC 2682	2M08515952+1155049	34.4 ± 0.0	0.06 ± 0.01	-11.00 ± 0.09	-3.10 ± 0.06	0.93	0.95	0.81	GM
NGC 2682	2M08515955+1246247	113.3 ± 0.2	-0.02 ± 0.01	-7.14 ± 0.07	-4.15 ± 0.05	0.00	0.00	0.00	NM
NGC 2682	2M08515963+1152576	33.0 ± 0.1	-0.01 ± 0.01	-10.91 ± 0.07	-2.66 ± 0.04	0.81	-1.00	0.47	DM
NGC 2682	2M08520041+1156070	34.1 ± 0.2	0.09 ± 0.01	-11.21 ± 0.06	-2.96 ± 0.03	0.99	-1.00	0.60	DM
NGC 2682	2M08520215+1149083	30.6 ± 0.2	-0.04 ± 0.01	-10.61 ± 0.05	-2.75 ± 0.03	0.05	-1.00	0.22	DM

Continued on next page

Table A.1 – Continued

Cluster name	2MASS ID	RV (km s^{-1})	[Fe/H] (dex)	μ_α (mas yr^{-1})	μ_δ (mas yr^{-1})	RV Prob	[Fe/H] Prob	PM Prob	Memb
NGC 2682	2M08520253+1207046	-15.3 ± 0.2	-0.36 ± 0.01	-1.41 ± 0.07	-3.64 ± 0.05	0.00	-1.00	0.00	NM
NGC 2682	2M08520276+1146039	37.3 ± 1.7	-0.01 ± 0.01	-11.27 ± 0.05	-3.17 ± 0.03	0.04	-1.00	0.29	DM
NGC 2682	2M08520356+1141238	34.1 ± 0.1	-0.05 ± 0.01	-10.82 ± 0.07	-2.76 ± 0.04	0.98	-1.00	0.60	DM
NGC 2682	2M08520474+1158291	30.1 ± 0.1	-0.03 ± 0.01	-12.06 ± 0.07	-2.98 ± 0.04	0.02	-1.00	0.00	NM
NGC 2682	2M08520629+1138411	44.9 ± 16.9	-0.14 ± 0.01	-11.46 ± 0.05	-3.25 ± 0.03	0.00	-1.00	0.06	NM
NGC 2682	2M08520741+1150221	34.2 ± 0.2	0.02 ± 0.01	-11.12 ± 0.04	-2.95 ± 0.03	0.97	-1.00	0.82	DM
NGC 2682	2M08520851+1155404	1.7 ± 4.7	-0.07 ± 0.01	-6.10 ± 0.06	5.65 ± 0.04	0.00	-1.00	0.00	NM
NGC 2682	2M08521097+1131491	33.8 ± 0.0	0.11 ± 0.01	-11.06 ± 0.06	-2.76 ± 0.04	1.00	0.67	0.67	GM
NGC 2682	2M08521134+1145380	33.1 ± 0.0	0.03 ± 0.01	-10.98 ± 0.07	-2.99 ± 0.04	0.83	-1.00	0.99	DM
NGC 2682	2M08521459+1046339	10.2 ± 0.3	0.12 ± 0.01	0.10 ± 0.06	-10.60 ± 0.05	0.00	-1.00	0.00	NM
NGC 2682	2M08521649+1147382	33.9 ± 0.3	0.06 ± 0.01	-11.01 ± 0.07	-2.74 ± 0.04	1.00	-1.00	0.67	DM
NGC 2682	2M08521656+1119380	33.8 ± 0.0	0.08 ± 0.01	-11.05 ± 0.07	-2.88 ± 0.05	1.00	1.00	0.90	GM
NGC 2682	2M08521664+1142300	32.2 ± 4.0	-0.11 ± 0.01	-10.94 ± 0.05	-2.95 ± 0.03	0.47	-1.00	0.99	DM
NGC 2682	2M08521752+1100352	-53.6 ± 0.2	-0.06 ± 0.01	4.64 ± 0.05	-25.72 ± 0.04	0.00	-1.00	0.00	NM
NGC 2682	2M08521856+1144263	33.7 ± 0.1	0.09 ± 0.01	-11.13 ± 0.07	-3.14 ± 0.05	0.99	0.90	0.58	GM
NGC 2682	2M08521868+1143246	32.7 ± 0.2	-0.06 ± 0.01	-10.97 ± 0.07	-2.86 ± 0.04	0.70	-1.00	0.94	DM
NGC 2682	2M08522003+1127362	33.9 ± 0.1	0.08 ± 0.01	-11.22 ± 0.07	-2.91 ± 0.04	1.00	1.00	0.54	GM
NGC 2682	2M08522086+1121472	34.9 ± 0.0	-0.23 ± 0.01	-6.84 ± 0.07	5.25 ± 0.05	0.74	0.00	0.00	NM
NGC 2682	2M08522332+1250027	6.4 ± 0.2	-0.08 ± 0.01	1.88 ± 0.05	2.73 ± 0.04	0.00	-1.00	0.00	NM
NGC 2682	2M08522636+1141277	33.4 ± 0.1	0.02 ± 0.01	-10.77 ± 0.08	-2.99 ± 0.05	0.94	0.31	0.70	GM
NGC 2682	2M08523751+1050537	6.7 ± 0.0	0.09 ± 0.01	-63.52 ± 0.06	-16.54 ± 0.04	0.00	-1.00	0.00	NM
NGC 2682	2M08523758+1141218	80.9 ± 0.7	-0.26 ± 0.01	-29.83 ± 0.08	-27.78 ± 0.05	0.00	-1.00	0.00	NM
NGC 2682	2M08524532+1050549	77.4 ± 0.0	-0.00 ± 0.01	-5.27 ± 0.05	-0.44 ± 0.03	0.00	0.00	0.00	NM
NGC 2682	2M08525040+1111066	41.6 ± 0.1	-0.06 ± 0.01	-1.39 ± 0.07	2.03 ± 0.05	0.00	0.00	0.00	NM
NGC 2682	2M08525347+1048530	-38.7 ± 0.0	0.37 ± 0.01	1.00 ± 0.07	-2.20 ± 0.05	0.00	0.00	0.00	NM
NGC 2682	2M08525428+1129482	33.1 ± 0.1	-0.28 ± 0.01	-1.27 ± 0.08	-2.35 ± 0.05	0.85	0.00	0.00	NM
NGC 2682	2M08525607+1112447	85.0 ± 0.3	-0.83 ± 0.01	-1.92 ± 0.05	-5.43 ± 0.04	0.00	0.00	0.00	NM
NGC 2682	2M08525625+1148539	32.8 ± 0.1	0.13 ± 0.01	-11.02 ± 0.08	-3.10 ± 0.05	0.74	0.31	0.80	GM
NGC 2682	2M08525848+1118539	66.9 ± 0.2	-0.32 ± 0.01	-2.81 ± 0.06	-9.02 ± 0.04	0.00	0.00	0.00	NM
NGC 2682	2M08525947+1210573	85.7 ± 0.2	-0.16 ± 0.01	-52.83 ± 0.15	-37.87 ± 0.12	0.00	-1.00	0.00	NM
NGC 2682	2M08530060+1141001	15.6 ± 0.0	0.11 ± 0.01	3.70 ± 0.08	2.57 ± 0.05	0.00	0.61	0.00	NM
NGC 2682	2M08530433+1054197	-5.3 ± 0.3	0.31 ± 0.01	-12.51 ± 0.10	-0.29 ± 0.06	0.00	-1.00	0.00	NM
NGC 2682	2M08530456+1129544	138.0 ± 0.3	-0.16 ± 0.01	-31.15 ± 0.08	14.94 ± 0.05	0.00	-1.00	0.00	NM
NGC 2682	2M08530651+1214374	357.1 ± 0.3	-1.32 ± 0.01	1.11 ± 0.05	-0.93 ± 0.04	0.00	0.00	0.00	NM
NGC 2682	2M08530745+1133583	39.5 ± 0.0	0.27 ± 0.01	2.32 ± 0.04	-21.58 ± 0.03	0.00	-1.00	0.00	NM
NGC 2682	2M08530766+1143005	86.3 ± 0.6	0.04 ± 0.01	5.32 ± 0.07	-31.15 ± 0.05	0.00	-1.00	0.00	NM
NGC 2682	2M08530772+1222365	68.4 ± 0.3	-0.41 ± 0.01	-28.85 ± 0.06	-15.43 ± 0.04	0.00	-1.00	0.00	NM
NGC 2682	2M08530915+1051224	1.2 ± 0.3	0.03 ± 0.01	3.04 ± 0.07	-14.03 ± 0.05	0.00	-1.00	0.00	NM
NGC 2682	2M08531108+1100596	102.4 ± 0.0	0.27 ± 0.01	-6.09 ± 0.06	5.32 ± 0.04	0.00	0.00	0.00	NM
NGC 2682	2M08531376+1104360	9.1 ± 0.3	-0.06 ± 0.01	-5.21 ± 0.07	7.94 ± 0.05	0.00	-1.00	0.00	NM
NGC 2682	2M08531969+1132235	87.5 ± 0.1	-1.54 ± 0.01	-0.50 ± 0.06	-17.11 ± 0.03	0.00	0.00	0.00	NM
NGC 2682	2M08532194+1050292	121.7 ± 0.1	-0.30 ± 0.01	-12.58 ± 0.07	-21.45 ± 0.05	0.00	0.00	0.00	NM
NGC 2682	2M08532214+1112230	33.7 ± 0.1	-0.45 ± 0.01	-0.03 ± 0.04	-0.68 ± 0.03	0.00	0.00	0.00	NM
NGC 2682	2M08532217+1241133	-4.4 ± 10.6	-0.05 ± 0.01	-3.26 ± 0.06	-15.70 ± 0.04	0.00	-1.00	0.00	NM
NGC 2682	2M08532241+1218406	-26.1 ± 0.1	-0.22 ± 0.01	-5.71 ± 0.07	-12.80 ± 0.06	0.00	0.00	0.00	NM
NGC 2682	2M08532275+1208484	23.6 ± 0.1	-0.27 ± 0.01	-3.18 ± 0.07	-2.96 ± 0.05	0.00	0.00	0.00	NM
NGC 2682	2M08532372+1119098	28.6 ± 0.3	-0.39 ± 0.01	11.31 ± 0.07	-8.55 ± 0.04	0.00	-1.00	0.00	NM
NGC 2682	2M08532742+1111047	23.6 ± 0.2	-0.32 ± 0.01	-17.25 ± 0.06	-6.57 ± 0.04	0.00	0.00	0.00	NM
NGC 2682	2M08532905+1223556	40.7 ± 0.4	0.41 ± 0.01	5.51 ± 0.05	-7.72 ± 0.04	0.00	-1.00	0.00	NM
NGC 2682	2M08533316+1112491	63.8 ± 0.1	-0.39 ± 0.01	-5.17 ± 0.06	-0.84 ± 0.04	0.00	0.00	0.00	NM
NGC 2682	2M08534172+1214386	53.3 ± 0.0	0.21 ± 0.01	-8.17 ± 0.06	-27.12 ± 0.04	0.00	-1.00	0.00	NM
NGC 2682	2M08534672+1123307	33.0 ± 0.1	0.07 ± 0.01	-11.24 ± 0.08	-2.79 ± 0.05	0.00	0.00	0.41	NM
NGC 2682	2M08534794+1202435	94.5 ± 0.4	0.07 ± 0.01	-1.89 ± 0.06	-3.05 ± 0.04	0.00	0.00	0.00	NM
NGC 2682	2M08534873+1201149	9.1 ± 0.3	0.14 ± 0.01	-10.47 ± 0.08	-17.24 ± 0.06	0.00	-1.00	0.00	NM
NGC 2682	2M08534927+1237197	46.7 ± 0.2	0.05 ± 0.01	24.33 ± 0.08	-73.72 ± 0.05	0.00	-1.00	0.00	NM
NGC 2682	2M08535731+1223031	40.1 ± 0.0	-0.24 ± 0.01	-5.99 ± 0.07	-3.71 ± 0.05	0.00	0.00	0.00	NM
NGC 2682	2M08540077+1141309	13.7 ± 0.3	0.13 ± 0.01	-1.66 ± 0.08	-6.21 ± 0.05	0.00	-1.00	0.00	NM
NGC 2682	2M08540404+1236352	79.5 ± 0.1	0.15 ± 0.01	-1.79 ± 0.07	-3.88 ± 0.05	0.00	0.00	0.00	NM
NGC 2682	2M08540487+1200199	34.6 ± 0.1	0.09 ± 0.01	-6.12 ± 0.08	0.47 ± 0.06	0.00	0.00	0.00	NM
NGC 2682	2M08540699+1212175	14.0 ± 0.1	0.14 ± 0.01	-4.72 ± 0.08	-2.48 ± 0.05	0.00	0.00	0.00	NM
NGC 2682	2M08540947+1214531	54.6 ± 0.3	-0.55 ± 0.01	-5.27 ± 0.07	-3.27 ± 0.05	0.00	0.00	0.00	NM
NGC 2682	2M08542116+1131162	39.3 ± 0.1	0.29 ± 0.01	-57.96 ± 0.06	-27.26 ± 0.04	0.00	-1.00	0.00	NM
NGC 2682	2M08542648+1105034	67.8 ± 0.4	0.00 ± 0.01	-25.46 ± 0.10	-18.13 ± 0.06	0.00	-1.00	0.00	NM

Continued on next page

Table A.1 – Continued

Cluster name	2MASS ID	RV (km s^{-1})	[Fe/H] (dex)	μ_α (mas yr^{-1})	μ_δ (mas yr^{-1})	RV Prob	[Fe/H] Prob	PM Prob	Memb
NGC 2682	2M08542841+1113088	-42.0 ± 38.2	-0.22 ± 0.01	-10.91 ± 0.08	-5.30 ± 0.05	0.00	-1.00	0.00	NM
NGC 2682	2M08543353+1219079	-3.5 ± 0.0	-0.31 ± 0.01	-8.01 ± 0.07	2.48 ± 0.05	0.00	0.00	0.00	NM
NGC 2682	2M08543373+1213417	62.6 ± 0.6	-1.07 ± 0.01	-0.11 ± 0.07	-2.99 ± 0.04	0.00	0.00	0.00	NM
NGC 2682	2M08543965+1229595	24.8 ± 0.1	0.15 ± 0.01	-25.16 ± 0.09	-7.70 ± 0.06	0.00	-1.00	0.00	NM
NGC 2682	2M08544343+1144570	38.3 ± 0.4	-0.04 ± 0.01	-15.61 ± 0.10	-4.05 ± 0.06	0.00	-1.00	0.00	NM
NGC 2682	2M08544465+1130053	4.0 ± 5.4	-0.27 ± 0.01	-4.11 ± 0.08	-4.55 ± 0.06	0.00	-1.00	0.00	NM
NGC 2682	2M08544504+1159398	-30.9 ± 0.4	-0.42 ± 0.01	30.34 ± 0.08	-51.95 ± 0.06	0.00	-1.00	0.00	NM
NGC 2682	2M08544578+1218431	23.8 ± 10.2	0.01 ± 0.01	-12.78 ± 0.11	-4.84 ± 0.07	0.00	-1.00	0.00	NM
NGC 2682	2M08544747+1109214	24.7 ± 0.4	0.02 ± 0.01	-105.09 ± 0.09	-62.67 ± 0.06	0.00	-1.00	0.00	NM
NGC 2682	2M08545333+1119571	6.7 ± 0.0	0.19 ± 0.01	-32.51 ± 0.07	-27.97 ± 0.05	0.00	-1.00	0.00	NM
NGC 2682	2M08545396+1135580	31.1 ± 0.4	0.18 ± 0.01	-17.30 ± 0.09	-8.98 ± 0.06	0.00	-1.00	0.00	NM
NGC 2682	2M08545627+1213146	33.8 ± 0.2	-0.12 ± 0.01	-6.55 ± 0.09	-6.48 ± 0.07	0.00	-1.00	0.00	NM
NGC 2682	2M08545739+1201313	61.6 ± 0.1	-0.11 ± 0.01	-6.57 ± 0.07	3.22 ± 0.05	0.00	0.00	0.00	NM
NGC 2682	2M08545806+1143034	63.5 ± 0.2	-0.30 ± 0.01	-3.18 ± 0.05	2.91 ± 0.03	0.00	0.00	0.00	NM
NGC 2682	2M08545897+1225409	21.4 ± 0.8	0.11 ± 0.01	-1.89 ± 0.05	-43.74 ± 0.03	0.00	-1.00	0.00	NM
NGC 2682	2M08550779+1149247	-18.5 ± 0.4	-0.15 ± 0.01	0.12 ± 0.75	-11.31 ± 0.44	0.00	-1.00	0.00	NM
NGC 2682	2M08551636+1148160	-48.0 ± 0.4	0.02 ± 0.01	3.42 ± 0.18	-28.09 ± 0.11	0.00	-1.00	0.00	NM
NGC 2682	2M08552972+1144050	54.1 ± 0.1	0.27 ± 0.01	-22.26 ± 0.60	-62.14 ± 0.47	0.00	-1.00	0.00	NM
NGC 2682	2M08553209+1136459	20.1 ± 0.2	0.12 ± 0.01	-30.35 ± 0.06	23.90 ± 0.04	0.00	-1.00	0.00	NM
NGC 2682	2M08554853+1145185	-28.5 ± 0.5	0.02 ± 0.01	26.16 ± 0.12	-15.86 ± 0.07	0.00	-1.00	0.00	NM

Appendix B

Table 2.6: DR14 OCAAM Open Cluster Member Star Abundances – Full Version

Table B.1: DR14 OCAAM Open Cluster Member Star Abundances (Full)

Cluster	2MASS ID	RV (km s^{-1})	[Fe/H] (dex)	[O/Fe] (dex)	[Mg/Fe] (dex)	[Ca/Fe] (dex)	[Si/Fe] (dex)	[S/Fe] (dex)
				[V/Fe] (dex)	[Cr/Fe] (dex)	[Mn/Fe] (dex)	[Co/Fe] (dex)	[Ni/Fe] (dex)
NGC 6791	2M19202870+3743169	-48.3 ± 0.4	0.46 ± 0.01	0.05 ± 0.03	-0.00 ± 0.02	-0.00 ± 0.03	-0.02 ± 0.02	-0.13 ± 0.07
				-0.05 ± 0.07	-0.23 ± 0.04	-0.23 ± 0.04	-0.76 ± 0.16	-0.01 ± 0.03
NGC 6791	2M19203005+3750191	-47.5 ± 0.0	0.43 ± 0.01	0.06 ± 0.03	0.06 ± 0.02	-0.01 ± 0.03	-0.02 ± 0.02	0.03 ± 0.06
				0.00 ± 0.06	-0.18 ± 0.04	-0.01 ± 0.03	-0.27 ± 0.09	0.00 ± 0.02
NGC 6791	2M19203485+3746298	-47.1 ± 0.1	0.44 ± 0.01	0.03 ± 0.03	0.05 ± 0.02	-0.04 ± 0.03	0.01 ± 0.02	-0.01 ± 0.06
				-0.29 ± 0.07	-0.13 ± 0.04	-0.02 ± 0.03	-0.20 ± 0.09	-0.05 ± 0.02
NGC 6791	2M19203519+3748579	-48.3 ± 0.0	0.35 ± 0.01	0.11 ± 0.01	0.13 ± 0.02	0.02 ± 0.02	0.04 ± 0.02	0.26 ± 0.05
				0.21 ± 0.04	0.02 ± 0.03	0.14 ± 0.02	0.15 ± 0.05	0.04 ± 0.01
NGC 6791	2M19203784+3745249	-48.6 ± 0.1	0.42 ± 0.01	0.06 ± 0.03	-0.01 ± 0.02	0.09 ± 0.03	-0.08 ± 0.02	-0.02 ± 0.07
				0.16 ± 0.07	-0.07 ± 0.04	-0.19 ± 0.04	-0.30 ± 0.14	-0.05 ± 0.03
NGC 6791	2M19203934+3748048	-46.8 ± 0.0	0.40 ± 0.01	0.07 ± 0.02	0.06 ± 0.02	-0.03 ± 0.02	-0.03 ± 0.02	0.10 ± 0.05
				0.04 ± 0.05	-0.18 ± 0.03	-0.07 ± 0.02	0.17 ± 0.07	-0.03 ± 0.02
NGC 6791	2M19204102+3743025	-47.9 ± 0.1	0.47 ± 0.01	0.00 ± 0.03	-0.06 ± 0.02	-0.03 ± 0.03	-0.15 ± 0.02	-0.06 ± 0.07
				-0.27 ± 0.08	-0.04 ± 0.05	-0.22 ± 0.04	0.26 ± 0.13	-0.03 ± 0.04
NGC 6791	2M19204485+3746215	-44.9 ± 0.1	0.38 ± 0.01	0.08 ± 0.02	0.11 ± 0.02	0.01 ± 0.02	0.05 ± 0.02	0.31 ± 0.06
				0.15 ± 0.05	-0.02 ± 0.03	0.12 ± 0.02	0.15 ± 0.06	-0.00 ± 0.02
NGC 6791	2M19204517+3744339	-48.4 ± 0.1	0.41 ± 0.01	0.06 ± 0.03	0.00 ± 0.02	-0.03 ± 0.03	-0.00 ± 0.02	0.04 ± 0.07
				-0.29 ± 0.07	-0.09 ± 0.04	-0.20 ± 0.03	-0.22 ± 0.11	-0.01 ± 0.03
NGC 6791	2M19204624+3749105	-46.1 ± 0.0	0.43 ± 0.01	0.02 ± 0.03	-0.04 ± 0.02	0.11 ± 0.03	0.02 ± 0.02	-0.03 ± 0.07
				0.00 ± 0.07	-0.06 ± 0.04	-0.24 ± 0.04	0.01 ± 0.12	-0.04 ± 0.03
NGC 6791	2M19204635+3750228	-45.3 ± 0.0	0.37 ± 0.01	0.09 ± 0.01	0.10 ± 0.01	0.04 ± 0.01	0.04 ± 0.02	0.06 ± 0.04
				-9.99 ± 9.99	-0.14 ± 0.02	0.15 ± 0.01	0.17 ± 0.03	0.03 ± 0.01
NGC 6791	2M19204971+3743426	-47.4 ± 0.2	0.32 ± 0.01	0.24 ± 0.01	0.13 ± 0.01	0.27 ± 0.02	0.09 ± 0.01	0.24 ± 0.04
				-9.99 ± 9.99	-0.20 ± 0.02	0.22 ± 0.01	0.22 ± 0.03	-0.01 ± 0.01

Continued on next page

Table B.1 – Continued

Cluster	2MASS ID	RV (km s^{-1})	[Fe/H] (dex)	[O/Fe] (dex)	[Mg/Fe] (dex)	[Ca/Fe] (dex)	[Si/Fe] (dex)	[S/Fe] (dex)
				[V/Fe] (dex)	[Cr/Fe] (dex)	[Mn/Fe] (dex)	[Co/Fe] (dex)	[Ni/Fe] (dex)
NGC 6791	2M19205038+3743335	-43.9 ± 5.6	0.37 ± 0.01	0.08 ± 0.04	0.13 ± 0.02	0.03 ± 0.04	0.06 ± 0.03	0.16 ± 0.08
				-0.22 ± 0.10	0.11 ± 0.05	0.04 ± 0.04	0.41 ± 0.14	-0.10 ± 0.03
NGC 6791	2M19205259+3744281	-45.4 ± 0.0	0.38 ± 0.01	0.11 ± 0.02	0.13 ± 0.02	0.03 ± 0.02	0.07 ± 0.02	0.22 ± 0.05
				0.17 ± 0.05	-0.04 ± 0.03	0.10 ± 0.02	0.27 ± 0.06	0.02 ± 0.02
NGC 6791	2M19205287+3745331	-46.0 ± 0.0	0.42 ± 0.01	0.05 ± 0.03	0.01 ± 0.02	0.04 ± 0.03	-0.01 ± 0.02	0.03 ± 0.06
				0.11 ± 0.07	-0.15 ± 0.04	-0.02 ± 0.03	0.10 ± 0.09	-0.00 ± 0.02
NGC 6791	2M19205338+3748282	-48.4 ± 0.1	0.44 ± 0.01	0.06 ± 0.01	0.06 ± 0.01	0.01 ± 0.01	0.01 ± 0.02	0.06 ± 0.04
				-9.99 ± 9.99	-0.11 ± 0.02	0.12 ± 0.01	-9.99 ± 9.99	0.02 ± 0.01
NGC 6791	2M19205368+3750236	-48.5 ± 0.1	0.46 ± 0.01	0.02 ± 0.03	0.04 ± 0.02	0.03 ± 0.03	-0.00 ± 0.02	0.04 ± 0.06
				0.02 ± 0.07	-0.13 ± 0.04	-0.11 ± 0.03	0.34 ± 0.09	0.02 ± 0.02
NGC 6791	2M19205510+3747162	-48.2 ± 0.0	0.37 ± 0.01	0.09 ± 0.01	0.09 ± 0.01	0.06 ± 0.01	0.04 ± 0.02	0.12 ± 0.04
				-9.99 ± 9.99	-0.08 ± 0.02	0.10 ± 0.02	0.17 ± 0.04	0.04 ± 0.01
NGC 6791	2M19205530+3743152	-47.9 ± 0.1	0.48 ± 0.01	0.08 ± 0.02	0.11 ± 0.02	-0.01 ± 0.02	0.00 ± 0.02	-0.10 ± 0.05
				-9.99 ± 9.99	-0.22 ± 0.03	0.07 ± 0.02	0.18 ± 0.06	-0.02 ± 0.01
NGC 6791	2M19205629+3744334	-49.0 ± 0.0	0.45 ± 0.01	0.07 ± 0.03	0.05 ± 0.02	0.00 ± 0.03	-0.04 ± 0.02	0.00 ± 0.06
				-0.24 ± 0.07	-0.10 ± 0.04	-0.03 ± 0.03	-0.05 ± 0.09	-0.01 ± 0.02
NGC 6791	2M19205784+3747067	-46.9 ± 0.9	0.42 ± 0.01	0.07 ± 0.03	0.08 ± 0.02	-0.00 ± 0.03	-0.03 ± 0.02	0.01 ± 0.06
				-0.04 ± 0.07	0.05 ± 0.04	0.13 ± 0.03	0.32 ± 0.10	0.02 ± 0.02
NGC 6791	2M19205958+3748108	-47.2 ± 0.2	0.54 ± 0.01	0.04 ± 0.03	-0.13 ± 0.02	0.10 ± 0.03	-0.16 ± 0.02	-0.18 ± 0.07
				0.04 ± 0.07	-0.23 ± 0.04	-0.38 ± 0.05	-9.99 ± 9.99	-0.10 ± 0.04
NGC 6791	2M19210052+3750188	-46.7 ± 0.0	0.33 ± 0.01	0.06 ± 0.03	0.02 ± 0.02	-0.01 ± 0.03	-0.03 ± 0.02	0.07 ± 0.06
				-0.06 ± 0.06	-0.11 ± 0.04	0.02 ± 0.03	0.08 ± 0.09	0.08 ± 0.02
NGC 6791	2M19210086+3745339	-45.8 ± 0.1	0.46 ± 0.01	0.05 ± 0.03	0.05 ± 0.02	0.01 ± 0.03	0.00 ± 0.02	0.14 ± 0.06
				0.04 ± 0.07	-0.18 ± 0.04	-0.06 ± 0.03	0.17 ± 0.09	0.05 ± 0.02

Continued on next page

Table B.1 – Continued

Cluster	2MASS ID	RV (km s^{-1})	[Fe/H] (dex)	[O/Fe] (dex)	[Mg/Fe] (dex)	[Ca/Fe] (dex)	[Si/Fe] (dex)	[S/Fe] (dex)
				[V/Fe] (dex)	[Cr/Fe] (dex)	[Mn/Fe] (dex)	[Co/Fe] (dex)	[Ni/Fe] (dex)
NGC 6791	2M19210112+3742134	-47.6 ± 0.1	0.43 ± 0.01	0.08 ± 0.02	0.12 ± 0.01	-0.00 ± 0.02	-0.00 ± 0.02	0.01 ± 0.04
				-9.99 ± 9.99	-0.12 ± 0.03	0.15 ± 0.02	0.23 ± 0.05	-0.01 ± 0.01
NGC 6791	2M19210426+3747187	-46.8 ± 0.1	0.41 ± 0.01	0.04 ± 0.01	0.05 ± 0.01	0.02 ± 0.02	0.01 ± 0.02	0.06 ± 0.04
				0.17 ± 0.04	-0.10 ± 0.02	0.10 ± 0.02	0.31 ± 0.05	0.06 ± 0.01
NGC 6791	2M19210483+3741036	-50.1 ± 0.0	0.43 ± 0.01	0.06 ± 0.02	0.11 ± 0.02	0.03 ± 0.02	0.01 ± 0.02	0.03 ± 0.05
				-9.99 ± 9.99	-0.05 ± 0.03	0.03 ± 0.02	-0.16 ± 0.08	-0.03 ± 0.02
NGC 6791	2M19210604+3752049	-48.0 ± 0.1	0.39 ± 0.01	0.12 ± 0.03	0.12 ± 0.02	0.02 ± 0.03	-0.03 ± 0.02	-0.00 ± 0.06
				-9.99 ± 9.99	-0.15 ± 0.04	0.15 ± 0.03	0.03 ± 0.11	0.07 ± 0.02
NGC 6791	2M19210629+3744596	-45.3 ± 0.1	0.44 ± 0.01	0.00 ± 0.03	0.00 ± 0.02	0.02 ± 0.03	-0.05 ± 0.02	-0.11 ± 0.06
				0.03 ± 0.07	-0.11 ± 0.04	-0.09 ± 0.03	0.02 ± 0.09	-0.04 ± 0.02
NGC 6791	2M19211007+3750008	-48.9 ± 0.1	0.38 ± 0.01	0.11 ± 0.02	0.13 ± 0.02	0.01 ± 0.02	0.03 ± 0.02	0.07 ± 0.05
				0.13 ± 0.06	-0.11 ± 0.03	0.14 ± 0.02	-0.08 ± 0.09	0.00 ± 0.02
NGC 6791	2M19211300+3743005	-48.1 ± 0.2	0.45 ± 0.01	0.04 ± 0.03	0.07 ± 0.02	-0.00 ± 0.03	-0.04 ± 0.02	0.02 ± 0.06
				-9.99 ± 9.99	-0.17 ± 0.04	0.03 ± 0.03	-0.59 ± 0.14	0.01 ± 0.02
NGC 6819	2M19404803+4008085	2.4 ± 0.1	0.09 ± 0.01	-0.01 ± 0.02	0.02 ± 0.02	0.01 ± 0.02	0.02 ± 0.02	-0.00 ± 0.05
				0.04 ± 0.06	0.02 ± 0.03	0.01 ± 0.02	0.07 ± 0.06	0.01 ± 0.01
NGC 6819	2M19404965+4014313	3.1 ± 0.0	0.12 ± 0.01	0.01 ± 0.03	0.01 ± 0.02	0.02 ± 0.02	0.00 ± 0.02	-0.03 ± 0.05
				0.06 ± 0.07	0.02 ± 0.04	0.03 ± 0.03	0.07 ± 0.08	0.02 ± 0.02
NGC 6819	2M19405020+4013109	4.3 ± 0.0	0.15 ± 0.01	0.00 ± 0.03	0.00 ± 0.02	-0.00 ± 0.02	-0.04 ± 0.02	-0.04 ± 0.05
				-0.02 ± 0.06	-0.02 ± 0.03	0.01 ± 0.02	0.03 ± 0.07	0.02 ± 0.01
NGC 6819	2M19405601+4013395	3.3 ± 0.1	0.09 ± 0.01	0.04 ± 0.04	-0.00 ± 0.02	0.02 ± 0.03	-0.13 ± 0.03	-0.07 ± 0.06
				-0.01 ± 0.09	-0.00 ± 0.05	0.02 ± 0.03	0.10 ± 0.10	0.00 ± 0.02
NGC 6819	2M19405797+4008174	4.5 ± 0.1	0.13 ± 0.01	0.00 ± 0.03	0.02 ± 0.02	0.00 ± 0.02	0.01 ± 0.02	-0.06 ± 0.05
				0.08 ± 0.07	0.03 ± 0.03	0.05 ± 0.02	0.03 ± 0.07	0.00 ± 0.01

Continued on next page

Table B.1 – Continued

Cluster	2MASS ID	RV (km s^{-1})	[Fe/H] (dex)	[O/Fe] (dex)	[Mg/Fe] (dex)	[Ca/Fe] (dex)	[Si/Fe] (dex)	[S/Fe] (dex)
				[V/Fe] (dex)	[Cr/Fe] (dex)	[Mn/Fe] (dex)	[Co/Fe] (dex)	[Ni/Fe] (dex)
NGC 6819	2M19410524+4014042	3.3 ± 0.1	0.14 ± 0.01	-0.03 ± 0.03	-0.01 ± 0.02	0.04 ± 0.02	0.02 ± 0.03	0.03 ± 0.05
				0.02 ± 0.07	0.02 ± 0.04	0.03 ± 0.03	-0.04 ± 0.08	0.04 ± 0.02
NGC 6819	2M19410622+4010532	3.2 ± 0.0	0.12 ± 0.01	0.07 ± 0.04	0.01 ± 0.02	0.02 ± 0.03	0.03 ± 0.03	-0.05 ± 0.06
				0.02 ± 0.08	-0.04 ± 0.04	0.02 ± 0.03	0.03 ± 0.10	0.02 ± 0.02
NGC 6819	2M19410858+4013299	2.3 ± 0.0	0.11 ± 0.01	-0.06 ± 0.03	0.00 ± 0.02	-0.01 ± 0.02	0.03 ± 0.02	-0.03 ± 0.05
				0.03 ± 0.06	0.03 ± 0.03	0.03 ± 0.02	0.08 ± 0.07	0.01 ± 0.01
NGC 6819	2M19410926+4014436	2.3 ± 0.1	0.13 ± 0.01	-0.03 ± 0.03	0.00 ± 0.02	-0.00 ± 0.02	-0.03 ± 0.02	-0.02 ± 0.05
				-0.04 ± 0.06	-0.00 ± 0.03	0.00 ± 0.02	0.01 ± 0.07	-0.02 ± 0.01
NGC 6819	2M19410991+4015495	2.5 ± 0.1	0.07 ± 0.01	-0.03 ± 0.03	-0.00 ± 0.02	0.05 ± 0.02	0.01 ± 0.03	0.02 ± 0.05
				0.13 ± 0.07	0.06 ± 0.04	0.00 ± 0.03	0.13 ± 0.08	0.03 ± 0.02
NGC 6819	2M19410994+4009056	2.9 ± 3.1	0.02 ± 0.01	0.01 ± 0.04	0.03 ± 0.02	0.02 ± 0.03	0.01 ± 0.03	-0.02 ± 0.07
				-0.13 ± 0.09	0.00 ± 0.05	0.03 ± 0.03	0.38 ± 0.12	0.07 ± 0.02
NGC 6819	2M19411102+4011116	3.0 ± 0.0	0.10 ± 0.01	-0.08 ± 0.03	0.01 ± 0.02	0.00 ± 0.02	0.07 ± 0.02	-0.00 ± 0.05
				0.05 ± 0.07	0.03 ± 0.03	0.06 ± 0.02	0.00 ± 0.08	0.01 ± 0.01
NGC 6819	2M19411115+4011422	4.6 ± 0.0	0.14 ± 0.01	-0.03 ± 0.02	0.02 ± 0.02	0.01 ± 0.02	0.02 ± 0.02	0.04 ± 0.04
				0.02 ± 0.06	0.04 ± 0.03	0.05 ± 0.02	0.08 ± 0.06	0.02 ± 0.01
NGC 6819	2M19411279+4012238	2.8 ± 0.0	0.12 ± 0.01	-0.03 ± 0.03	0.01 ± 0.02	0.03 ± 0.02	0.02 ± 0.02	-0.03 ± 0.05
				0.02 ± 0.07	0.04 ± 0.03	0.07 ± 0.02	-0.02 ± 0.07	0.00 ± 0.01
NGC 6819	2M19411319+4014567	-1.8 ± 0.1	0.10 ± 0.01	0.01 ± 0.02	-0.01 ± 0.02	0.00 ± 0.02	-0.03 ± 0.02	-0.02 ± 0.04
				-0.04 ± 0.04	-0.02 ± 0.02	0.00 ± 0.02	-0.02 ± 0.04	-0.02 ± 0.01
NGC 6819	2M19411355+4012205	2.6 ± 0.1	0.09 ± 0.01	-0.04 ± 0.03	-0.01 ± 0.02	-0.01 ± 0.02	0.02 ± 0.02	0.02 ± 0.05
				-0.06 ± 0.07	0.00 ± 0.03	0.02 ± 0.02	0.01 ± 0.07	0.01 ± 0.01
NGC 6819	2M19411476+4011008	1.0 ± 0.2	0.15 ± 0.01	-0.04 ± 0.03	0.01 ± 0.02	-0.00 ± 0.02	0.03 ± 0.02	-0.01 ± 0.05
				0.04 ± 0.07	-0.01 ± 0.03	0.04 ± 0.02	0.14 ± 0.07	0.02 ± 0.01

Continued on next page

Table B.1 – Continued

Cluster	2MASS ID	RV (km s^{-1})	[Fe/H] (dex)	[O/Fe] (dex)	[Mg/Fe] (dex)	[Ca/Fe] (dex)	[Si/Fe] (dex)	[S/Fe] (dex)
				[V/Fe] (dex)	[Cr/Fe] (dex)	[Mn/Fe] (dex)	[Co/Fe] (dex)	[Ni/Fe] (dex)
NGC 6819	2M19411564+4010105	1.6 ± 0.1	0.15 ± 0.01	-0.04 ± 0.03	-0.02 ± 0.02	0.02 ± 0.02	-0.01 ± 0.02	-0.07 ± 0.05
				0.11 ± 0.07	0.00 ± 0.04	0.05 ± 0.03	-0.06 ± 0.08	-0.00 ± 0.02
NGC 6819	2M19411593+4011114	5.2 ± 0.1	0.11 ± 0.01	0.02 ± 0.04	0.03 ± 0.02	0.04 ± 0.02	0.04 ± 0.03	-0.03 ± 0.05
				-0.02 ± 0.08	0.06 ± 0.04	0.07 ± 0.03	-0.07 ± 0.09	0.02 ± 0.02
NGC 6819	2M19411631+4005508	-1.0 ± 0.0	0.08 ± 0.01	-0.06 ± 0.03	-0.00 ± 0.02	0.00 ± 0.02	0.02 ± 0.02	-0.05 ± 0.05
				0.05 ± 0.07	0.05 ± 0.03	0.03 ± 0.02	0.12 ± 0.07	0.03 ± 0.01
NGC 6819	2M19411705+4010517	1.4 ± 0.1	0.07 ± 0.01	0.01 ± 0.02	-0.00 ± 0.02	0.00 ± 0.02	-0.00 ± 0.02	-0.05 ± 0.04
				-0.01 ± 0.04	-0.02 ± 0.02	0.02 ± 0.02	-0.03 ± 0.04	-0.01 ± 0.01
NGC 6819	2M19411776+4009158	-1.0 ± 0.5	0.12 ± 0.01	-0.02 ± 0.03	0.01 ± 0.02	-0.01 ± 0.02	0.03 ± 0.02	0.02 ± 0.05
				-0.05 ± 0.08	0.04 ± 0.03	0.05 ± 0.02	-0.02 ± 0.08	-0.01 ± 0.01
NGC 6819	2M19411893+4011408	1.0 ± 0.1	0.10 ± 0.01	-0.04 ± 0.03	-0.01 ± 0.02	0.02 ± 0.02	-0.04 ± 0.02	0.01 ± 0.05
				0.10 ± 0.06	0.05 ± 0.03	0.05 ± 0.02	-0.04 ± 0.07	0.03 ± 0.01
NGC 6819	2M19412136+4011002	1.9 ± 0.0	0.11 ± 0.01	-0.06 ± 0.03	-0.02 ± 0.02	0.05 ± 0.02	-0.03 ± 0.02	0.00 ± 0.06
				0.07 ± 0.07	0.05 ± 0.04	0.03 ± 0.03	0.01 ± 0.08	0.06 ± 0.02
NGC 6819	2M19412147+4013573	1.5 ± 0.0	0.13 ± 0.01	-0.03 ± 0.03	-0.01 ± 0.02	-0.01 ± 0.02	0.02 ± 0.02	0.03 ± 0.05
				0.10 ± 0.06	0.03 ± 0.03	0.02 ± 0.02	0.04 ± 0.07	-0.00 ± 0.01
NGC 6819	2M19412176+4012111	0.6 ± 0.2	0.14 ± 0.01	-0.04 ± 0.02	0.01 ± 0.02	-0.01 ± 0.02	-0.01 ± 0.02	-0.02 ± 0.04
				0.06 ± 0.06	0.02 ± 0.03	0.00 ± 0.02	0.04 ± 0.06	0.01 ± 0.01
NGC 6819	2M19412222+4016442	2.7 ± 0.1	0.12 ± 0.01	-0.05 ± 0.02	-0.01 ± 0.02	0.00 ± 0.02	-0.01 ± 0.02	-0.01 ± 0.05
				-0.05 ± 0.06	0.04 ± 0.03	-0.00 ± 0.02	0.16 ± 0.06	-0.01 ± 0.01
NGC 6819	2M19412369+4012355	3.7 ± 0.0	0.08 ± 0.01	0.01 ± 0.02	0.00 ± 0.02	0.00 ± 0.02	-0.00 ± 0.02	-0.01 ± 0.04
				-0.03 ± 0.05	0.03 ± 0.03	-0.03 ± 0.02	0.07 ± 0.05	0.03 ± 0.01
NGC 6819	2M19412658+4011418	2.2 ± 0.0	0.09 ± 0.01	0.01 ± 0.02	-0.00 ± 0.02	0.01 ± 0.02	0.00 ± 0.02	-0.01 ± 0.04
				-0.06 ± 0.05	0.03 ± 0.03	0.03 ± 0.02	0.03 ± 0.05	0.04 ± 0.01

Continued on next page

Table B.1 – Continued

Cluster	2MASS ID	RV (km s^{-1})	[Fe/H] (dex)	[O/Fe] (dex)	[Mg/Fe] (dex)	[Ca/Fe] (dex)	[Si/Fe] (dex)	[S/Fe] (dex)
				[V/Fe] (dex)	[Cr/Fe] (dex)	[Mn/Fe] (dex)	[Co/Fe] (dex)	[Ni/Fe] (dex)
NGC 6819	2M19412707+4012283	0.8 ± 0.1	0.09 ± 0.01	-0.01 ± 0.02	-0.00 ± 0.02	0.01 ± 0.02	-0.02 ± 0.02	-0.04 ± 0.05
				0.04 ± 0.06	0.06 ± 0.03	0.06 ± 0.02	0.08 ± 0.06	0.02 ± 0.01
NGC 6819	2M19412915+4013040	1.4 ± 0.0	0.11 ± 0.01	-0.00 ± 0.03	0.00 ± 0.02	0.02 ± 0.02	-0.01 ± 0.02	-0.07 ± 0.05
				0.18 ± 0.07	0.01 ± 0.03	0.06 ± 0.02	0.00 ± 0.07	0.03 ± 0.01
NGC 6819	2M19412942+4014199	3.5 ± 0.0	0.11 ± 0.01	-0.00 ± 0.03	0.02 ± 0.02	0.07 ± 0.02	-0.02 ± 0.02	-0.06 ± 0.05
				0.05 ± 0.07	0.06 ± 0.04	0.04 ± 0.03	0.18 ± 0.08	0.08 ± 0.02
NGC 6819	2M19412953+4012210	2.9 ± 0.2	0.15 ± 0.01	-0.04 ± 0.03	0.01 ± 0.02	-0.03 ± 0.02	-0.00 ± 0.02	-0.00 ± 0.05
				0.02 ± 0.06	-0.07 ± 0.03	0.02 ± 0.02	0.07 ± 0.07	-0.01 ± 0.01
NGC 6819	2M19413027+4015218	2.1 ± 0.0	0.12 ± 0.01	-0.07 ± 0.03	-0.01 ± 0.02	-0.02 ± 0.02	0.03 ± 0.02	-0.06 ± 0.05
				-0.04 ± 0.06	0.01 ± 0.03	0.02 ± 0.02	0.02 ± 0.07	-0.00 ± 0.01
NGC 6819	2M19413031+4009005	6.2 ± 0.1	0.09 ± 0.01	-0.03 ± 0.02	-0.03 ± 0.02	-0.00 ± 0.02	-0.01 ± 0.02	-0.03 ± 0.04
				0.01 ± 0.04	-0.05 ± 0.02	0.02 ± 0.02	0.04 ± 0.04	0.01 ± 0.01
NGC 6819	2M19413330+4012349	4.3 ± 0.0	0.07 ± 0.01	0.00 ± 0.03	-0.00 ± 0.02	0.02 ± 0.02	0.02 ± 0.02	-0.04 ± 0.05
				-0.00 ± 0.06	0.03 ± 0.03	0.01 ± 0.02	0.04 ± 0.06	-0.00 ± 0.01
NGC 6811	2M19365580+4627376	7.4 ± 0.1	-0.02 ± 0.01	-0.11 ± 0.04	-0.02 ± 0.02	-0.02 ± 0.02	-0.00 ± 0.03	0.08 ± 0.05
				-0.03 ± 0.08	0.03 ± 0.04	0.00 ± 0.03	-0.13 ± 0.08	-0.04 ± 0.02
NGC 6811	2M19365712+4622425	7.9 ± 0.0	-0.03 ± 0.01	-0.11 ± 0.04	-0.01 ± 0.02	0.03 ± 0.02	-0.00 ± 0.03	-0.02 ± 0.05
				0.00 ± 0.08	0.01 ± 0.04	-0.01 ± 0.03	-0.37 ± 0.08	-0.01 ± 0.02
NGC 6811	2M19370267+4623130	8.1 ± 0.0	0.01 ± 0.01	-0.10 ± 0.04	-0.02 ± 0.02	0.02 ± 0.02	-0.01 ± 0.03	0.04 ± 0.05
				-0.12 ± 0.08	-0.02 ± 0.04	0.01 ± 0.02	-0.28 ± 0.08	-0.01 ± 0.02
NGC 6811	2M19373462+4624098	7.7 ± 0.0	0.02 ± 0.01	-0.04 ± 0.03	-0.03 ± 0.02	-0.04 ± 0.02	0.02 ± 0.03	0.09 ± 0.05
				-0.04 ± 0.07	0.01 ± 0.04	-0.02 ± 0.02	-0.07 ± 0.07	-0.04 ± 0.01
Berkeley 53	2M20554232+5106153	-35.6 ± 0.0	-0.01 ± 0.01	-0.04 ± 0.03	-0.02 ± 0.02	0.00 ± 0.02	-0.01 ± 0.02	0.09 ± 0.05
				0.09 ± 0.07	-0.00 ± 0.03	-0.00 ± 0.02	-0.09 ± 0.06	-0.02 ± 0.01

Continued on next page

Table B.1 – Continued

Cluster	2MASS ID	RV (km s^{-1})	[Fe/H] (dex)	[O/Fe] (dex)	[Mg/Fe] (dex)	[Ca/Fe] (dex)	[Si/Fe] (dex)	[S/Fe] (dex)
				[V/Fe] (dex)	[Cr/Fe] (dex)	[Mn/Fe] (dex)	[Co/Fe] (dex)	[Ni/Fe] (dex)
Berkeley 53	2M20554936+5106545	-36.9 ± 0.1	0.01 ± 0.01	-0.01 ± 0.02	-0.02 ± 0.02	-0.01 ± 0.02	-0.01 ± 0.02	0.01 ± 0.05
				-0.11 ± 0.05	-0.02 ± 0.03	-0.01 ± 0.02	-0.11 ± 0.05	-0.03 ± 0.01
Berkeley 53	2M20554998+5102175	-36.1 ± 0.0	-0.00 ± 0.01	-0.00 ± 0.03	-0.01 ± 0.02	0.00 ± 0.03	-0.02 ± 0.03	-0.04 ± 0.06
				-0.04 ± 0.08	-0.06 ± 0.04	-0.01 ± 0.03	-0.51 ± 0.10	-0.01 ± 0.02
Berkeley 53	2M20555959+5100466	-36.7 ± 0.0	-0.03 ± 0.01	-0.01 ± 0.05	-0.02 ± 0.02	0.08 ± 0.04	0.06 ± 0.03	0.00 ± 0.09
				-0.01 ± 0.11	-0.08 ± 0.06	-0.06 ± 0.04	-0.82 ± 0.26	-0.02 ± 0.03
Berkeley 53	2M20561018+5102389	-36.3 ± 0.2	0.01 ± 0.01	-0.04 ± 0.03	-0.01 ± 0.02	-0.01 ± 0.02	0.03 ± 0.02	0.06 ± 0.05
				0.11 ± 0.07	0.01 ± 0.03	0.01 ± 0.02	-0.05 ± 0.07	-0.03 ± 0.01
NGC 7789	2M23554966+5639180	-56.9 ± 0.1	0.09 ± 0.01	-0.03 ± 0.02	-0.01 ± 0.02	-0.04 ± 0.02	-0.05 ± 0.02	-0.15 ± 0.05
				0.03 ± 0.05	0.01 ± 0.03	0.00 ± 0.02	-0.06 ± 0.05	-0.04 ± 0.01
NGC 7789	2M23562953+5648399	-55.4 ± 0.0	-0.01 ± 0.01	-0.05 ± 0.03	-0.03 ± 0.02	-0.03 ± 0.02	0.00 ± 0.03	0.03 ± 0.05
				0.03 ± 0.07	0.01 ± 0.04	-0.01 ± 0.02	0.08 ± 0.07	-0.02 ± 0.01
NGC 7789	2M23563930+5645242	-55.1 ± 0.1	0.04 ± 0.01	-0.06 ± 0.03	-0.03 ± 0.02	-0.01 ± 0.02	-0.03 ± 0.03	0.01 ± 0.05
				0.08 ± 0.07	0.01 ± 0.03	-0.01 ± 0.02	-0.12 ± 0.08	-0.02 ± 0.01
NGC 7789	2M23564304+5650477	-53.4 ± 0.0	0.06 ± 0.01	-0.07 ± 0.03	-0.02 ± 0.02	-0.02 ± 0.02	-0.01 ± 0.02	-0.01 ± 0.05
				0.14 ± 0.07	0.05 ± 0.03	0.00 ± 0.02	-0.03 ± 0.07	-0.00 ± 0.01
NGC 7789	2M23565053+5649208	-50.6 ± 0.0	0.01 ± 0.01	-0.05 ± 0.03	-0.04 ± 0.02	-0.00 ± 0.02	-0.01 ± 0.03	-0.01 ± 0.05
				-0.01 ± 0.07	0.00 ± 0.04	-0.03 ± 0.02	-0.14 ± 0.07	-0.03 ± 0.01
NGC 7789	2M23565751+5645272	-55.2 ± 0.0	0.06 ± 0.01	-0.04 ± 0.02	-0.01 ± 0.02	-0.00 ± 0.02	-0.02 ± 0.02	-0.04 ± 0.05
				0.00 ± 0.06	0.04 ± 0.03	-0.02 ± 0.02	-0.02 ± 0.06	-0.02 ± 0.01
NGC 7789	2M23570895+5648504	-54.7 ± 0.0	0.08 ± 0.01	-0.05 ± 0.03	-0.02 ± 0.02	-0.01 ± 0.02	-0.02 ± 0.02	-0.02 ± 0.05
				-0.02 ± 0.07	0.02 ± 0.03	-0.01 ± 0.02	-0.06 ± 0.08	-0.03 ± 0.01
NGC 7789	2M23571400+5640586	-53.9 ± 0.2	0.07 ± 0.01	-0.03 ± 0.02	-0.02 ± 0.02	-0.02 ± 0.02	-0.01 ± 0.02	0.09 ± 0.05
				-0.03 ± 0.06	0.03 ± 0.03	0.01 ± 0.02	0.00 ± 0.06	-0.03 ± 0.01

Continued on next page

Table B.1 – Continued

Cluster	2MASS ID	RV (km s^{-1})	[Fe/H] (dex)	[O/Fe] (dex)	[Mg/Fe] (dex)	[Ca/Fe] (dex)	[Si/Fe] (dex)	[S/Fe] (dex)
				[V/Fe] (dex)	[Cr/Fe] (dex)	[Mn/Fe] (dex)	[Co/Fe] (dex)	[Ni/Fe] (dex)
NGC 7789	2M23571728+5645333	-55.1 ± 0.1	0.04 ± 0.01	0.02 ± 0.04	-0.00 ± 0.02	-0.03 ± 0.02	-0.01 ± 0.03	0.06 ± 0.05
				-0.20 ± 0.08	-0.10 ± 0.04	-0.04 ± 0.03	0.05 ± 0.09	-0.05 ± 0.02
NGC 7789	2M23571847+5650271	-55.5 ± 0.1	0.01 ± 0.01	-0.03 ± 0.03	-0.01 ± 0.02	-0.04 ± 0.02	0.01 ± 0.02	0.04 ± 0.05
				-0.12 ± 0.07	0.02 ± 0.03	-0.00 ± 0.02	-0.30 ± 0.07	-0.02 ± 0.01
NGC 7789	2M23572242+5641459	-54.9 ± 0.1	0.06 ± 0.01	-0.05 ± 0.02	-0.03 ± 0.02	-0.05 ± 0.02	-0.03 ± 0.02	-0.00 ± 0.05
				-0.05 ± 0.06	0.01 ± 0.03	-0.03 ± 0.02	-0.10 ± 0.06	-0.05 ± 0.01
NGC 7789	2M23573184+5641221	-55.8 ± 0.1	0.05 ± 0.01	-0.03 ± 0.02	-0.03 ± 0.02	-0.02 ± 0.02	-0.02 ± 0.02	-0.02 ± 0.05
				-0.08 ± 0.05	0.00 ± 0.03	-0.01 ± 0.02	-0.05 ± 0.05	-0.05 ± 0.01
NGC 7789	2M23573563+5640000	-54.7 ± 0.1	0.08 ± 0.01	0.02 ± 0.03	-0.02 ± 0.02	-0.01 ± 0.02	-0.04 ± 0.03	-0.02 ± 0.05
				0.08 ± 0.08	-0.15 ± 0.04	-0.05 ± 0.02	-0.19 ± 0.08	-0.05 ± 0.02
NGC 7789	2M23575438+5647439	-53.6 ± 0.1	0.04 ± 0.01	-0.05 ± 0.03	-0.00 ± 0.02	-0.01 ± 0.02	0.00 ± 0.03	0.02 ± 0.05
				0.03 ± 0.08	0.05 ± 0.04	0.00 ± 0.02	0.02 ± 0.08	-0.01 ± 0.01
NGC 7789	2M23580015+5650125	-54.5 ± 0.1	0.02 ± 0.01	-0.00 ± 0.02	-0.02 ± 0.02	0.01 ± 0.02	-0.01 ± 0.02	-0.02 ± 0.05
				-0.09 ± 0.05	0.02 ± 0.03	-0.01 ± 0.02	-0.03 ± 0.05	-0.03 ± 0.01
NGC 7789	2M23580275+5647208	-54.4 ± 0.0	0.04 ± 0.01	-0.07 ± 0.03	-0.03 ± 0.02	-0.02 ± 0.02	-0.02 ± 0.02	-0.04 ± 0.05
				0.12 ± 0.06	0.04 ± 0.03	0.00 ± 0.02	-0.14 ± 0.07	-0.02 ± 0.01
NGC 7789	2M23581471+5651466	-56.1 ± 0.0	0.06 ± 0.01	-0.02 ± 0.02	-0.03 ± 0.02	-0.02 ± 0.02	0.00 ± 0.02	0.01 ± 0.04
				-0.10 ± 0.05	-0.01 ± 0.03	0.01 ± 0.02	-0.06 ± 0.05	-0.01 ± 0.01
FSR 0494	2M00253373+6345239	-64.2 ± 0.0	0.03 ± 0.01	-0.12 ± 0.05	-0.02 ± 0.02	-0.00 ± 0.03	-0.04 ± 0.03	0.09 ± 0.07
				0.12 ± 0.11	0.01 ± 0.06	0.03 ± 0.04	-0.18 ± 0.13	0.03 ± 0.03
FSR 0494	2M00253400+6346574	-64.3 ± 0.1	0.02 ± 0.01	-0.05 ± 0.05	-0.05 ± 0.02	0.00 ± 0.04	-0.02 ± 0.03	-0.07 ± 0.07
				0.17 ± 0.11	0.05 ± 0.06	-0.01 ± 0.04	-0.09 ± 0.13	-0.02 ± 0.03
FSR 0494	2M00253826+6344101	-63.5 ± 0.1	0.01 ± 0.01	-0.02 ± 0.05	-0.03 ± 0.02	-0.02 ± 0.03	0.02 ± 0.03	0.07 ± 0.07
				-0.05 ± 0.11	0.08 ± 0.06	-0.01 ± 0.04	0.19 ± 0.14	-0.02 ± 0.03

Continued on next page

Table B.1 – Continued

Cluster	2MASS ID	RV (km s^{-1})	[Fe/H] (dex)	[O/Fe] (dex)	[Mg/Fe] (dex)	[Ca/Fe] (dex)	[Si/Fe] (dex)	[S/Fe] (dex)
				[V/Fe] (dex)	[Cr/Fe] (dex)	[Mn/Fe] (dex)	[Co/Fe] (dex)	[Ni/Fe] (dex)
FSR 0494	2M00255011+6343565	-60.4 ± 0.1	0.01 ± 0.01	0.01 ± 0.05	-0.07 ± 0.02	-0.01 ± 0.04	-0.06 ± 0.03	-0.12 ± 0.07
				0.29 ± 0.11	0.05 ± 0.06	0.04 ± 0.04	0.42 ± 0.15	0.03 ± 0.03
FSR 0494	2M00260027+6343287	-63.9 ± 0.1	-0.02 ± 0.01	-0.05 ± 0.06	-0.02 ± 0.02	0.01 ± 0.04	0.01 ± 0.03	-0.00 ± 0.08
				0.07 ± 0.11	-0.04 ± 0.06	0.03 ± 0.04	-0.09 ± 0.14	-0.00 ± 0.03
NGC 188	2M00344509+8512058	-38.8 ± 6.8	0.07 ± 0.01	-0.01 ± 0.06	0.10 ± 0.02	-0.01 ± 0.03	0.04 ± 0.03	0.27 ± 0.07
				0.05 ± 0.12	-0.17 ± 0.06	0.04 ± 0.04	-9.99 ± 9.99	0.09 ± 0.03
NGC 188	2M00415197+8527070	-42.6 ± 0.1	0.17 ± 0.01	0.01 ± 0.02	0.03 ± 0.02	-0.03 ± 0.02	0.01 ± 0.02	-0.03 ± 0.04
				0.05 ± 0.06	0.03 ± 0.03	0.10 ± 0.02	0.14 ± 0.06	0.03 ± 0.01
NGC 188	2M00422570+8516219	-40.3 ± 0.0	0.14 ± 0.01	0.02 ± 0.02	0.04 ± 0.02	-0.03 ± 0.02	0.01 ± 0.02	0.01 ± 0.04
				0.06 ± 0.06	0.03 ± 0.03	0.11 ± 0.02	0.08 ± 0.06	0.02 ± 0.01
NGC 188	2M00444460+8532163	-42.2 ± 0.1	0.14 ± 0.01	0.02 ± 0.03	0.05 ± 0.02	-0.04 ± 0.02	-0.01 ± 0.02	-0.03 ± 0.05
				0.17 ± 0.07	0.02 ± 0.03	0.08 ± 0.02	0.04 ± 0.07	0.08 ± 0.01
NGC 188	2M00454489+8504180	-42.6 ± 0.8	0.12 ± 0.01	0.14 ± 0.04	0.05 ± 0.02	-0.00 ± 0.03	-0.03 ± 0.03	-0.03 ± 0.07
				-0.16 ± 0.09	-0.10 ± 0.05	0.02 ± 0.04	0.44 ± 0.12	0.03 ± 0.02
NGC 188	2M00463920+8523336	-41.0 ± 4.9	0.13 ± 0.01	0.02 ± 0.02	0.05 ± 0.02	-0.00 ± 0.02	0.02 ± 0.02	-0.04 ± 0.04
				-0.07 ± 0.05	0.01 ± 0.03	0.10 ± 0.02	0.11 ± 0.05	0.04 ± 0.01
NGC 188	2M00472975+8524140	-40.9 ± 0.0	0.18 ± 0.01	-0.01 ± 0.02	0.03 ± 0.02	-0.02 ± 0.02	0.00 ± 0.02	-0.01 ± 0.04
				-0.04 ± 0.06	0.02 ± 0.03	0.09 ± 0.02	0.22 ± 0.06	0.00 ± 0.01
NGC 188	2M00512176+8512377	-40.2 ± 0.1	0.13 ± 0.01	0.04 ± 0.03	0.06 ± 0.02	-0.00 ± 0.02	0.01 ± 0.02	0.02 ± 0.05
				0.00 ± 0.06	0.04 ± 0.03	0.12 ± 0.02	0.10 ± 0.06	0.05 ± 0.01
NGC 188	2M00533497+8511145	-42.1 ± 0.1	0.10 ± 0.01	0.02 ± 0.03	0.05 ± 0.02	-0.02 ± 0.02	-0.01 ± 0.02	-0.01 ± 0.05
				0.14 ± 0.06	0.03 ± 0.03	0.08 ± 0.02	0.12 ± 0.06	0.04 ± 0.01
NGC 188	2M00533572+8520583	-42.7 ± 0.1	0.16 ± 0.01	0.01 ± 0.02	0.05 ± 0.02	-0.00 ± 0.02	0.02 ± 0.02	-0.04 ± 0.04
				0.03 ± 0.06	0.01 ± 0.03	0.08 ± 0.02	0.05 ± 0.06	0.05 ± 0.01

Continued on next page

Table B.1 – Continued

Cluster	2MASS ID	RV (km s^{-1})	[Fe/H] (dex)	[O/Fe] (dex)	[Mg/Fe] (dex)	[Ca/Fe] (dex)	[Si/Fe] (dex)	[S/Fe] (dex)
				[V/Fe] (dex)	[Cr/Fe] (dex)	[Mn/Fe] (dex)	[Co/Fe] (dex)	[Ni/Fe] (dex)
NGC 188	2M00541152+8515231	-42.1 ± 0.1	0.14 ± 0.01	-0.01 ± 0.02	0.03 ± 0.02	-0.03 ± 0.02	0.04 ± 0.02	0.04 ± 0.04
				0.02 ± 0.06	-0.01 ± 0.03	0.10 ± 0.02	0.06 ± 0.06	0.01 ± 0.01
NGC 188	2M00543664+8501152	-42.4 ± 0.0	0.16 ± 0.01	-0.02 ± 0.02	0.04 ± 0.02	-0.05 ± 0.02	0.02 ± 0.02	-0.04 ± 0.04
				0.04 ± 0.06	-0.01 ± 0.03	0.05 ± 0.02	0.02 ± 0.06	0.02 ± 0.01
NGC 188	2M00571844+8510288	-42.0 ± 0.0	0.18 ± 0.01	0.03 ± 0.02	0.05 ± 0.02	-0.02 ± 0.02	0.01 ± 0.02	0.02 ± 0.04
				0.10 ± 0.06	0.01 ± 0.03	0.12 ± 0.02	0.18 ± 0.06	0.04 ± 0.01
IC 166	2M01514975+6150556	-39.8 ± 0.4	-0.05 ± 0.01	0.05 ± 0.06	0.05 ± 0.02	-0.07 ± 0.04	0.05 ± 0.03	-0.07 ± 0.08
				0.14 ± 0.11	0.07 ± 0.06	-0.00 ± 0.04	0.24 ± 0.13	-0.04 ± 0.03
IC 166	2M01515473+6148552	-39.8 ± 0.3	-0.08 ± 0.01	-0.01 ± 0.06	0.05 ± 0.02	-0.03 ± 0.04	0.10 ± 0.03	0.27 ± 0.08
				0.53 ± 0.11	-0.06 ± 0.06	0.00 ± 0.04	0.34 ± 0.13	-0.02 ± 0.03
IC 166	2M01520209+6147453	-39.8 ± 0.2	-0.01 ± 0.01	0.09 ± 0.06	0.03 ± 0.02	-0.02 ± 0.04	0.06 ± 0.03	-0.12 ± 0.08
				-0.57 ± 0.13	-0.02 ± 0.07	0.01 ± 0.05	-0.34 ± 0.21	-0.05 ± 0.03
IC 166	2M01520770+6150058	-40.0 ± 0.4	-0.09 ± 0.01	-0.02 ± 0.07	-0.06 ± 0.03	-0.01 ± 0.05	-0.05 ± 0.04	-0.20 ± 0.09
				0.21 ± 0.13	-0.04 ± 0.08	0.02 ± 0.06	-0.40 ± 0.28	0.00 ± 0.04
IC 166	2M01521347+6152558	-44.1 ± 0.7	-0.05 ± 0.01	0.00 ± 0.06	0.02 ± 0.02	-0.02 ± 0.04	0.08 ± 0.03	0.01 ± 0.09
				-0.16 ± 0.12	0.06 ± 0.07	-0.01 ± 0.05	0.03 ± 0.17	-0.01 ± 0.03
IC 166	2M01521509+6151407	-40.2 ± 0.2	-0.05 ± 0.01	0.04 ± 0.05	-0.00 ± 0.02	0.05 ± 0.03	0.09 ± 0.03	-0.00 ± 0.07
				0.05 ± 0.11	0.00 ± 0.06	0.02 ± 0.04	-0.24 ± 0.16	-0.02 ± 0.03
IC 166	2M01522060+6150364	-37.4 ± 0.1	-0.04 ± 0.01	-0.10 ± 0.06	0.05 ± 0.02	-0.02 ± 0.04	0.05 ± 0.03	0.23 ± 0.08
				-0.47 ± 0.12	-0.08 ± 0.07	-0.02 ± 0.04	-0.11 ± 0.21	-0.05 ± 0.03
IC 166	2M01522357+6154011	-40.0 ± 0.2	-0.09 ± 0.01	-0.09 ± 0.06	0.05 ± 0.02	0.06 ± 0.04	0.09 ± 0.03	-0.02 ± 0.08
				-0.21 ± 0.12	0.04 ± 0.06	0.02 ± 0.04	-2.15 ± 0.70	-0.00 ± 0.03
IC 166	2M01522953+6151427	-41.3 ± 0.1	-0.04 ± 0.01	-0.03 ± 0.04	-0.04 ± 0.02	-0.01 ± 0.03	0.00 ± 0.03	0.06 ± 0.06
				-0.08 ± 0.08	-0.01 ± 0.04	-0.06 ± 0.03	-0.03 ± 0.09	-0.03 ± 0.02

Continued on next page

Table B.1 – Continued

Cluster	2MASS ID	RV (km s^{-1})	[Fe/H] (dex)	[O/Fe] (dex)	[Mg/Fe] (dex)	[Ca/Fe] (dex)	[Si/Fe] (dex)	[S/Fe] (dex)
				[V/Fe] (dex)	[Cr/Fe] (dex)	[Mn/Fe] (dex)	[Co/Fe] (dex)	[Ni/Fe] (dex)
IC 166	2M01523324+6152050	-42.2 ± 0.1	-0.06 ± 0.01	-0.08 ± 0.06	0.02 ± 0.02	-0.05 ± 0.04	0.10 ± 0.03	0.01 ± 0.12
				-0.41 ± 0.12	0.10 ± 0.07	0.02 ± 0.05	-0.75 ± 0.36	-0.03 ± 0.03
IC 166	2M01523513+6154318	-39.3 ± 0.1	-0.08 ± 0.01	0.00 ± 0.05	0.03 ± 0.02	0.01 ± 0.03	0.11 ± 0.03	0.15 ± 0.07
				-0.20 ± 0.11	-0.02 ± 0.06	-0.04 ± 0.04	-0.13 ± 0.16	-0.00 ± 0.03
IC 166	2M01524136+6151507	-42.0 ± 0.0	-0.05 ± 0.01	0.05 ± 0.06	-0.02 ± 0.02	0.08 ± 0.04	0.03 ± 0.03	-0.11 ± 0.08
				-0.14 ± 0.12	-0.07 ± 0.06	0.03 ± 0.04	-0.88 ± 0.40	-0.02 ± 0.03
IC 166	2M01524515+6153369	-39.9 ± 0.2	-0.08 ± 0.01	-0.11 ± 0.05	0.05 ± 0.02	-0.00 ± 0.03	0.08 ± 0.03	0.29 ± 0.07
				-0.16 ± 0.11	0.07 ± 0.06	-0.01 ± 0.04	-9.99 ± 9.99	-0.05 ± 0.03
IC 166	2M01525074+6145411	-39.7 ± 0.1	-0.09 ± 0.01	0.06 ± 0.06	0.09 ± 0.02	0.02 ± 0.04	0.22 ± 0.03	0.04 ± 0.09
				-9.99 ± 9.99	0.06 ± 0.07	0.04 ± 0.05	-0.75 ± 0.32	-0.02 ± 0.04
IC 166	2M01525543+6148504	-41.7 ± 0.2	-0.07 ± 0.01	-0.17 ± 0.05	0.01 ± 0.02	-0.03 ± 0.03	0.06 ± 0.03	0.02 ± 0.07
				-0.17 ± 0.10	-0.06 ± 0.05	0.01 ± 0.04	-0.62 ± 0.23	-0.03 ± 0.03
Berkeley 66	2M03040128+5846422	-50.2 ± 0.0	-0.11 ± 0.01	0.22 ± 0.05	0.10 ± 0.03	0.04 ± 0.04	0.05 ± 0.03	0.01 ± 0.09
				0.19 ± 0.11	0.02 ± 0.07	-0.03 ± 0.05	0.35 ± 0.14	-0.12 ± 0.04
Berkeley 66	2M03040371+5844017	-49.8 ± 0.1	-0.14 ± 0.01	0.04 ± 0.05	0.07 ± 0.02	-0.03 ± 0.04	0.10 ± 0.03	-0.07 ± 0.08
				-0.26 ± 0.10	-0.01 ± 0.06	-0.06 ± 0.04	0.04 ± 0.14	-0.05 ± 0.03
Berkeley 66	2M03041010+5845484	-50.4 ± 0.0	-0.15 ± 0.01	0.05 ± 0.03	0.05 ± 0.02	0.02 ± 0.03	0.03 ± 0.03	0.06 ± 0.06
				-0.18 ± 0.07	0.09 ± 0.04	-0.05 ± 0.03	-0.03 ± 0.07	0.03 ± 0.02
Berkeley 66	2M03041368+5843387	-49.9 ± 0.1	-0.14 ± 0.01	-0.01 ± 0.05	-0.00 ± 0.02	-0.07 ± 0.04	0.04 ± 0.03	0.06 ± 0.08
				-0.34 ± 0.10	-0.05 ± 0.06	-0.04 ± 0.04	-0.42 ± 0.22	-0.02 ± 0.03
Berkeley 66	2M03042113+5845433	-50.7 ± 0.0	-0.14 ± 0.01	0.07 ± 0.02	0.08 ± 0.02	0.03 ± 0.02	0.04 ± 0.02	-0.01 ± 0.05
				-0.07 ± 0.04	0.02 ± 0.03	-0.06 ± 0.02	0.01 ± 0.04	-0.03 ± 0.01
Berkeley 66	2M03042797+5845042	-49.9 ± 0.1	-0.11 ± 0.01	-0.13 ± 0.05	0.05 ± 0.03	0.02 ± 0.04	0.04 ± 0.03	0.02 ± 0.09
				-0.21 ± 0.11	-0.02 ± 0.07	-0.09 ± 0.05	-0.02 ± 0.17	0.02 ± 0.04

Continued on next page

Table B.1 – Continued

Cluster	2MASS ID	RV (km s^{-1})	[Fe/H] (dex)	[O/Fe] (dex)	[Mg/Fe] (dex)	[Ca/Fe] (dex)	[Si/Fe] (dex)	[S/Fe] (dex)
				[V/Fe] (dex)	[Cr/Fe] (dex)	[Mn/Fe] (dex)	[Co/Fe] (dex)	[Ni/Fe] (dex)
NGC 1245	2M03140839+4716330	-29.1 ± 0.0	-0.04 ± 0.01	-0.09 ± 0.05	-0.05 ± 0.02	0.02 ± 0.03	0.03 ± 0.03	0.13 ± 0.06
				0.00 ± 0.10	0.05 ± 0.05	-0.03 ± 0.03	0.07 ± 0.14	-0.04 ± 0.02
NGC 1245	2M03141134+4709173	-29.4 ± 0.0	-0.05 ± 0.01	-0.05 ± 0.02	-0.05 ± 0.02	0.01 ± 0.02	0.00 ± 0.02	-0.06 ± 0.05
				-0.05 ± 0.06	-0.01 ± 0.03	-0.06 ± 0.02	-0.09 ± 0.06	-0.05 ± 0.01
NGC 1245	2M03141268+4717315	-29.9 ± 0.1	-0.09 ± 0.01	0.04 ± 0.04	-0.03 ± 0.02	0.02 ± 0.02	-0.00 ± 0.03	0.04 ± 0.06
				0.08 ± 0.09	0.04 ± 0.05	0.02 ± 0.03	-0.10 ± 0.10	-0.02 ± 0.02
NGC 1245	2M03142464+4711327	-29.9 ± 0.2	-0.06 ± 0.01	-0.09 ± 0.05	-0.06 ± 0.02	-0.00 ± 0.03	0.04 ± 0.03	-0.08 ± 0.06
				0.06 ± 0.10	0.06 ± 0.05	0.02 ± 0.03	0.05 ± 0.11	-0.00 ± 0.02
NGC 1245	2M03143100+4714204	-30.3 ± 0.0	-0.06 ± 0.01	-0.14 ± 0.04	-0.05 ± 0.02	-0.06 ± 0.02	0.04 ± 0.03	0.05 ± 0.06
				0.04 ± 0.09	-0.05 ± 0.05	0.00 ± 0.03	0.20 ± 0.10	-0.03 ± 0.02
NGC 1245	2M03143256+4716277	-28.2 ± 0.1	-0.07 ± 0.01	-0.11 ± 0.05	0.00 ± 0.02	-0.04 ± 0.03	0.04 ± 0.03	0.04 ± 0.06
				0.04 ± 0.10	-0.02 ± 0.05	-0.01 ± 0.03	-0.13 ± 0.10	-0.05 ± 0.02
NGC 1245	2M03143819+4720444	-29.2 ± 0.0	-0.04 ± 0.01	0.03 ± 0.04	0.00 ± 0.02	-0.02 ± 0.02	0.01 ± 0.03	0.05 ± 0.05
				0.04 ± 0.09	0.02 ± 0.04	-0.02 ± 0.03	-0.06 ± 0.09	-0.03 ± 0.02
NGC 1245	2M03143888+4718202	-28.3 ± 0.0	-0.08 ± 0.01	0.05 ± 0.05	-0.01 ± 0.02	-0.02 ± 0.03	0.04 ± 0.03	0.02 ± 0.06
				0.22 ± 0.10	0.04 ± 0.05	-0.04 ± 0.03	0.59 ± 0.12	-0.03 ± 0.02
NGC 1245	2M03143977+4714400	-26.6 ± 0.7	-0.06 ± 0.01	-0.10 ± 0.04	-0.04 ± 0.02	0.02 ± 0.02	0.02 ± 0.03	-0.04 ± 0.05
				0.03 ± 0.09	0.02 ± 0.04	0.01 ± 0.03	-0.13 ± 0.09	-0.02 ± 0.02
NGC 1245	2M03144021+4715280	-29.9 ± 0.0	-0.05 ± 0.01	0.04 ± 0.04	-0.02 ± 0.02	-0.03 ± 0.02	0.03 ± 0.03	0.09 ± 0.05
				0.04 ± 0.09	-0.04 ± 0.04	0.01 ± 0.03	0.08 ± 0.09	-0.05 ± 0.02
NGC 1245	2M03144698+4711579	-30.4 ± 0.1	-0.07 ± 0.01	-0.01 ± 0.05	-0.03 ± 0.02	-0.00 ± 0.03	0.04 ± 0.03	0.07 ± 0.06
				0.10 ± 0.10	-0.01 ± 0.05	-0.03 ± 0.03	-0.07 ± 0.10	-0.06 ± 0.02
NGC 1245	2M03145265+4719245	-29.1 ± 0.1	-0.10 ± 0.01	-0.03 ± 0.04	-0.02 ± 0.02	0.01 ± 0.03	0.07 ± 0.03	-0.14 ± 0.06
				0.15 ± 0.10	0.03 ± 0.05	-0.01 ± 0.03	-0.21 ± 0.15	-0.05 ± 0.02

Continued on next page

Table B.1 – Continued

Cluster	2MASS ID	RV (km s^{-1})	[Fe/H] (dex)	[O/Fe] (dex)	[Mg/Fe] (dex)	[Ca/Fe] (dex)	[Si/Fe] (dex)	[S/Fe] (dex)
				[V/Fe] (dex)	[Cr/Fe] (dex)	[Mn/Fe] (dex)	[Co/Fe] (dex)	[Ni/Fe] (dex)
NGC 1245	2M03145273+4714033	-29.5 ± 0.1	-0.06 ± 0.01	0.03 ± 0.04	-0.03 ± 0.02	-0.02 ± 0.02	0.01 ± 0.03	-0.09 ± 0.06
				0.03 ± 0.09	-0.04 ± 0.04	0.02 ± 0.03	-0.45 ± 0.13	-0.02 ± 0.02
NGC 1245	2M03145518+4712146	-30.2 ± 0.1	-0.03 ± 0.01	-0.04 ± 0.04	-0.00 ± 0.02	-0.03 ± 0.02	0.05 ± 0.03	0.04 ± 0.05
				0.06 ± 0.09	0.01 ± 0.04	-0.02 ± 0.03	-0.12 ± 0.09	-0.05 ± 0.02
NGC 1245	2M03145841+4708245	-29.4 ± 0.0	-0.10 ± 0.01	-0.10 ± 0.05	-0.04 ± 0.02	-0.02 ± 0.03	0.01 ± 0.03	-0.01 ± 0.06
				-0.07 ± 0.10	0.01 ± 0.05	-0.00 ± 0.03	0.05 ± 0.13	-0.05 ± 0.02
NGC 1245	2M03145950+4721138	-29.3 ± 0.1	-0.00 ± 0.01	-0.03 ± 0.04	-0.01 ± 0.02	-0.04 ± 0.02	0.01 ± 0.03	-0.08 ± 0.06
				0.03 ± 0.09	0.03 ± 0.04	-0.00 ± 0.03	-2.27 ± 0.24	-0.04 ± 0.02
NGC 1245	2M03150241+4719582	-28.9 ± 0.1	-0.07 ± 0.01	-0.16 ± 0.05	-0.06 ± 0.02	0.07 ± 0.03	-0.01 ± 0.03	-0.05 ± 0.06
				-0.03 ± 0.10	-0.01 ± 0.05	-0.02 ± 0.03	-0.12 ± 0.16	-0.07 ± 0.02
NGC 1245	2M03150510+4714411	-30.3 ± 0.0	-0.04 ± 0.01	0.07 ± 0.05	-0.00 ± 0.02	-0.00 ± 0.03	0.02 ± 0.03	0.04 ± 0.06
				-0.01 ± 0.10	-0.02 ± 0.05	-0.02 ± 0.03	-0.16 ± 0.14	-0.03 ± 0.02
NGC 1245	2M03150614+4716352	-29.1 ± 0.1	-0.06 ± 0.01	-0.12 ± 0.04	-0.04 ± 0.02	-0.01 ± 0.02	0.03 ± 0.03	-0.05 ± 0.06
				-0.00 ± 0.09	0.05 ± 0.05	0.02 ± 0.03	-0.55 ± 0.16	-0.03 ± 0.02
NGC 1245	2M03151244+4708556	-28.5 ± 0.1	-0.07 ± 0.01	-0.03 ± 0.04	-0.04 ± 0.02	0.02 ± 0.03	0.02 ± 0.03	0.09 ± 0.06
				0.08 ± 0.10	-0.02 ± 0.05	0.01 ± 0.03	-0.22 ± 0.12	-0.03 ± 0.02
NGC 1245	2M03151253+4717291	-29.3 ± 0.1	-0.06 ± 0.01	0.11 ± 0.04	0.00 ± 0.02	0.03 ± 0.02	0.04 ± 0.03	-0.01 ± 0.06
				0.06 ± 0.09	0.02 ± 0.04	-0.02 ± 0.03	0.01 ± 0.09	-0.06 ± 0.02
NGC 1245	2M03151881+4712051	-28.4 ± 0.1	-0.06 ± 0.01	-0.03 ± 0.04	-0.03 ± 0.02	0.02 ± 0.02	-0.01 ± 0.03	-0.03 ± 0.06
				0.01 ± 0.09	0.01 ± 0.04	0.00 ± 0.03	-0.03 ± 0.10	-0.05 ± 0.02
NGC 1245	2M03151975+4713477	-29.4 ± 0.1	-0.06 ± 0.01	0.00 ± 0.04	0.00 ± 0.02	0.01 ± 0.02	0.04 ± 0.03	-0.00 ± 0.05
				0.11 ± 0.09	0.03 ± 0.04	-0.03 ± 0.03	-0.25 ± 0.11	-0.04 ± 0.02
King 7	2M03590443+5148003	-10.8 ± 0.1	-0.06 ± 0.01	-0.04 ± 0.03	-0.02 ± 0.02	-0.01 ± 0.02	0.04 ± 0.03	0.07 ± 0.05
				-0.11 ± 0.07	0.04 ± 0.04	0.04 ± 0.02	-0.05 ± 0.07	-0.05 ± 0.01

Continued on next page

Table B.1 – Continued

Cluster	2MASS ID	RV (km s^{-1})	[Fe/H] (dex)	[O/Fe] (dex)	[Mg/Fe] (dex)	[Ca/Fe] (dex)	[Si/Fe] (dex)	[S/Fe] (dex)
				[V/Fe] (dex)	[Cr/Fe] (dex)	[Mn/Fe] (dex)	[Co/Fe] (dex)	[Ni/Fe] (dex)
King 7	2M03590818+5145215	-15.4 ± 2.5	-0.03 ± 0.01	-0.03 ± 0.02	-0.02 ± 0.02	-0.01 ± 0.02	-0.01 ± 0.02	0.01 ± 0.05
				-0.11 ± 0.05	0.03 ± 0.03	0.01 ± 0.02	-0.06 ± 0.05	-0.08 ± 0.01
King 7	2M03591013+5145193	-10.5 ± 0.0	-0.06 ± 0.01	-0.01 ± 0.03	0.01 ± 0.02	0.02 ± 0.02	0.04 ± 0.02	0.18 ± 0.05
				-0.08 ± 0.07	0.03 ± 0.03	0.00 ± 0.02	-0.08 ± 0.07	-0.04 ± 0.01
King 7	2M03592828+5148425	-10.9 ± 0.1	-0.06 ± 0.01	0.00 ± 0.03	0.00 ± 0.02	0.02 ± 0.02	0.07 ± 0.03	0.14 ± 0.05
				0.05 ± 0.07	0.01 ± 0.04	0.07 ± 0.02	0.03 ± 0.07	-0.04 ± 0.01
NGC 1798	2M05112446+4740027	3.4 ± 0.0	-0.16 ± 0.01	-0.01 ± 0.02	-0.02 ± 0.02	-0.02 ± 0.02	-0.00 ± 0.02	0.07 ± 0.05
				-0.07 ± 0.06	0.01 ± 0.03	-0.07 ± 0.02	-0.07 ± 0.05	-0.03 ± 0.01
NGC 1798	2M05113450+4741177	-2.3 ± 1.5	-0.19 ± 0.01	-0.13 ± 0.06	-0.03 ± 0.02	0.06 ± 0.04	0.07 ± 0.03	0.08 ± 0.08
				-0.24 ± 0.12	-0.07 ± 0.06	-0.05 ± 0.04	-0.45 ± 0.27	-0.03 ± 0.03
NGC 1798	2M05113666+4741482	2.9 ± 0.1	-0.17 ± 0.01	0.01 ± 0.03	-0.02 ± 0.02	0.03 ± 0.02	0.02 ± 0.03	-0.02 ± 0.06
				-0.11 ± 0.07	0.04 ± 0.04	-0.05 ± 0.03	-0.01 ± 0.07	-0.01 ± 0.02
NGC 1798	2M05113768+4742329	3.2 ± 0.1	-0.20 ± 0.01	-0.05 ± 0.04	-0.02 ± 0.02	0.02 ± 0.03	0.02 ± 0.03	-0.10 ± 0.06
				0.11 ± 0.08	-0.00 ± 0.05	-0.07 ± 0.03	-0.38 ± 0.12	-0.03 ± 0.02
NGC 1798	2M05114006+4739238	2.4 ± 0.0	-0.17 ± 0.01	0.01 ± 0.03	0.01 ± 0.02	0.02 ± 0.02	0.01 ± 0.03	-0.02 ± 0.06
				0.12 ± 0.08	0.05 ± 0.04	-0.06 ± 0.03	-0.09 ± 0.07	-0.03 ± 0.02
NGC 1798	2M05114134+4740406	0.8 ± 0.1	-0.17 ± 0.01	0.07 ± 0.05	-0.00 ± 0.02	0.03 ± 0.03	-0.01 ± 0.03	0.02 ± 0.07
				-0.08 ± 0.09	-0.03 ± 0.06	-0.09 ± 0.04	0.13 ± 0.10	-0.03 ± 0.03
NGC 1798	2M05114422+4741517	3.3 ± 0.1	-0.16 ± 0.01	0.09 ± 0.06	-0.01 ± 0.02	0.04 ± 0.04	0.01 ± 0.04	-0.00 ± 0.08
				-0.09 ± 0.12	-0.02 ± 0.07	-0.10 ± 0.05	-0.67 ± 0.32	-0.05 ± 0.03
NGC 1798	2M05114626+4743422	1.9 ± 0.0	-0.17 ± 0.01	-0.01 ± 0.04	0.01 ± 0.02	0.03 ± 0.03	-0.01 ± 0.03	0.01 ± 0.07
				0.10 ± 0.08	-0.01 ± 0.05	-0.08 ± 0.03	-0.08 ± 0.08	-0.01 ± 0.02
NGC 1798	2M05114795+4740258	1.9 ± 0.0	-0.21 ± 0.01	0.07 ± 0.02	0.00 ± 0.02	0.02 ± 0.02	0.02 ± 0.02	0.03 ± 0.05
				-0.03 ± 0.04	-0.01 ± 0.03	-0.04 ± 0.02	0.02 ± 0.04	-0.01 ± 0.01

Continued on next page

Table B.1 – Continued

Cluster	2MASS ID	RV (km s^{-1})	[Fe/H] (dex)	[O/Fe] (dex)	[Mg/Fe] (dex)	[Ca/Fe] (dex)	[Si/Fe] (dex)	[S/Fe] (dex)
				[V/Fe] (dex)	[Cr/Fe] (dex)	[Mn/Fe] (dex)	[Co/Fe] (dex)	[Ni/Fe] (dex)
Berkeley 17	2M05202118+3035544	-73.6 ± 0.1	-0.10 ± 0.01	-0.00 ± 0.03	0.05 ± 0.02	-0.00 ± 0.02	0.02 ± 0.03	0.04 ± 0.05
				0.11 ± 0.07	0.03 ± 0.04	0.02 ± 0.02	-0.04 ± 0.07	0.04 ± 0.02
Berkeley 17	2M05202905+3032414	-73.5 ± 0.1	-0.13 ± 0.01	0.03 ± 0.04	0.07 ± 0.02	0.07 ± 0.03	0.00 ± 0.03	0.13 ± 0.07
				0.13 ± 0.09	0.04 ± 0.05	0.03 ± 0.04	0.12 ± 0.10	0.04 ± 0.03
Berkeley 17	2M05203121+3035067	-73.2 ± 0.1	-0.12 ± 0.01	0.06 ± 0.03	0.08 ± 0.02	0.03 ± 0.02	0.03 ± 0.03	0.09 ± 0.05
				-0.06 ± 0.07	0.06 ± 0.04	-0.01 ± 0.03	0.10 ± 0.07	0.05 ± 0.02
Berkeley 17	2M05203650+3030351	-74.2 ± 0.1	-0.06 ± 0.01	0.04 ± 0.02	0.05 ± 0.02	-0.01 ± 0.02	0.01 ± 0.02	0.03 ± 0.05
				-0.06 ± 0.05	0.02 ± 0.03	-0.05 ± 0.02	0.07 ± 0.05	0.02 ± 0.01
Berkeley 17	2M05203799+3034414	-73.1 ± 0.2	-0.08 ± 0.01	0.04 ± 0.02	0.05 ± 0.02	-0.02 ± 0.02	-0.01 ± 0.02	0.04 ± 0.05
				-0.00 ± 0.05	0.02 ± 0.03	-0.05 ± 0.02	0.04 ± 0.05	0.02 ± 0.01
Berkeley 17	2M05204143+3036042	-73.1 ± 0.1	-0.14 ± 0.01	0.06 ± 0.03	0.09 ± 0.02	0.03 ± 0.02	0.03 ± 0.03	0.08 ± 0.05
				0.01 ± 0.08	-0.00 ± 0.04	-0.02 ± 0.03	0.09 ± 0.07	0.05 ± 0.02
Berkeley 17	2M05204488+3038020	-73.1 ± 0.1	-0.13 ± 0.01	0.01 ± 0.03	0.07 ± 0.02	0.00 ± 0.02	0.02 ± 0.03	0.01 ± 0.05
				0.03 ± 0.07	0.01 ± 0.04	-0.01 ± 0.02	0.02 ± 0.07	0.02 ± 0.02
Berkeley 71	2M05404312+3217303	-10.0 ± 0.2	-0.21 ± 0.01	0.03 ± 0.06	-0.00 ± 0.02	0.03 ± 0.03	0.02 ± 0.03	0.05 ± 0.07
				0.11 ± 0.11	0.02 ± 0.06	-0.04 ± 0.04	-0.55 ± 0.24	-0.01 ± 0.02
Berkeley 71	2M05405311+3215557	-9.2 ± 0.1	-0.25 ± 0.01	-0.07 ± 0.05	0.03 ± 0.02	0.02 ± 0.03	0.09 ± 0.03	0.18 ± 0.06
				0.14 ± 0.10	0.02 ± 0.05	-0.04 ± 0.03	-0.37 ± 0.13	-0.05 ± 0.02
Berkeley 71	2M05405316+3215197	-9.4 ± 0.1	-0.23 ± 0.01	-0.05 ± 0.04	0.03 ± 0.02	-0.02 ± 0.02	0.08 ± 0.03	0.28 ± 0.05
				-0.00 ± 0.09	-0.01 ± 0.04	0.00 ± 0.03	-0.10 ± 0.09	-0.01 ± 0.02
Berkeley 71	2M05405442+3217298	-10.1 ± 0.1	-0.17 ± 0.01	0.10 ± 0.06	0.00 ± 0.02	0.04 ± 0.03	0.08 ± 0.03	0.04 ± 0.07
				-0.08 ± 0.11	-0.03 ± 0.06	-0.04 ± 0.04	0.22 ± 0.12	-0.05 ± 0.03
Berkeley 71	2M05405484+3215567	-9.3 ± 0.1	-0.17 ± 0.01	0.14 ± 0.06	0.14 ± 0.02	0.06 ± 0.03	0.06 ± 0.03	0.17 ± 0.07
				0.08 ± 0.11	-0.08 ± 0.06	-0.08 ± 0.04	-0.11 ± 0.14	-0.01 ± 0.02

Continued on next page

Table B.1 – Continued

Cluster	2MASS ID	RV (km s^{-1})	[Fe/H] (dex)	[O/Fe] (dex)	[Mg/Fe] (dex)	[Ca/Fe] (dex)	[Si/Fe] (dex)	[S/Fe] (dex)
				[V/Fe] (dex)	[Cr/Fe] (dex)	[Mn/Fe] (dex)	[Co/Fe] (dex)	[Ni/Fe] (dex)
Berkeley 71	2M05405503+3214099	-9.9 ± 0.1	-0.20 ± 0.01	0.12 ± 0.06	-0.00 ± 0.02	0.02 ± 0.03	0.04 ± 0.03	0.13 ± 0.07
				0.14 ± 0.12	0.15 ± 0.06	-0.01 ± 0.04	0.01 ± 0.14	0.01 ± 0.03
Berkeley 71	2M05405956+3215182	-3.3 ± 0.4	-0.16 ± 0.01	-0.11 ± 0.06	-0.00 ± 0.02	0.04 ± 0.04	0.04 ± 0.03	0.07 ± 0.07
				-0.14 ± 0.12	-0.01 ± 0.06	-0.03 ± 0.04	-0.09 ± 0.13	-0.06 ± 0.03
Teutsch 51	2M05534332+2649595	17.5 ± 0.1	-0.28 ± 0.01	0.12 ± 0.09	0.01 ± 0.03	0.07 ± 0.05	0.08 ± 0.04	-0.02 ± 0.10
				-0.11 ± 0.14	-0.04 ± 0.09	-0.02 ± 0.06	0.42 ± 0.21	0.02 ± 0.04
Teutsch 51	2M05534659+2651366	14.4 ± 0.1	-0.25 ± 0.01	0.05 ± 0.07	0.01 ± 0.03	0.04 ± 0.05	-0.03 ± 0.04	-0.01 ± 0.09
				0.01 ± 0.13	0.06 ± 0.08	0.01 ± 0.05	-0.04 ± 0.16	-0.02 ± 0.04
Teutsch 51	2M05534689+2648234	17.1 ± 0.0	-0.25 ± 0.01	0.04 ± 0.08	-0.00 ± 0.03	0.04 ± 0.05	0.04 ± 0.04	-0.08 ± 0.09
				0.14 ± 0.14	0.13 ± 0.08	-0.04 ± 0.06	0.18 ± 0.16	-0.01 ± 0.04
Teutsch 51	2M05535631+2648351	17.8 ± 0.2	-0.32 ± 0.01	0.05 ± 0.07	0.04 ± 0.03	0.01 ± 0.04	0.14 ± 0.04	0.26 ± 0.09
				0.08 ± 0.13	0.04 ± 0.08	-0.12 ± 0.05	-0.19 ± 0.26	-0.01 ± 0.04
Teutsch 51	2M05535767+2649296	18.2 ± 0.1	-0.32 ± 0.01	0.15 ± 0.06	0.00 ± 0.03	-0.01 ± 0.05	0.09 ± 0.04	-0.12 ± 0.09
				-0.12 ± 0.12	0.06 ± 0.08	0.00 ± 0.05	0.10 ± 0.14	-0.02 ± 0.04
King 5	2M03140915+5237511	-42.6 ± 0.1	-0.12 ± 0.01	-0.01 ± 0.05	-0.00 ± 0.02	-0.03 ± 0.03	0.07 ± 0.03	0.09 ± 0.06
				0.12 ± 0.10	0.09 ± 0.05	0.01 ± 0.03	-0.09 ± 0.10	0.00 ± 0.02
King 5	2M03142548+5247355	-43.5 ± 0.1	-0.07 ± 0.01	-0.00 ± 0.02	-0.02 ± 0.02	-0.02 ± 0.02	0.01 ± 0.02	-0.01 ± 0.05
				-0.18 ± 0.05	0.02 ± 0.03	-0.02 ± 0.02	-0.07 ± 0.05	-0.01 ± 0.01
King 5	2M03142784+5242408	-45.0 ± 0.1	-0.12 ± 0.01	-0.00 ± 0.04	-0.01 ± 0.02	0.04 ± 0.02	0.07 ± 0.03	0.05 ± 0.05
				-0.03 ± 0.08	-0.00 ± 0.04	-0.00 ± 0.03	-0.02 ± 0.08	-0.02 ± 0.02
King 5	2M03144335+5242143	-47.0 ± 1.8	-0.10 ± 0.01	0.02 ± 0.04	-0.02 ± 0.02	0.01 ± 0.02	0.03 ± 0.03	0.08 ± 0.05
				0.10 ± 0.08	0.06 ± 0.04	-0.02 ± 0.03	0.23 ± 0.08	-0.01 ± 0.02
King 5	2M03154012+5242565	-43.6 ± 0.2	-0.13 ± 0.01	0.01 ± 0.05	-0.04 ± 0.02	-0.00 ± 0.03	-0.00 ± 0.03	0.12 ± 0.08
				-0.08 ± 0.10	0.03 ± 0.05	-0.11 ± 0.03	-0.07 ± 0.10	-0.02 ± 0.02

Continued on next page

Table B.1 – Continued

Cluster	2MASS ID	RV (km s^{-1})	[Fe/H] (dex)	[O/Fe] (dex)	[Mg/Fe] (dex)	[Ca/Fe] (dex)	[Si/Fe] (dex)	[S/Fe] (dex)
				[V/Fe] (dex)	[Cr/Fe] (dex)	[Mn/Fe] (dex)	[Co/Fe] (dex)	[Ni/Fe] (dex)
NGC 2158	2M06070155+2401470	27.9 ± 0.1	-0.16 ± 0.01	0.10 ± 0.05	0.03 ± 0.02	-0.03 ± 0.04	0.04 ± 0.03	0.12 ± 0.08
				-0.15 ± 0.10	0.02 ± 0.06	-0.07 ± 0.04	0.08 ± 0.12	0.00 ± 0.03
NGC 2158	2M06070415+2409180	26.0 ± 0.1	-0.12 ± 0.01	0.13 ± 0.06	0.03 ± 0.03	-0.01 ± 0.04	0.07 ± 0.03	-0.09 ± 0.10
				-0.13 ± 0.11	0.11 ± 0.07	-0.04 ± 0.05	-0.36 ± 0.15	0.03 ± 0.04
NGC 2158	2M06071494+2407517	26.8 ± 0.1	-0.15 ± 0.01	0.01 ± 0.03	0.02 ± 0.02	-0.03 ± 0.02	0.00 ± 0.03	0.22 ± 0.05
				-0.04 ± 0.06	-0.02 ± 0.04	-0.07 ± 0.03	-0.07 ± 0.06	0.00 ± 0.02
NGC 2158	2M06071696+2402007	25.6 ± 0.1	-0.13 ± 0.01	-0.05 ± 0.05	0.04 ± 0.02	0.00 ± 0.04	0.04 ± 0.03	0.19 ± 0.08
				-0.38 ± 0.11	0.01 ± 0.06	-0.05 ± 0.04	-0.33 ± 0.12	0.01 ± 0.03
NGC 2158	2M06071764+2410276	25.8 ± 0.1	-0.22 ± 0.01	0.02 ± 0.05	0.03 ± 0.02	-0.00 ± 0.04	0.03 ± 0.03	0.26 ± 0.07
				-0.11 ± 0.11	-0.06 ± 0.06	-0.03 ± 0.04	-0.51 ± 0.14	-0.05 ± 0.03
NGC 2158	2M06071787+2405542	29.1 ± 0.0	-0.09 ± 0.01	0.02 ± 0.02	0.00 ± 0.02	-0.00 ± 0.02	-0.01 ± 0.02	0.07 ± 0.05
				-0.10 ± 0.06	-0.01 ± 0.03	-0.10 ± 0.02	-0.01 ± 0.05	-0.03 ± 0.01
NGC 2158	2M06071913+2400148	28.5 ± 0.2	-0.16 ± 0.01	0.16 ± 0.06	0.02 ± 0.02	-0.05 ± 0.04	0.01 ± 0.03	0.11 ± 0.08
				0.06 ± 0.11	-0.05 ± 0.07	-0.09 ± 0.05	0.09 ± 0.13	0.01 ± 0.03
NGC 2158	2M06072041+2407463	28.6 ± 0.2	-0.18 ± 0.01	0.05 ± 0.05	0.05 ± 0.03	-0.05 ± 0.04	0.01 ± 0.03	-0.02 ± 0.09
				-0.11 ± 0.11	0.13 ± 0.07	-0.02 ± 0.05	0.02 ± 0.13	-0.00 ± 0.03
NGC 2158	2M06072443+2400524	28.5 ± 0.1	-0.16 ± 0.01	-0.06 ± 0.05	0.01 ± 0.02	-0.03 ± 0.04	0.01 ± 0.03	0.04 ± 0.09
				-0.19 ± 0.10	-0.04 ± 0.06	-0.06 ± 0.04	-0.23 ± 0.12	0.00 ± 0.03
NGC 2158	2M06072624+2409568	25.1 ± 0.0	-0.17 ± 0.01	-0.06 ± 0.05	0.04 ± 0.02	-0.01 ± 0.04	-0.00 ± 0.03	0.19 ± 0.08
				0.08 ± 0.11	0.09 ± 0.06	-0.01 ± 0.04	-0.27 ± 0.12	0.04 ± 0.03
NGC 2158	2M06072907+2402151	27.9 ± 0.1	-0.12 ± 0.01	0.01 ± 0.05	0.04 ± 0.02	0.04 ± 0.03	0.04 ± 0.03	0.08 ± 0.07
				-0.19 ± 0.10	-0.11 ± 0.05	-0.04 ± 0.04	-0.11 ± 0.11	-0.03 ± 0.03
NGC 2158	2M06072918+2408185	29.2 ± 0.1	-0.15 ± 0.01	-0.05 ± 0.05	0.02 ± 0.02	0.04 ± 0.03	0.00 ± 0.03	0.02 ± 0.07
				-0.18 ± 0.10	-0.26 ± 0.05	-0.01 ± 0.04	0.12 ± 0.11	-0.04 ± 0.02

Continued on next page

Table B.1 – Continued

Cluster	2MASS ID	RV (km s^{-1})	[Fe/H] (dex)	[O/Fe] (dex)	[Mg/Fe] (dex)	[Ca/Fe] (dex)	[Si/Fe] (dex)	[S/Fe] (dex)
				[V/Fe] (dex)	[Cr/Fe] (dex)	[Mn/Fe] (dex)	[Co/Fe] (dex)	[Ni/Fe] (dex)
NGC 2158	2M06073636+2405001	29.1 ± 0.1	-0.13 ± 0.01	0.01 ± 0.05	0.05 ± 0.02	0.06 ± 0.03	0.04 ± 0.03	0.13 ± 0.08
				-0.31 ± 0.10	-0.13 ± 0.06	-0.01 ± 0.04	-0.06 ± 0.11	-0.01 ± 0.03
NGC 2158	2M06073917+2409098	29.5 ± 0.1	-0.11 ± 0.01	-0.06 ± 0.05	0.03 ± 0.02	-0.00 ± 0.04	0.06 ± 0.03	0.03 ± 0.08
				-0.02 ± 0.10	-0.12 ± 0.06	-0.05 ± 0.04	0.13 ± 0.12	-0.04 ± 0.03
NGC 2158	2M06073998+2403546	29.0 ± 0.0	-0.17 ± 0.01	0.01 ± 0.05	0.06 ± 0.02	0.01 ± 0.03	0.05 ± 0.03	0.10 ± 0.08
				-0.32 ± 0.10	-0.27 ± 0.06	-0.06 ± 0.04	0.22 ± 0.11	-0.05 ± 0.03
NGC 2158	2M06074162+2405540	26.6 ± 0.1	-0.14 ± 0.01	-0.13 ± 0.05	0.04 ± 0.02	-0.02 ± 0.03	0.03 ± 0.03	0.14 ± 0.08
				-0.05 ± 0.10	-0.15 ± 0.06	-0.05 ± 0.04	-0.08 ± 0.11	-0.02 ± 0.03
NGC 2158	2M06074272+2402514	25.0 ± 0.1	-0.19 ± 0.01	0.03 ± 0.05	0.05 ± 0.02	0.06 ± 0.03	0.02 ± 0.03	0.17 ± 0.09
				-0.38 ± 0.11	-0.24 ± 0.06	-0.04 ± 0.04	0.33 ± 0.11	-0.05 ± 0.03
NGC 2158	2M06075243+2403561	25.9 ± 0.1	-0.15 ± 0.01	-0.08 ± 0.05	0.06 ± 0.02	0.02 ± 0.03	0.01 ± 0.03	0.11 ± 0.08
				-0.13 ± 0.10	-0.21 ± 0.05	-0.02 ± 0.04	-0.28 ± 0.11	-0.02 ± 0.02
NGC 2420	2M07380545+2136507	73.3 ± 0.5	-0.14 ± 0.01	0.01 ± 0.03	0.03 ± 0.02	0.02 ± 0.02	-0.04 ± 0.03	-0.02 ± 0.05
				0.01 ± 0.08	0.09 ± 0.04	-0.05 ± 0.03	-0.36 ± 0.08	-0.03 ± 0.02
NGC 2420	2M07380599+2133071	75.1 ± 0.2	-0.13 ± 0.01	0.12 ± 0.05	-0.08 ± 0.02	0.09 ± 0.02	0.00 ± 0.03	-0.00 ± 0.05
				-0.16 ± 0.09	0.04 ± 0.04	-0.05 ± 0.03	-0.60 ± 0.19	0.00 ± 0.02
NGC 2420	2M07380627+2136542	73.8 ± 0.1	-0.14 ± 0.01	0.02 ± 0.03	0.00 ± 0.02	0.01 ± 0.02	-0.00 ± 0.03	0.01 ± 0.05
				0.04 ± 0.07	-0.06 ± 0.04	-0.07 ± 0.02	-0.22 ± 0.07	-0.00 ± 0.02
NGC 2420	2M07381507+2134589	74.3 ± 0.1	-0.14 ± 0.01	-0.00 ± 0.02	-0.02 ± 0.02	-0.02 ± 0.02	0.00 ± 0.02	0.04 ± 0.05
				-0.20 ± 0.05	-0.01 ± 0.03	-0.08 ± 0.02	-0.04 ± 0.04	-0.03 ± 0.01
NGC 2420	2M07381549+2138015	74.6 ± 0.1	-0.14 ± 0.01	-0.00 ± 0.03	-0.00 ± 0.02	0.03 ± 0.02	0.02 ± 0.03	0.04 ± 0.05
				-0.02 ± 0.08	-0.11 ± 0.04	-0.06 ± 0.03	-0.04 ± 0.07	-0.02 ± 0.02
NGC 2420	2M07381972+2136522	74.6 ± 0.1	-0.12 ± 0.01	0.18 ± 0.05	0.01 ± 0.02	0.07 ± 0.02	0.00 ± 0.03	-0.07 ± 0.05
				-0.15 ± 0.10	-0.04 ± 0.04	-0.00 ± 0.03	-0.36 ± 0.15	-0.03 ± 0.02

Continued on next page

Table B.1 – Continued

Cluster	2MASS ID	RV (km s^{-1})	[Fe/H] (dex)	[O/Fe] (dex)	[Mg/Fe] (dex)	[Ca/Fe] (dex)	[Si/Fe] (dex)	[S/Fe] (dex)
				[V/Fe] (dex)	[Cr/Fe] (dex)	[Mn/Fe] (dex)	[Co/Fe] (dex)	[Ni/Fe] (dex)
NGC 2420	2M07382114+2131418	74.3 ± 0.0	-0.09 ± 0.01	0.08 ± 0.04	0.02 ± 0.02	0.03 ± 0.02	0.05 ± 0.03	0.06 ± 0.06
				-0.24 ± 0.09	-0.27 ± 0.04	-0.04 ± 0.03	-0.49 ± 0.09	-0.02 ± 0.02
NGC 2420	2M07382148+2135050	74.3 ± 0.0	-0.10 ± 0.01	0.07 ± 0.03	-0.00 ± 0.02	0.05 ± 0.02	0.01 ± 0.03	0.07 ± 0.05
				0.02 ± 0.08	-0.08 ± 0.04	-0.02 ± 0.03	-0.12 ± 0.07	-0.01 ± 0.02
NGC 2420	2M07382195+2135508	73.5 ± 0.2	-0.09 ± 0.01	-0.03 ± 0.03	0.02 ± 0.02	0.02 ± 0.02	0.01 ± 0.03	0.01 ± 0.05
				-0.03 ± 0.08	0.03 ± 0.04	-0.04 ± 0.02	-0.22 ± 0.07	-0.03 ± 0.02
NGC 2420	2M07382327+2132569	73.5 ± 0.2	-0.16 ± 0.01	0.14 ± 0.05	-0.01 ± 0.02	0.06 ± 0.03	0.03 ± 0.03	-0.02 ± 0.06
				-0.10 ± 0.11	-0.14 ± 0.05	-0.06 ± 0.04	-0.23 ± 0.17	-0.03 ± 0.02
NGC 2420	2M07382501+2133283	74.4 ± 0.2	-0.12 ± 0.01	0.07 ± 0.06	0.02 ± 0.02	0.05 ± 0.03	0.01 ± 0.03	-0.10 ± 0.07
				-0.41 ± 0.12	0.01 ± 0.06	-0.02 ± 0.04	0.20 ± 0.13	-0.06 ± 0.03
NGC 2420	2M07382670+2128514	74.5 ± 0.1	-0.07 ± 0.01	0.06 ± 0.04	0.00 ± 0.02	0.01 ± 0.02	0.01 ± 0.03	-0.11 ± 0.06
				-0.22 ± 0.08	-0.19 ± 0.04	-0.05 ± 0.03	-0.16 ± 0.08	-0.02 ± 0.02
NGC 2420	2M07382696+2138244	73.9 ± 0.1	-0.11 ± 0.01	0.03 ± 0.03	-0.01 ± 0.02	0.02 ± 0.02	0.00 ± 0.03	0.08 ± 0.05
				-0.04 ± 0.07	0.02 ± 0.04	-0.04 ± 0.02	0.03 ± 0.07	-0.00 ± 0.02
NGC 2420	2M07382984+2134509	75.1 ± 0.2	-0.13 ± 0.01	0.00 ± 0.03	0.02 ± 0.02	0.04 ± 0.02	-0.02 ± 0.03	-0.04 ± 0.05
				-0.00 ± 0.07	-0.00 ± 0.04	-0.05 ± 0.02	-0.17 ± 0.07	-0.03 ± 0.02
NGC 2420	2M07383760+2134119	73.9 ± 0.0	-0.15 ± 0.01	-0.01 ± 0.04	0.05 ± 0.02	0.02 ± 0.02	0.02 ± 0.03	-0.02 ± 0.05
				0.09 ± 0.08	0.08 ± 0.04	-0.02 ± 0.03	0.01 ± 0.07	-0.02 ± 0.02
NGC 2682	2M08492491+1144057	35.1 ± 1.5	0.11 ± 0.01	-0.05 ± 0.03	0.02 ± 0.02	-0.02 ± 0.02	-0.07 ± 0.02	-0.04 ± 0.05
				-0.09 ± 0.07	-0.03 ± 0.03	0.01 ± 0.02	0.03 ± 0.07	0.04 ± 0.01
NGC 2682	2M08501230+1151246	32.7 ± 0.0	0.02 ± 0.01	0.04 ± 0.02	-0.04 ± 0.02	-0.02 ± 0.02	-0.01 ± 0.02	-0.06 ± 0.05
				0.01 ± 0.04	-0.06 ± 0.03	0.05 ± 0.02	0.09 ± 0.04	0.01 ± 0.01
NGC 2682	2M08503613+1143180	34.3 ± 0.1	0.02 ± 0.01	-0.01 ± 0.04	0.01 ± 0.02	-0.00 ± 0.02	-0.06 ± 0.03	0.11 ± 0.06
				-0.04 ± 0.09	0.04 ± 0.04	-0.01 ± 0.03	-0.13 ± 0.09	0.04 ± 0.02

Continued on next page

Table B.1 – Continued

Cluster	2MASS ID	RV (km s^{-1})	[Fe/H] (dex)	[O/Fe] (dex)	[Mg/Fe] (dex)	[Ca/Fe] (dex)	[Si/Fe] (dex)	[S/Fe] (dex)
				[V/Fe] (dex)	[Cr/Fe] (dex)	[Mn/Fe] (dex)	[Co/Fe] (dex)	[Ni/Fe] (dex)
NGC 2682	2M08504964+1135089	34.9 ± 0.1	0.09 ± 0.01	-0.04 ± 0.03	-0.00 ± 0.02	-0.03 ± 0.02	-0.03 ± 0.02	0.00 ± 0.05
				-0.04 ± 0.06	0.09 ± 0.03	0.03 ± 0.02	0.04 ± 0.07	0.04 ± 0.01
NGC 2682	2M08504994+1149127	33.8 ± 0.1	0.01 ± 0.01	-0.08 ± 0.04	0.00 ± 0.02	-0.03 ± 0.02	-0.03 ± 0.03	0.02 ± 0.06
				-0.34 ± 0.09	-0.16 ± 0.04	0.02 ± 0.03	0.13 ± 0.10	0.03 ± 0.02
NGC 2682	2M08505816+1152223	34.0 ± 0.1	0.08 ± 0.01	-0.03 ± 0.03	0.00 ± 0.02	0.00 ± 0.02	-0.04 ± 0.03	-0.03 ± 0.05
				0.03 ± 0.08	-0.01 ± 0.04	0.02 ± 0.02	-0.09 ± 0.08	0.03 ± 0.01
NGC 2682	2M08510839+1147121	33.5 ± 0.2	0.08 ± 0.01	-0.06 ± 0.03	0.01 ± 0.02	-0.01 ± 0.02	-0.03 ± 0.02	-0.04 ± 0.05
				-0.23 ± 0.07	-0.05 ± 0.03	-0.00 ± 0.02	0.02 ± 0.07	0.04 ± 0.01
NGC 2682	2M08511269+1152423	34.3 ± 0.1	0.08 ± 0.01	-0.04 ± 0.03	-0.00 ± 0.02	-0.02 ± 0.02	-0.01 ± 0.02	-0.03 ± 0.05
				-0.03 ± 0.07	-0.02 ± 0.03	0.04 ± 0.02	0.07 ± 0.07	0.01 ± 0.01
NGC 2682	2M08511704+1150464	33.6 ± 0.1	0.05 ± 0.01	-0.01 ± 0.03	0.01 ± 0.02	-0.01 ± 0.02	-0.02 ± 0.02	-0.03 ± 0.05
				-0.14 ± 0.06	0.03 ± 0.03	0.00 ± 0.02	-0.02 ± 0.06	0.01 ± 0.01
NGC 2682	2M08511710+1148160	33.6 ± 0.0	0.10 ± 0.01	0.01 ± 0.02	0.01 ± 0.02	0.00 ± 0.02	0.01 ± 0.02	-0.05 ± 0.04
				-0.06 ± 0.05	-0.01 ± 0.03	-0.01 ± 0.02	0.12 ± 0.05	-0.00 ± 0.01
NGC 2682	2M08511897+1158110	34.0 ± 0.1	0.05 ± 0.01	0.00 ± 0.03	0.03 ± 0.02	-0.02 ± 0.02	-0.04 ± 0.02	0.00 ± 0.05
				0.04 ± 0.07	0.00 ± 0.03	0.02 ± 0.02	-0.10 ± 0.07	0.04 ± 0.01
NGC 2682	2M08512156+1146061	34.9 ± 0.1	0.12 ± 0.01	-0.05 ± 0.03	0.01 ± 0.02	-0.01 ± 0.02	-0.02 ± 0.02	-0.05 ± 0.05
				-0.22 ± 0.06	0.01 ± 0.03	0.01 ± 0.02	-0.07 ± 0.07	0.02 ± 0.01
NGC 2682	2M08512280+1148016	33.8 ± 0.0	0.12 ± 0.01	-0.02 ± 0.03	0.02 ± 0.02	-0.00 ± 0.02	0.02 ± 0.02	-0.06 ± 0.05
				0.02 ± 0.06	0.01 ± 0.03	0.03 ± 0.02	0.05 ± 0.07	-0.00 ± 0.01
NGC 2682	2M08512618+1153520	34.2 ± 0.0	0.07 ± 0.01	-0.03 ± 0.03	-0.00 ± 0.02	-0.03 ± 0.02	-0.00 ± 0.02	-0.00 ± 0.05
				0.01 ± 0.07	-0.02 ± 0.03	0.03 ± 0.02	0.04 ± 0.07	0.02 ± 0.01
NGC 2682	2M08512898+1150330	33.5 ± 0.0	0.08 ± 0.01	-0.02 ± 0.03	-0.00 ± 0.02	-0.05 ± 0.02	0.01 ± 0.02	-0.06 ± 0.05
				-0.22 ± 0.06	-0.05 ± 0.03	0.04 ± 0.02	0.13 ± 0.06	0.02 ± 0.01

Continued on next page

Table B.1 – Continued

Cluster	2MASS ID	RV (km s^{-1})	[Fe/H] (dex)	[O/Fe] (dex)	[Mg/Fe] (dex)	[Ca/Fe] (dex)	[Si/Fe] (dex)	[S/Fe] (dex)
				[V/Fe] (dex)	[Cr/Fe] (dex)	[Mn/Fe] (dex)	[Co/Fe] (dex)	[Ni/Fe] (dex)
NGC 2682	2M08512935+1145275	33.1 ± 0.1	0.04 ± 0.01	-0.12 ± 0.04	0.02 ± 0.02	0.03 ± 0.02	-0.06 ± 0.03	0.04 ± 0.05
				-0.39 ± 0.08	-0.15 ± 0.04	0.01 ± 0.02	-0.03 ± 0.08	0.02 ± 0.01
NGC 2682	2M08513044+1148582	30.1 ± 6.1	0.09 ± 0.01	-0.05 ± 0.03	-0.01 ± 0.02	-0.01 ± 0.02	-0.02 ± 0.02	-0.03 ± 0.05
				-0.13 ± 0.07	-0.04 ± 0.03	-0.00 ± 0.02	-0.03 ± 0.07	-0.00 ± 0.01
NGC 2682	2M08513577+1153347	34.0 ± 0.1	0.08 ± 0.01	-0.06 ± 0.03	0.01 ± 0.02	-0.03 ± 0.02	-0.05 ± 0.02	0.02 ± 0.05
				-0.03 ± 0.07	-0.01 ± 0.03	0.01 ± 0.02	-0.09 ± 0.07	-0.02 ± 0.01
NGC 2682	2M08513862+1220141	33.7 ± 0.1	0.04 ± 0.01	0.04 ± 0.04	-0.00 ± 0.02	-0.02 ± 0.02	-0.05 ± 0.03	-0.03 ± 0.05
				0.10 ± 0.08	0.00 ± 0.04	0.01 ± 0.02	-0.08 ± 0.08	0.03 ± 0.01
NGC 2682	2M08513938+1151456	34.0 ± 0.1	0.05 ± 0.01	-0.02 ± 0.03	0.02 ± 0.02	-0.02 ± 0.02	-0.04 ± 0.02	-0.05 ± 0.05
				0.06 ± 0.07	0.02 ± 0.03	0.02 ± 0.02	0.06 ± 0.07	0.02 ± 0.01
NGC 2682	2M08514234+1150076	34.3 ± 0.0	0.09 ± 0.01	0.00 ± 0.03	0.05 ± 0.02	-0.01 ± 0.02	-0.07 ± 0.02	-0.05 ± 0.05
				-0.18 ± 0.07	-0.01 ± 0.03	0.02 ± 0.02	0.01 ± 0.07	0.01 ± 0.01
NGC 2682	2M08514235+1151230	33.5 ± 0.1	0.07 ± 0.01	-0.04 ± 0.03	-0.00 ± 0.02	-0.03 ± 0.02	-0.02 ± 0.02	-0.02 ± 0.05
				-0.04 ± 0.06	-0.07 ± 0.03	0.02 ± 0.02	0.07 ± 0.07	0.01 ± 0.01
NGC 2682	2M08514388+1156425	32.9 ± 0.0	0.07 ± 0.01	-0.03 ± 0.03	0.02 ± 0.02	0.01 ± 0.02	0.00 ± 0.02	-0.06 ± 0.05
				-0.15 ± 0.07	-0.25 ± 0.03	0.03 ± 0.02	-0.01 ± 0.07	0.01 ± 0.01
NGC 2682	2M08514474+1146460	33.1 ± 0.1	0.01 ± 0.01	0.00 ± 0.04	0.02 ± 0.02	0.01 ± 0.02	-0.03 ± 0.03	-0.01 ± 0.05
				0.04 ± 0.08	-0.00 ± 0.04	0.04 ± 0.02	-0.29 ± 0.08	0.06 ± 0.02
NGC 2682	2M08514507+1147459	33.0 ± 0.0	0.10 ± 0.01	-0.06 ± 0.03	0.00 ± 0.02	-0.02 ± 0.02	-0.05 ± 0.02	0.01 ± 0.05
				-0.34 ± 0.07	0.01 ± 0.03	-0.03 ± 0.02	-0.02 ± 0.07	-0.00 ± 0.01
NGC 2682	2M08514883+1156511	34.3 ± 0.1	0.01 ± 0.01	-0.11 ± 0.03	0.04 ± 0.02	-0.01 ± 0.02	-0.04 ± 0.03	0.10 ± 0.05
				0.25 ± 0.08	-0.03 ± 0.04	-0.00 ± 0.02	-0.18 ± 0.08	0.03 ± 0.01
NGC 2682	2M08515020+1146069	37.3 ± 0.4	0.07 ± 0.01	-0.04 ± 0.03	-0.00 ± 0.02	-0.03 ± 0.02	-0.01 ± 0.03	0.01 ± 0.05
				-0.27 ± 0.08	-0.02 ± 0.04	0.00 ± 0.02	0.07 ± 0.08	0.03 ± 0.01

Continued on next page

Table B.1 – Continued

Cluster	2MASS ID	RV (km s^{-1})	[Fe/H] (dex)	[O/Fe] (dex)	[Mg/Fe] (dex)	[Ca/Fe] (dex)	[Si/Fe] (dex)	[S/Fe] (dex)
				[V/Fe] (dex)	[Cr/Fe] (dex)	[Mn/Fe] (dex)	[Co/Fe] (dex)	[Ni/Fe] (dex)
NGC 2682	2M08515567+1217573	33.5 ± 0.1	0.01 ± 0.01	0.05 ± 0.04	-0.00 ± 0.02	-0.00 ± 0.02	-0.02 ± 0.03	0.00 ± 0.05
				0.04 ± 0.09	0.05 ± 0.04	0.02 ± 0.03	0.04 ± 0.09	0.04 ± 0.02
NGC 2682	2M08515952+1155049	34.4 ± 0.0	0.06 ± 0.01	-0.04 ± 0.03	-0.02 ± 0.02	-0.02 ± 0.02	-0.00 ± 0.02	-0.03 ± 0.05
				-0.12 ± 0.07	-0.00 ± 0.03	-0.01 ± 0.02	-0.04 ± 0.07	0.02 ± 0.01
NGC 2682	2M08521097+1131491	33.8 ± 0.0	0.11 ± 0.01	-0.01 ± 0.02	0.01 ± 0.02	-0.00 ± 0.02	-0.01 ± 0.02	-0.07 ± 0.05
				-0.02 ± 0.06	0.02 ± 0.03	0.00 ± 0.02	0.02 ± 0.06	-0.00 ± 0.01
NGC 2682	2M08521656+1119380	33.8 ± 0.0	0.08 ± 0.01	-0.06 ± 0.02	-0.01 ± 0.02	-0.02 ± 0.02	-0.03 ± 0.02	-0.05 ± 0.04
				-0.08 ± 0.05	-0.01 ± 0.03	-0.01 ± 0.02	0.04 ± 0.05	0.01 ± 0.01
NGC 2682	2M08521856+1144263	33.7 ± 0.1	0.09 ± 0.01	-0.06 ± 0.03	0.00 ± 0.02	-0.05 ± 0.02	0.01 ± 0.02	-0.04 ± 0.05
				-0.05 ± 0.06	-0.01 ± 0.03	0.03 ± 0.02	0.08 ± 0.06	0.01 ± 0.01
NGC 2682	2M08522003+1127362	33.9 ± 0.1	0.08 ± 0.01	-0.02 ± 0.03	0.01 ± 0.02	-0.01 ± 0.02	-0.03 ± 0.02	-0.12 ± 0.05
				-0.06 ± 0.07	-0.01 ± 0.03	0.01 ± 0.02	0.02 ± 0.08	0.02 ± 0.01
NGC 2682	2M08522636+1141277	33.4 ± 0.1	0.02 ± 0.01	-0.03 ± 0.03	0.04 ± 0.02	-0.02 ± 0.02	-0.00 ± 0.03	0.02 ± 0.05
				-0.01 ± 0.07	0.12 ± 0.04	-0.02 ± 0.02	-0.09 ± 0.08	0.04 ± 0.01
NGC 2682	2M08525625+1148539	32.8 ± 0.1	0.13 ± 0.01	-0.03 ± 0.03	0.02 ± 0.02	-0.04 ± 0.02	-0.03 ± 0.02	0.03 ± 0.05
				-0.02 ± 0.07	0.08 ± 0.03	0.04 ± 0.02	0.03 ± 0.07	0.03 ± 0.01

Appendix C

Table 3.1: OCCAM DR16 Sample - Basic Parameters – Full Version

Table C.1: OCCAM DR16 Sample - Basic Parameters (Full)

Cluster name	Qual flag	l deg	b deg	R (')	Age Gyr	R_{GC} (kpc)	μ_α (mas yr^{-1})	μ_δ (mas yr^{-1})	RV (km s^{-1})	[Fe/H] (dex)	Num stars
Czernik 21	1	171.8933	0.4622	6.6	2.24	12.27	2.38 ± 0.09	-1.04 ± 0.07	45.0 ± 0.3	-0.32 ± 0.01	2
Berkeley 71	2	176.6384	0.8936	4.8	1.05	11.26	0.69 ± 0.08	-1.66 ± 0.06	-9.4 ± 0.3	-0.23 ± 0.04	6
Chupina 1	0	215.3987	31.6938	5.0	0.01	8.57	-10.89 ± 0.14	-2.77 ± 0.10	33.8 ± 0.2	-0.00 ± 0.02	2
NGC 188	2	122.8416	22.3840	17.7	4.47	9.14	-2.33 ± 0.04	-0.92 ± 0.03	-41.4 ± 1.1	0.09 ± 0.02	14
NGC 2202	0	203.5978	-4.8847	4.8	1.58	9.80	-0.97 ± 0.03	0.53 ± 0.03	52.8 ± 0.1	-0.14 ± 0.01	1
NGC 1245	2	146.6533	-8.9081	11.4	1.06	10.60	0.51 ± 0.04	-1.63 ± 0.03	-29.0 ± 0.8	-0.08 ± 0.02	24
NGC 2243	1	239.4800	-18.0146	5.1	1.36	10.78	-1.28 ± 0.02	5.50 ± 0.02	59.8 ± 0.4	-0.46 ± 0.03	8
Czernik 7	0	131.1573	0.5299	3.9	1.31	10.23	-0.39 ± 0.01	-0.45 ± 0.02	-39.5 ± 0.0	-0.07 ± 0.01	1
FSR 0687	0	156.9333	0.9670	5.0	0.00	11.50	0.53 ± 0.08	0.35 ± 0.05	-29.3 ± 0.4	-0.15 ± 0.02	1
NGC 1802	0	179.5885	-9.2419	4.8	1.41	10.07	2.01 ± 0.04	-0.62 ± 0.27	35.0 ± 0.6	-0.30 ± 0.01	2
FSR 0940	0	195.5557	-1.2914	5.1	2.51	10.35	0.47 ± 0.05	-2.51 ± 0.04	71.8 ± 0.1	-0.23 ± 0.01	1
NGC 1907	1	172.6189	0.3057	5.4	0.40	9.59	-0.06 ± 0.07	-3.54 ± 0.06	2.8 ± 0.2	-0.08 ± 0.01	3
NGC 6811	2	79.2233	12.0047	7.2	0.64	7.86	-3.44 ± 0.06	-8.73 ± 0.04	8.0 ± 0.3	-0.05 ± 0.02	4
FSR 0852	0	184.1286	-0.4317	4.8	1.00	10.14	1.09 ± 0.08	-1.97 ± 0.06	27.1 ± 0.2	-0.31 ± 0.01	1
Collinder 95	0	201.8031	0.0402	5.4	0.02	8.59	-2.05 ± 0.14	-5.46 ± 0.14	19.7 ± 1.6	-0.14 ± 0.02	1
L 1641S	0	212.4711	-19.0105	12.9	0.00	8.40	0.36 ± 0.16	-0.50 ± 0.13	22.0 ± 2.0	-0.05 ± 0.05	11
NGC 2311	0	217.7569	-0.6935	6.0	0.65	9.85	-1.46 ± 0.08	0.80 ± 0.07	100.5 ± 0.2	-0.32 ± 0.01	1
FSR 0716	1	162.2554	3.6174	3.9	0.64	12.35	-0.33 ± 0.04	-1.77 ± 0.03	20.8 ±13.7	-0.40 ± 0.01	1
King 2	1	122.8645	-4.6707	3.0	4.68	11.90	-1.49 ± 0.02	-0.92 ± 0.02	-135.5 ± 0.0	-0.36 ± 0.01	1
IC 348	0	160.5067	-17.8063	7.5	0.01	8.43	4.38 ± 0.26	-6.26 ± 0.12	16.7 ± 0.3	-0.11 ± 0.02	2
Koposov 62	0	187.2643	4.1906	4.2	2.60	11.41	-0.02 ± 0.04	-0.43 ± 0.03	51.8 ± 0.0	-0.27 ± 0.01	1
Briceno 1	0	200.9817	-18.3440	30.0	0.01	8.30	1.45 ± 0.10	-0.08 ± 0.09	21.0 ± 1.0	-0.06 ± 0.06	30
Melotte 20	1	147.4872	-6.5275	120.0	0.05	8.15	23.34 ± 0.13	-25.80 ± 0.11	1.0 ± 1.3	0.01 ± 0.05	60
Berkeley 31	1	206.2232	5.1295	3.0	2.00	13.85	0.24 ± 0.06	-1.08 ± 0.06	59.6 ± 0.3	-0.45 ± 0.01	1
Czernik 20	1	168.2836	1.4287	6.6	1.55	9.97	0.58 ± 0.05	-1.56 ± 0.04	31.4 ± 2.4	-0.16 ± 0.03	7
Trumpler 5	1	202.8071	1.0182	13.5	3.16	10.59	-0.58 ± 0.06	0.23 ± 0.04	50.5 ± 0.4	-0.44 ± 0.01	3
Berkeley 66	2	139.4199	0.1803	3.3	1.41	14.08	0.01 ± 0.15	-0.10 ± 0.12	-50.0 ± 0.2	-0.19 ± 0.03	5
NGC 6866	1	79.5648	6.8354	5.1	0.44	7.87	-1.18 ± 0.04	-5.91 ± 0.08	14.2 ± 0.4	0.01 ± 0.01	2

Continued on next page

Table C.1 – Continued

Cluster name	Qual flag	l deg	b deg	R (')	Age Gyr	R_{GC} (kpc)	μ_α (mas yr^{-1})	μ_δ (mas yr^{-1})	RV (km s^{-1})	[Fe/H] (dex)	Num stars
SAI 16	1	131.4481	0.6267	2.7	1.41	11.69	-0.70 ± 0.03	-0.37 ± 0.04	-61.2 ± 0.2	-0.28 ± 0.01	1
NGC 2204	1	226.0090	-16.1042	6.3	1.95	10.85	-0.58 ± 0.04	1.95 ± 0.04	91.9 ± 0.9	-0.26 ± 0.02	12
Saurer 1	0	214.6969	7.3830	2.7	3.98	20.69	-0.36 ± 0.05	-0.39 ± 0.04	105.0 ± 0.0	-0.42 ± 0.01	1
ASCC 19	0	204.8628	-19.4804	15.0	0.03	8.27	1.24 ± 0.12	-1.14 ± 0.13	23.0 ± 1.4	-0.05 ± 0.05	10
VVV CL006	0	295.7470	-0.2071	5.0	nan	7.24	-7.74 ± 0.04	1.28 ± 0.03	-14.1 ± 0.1	0.16 ± 0.01	2
NGC 6705	1	27.2873	-2.7594	9.0	0.32	6.50	-1.56 ± 0.08	-4.17 ± 0.07	35.4 ± 1.0	0.12 ± 0.04	12
NGC 136	0	120.5684	-1.2707	3.3	0.25	10.25	-1.63 ± 0.02	-0.53 ± 0.02	-51.9 ± 0.0	-0.23 ± 0.01	1
NGC 2479	1	236.0065	5.3789	6.3	1.04	8.83	-4.30 ± 0.03	1.09 ± 0.03	41.6 ± 0.0	-0.03 ± 0.01	1
NGC 1193	1	146.8058	-12.1708	2.4	2.00	13.30	-0.22 ± 0.10	-0.36 ± 0.07	-84.7 ± 0.2	-0.34 ± 0.01	3
FSR 0496	0	120.2273	1.2882	4.5	1.14	8.62	2.20 ± 0.03	-0.77 ± 0.03	-23.3 ± 0.1	-0.10 ± 0.01	1
FSR 0394	1	108.3181	-0.8073	2.7	1.58	10.50	-3.84 ± 0.05	-1.20 ± 0.05	-70.3 ± 0.2	-0.10 ± 0.01	3
Collinder 92	0	205.1263	-3.9845	6.0	1.40	10.47	-0.04 ± 0.04	0.23 ± 0.03	84.9 ± 0.2	-0.42 ± 0.01	1
Ruprecht 96	0	295.9135	-0.1075	4.6	1.15	7.54	-5.48 ± 0.04	0.81 ± 0.03	-6.3 ± 0.1	0.03 ± 0.01	1
NGC 6791	2	69.9658	10.9080	6.3	4.42	7.80	-0.44 ± 0.03	-2.25 ± 0.03	-46.9 ± 1.3	0.35 ± 0.04	36
NGC 2678	0	216.0348	31.4206	6.5	2.29	8.58	-11.01 ± 0.05	-3.08 ± 0.03	34.1 ± 0.1	0.00 ± 0.01	1
NGC 1977	0	208.5157	-19.0685	10.2	0.00	8.30	1.09 ± 0.15	-0.91 ± 0.46	29.6 ± 2.1	-0.21 ± 0.04	3
Berkeley 20	1	203.4881	-17.3755	4.2	6.03	15.68	1.04 ± 0.07	-0.16 ± 0.05	78.8 ± 0.0	-0.40 ± 0.01	1
Berkeley 98	1	103.8443	-5.6638	4.5	2.09	9.87	-1.41 ± 0.04	-3.23 ± 0.03	-64.9 ± 0.0	-0.00 ± 0.01	2
NGC 2232	0	214.5457	-7.4008	9.9	0.05	8.27	0.13 ± 0.11	1.42 ± 0.22	81.4 ± 0.4	-0.36 ± 0.01	2
ASCC 116	0	99.4864	-0.3121	3.6	0.09	8.38	-1.40 ± 0.03	-2.03 ± 0.02	-22.5 ± 0.1	-0.13 ± 0.01	1
NGC 1664	1	161.7036	-0.4372	11.4	0.56	9.15	1.84 ± 0.07	-5.76 ± 0.04	7.0 ± 0.1	-0.03 ± 0.01	1
BH 211	1	344.9657	0.4577	5.0	0.51	6.28	-0.68 ± 0.09	-2.04 ± 0.08	-49.0 ± 0.4	0.21 ± 0.02	2
Teutsch 12	1	197.9215	0.5810	5.0	0.30	11.16	-0.76 ± 0.05	-0.94 ± 0.04	52.0 ± 0.1	-0.17 ± 0.01	1
King 5	2	143.7732	-4.2760	8.4	1.23	9.86	-0.27 ± 0.09	-1.37 ± 0.08	-44.1 ± 1.5	-0.14 ± 0.01	5
Dol Dzim 4	0	181.3930	-3.4099	6.0	0.10	11.78	0.64 ± 0.05	0.23 ± 0.04	48.0 ± 0.1	-0.47 ± 0.01	1
NGC 1798	2	160.6994	4.8502	5.4	2.00	13.05	0.83 ± 0.04	-0.31 ± 0.04	2.7 ± 0.8	-0.27 ± 0.03	8
Basel 11b	1	187.4276	-1.0927	5.1	0.95	9.31	1.08 ± 0.05	-4.22 ± 0.05	3.2 ± 0.0	-0.00 ± 0.01	1
Collinder 70	0	204.8629	-17.1827	21.6	0.03	8.33	1.77 ± 0.42	-0.92 ± 0.34	20.3 ± 4.2	-0.10 ± 0.06	8

Continued on next page

Table C.1 – Continued

Cluster name	Qual flag	l deg	b deg	R (')	Age Gyr	R_{GC} (kpc)	μ_α (mas yr^{-1})	μ_δ (mas yr^{-1})	RV (km s^{-1})	[Fe/H] (dex)	Num stars
IC 1369	1	89.6019	-0.4154	5.1	0.35	8.37	-4.68 ± 0.05	-5.55 ± 0.04	-48.5 ± 0.1	-0.08 ± 0.03	3
NGC 2264	0	202.9506	2.1918	11.4	0.01	8.60	-1.63 ± 0.12	-3.58 ± 0.10	22.4 ± 3.3	-0.17 ± 0.06	24
Berkeley 9	1	146.0671	-2.8254	3.9	2.00	9.32	1.57 ± 0.10	-0.10 ± 0.10	-16.9 ± 1.1	-0.09 ± 0.06	3
Melotte 71	1	228.9457	4.5164	14.4	0.94	9.80	-2.38 ± 0.04	4.13 ± 0.06	50.5 ± 0.7	-0.13 ± 0.02	4
Czernik 30	1	226.3319	4.1618	3.2	1.58	13.61	-0.69 ± 0.03	-0.10 ± 0.04	81.3 ± 0.3	-0.40 ± 0.01	2
Trumpler 3	0	138.0679	4.4927	14.1	0.10	8.47	1.00 ± 0.04	-1.05 ± 0.05	-10.1 ±11.5	0.14 ± 0.01	1
FSR 0823	0	179.1315	-0.2444	3.0	0.64	9.10	1.30 ± 0.13	-2.07 ± 0.11	5.4 ± 0.0	-0.20 ± 0.01	1
Sigma Orionis	0	206.8107	-17.3462	5.0	0.01	8.34	1.23 ± 0.13	-0.46 ± 0.13	30.7 ± 1.2	-0.15 ± 0.05	10
Berkeley 17	2	175.6574	-3.6494	7.2	3.98	9.79	2.69 ± 0.05	-0.35 ± 0.04	-73.4 ± 0.3	-0.16 ± 0.02	7
King 8	0	176.3879	3.1012	3.6	1.01	12.49	0.89 ± 0.15	-1.47 ± 0.12	-0.9 ± 0.1	-0.16 ± 0.01	1
FSR 0546	0	127.5948	3.3934	5.4	1.00	9.73	-0.57 ± 0.04	0.38 ± 0.04	-33.4 ± 0.1	-0.13 ± 0.01	1
King 12	0	116.1253	-0.1384	3.6	0.01	9.31	-3.51 ± 0.03	-1.75 ± 0.02	-80.4 ± 0.0	0.39 ± 0.01	1
ASCC 18	0	202.0212	-18.4242	13.2	0.01	8.28	1.13 ± 0.05	-0.31 ± 0.04	21.2 ± 0.1	-0.14 ± 0.01	1
Berkeley 43	1	45.6843	-0.1391	6.3	0.61	7.12	-0.92 ± 0.08	-3.27 ± 0.07	30.0 ± 0.1	0.03 ± 0.01	1
SAI 116	1	295.7611	-0.2217	3.6	0.48	7.29	-7.74 ± 0.04	1.28 ± 0.03	-14.1 ± 0.1	0.16 ± 0.01	2
ASCC 21	0	199.9498	-16.5116	19.2	0.01	8.34	1.28 ± 0.23	-0.29 ± 0.05	20.0 ± 0.7	-0.18 ± 0.01	3
Ruprecht 82	1	277.7085	-0.4503	3.1	0.23	8.01	-6.39 ± 0.04	4.38 ± 0.04	2.1 ± 0.1	-0.03 ± 0.01	1
Collinder 69	0	195.1694	-12.0054	15.6	0.01	8.39	0.94 ± 0.13	-1.99 ± 0.10	28.1 ± 1.9	-0.12 ± 0.04	30
FSR 0816	0	177.0913	0.2039	3.9	0.06	10.22	0.90 ± 0.06	-3.32 ± 0.30	-18.4 ± 1.9	-0.10 ± 0.02	2
NGC 2355	1	203.3897	11.8027	6.0	0.79	9.95	-3.38 ± 0.06	-1.33 ± 0.06	35.5 ± 0.0	-0.14 ± 0.01	1
NGC 1980	0	209.5301	-19.5798	9.3	0.00	8.43	1.26 ± 0.09	0.76 ± 0.08	26.2 ± 1.0	-0.08 ± 0.04	9
FSR 0494	2	120.0882	1.0206	5.7	2.00	11.43	-2.52 ± 0.04	-0.86 ± 0.04	-64.0 ± 0.3	-0.01 ± 0.01	4
Berkeley 79	0	31.1631	0.9187	3.9	0.01	6.05	-0.76 ± 0.06	-2.01 ± 0.05	13.4 ± 0.1	0.32 ± 0.01	1
FSR 0656	0	148.5631	0.3661	4.8	0.79	9.22	1.70 ± 0.06	-0.60 ± 0.05	-43.6 ± 0.0	-0.32 ± 0.01	1
NGC 358	0	124.5435	-0.8071	5.0	0.00	11.15	-0.88 ± 0.03	-0.59 ± 0.03	-71.0 ± 0.0	-0.31 ± 0.01	1
Chupina 5	0	215.8374	32.3036	5.0	0.00	8.58	-11.02 ± 0.05	-3.10 ± 0.03	33.2 ± 0.1	0.09 ± 0.01	1
King 7	2	149.7993	-1.0215	11.1	0.71	10.36	0.97 ± 0.12	-1.35 ± 0.10	-9.7 ± 1.4	-0.13 ± 0.05	6
NGC 2158	2	186.6394	1.7807	8.4	2.14	12.75	-0.24 ± 0.05	-2.00 ± 0.04	27.7 ± 1.5	-0.21 ± 0.02	18

Continued on next page

Table C.1 – Continued

Cluster name	Qual flag	l deg	b deg	R (')	Age Gyr	R_{GC} (kpc)	μ_α (mas yr^{-1})	μ_δ (mas yr^{-1})	RV (km s^{-1})	[Fe/H] (dex)	Num stars
Teutsch 10	0	179.9590	-0.2798	4.5	0.06	10.60	0.84 ± 0.05	-1.90 ± 0.04	5.6 ± 7.5	-0.27 ± 0.01	1
Teutsch 51	2	182.7401	0.4760	2.7	0.53	11.78	0.62 ± 0.10	-0.29 ± 0.09	17.7 ± 0.4	-0.33 ± 0.02	4
NGC 2420	2	198.1134	19.6318	7.5	2.32	10.61	-1.14 ± 0.06	-2.11 ± 0.04	74.4 ± 0.6	-0.19 ± 0.03	15
NGC 2318	0	226.0191	-4.4369	4.5	0.56	9.27	-1.94 ± 0.04	-2.30 ± 0.04	8.6 ± 0.0	-0.03 ± 0.01	1
Teutsch 84	1	344.4404	-0.4504	5.1	0.99	4.80	-1.94 ± 0.11	-1.08 ± 0.12	-58.4 ± 2.1	0.20 ± 0.01	2
ASCC 16	0	201.0701	-18.5210	18.6	0.01	8.35	1.44 ± 0.09	-0.19 ± 0.08	21.0 ± 0.9	-0.05 ± 0.05	17
NGC 752	1	137.0013	-23.2815	39.0	1.35	8.31	9.83 ± 0.05	-11.90 ± 0.06	5.6 ± 0.3	-0.04 ± 0.01	1
NGC 7789	2	115.5392	-5.3644	14.4	1.84	8.92	-0.95 ± 0.04	-1.91 ± 0.04	-54.6 ± 1.3	-0.01 ± 0.02	17
Chupina 4	0	215.1593	32.2925	5.0	0.00	8.63	-10.99 ± 0.06	-2.86 ± 0.04	33.8 ± 0.1	-0.00 ± 0.01	1
Berkeley 19	1	176.9181	-3.6224	3.3	3.16	12.79	0.64 ± 0.03	-0.23 ± 0.02	17.8 ± 0.0	-0.32 ± 0.01	1
NGC 6819	2	73.9834	8.4882	6.9	1.62	7.69	-2.96 ± 0.03	-3.87 ± 0.03	2.7 ± 1.7	0.05 ± 0.03	37
NGC 1981	0	208.0754	-18.9818	9.0	0.01	8.33	1.11 ± 0.04	0.58 ± 0.03	28.8 ± 0.2	-0.18 ± 0.01	1
NGC 6383	0	355.6742	0.0462	6.9	0.00	6.82	2.61 ± 0.07	-1.84 ± 0.06	7.7 ± 0.0	-0.39 ± 0.03	1
ASCC 20	0	201.6623	-17.5165	15.6	0.01	8.35	1.42 ± 0.07	-1.90 ± 0.06	19.4 ± 0.6	0.02 ± 0.01	1
NGC 2682	2	215.6906	31.9221	33.0	3.43	8.62	-11.05 ± 0.06	-2.98 ± 0.04	33.9 ± 0.7	0.01 ± 0.03	32
Chupina 3	0	216.1467	31.7593	5.0	0.00	8.58	-11.05 ± 0.04	-2.83 ± 0.05	34.2 ± 0.6	0.01 ± 0.02	5
IC 166	2	130.0502	-0.1616	7.5	1.00	11.68	-1.45 ± 0.04	1.15 ± 0.05	-40.0 ± 1.3	-0.10 ± 0.03	18
NGC 2324	1	213.4597	3.3065	8.7	0.48	11.40	-0.31 ± 0.05	-0.11 ± 0.04	42.2 ± 0.2	-0.19 ± 0.02	4
Platais 4	0	180.4786	-10.7804	15.0	0.35	8.27	0.20 ± 0.07	-1.87 ± 0.04	15.2 ± 0.1	-0.31 ± 0.01	1
Czernik 23	1	180.5378	0.8205	3.3	0.30	10.45	0.07 ± 0.06	-1.84 ± 0.05	18.0 ± 0.1	-0.28 ± 0.01	1
NGC 4337	1	299.3036	4.5613	6.6	1.41	7.05	-8.88 ± 0.03	1.48 ± 0.04	-18.2 ± 1.0	0.24 ± 0.03	7
NGC 2447	1	240.0507	0.1488	15.0	0.48	8.56	-3.67 ± 0.05	5.01 ± 0.04	23.5 ± 0.6	-0.08 ± 0.01	3
Berkeley 53	2	90.3051	3.7555	7.5	1.23	8.67	-3.84 ± 0.10	-5.65 ± 0.09	-35.9 ± 0.8	-0.08 ± 0.02	6
NGC 1912	1	172.3115	0.7010	9.6	0.22	9.13	1.99 ± 0.06	-4.74 ± 0.04	-0.7 ± 0.4	-0.14 ± 0.01	1
NGC 1857	1	168.4442	1.2218	4.5	0.47	11.25	0.75 ± 0.07	-1.20 ± 0.05	1.3 ± 0.1	-0.14 ± 0.01	1
FSR 0304	0	93.5597	0.6456	3.6	0.61	8.21	-3.90 ± 0.23	-4.94 ± 0.26	-68.3 ± 1.5	-0.07 ± 0.01	3
NGC 2304	1	197.2162	8.8965	4.8	0.68	11.73	-0.12 ± 0.05	-1.52 ± 0.05	51.5 ± 0.1	-0.12 ± 0.02	2
Ruprecht 147	1	21.0089	-12.7301	30.0	2.14	7.75	-0.87 ± 0.10	-26.72 ± 0.10	42.4 ± 1.5	0.12 ± 0.03	27

Continued on next page

Table C.1 – Continued

Cluster name	Qual flag	l deg	b deg	R (')	Age Gyr	R_{GC} (kpc)	μ_α (mas yr^{-1})	μ_δ (mas yr^{-1})	RV (km s^{-1})	[Fe/H] (dex)	Num stars
Teutsch 5	0	167.5834	-4.1143	4.8	2.40	10.94	0.23 ± 0.04	-1.46 ± 0.03	-74.7 ± 0.1	-0.35 ± 0.01	1
FSR 1113	1	216.2903	3.2530	4.2	0.20	13.13	-0.46 ± 0.03	1.84 ± 0.03	69.0 ± 0.1	-0.30 ± 0.01	1
Berkeley 29	1	197.9438	7.9747	3.6	1.26	18.47	0.15 ± 0.04	-1.01 ± 0.04	25.9 ± 0.7	-0.49 ± 0.03	3
NGC 2240	0	179.2125	11.8825	3.6	1.58	9.52	0.77 ± 0.05	-1.71 ± 0.04	26.4 ± 0.1	-0.15 ± 0.01	1
Berkeley 91	0	90.0183	0.2805	3.6	0.25	12.40	-1.56 ± 0.10	-3.43 ± 0.09	-51.1 ± 0.2	0.09 ± 0.01	1
Collinder 220	1	284.5606	-0.3325	5.7	0.37	7.76	-7.33 ± 0.03	2.68 ± 0.03	-12.5 ± 0.0	-0.08 ± 0.01	1
Haffner 4	1	227.9381	-3.6156	4.5	1.30	11.47	-0.48 ± 0.03	0.92 ± 0.03	59.5 ± 0.1	-0.16 ± 0.01	1
FSR 0542	0	126.8224	0.3731	5.1	0.22	9.29	-2.09 ± 0.04	-0.11 ± 0.05	-74.0 ± 0.1	-0.23 ± 0.01	1
Berkeley 44	1	53.2093	3.3443	6.3	1.41	7.00	-0.17 ± 0.05	-3.17 ± 0.05	23.0 ± 0.1	-0.00 ± 0.01	1
FSR 0942	0	195.5903	-3.5955	6.0	1.00	10.02	-0.46 ± 0.04	0.22 ± 0.03	29.3 ± 0.0	-0.28 ± 0.01	1
NGC 7058	1	92.8783	0.6124	5.1	0.22	8.03	7.41 ± 0.10	2.76 ± 0.14	-19.1 ± 0.3	0.03 ± 0.04	3
Berkeley 33	1	225.4429	-4.5932	3.0	1.10	11.84	-0.69 ± 0.04	1.56 ± 0.04	77.5 ± 0.4	-0.30 ± 0.01	2
Melotte 22	1	166.2047	-23.4834	150.0	0.14	8.12	20.35 ± 0.11	-44.59 ± 0.08	6.1 ± 0.9	-0.00 ± 0.05	79
NGC 7062	1	89.9667	-2.7397	3.6	0.69	8.16	-1.84 ± 0.04	-4.08 ± 0.04	-22.0 ± 0.1	0.01 ± 0.01	1
FSR 0667	1	151.1544	-0.6481	2.7	0.12	9.63	0.64 ± 0.05	-4.01 ± 0.04	3.7 ± 0.8	-0.02 ± 0.01	1
Czernik 18	1	168.2530	-12.3062	4.2	0.48	9.21	2.20 ± 0.23	-2.89 ± 0.13	-15.3 ± 0.3	-0.07 ± 0.02	1

Appendix D

Table 3.2: OCCAM DR16 Sample - Detailed Chemistry – Full Version

Table D.1: OCCAM DR16 Sample - Detailed Chemistry (Full)

Cluster name	[Fe/H] (dex)	[O/Fe] (dex)	[Na/Fe] (dex)	[Mg/Fe] (dex)	[Al/Fe] (dex)	[Si/Fe] (dex)	[S/Fe] (dex)	[K/Fe] (dex)
	[Ca/Fe] (dex)	[Ti/Fe] (dex)	[V/Fe] (dex)	[Cr/Fe] (dex)	[Mn/Fe] (dex)	[Co/Fe] (dex)	[Ni/Fe] (dex)	[Cu/Fe] (dex)
Czernik 21	-0.32 ± 0.01	0.20 ± 0.08	0.06 ± 0.06	-0.04 ± 0.02	0.04 ± 0.03	-0.01 ± 0.02	-0.03 ± 0.05	0.05 ± 0.05
	0.09 ± 0.03	-0.01 ± 0.03	—	0.01 ± 0.05	-0.01 ± 0.03	0.02 ± 0.15	0.03 ± 0.02	-0.04 ± 0.06
Berkeley 71	-0.23 ± 0.04	—	0.11 ± 0.11	-0.00 ± 0.01	-0.04 ± 0.06	-0.01 ± 0.02	0.12 ± 0.07	-0.02 ± 0.04
	0.05 ± 0.03	0.04 ± 0.05	—	-0.13 ± 0.06	-0.03 ± 0.02	-0.13 ± 0.12	-0.01 ± 0.02	0.08 ± 0.10
Chupina 1	-0.00 ± 0.02	—	—	0.03 ± 0.03	0.07 ± 0.03	0.07 ± 0.04	0.04 ± 0.05	0.06 ± 0.05
	-0.01 ± 0.07	—	—	0.06 ± 0.10	0.00 ± 0.07	-0.12 ± 0.20	0.05 ± 0.03	-0.58 ± 0.11
NGC 188	0.09 ± 0.02	-0.00 ± 0.05	-0.01 ± 0.18	0.02 ± 0.02	0.04 ± 0.09	0.03 ± 0.01	0.01 ± 0.05	0.05 ± 0.05
	-0.02 ± 0.04	0.03 ± 0.03	-0.03 ± 0.14	0.04 ± 0.04	0.08 ± 0.04	0.08 ± 0.07	0.04 ± 0.03	0.02 ± 0.07
NGC 2202	-0.14 ± 0.01	0.10 ± 0.02	-0.07 ± 0.05	-0.05 ± 0.01	0.08 ± 0.02	-0.00 ± 0.01	-0.08 ± 0.04	0.02 ± 0.04
	0.04 ± 0.02	0.01 ± 0.02	—	-0.02 ± 0.04	0.01 ± 0.02	0.09 ± 0.05	0.01 ± 0.02	0.11 ± 0.05
NGC 1245	-0.08 ± 0.02	-0.04 ± 0.01	0.06 ± 0.13	-0.03 ± 0.03	-0.01 ± 0.03	-0.03 ± 0.02	-0.00 ± 0.06	-0.02 ± 0.04
	0.01 ± 0.03	-0.02 ± 0.04	-0.17 ± 0.04	-0.01 ± 0.07	-0.01 ± 0.02	-0.17 ± 0.36	-0.03 ± 0.02	-0.14 ± 0.11
NGC 2243	-0.46 ± 0.03	0.11 ± 0.06	0.12 ± 0.21	0.05 ± 0.02	0.05 ± 0.04	0.04 ± 0.02	0.17 ± 0.06	0.10 ± 0.07
	0.04 ± 0.04	-0.05 ± 0.05	0.25 ± 0.06	-0.01 ± 0.10	-0.07 ± 0.03	0.06 ± 0.10	0.00 ± 0.03	0.10 ± 0.11
Czernik 7	-0.07 ± 0.01	0.02 ± 0.01	-0.04 ± 0.04	-0.00 ± 0.01	0.01 ± 0.02	0.04 ± 0.01	-0.02 ± 0.03	0.03 ± 0.03
	0.02 ± 0.01	-0.06 ± 0.02	0.04 ± 0.05	-0.02 ± 0.03	-0.02 ± 0.01	0.00 ± 0.04	-0.01 ± 0.01	0.01 ± 0.03
FSR 0687	-0.15 ± 0.02	—	0.17 ± 0.08	-0.01 ± 0.02	0.12 ± 0.04	-0.04 ± 0.02	0.04 ± 0.06	-0.05 ± 0.06
	0.02 ± 0.03	0.16 ± 0.04	—	-0.30 ± 0.07	-0.03 ± 0.03	0.13 ± 0.09	-0.01 ± 0.03	0.10 ± 0.07
NGC 1802	-0.30 ± 0.01	0.04 ± 0.03	-0.12 ± 0.08	0.07 ± 0.02	0.01 ± 0.04	0.03 ± 0.06	0.01 ± 0.06	-0.06 ± 0.07
	0.01 ± 0.03	-0.08 ± 0.04	-1.13 ± 0.09	0.02 ± 0.07	-0.04 ± 0.03	-0.45 ± 0.17	-0.02 ± 0.03	-0.04 ± 0.08
FSR 0940	-0.23 ± 0.01	0.11 ± 0.02	-0.07 ± 0.06	-0.01 ± 0.01	0.12 ± 0.02	0.01 ± 0.01	0.05 ± 0.04	0.33 ± 0.04
	0.01 ± 0.02	0.06 ± 0.03	—	-0.00 ± 0.05	0.03 ± 0.02	0.02 ± 0.06	0.07 ± 0.02	0.02 ± 0.05
NGC 1907	-0.08 ± 0.01	-0.04 ± 0.02	0.14 ± 0.07	-0.04 ± 0.01	-0.06 ± 0.02	-0.01 ± 0.01	0.09 ± 0.03	-0.05 ± 0.04
	0.01 ± 0.01	-0.02 ± 0.03	—	0.02 ± 0.03	-0.00 ± 0.02	-0.03 ± 0.04	-0.03 ± 0.01	0.03 ± 0.04

Continued on next page

Table D.1 – Continued

Cluster name	[Fe/H] (dex)	[O/Fe] (dex)	[Na/Fe] (dex)	[Mg/Fe] (dex)	[Al/Fe] (dex)	[Si/Fe] (dex)	[S/Fe] (dex)	[K/Fe] (dex)
	[Ca/Fe] (dex)	[Ti/Fe] (dex)	[V/Fe] (dex)	[Cr/Fe] (dex)	[Mn/Fe] (dex)	[Co/Fe] (dex)	[Ni/Fe] (dex)	[Cu/Fe] (dex)
NGC 6811	-0.05 ± 0.02	-0.04 ± 0.02	0.06 ± 0.07	-0.04 ± 0.01	-0.07 ± 0.03	-0.02 ± 0.01	0.05 ± 0.04	-0.06 ± 0.05
	0.02 ± 0.01	0.00 ± 0.02	—	0.05 ± 0.03	0.01 ± 0.02	-0.16 ± 0.12	-0.03 ± 0.01	-0.06 ± 0.10
FSR 0852	-0.31 ± 0.01	—	0.28 ± 0.08	0.01 ± 0.02	0.05 ± 0.04	0.03 ± 0.02	0.32 ± 0.06	0.07 ± 0.07
	0.02 ± 0.03	-0.10 ± 0.04	—	-0.12 ± 0.07	0.00 ± 0.03	-0.43 ± 0.09	0.02 ± 0.03	0.19 ± 0.08
Collinder 95	-0.14 ± 0.02	-0.08 ± 0.01	—	-0.07 ± 0.02	-0.12 ± 0.04	-0.04 ± 0.01	—	—
	0.01 ± 0.02	—	—	—	—	-0.23 ± 0.12	-0.13 ± 0.04	0.07 ± 0.06
L 1641S	-0.05 ± 0.05	-0.08 ± 0.05	—	-0.12 ± 0.04	-0.09 ± 0.16	-0.09 ± 0.05	0.22 ± 0.25	0.07 ± 0.04
	-0.05 ± 0.11	-0.10 ± 0.13	—	-0.04 ± 0.06	-0.13 ± 0.04	-0.28 ± 0.27	-0.04 ± 0.10	0.02 ± 0.10
NGC 2311	-0.32 ± 0.01	0.12 ± 0.03	-0.07 ± 0.08	-0.03 ± 0.02	0.15 ± 0.03	0.02 ± 0.02	-0.05 ± 0.06	0.09 ± 0.06
	0.04 ± 0.03	-0.03 ± 0.04	—	0.05 ± 0.07	-0.00 ± 0.03	-0.12 ± 0.08	0.02 ± 0.03	0.06 ± 0.07
FSR 0716	-0.40 ± 0.01	—	0.05 ± 0.07	-0.07 ± 0.02	0.01 ± 0.03	-0.05 ± 0.02	0.03 ± 0.05	0.02 ± 0.05
	0.04 ± 0.03	0.03 ± 0.04	—	0.09 ± 0.06	-0.02 ± 0.03	-0.41 ± 0.08	0.02 ± 0.02	0.09 ± 0.07
King 2	-0.36 ± 0.01	0.08 ± 0.01	-0.27 ± 0.04	0.10 ± 0.01	0.03 ± 0.02	0.02 ± 0.01	0.22 ± 0.03	0.10 ± 0.03
	0.03 ± 0.01	—	-0.03 ± 0.04	0.03 ± 0.03	0.05 ± 0.02	0.00 ± 0.03	0.05 ± 0.01	0.17 ± 0.03
IC 348	-0.11 ± 0.02	-0.06 ± 0.02	—	-0.07 ± 0.02	0.03 ± 0.08	-0.02 ± 0.05	—	—
	-0.24 ± 0.02	—	—	—	—	0.19 ± 0.12	-0.16 ± 0.09	-0.02 ± 0.09
Koposov 62	-0.27 ± 0.01	0.02 ± 0.01	0.01 ± 0.04	0.01 ± 0.01	-0.03 ± 0.02	0.04 ± 0.01	0.11 ± 0.03	0.05 ± 0.03
	0.02 ± 0.01	-0.03 ± 0.02	0.53 ± 0.04	-0.03 ± 0.03	-0.01 ± 0.01	0.02 ± 0.03	-0.02 ± 0.01	0.06 ± 0.03
Briceno 1	-0.06 ± 0.06	-0.06 ± 0.03	-0.80 ± 0.05	-0.06 ± 0.06	-0.15 ± 0.07	-0.08 ± 0.04	0.03 ± 0.10	0.04 ± 0.02
	-0.04 ± 0.09	-0.12 ± 0.08	—	-0.05 ± 0.07	-0.07 ± 0.11	-0.48 ± 0.10	-0.05 ± 0.03	0.16 ± 0.09
Melotte 20	0.01 ± 0.05	-0.02 ± 0.04	—	-0.03 ± 0.06	-0.13 ± 0.14	-0.00 ± 0.07	0.04 ± 0.12	0.03 ± 0.07
	0.01 ± 0.10	-0.04 ± 0.21	-0.07 ± 0.05	-0.04 ± 0.11	-0.04 ± 0.10	-0.04 ± 0.39	-0.07 ± 0.08	0.12 ± 0.15
Berkeley 31	-0.45 ± 0.01	0.08 ± 0.01	0.01 ± 0.04	0.11 ± 0.01	-0.03 ± 0.02	0.04 ± 0.01	0.04 ± 0.04	—
	0.06 ± 0.01	—	0.07 ± 0.03	0.05 ± 0.03	—	0.10 ± 0.03	0.01 ± 0.02	—
Czernik 20	-0.16 ± 0.03	—	0.02 ± 0.15	-0.02 ± 0.03	-0.00 ± 0.03	-0.02 ± 0.02	0.06 ± 0.06	0.05 ± 0.07
	0.03 ± 0.04	-0.01 ± 0.10	—	-0.01 ± 0.08	-0.03 ± 0.03	-0.25 ± 0.38	-0.03 ± 0.02	-0.14 ± 0.17

Continued on next page

Table D.1 – Continued

Cluster name	[Fe/H] (dex)	[O/Fe] (dex)	[Na/Fe] (dex)	[Mg/Fe] (dex)	[Al/Fe] (dex)	[Si/Fe] (dex)	[S/Fe] (dex)	[K/Fe] (dex)
	[Ca/Fe] (dex)	[Ti/Fe] (dex)	[V/Fe] (dex)	[Cr/Fe] (dex)	[Mn/Fe] (dex)	[Co/Fe] (dex)	[Ni/Fe] (dex)	[Cu/Fe] (dex)
Trumpler 5	-0.44 ± 0.01	0.08 ± 0.02	0.16 ± 0.14	0.04 ± 0.02	0.07 ± 0.05	0.04 ± 0.01	0.03 ± 0.06	0.17 ± 0.07
	0.06 ± 0.04	-0.02 ± 0.03	0.16 ± 0.28	0.03 ± 0.07	-0.04 ± 0.03	-0.08 ± 0.08	0.01 ± 0.02	0.11 ± 0.08
Berkeley 66	-0.19 ± 0.03	0.03 ± 0.12	-0.15 ± 0.32	0.11 ± 0.02	0.16 ± 0.23	0.03 ± 0.02	0.07 ± 0.07	0.04 ± 0.06
	0.04 ± 0.02	0.00 ± 0.05	0.03 ± 0.07	0.03 ± 0.06	-0.04 ± 0.04	0.02 ± 0.07	-0.02 ± 0.04	0.11 ± 0.06
NGC 6866	0.01 ± 0.01	—	-0.00 ± 0.04	-0.05 ± 0.01	-0.04 ± 0.02	-0.04 ± 0.01	0.04 ± 0.03	-0.06 ± 0.03
	0.01 ± 0.02	0.01 ± 0.02	—	0.03 ± 0.05	0.02 ± 0.01	-0.14 ± 0.08	-0.03 ± 0.01	0.02 ± 0.03
SAI 16	-0.28 ± 0.01	—	-0.07 ± 0.08	-0.06 ± 0.02	-0.43 ± 0.04	-0.09 ± 0.02	0.17 ± 0.06	0.28 ± 0.06
	0.18 ± 0.03	-0.01 ± 0.04	—	0.18 ± 0.07	-0.00 ± 0.03	-0.02 ± 0.09	-0.02 ± 0.03	-0.07 ± 0.07
NGC 2204	-0.26 ± 0.02	0.02 ± 0.05	0.02 ± 0.18	0.00 ± 0.05	-0.05 ± 0.06	0.00 ± 0.03	-0.06 ± 0.11	0.01 ± 0.05
	0.03 ± 0.02	-0.05 ± 0.03	0.03 ± 0.18	0.02 ± 0.05	-0.04 ± 0.03	-0.03 ± 0.17	-0.02 ± 0.02	0.11 ± 0.10
Saurer 1	-0.42 ± 0.01	0.05 ± 0.01	-0.02 ± 0.05	0.02 ± 0.02	-0.05 ± 0.03	0.01 ± 0.01	0.22 ± 0.05	0.12 ± 0.05
	-0.00 ± 0.02	—	-0.02 ± 0.05	0.05 ± 0.05	—	0.09 ± 0.04	0.05 ± 0.02	—
ASCC 19	-0.05 ± 0.05	-0.02 ± 0.03	—	-0.11 ± 0.07	-0.07 ± 0.12	-0.07 ± 0.07	0.08 ± 0.23	0.21 ± 0.29
	0.07 ± 0.13	-0.11 ± 0.10	—	-0.04 ± 0.10	-0.07 ± 0.07	-0.21 ± 0.16	-0.07 ± 0.05	0.08 ± 0.10
VVV CL006	0.16 ± 0.01	-0.03 ± 0.01	0.19 ± 0.10	-0.02 ± 0.01	-0.04 ± 0.02	0.04 ± 0.01	0.06 ± 0.02	-0.11 ± 0.02
	-0.03 ± 0.01	-0.01 ± 0.01	-0.09 ± 0.08	-0.09 ± 0.02	0.12 ± 0.03	0.06 ± 0.05	0.01 ± 0.01	0.03 ± 0.03
NGC 6705	0.12 ± 0.04	-0.05 ± 0.02	0.23 ± 0.04	-0.07 ± 0.02	-0.13 ± 0.03	0.01 ± 0.01	0.07 ± 0.02	-0.16 ± 0.06
	-0.03 ± 0.02	-0.00 ± 0.02	-0.01 ± 0.04	-0.03 ± 0.04	0.11 ± 0.02	0.04 ± 0.03	0.03 ± 0.01	0.17 ± 0.07
NGC 136	-0.23 ± 0.01	—	-0.10 ± 0.05	-0.03 ± 0.01	-0.08 ± 0.02	-0.01 ± 0.01	0.22 ± 0.03	0.09 ± 0.03
	0.01 ± 0.01	0.08 ± 0.02	—	-0.02 ± 0.04	-0.01 ± 0.02	-0.00 ± 0.05	-0.05 ± 0.01	0.29 ± 0.04
NGC 2479	-0.03 ± 0.01	—	0.11 ± 0.04	-0.05 ± 0.01	-0.03 ± 0.02	-0.00 ± 0.01	0.06 ± 0.03	-0.17 ± 0.03
	0.01 ± 0.01	-0.01 ± 0.02	—	-0.03 ± 0.03	0.02 ± 0.01	-0.04 ± 0.04	-0.01 ± 0.01	-0.02 ± 0.03
NGC 1193	-0.34 ± 0.01	0.07 ± 0.02	-0.10 ± 0.17	0.08 ± 0.02	-0.01 ± 0.09	0.02 ± 0.01	0.10 ± 0.05	0.19 ± 0.06
	0.07 ± 0.03	0.00 ± 0.03	0.13 ± 0.07	0.01 ± 0.05	-0.05 ± 0.03	0.03 ± 0.08	0.05 ± 0.03	0.05 ± 0.11
FSR 0496	-0.10 ± 0.01	-0.01 ± 0.02	0.08 ± 0.04	-0.01 ± 0.01	0.00 ± 0.02	0.00 ± 0.01	0.04 ± 0.03	0.04 ± 0.03
	0.04 ± 0.01	-0.01 ± 0.02	—	-0.06 ± 0.03	-0.05 ± 0.02	-0.06 ± 0.04	-0.03 ± 0.01	-0.08 ± 0.04

Continued on next page

Table D.1 – Continued

Cluster name	[Fe/H] (dex)	[O/Fe] (dex)	[Na/Fe] (dex)	[Mg/Fe] (dex)	[Al/Fe] (dex)	[Si/Fe] (dex)	[S/Fe] (dex)	[K/Fe] (dex)
	[Ca/Fe] (dex)	[Ti/Fe] (dex)	[V/Fe] (dex)	[Cr/Fe] (dex)	[Mn/Fe] (dex)	[Co/Fe] (dex)	[Ni/Fe] (dex)	[Cu/Fe] (dex)
FSR 0394	-0.10 ± 0.01	-0.07 ± 0.05	0.10 ± 0.23	-0.01 ± 0.01	0.10 ± 0.06	-0.03 ± 0.01	0.06 ± 0.05	0.03 ± 0.04
	0.02 ± 0.02	-0.05 ± 0.03	-0.14 ± 0.06	0.03 ± 0.05	-0.04 ± 0.02	-0.08 ± 0.06	-0.02 ± 0.02	0.01 ± 0.05
Collinder 92	-0.42 ± 0.01	0.12 ± 0.03	-0.08 ± 0.07	-0.01 ± 0.02	0.07 ± 0.03	0.01 ± 0.02	-0.08 ± 0.06	0.10 ± 0.06
	-0.02 ± 0.03	-0.05 ± 0.04	—	-0.07 ± 0.06	-0.03 ± 0.03	-0.14 ± 0.08	0.03 ± 0.02	-0.07 ± 0.07
Ruprecht 96	0.03 ± 0.01	-0.12 ± 0.01	0.22 ± 0.03	-0.09 ± 0.01	-0.09 ± 0.02	-0.05 ± 0.01	0.00 ± 0.03	-0.12 ± 0.03
	-0.02 ± 0.01	0.03 ± 0.01	-0.01 ± 0.04	0.01 ± 0.03	0.02 ± 0.01	0.05 ± 0.03	-0.01 ± 0.01	0.09 ± 0.03
NGC 6791	0.35 ± 0.04	0.04 ± 0.03	0.08 ± 0.06	0.11 ± 0.03	0.01 ± 0.07	0.01 ± 0.03	-0.02 ± 0.05	0.03 ± 0.10
	-0.02 ± 0.03	0.09 ± 0.05	-0.06 ± 0.30	-0.02 ± 0.09	0.01 ± 0.13	0.11 ± 0.08	0.01 ± 0.04	0.14 ± 0.07
NGC 2678	0.00 ± 0.01	—	—	0.03 ± 0.01	0.12 ± 0.02	0.03 ± 0.01	-0.04 ± 0.04	0.05 ± 0.04
	0.01 ± 0.02	-0.26 ± 0.06	—	-0.29 ± 0.06	0.02 ± 0.02	-0.33 ± 0.15	-0.03 ± 0.02	-0.07 ± 0.08
NGC 1977	-0.21 ± 0.04	-0.07 ± 0.01	—	-0.14 ± 0.01	-0.24 ± 0.14	-0.10 ± 0.01	0.16 ± 0.05	0.09 ± 0.02
	0.02 ± 0.06	-0.05 ± 0.02	—	-0.01 ± 0.10	-0.08 ± 0.02	-0.12 ± 0.10	0.00 ± 0.06	0.07 ± 0.04
Berkeley 20	-0.40 ± 0.01	0.04 ± 0.02	0.25 ± 0.07	-0.02 ± 0.02	0.12 ± 0.04	0.09 ± 0.02	0.01 ± 0.07	0.03 ± 0.07
	0.01 ± 0.03	-0.10 ± 0.03	-0.01 ± 0.09	0.01 ± 0.07	0.01 ± 0.03	0.05 ± 0.07	0.05 ± 0.03	0.12 ± 0.07
Berkeley 98	-0.00 ± 0.01	-0.00 ± 0.02	-0.21 ± 0.14	-0.00 ± 0.01	0.05 ± 0.07	0.02 ± 0.01	0.15 ± 0.07	0.02 ± 0.04
	-0.01 ± 0.02	-0.08 ± 0.04	0.06 ± 0.06	0.06 ± 0.04	-0.03 ± 0.02	0.05 ± 0.05	-0.01 ± 0.02	0.03 ± 0.04
NGC 2232	-0.36 ± 0.01	0.05 ± 0.02	-0.01 ± 0.04	0.09 ± 0.02	-0.04 ± 0.02	0.00 ± 0.01	0.06 ± 0.06	0.05 ± 0.03
	0.04 ± 0.01	—	-0.03 ± 0.04	0.03 ± 0.03	—	-0.02 ± 0.04	-0.02 ± 0.02	—
ASCC 116	-0.13 ± 0.01	-0.01 ± 0.01	0.06 ± 0.04	0.01 ± 0.01	0.02 ± 0.02	0.02 ± 0.01	0.07 ± 0.03	0.03 ± 0.03
	0.04 ± 0.01	-0.04 ± 0.02	—	-0.03 ± 0.03	-0.03 ± 0.01	-0.10 ± 0.04	0.01 ± 0.01	-0.09 ± 0.03
NGC 1664	-0.03 ± 0.01	—	0.11 ± 0.04	-0.07 ± 0.01	-0.05 ± 0.02	0.01 ± 0.01	0.04 ± 0.03	-0.05 ± 0.03
	0.01 ± 0.01	-0.02 ± 0.02	—	-0.01 ± 0.03	-0.00 ± 0.02	-0.00 ± 0.04	-0.02 ± 0.01	-0.06 ± 0.04
BH 211	0.21 ± 0.02	-0.06 ± 0.01	0.22 ± 0.03	-0.05 ± 0.03	-0.02 ± 0.02	-0.00 ± 0.03	0.02 ± 0.02	0.01 ± 0.08
	-0.04 ± 0.01	-0.02 ± 0.03	-0.34 ± 0.04	-0.02 ± 0.05	0.08 ± 0.01	-0.01 ± 0.03	0.00 ± 0.01	0.02 ± 0.04
Teutsch 12	-0.17 ± 0.01	—	0.31 ± 0.06	-0.05 ± 0.02	0.08 ± 0.03	-0.02 ± 0.02	0.04 ± 0.04	-0.02 ± 0.05
	0.04 ± 0.02	-0.02 ± 0.03	—	0.01 ± 0.05	-0.07 ± 0.03	-0.58 ± 0.07	-0.03 ± 0.02	0.11 ± 0.06

Continued on next page

Table D.1 – Continued

Cluster name	[Fe/H] (dex)	[O/Fe] (dex)	[Na/Fe] (dex)	[Mg/Fe] (dex)	[Al/Fe] (dex)	[Si/Fe] (dex)	[S/Fe] (dex)	[K/Fe] (dex)
	[Ca/Fe] (dex)	[Ti/Fe] (dex)	[V/Fe] (dex)	[Cr/Fe] (dex)	[Mn/Fe] (dex)	[Co/Fe] (dex)	[Ni/Fe] (dex)	[Cu/Fe] (dex)
King 5	-0.14 ± 0.01	-0.01 ± 0.01	0.04 ± 0.05	-0.02 ± 0.02	-0.01 ± 0.04	0.00 ± 0.02	0.04 ± 0.04	0.05 ± 0.05
	0.02 ± 0.03	0.00 ± 0.03	-0.16 ± 0.04	-0.00 ± 0.06	-0.02 ± 0.03	0.02 ± 0.07	-0.03 ± 0.02	0.02 ± 0.04
Dol Dzim 4	-0.47 ± 0.01	0.18 ± 0.03	-0.14 ± 0.08	0.09 ± 0.02	0.11 ± 0.03	0.06 ± 0.02	0.11 ± 0.06	0.22 ± 0.06
	0.05 ± 0.03	-0.02 ± 0.03	0.36 ± 0.10	-0.41 ± 0.07	-0.09 ± 0.03	-0.02 ± 0.08	0.03 ± 0.03	0.17 ± 0.07
NGC 1798	-0.27 ± 0.03	0.01 ± 0.03	0.13 ± 0.08	0.00 ± 0.02	0.03 ± 0.06	0.01 ± 0.01	0.04 ± 0.07	0.01 ± 0.12
	0.04 ± 0.02	-0.05 ± 0.03	0.03 ± 0.10	-0.02 ± 0.05	-0.03 ± 0.02	-0.41 ± 0.60	-0.02 ± 0.02	-0.00 ± 0.08
Basel 11b	-0.00 ± 0.01	-0.02 ± 0.01	0.04 ± 0.04	-0.04 ± 0.01	-0.07 ± 0.02	0.01 ± 0.01	0.08 ± 0.03	0.04 ± 0.03
	-0.02 ± 0.01	-0.05 ± 0.02	0.10 ± 0.04	-0.05 ± 0.03	0.04 ± 0.01	-0.06 ± 0.03	-0.03 ± 0.01	-0.19 ± 0.03
Collinder 70	-0.10 ± 0.06	-0.14 ± 0.10	0.23 ± 0.05	-0.14 ± 0.13	-0.18 ± 0.24	-0.14 ± 0.10	-0.10 ± 0.23	0.02 ± 0.21
	-0.04 ± 0.19	-0.04 ± 0.14	—	0.05 ± 0.09	0.07 ± 0.11	-0.19 ± 0.36	-0.05 ± 0.13	0.09 ± 0.08
IC 1369	-0.08 ± 0.03	-0.08 ± 0.02	0.08 ± 0.10	-0.04 ± 0.02	-0.11 ± 0.02	-0.01 ± 0.01	0.09 ± 0.07	0.02 ± 0.03
	0.01 ± 0.04	-0.08 ± 0.02	—	0.01 ± 0.04	0.04 ± 0.03	-0.04 ± 0.04	-0.06 ± 0.01	0.09 ± 0.04
NGC 2264	-0.17 ± 0.06	-0.10 ± 0.05	—	-0.09 ± 0.06	-0.04 ± 0.16	-0.07 ± 0.07	0.20 ± 0.42	0.16 ± 0.09
	-0.01 ± 0.10	-0.09 ± 0.14	-0.08 ± 0.06	-0.07 ± 0.13	-0.07 ± 0.06	-0.30 ± 0.25	-0.04 ± 0.07	0.16 ± 0.19
Berkeley 9	-0.09 ± 0.06	—	-0.31 ± 0.66	0.03 ± 0.08	0.11 ± 0.20	-0.01 ± 0.04	0.12 ± 0.07	-0.08 ± 0.19
	0.07 ± 0.06	-0.02 ± 0.02	—	0.05 ± 0.09	-0.11 ± 0.09	0.15 ± 0.25	0.01 ± 0.07	0.01 ± 0.10
Melotte 71	-0.13 ± 0.02	—	0.01 ± 0.06	-0.05 ± 0.01	-0.01 ± 0.02	-0.01 ± 0.01	0.07 ± 0.03	0.03 ± 0.03
	0.04 ± 0.01	-0.01 ± 0.03	—	0.04 ± 0.07	-0.00 ± 0.02	-0.15 ± 0.09	-0.02 ± 0.01	-0.01 ± 0.05
Czernik 30	-0.40 ± 0.01	0.05 ± 0.02	-0.10 ± 0.06	-0.02 ± 0.02	0.06 ± 0.03	0.00 ± 0.02	0.22 ± 0.05	0.00 ± 0.05
	0.02 ± 0.02	-0.06 ± 0.02	-0.10 ± 0.09	-0.05 ± 0.05	-0.02 ± 0.02	0.01 ± 0.05	0.03 ± 0.02	0.12 ± 0.05
Trumpler 3	0.14 ± 0.01	0.02 ± 0.01	0.03 ± 0.04	0.03 ± 0.01	-0.19 ± 0.02	-0.00 ± 0.01	0.12 ± 0.03	-0.08 ± 0.03
	-0.03 ± 0.01	0.09 ± 0.02	-0.02 ± 0.05	-0.02 ± 0.03	0.02 ± 0.01	0.05 ± 0.03	0.10 ± 0.01	0.24 ± 0.03
FSR 0823	-0.20 ± 0.01	0.06 ± 0.02	0.17 ± 0.06	0.04 ± 0.02	0.10 ± 0.03	0.09 ± 0.02	0.15 ± 0.05	0.05 ± 0.05
	0.03 ± 0.02	0.04 ± 0.03	—	-0.15 ± 0.05	-0.06 ± 0.02	-0.02 ± 0.07	-0.01 ± 0.02	0.11 ± 0.06
Sigma Orionis	-0.15 ± 0.05	-0.10 ± 0.06	—	-0.11 ± 0.06	-0.20 ± 0.16	-0.07 ± 0.06	—	0.09 ± 0.02
	-0.08 ± 0.10	-0.19 ± 0.02	—	-0.09 ± 0.03	-0.03 ± 0.03	-0.20 ± 0.27	-0.06 ± 0.09	0.16 ± 0.08

Continued on next page

Table D.1 – Continued

Cluster name	[Fe/H] (dex)	[O/Fe] (dex)	[Na/Fe] (dex)	[Mg/Fe] (dex)	[Al/Fe] (dex)	[Si/Fe] (dex)	[S/Fe] (dex)	[K/Fe] (dex)
	[Ca/Fe] (dex)	[Ti/Fe] (dex)	[V/Fe] (dex)	[Cr/Fe] (dex)	[Mn/Fe] (dex)	[Co/Fe] (dex)	[Ni/Fe] (dex)	[Cu/Fe] (dex)
Berkeley 17	-0.16 ± 0.02	0.04 ± 0.02	-0.10 ± 0.15	0.05 ± 0.02	0.04 ± 0.04	0.03 ± 0.01	0.09 ± 0.05	0.08 ± 0.05
	0.02 ± 0.02	0.00 ± 0.03	0.08 ± 0.11	-0.02 ± 0.04	-0.01 ± 0.02	0.03 ± 0.04	0.03 ± 0.02	0.10 ± 0.06
King 8	-0.16 ± 0.01	-0.06 ± 0.02	0.16 ± 0.05	-0.02 ± 0.01	0.02 ± 0.02	-0.02 ± 0.01	0.07 ± 0.04	-0.05 ± 0.04
	0.02 ± 0.02	-0.03 ± 0.02	0.08 ± 0.07	-0.00 ± 0.04	-0.04 ± 0.02	-0.06 ± 0.05	-0.03 ± 0.02	-0.02 ± 0.04
FSR 0546	-0.13 ± 0.01	0.04 ± 0.03	-0.31 ± 0.07	-0.01 ± 0.02	0.18 ± 0.03	0.01 ± 0.02	0.15 ± 0.05	0.02 ± 0.06
	0.06 ± 0.02	-0.03 ± 0.03	—	0.08 ± 0.06	0.01 ± 0.03	0.01 ± 0.07	0.02 ± 0.02	-0.13 ± 0.06
King 12	0.39 ± 0.01	-0.04 ± 0.02	0.19 ± 0.05	0.02 ± 0.01	0.01 ± 0.03	-0.06 ± 0.01	-0.09 ± 0.04	-0.13 ± 0.04
	-0.03 ± 0.01	0.09 ± 0.02	0.16 ± 0.07	0.13 ± 0.04	0.03 ± 0.02	0.19 ± 0.05	0.03 ± 0.02	-0.04 ± 0.04
ASCC 18	-0.14 ± 0.01	-0.04 ± 0.02	—	-0.15 ± 0.01	-0.06 ± 0.03	-0.08 ± 0.01	0.29 ± 0.07	0.09 ± 0.02
	0.06 ± 0.02	-0.20 ± 0.03	—	-0.08 ± 0.05	-0.20 ± 0.03	-0.50 ± 0.14	-0.06 ± 0.02	0.15 ± 0.07
Berkeley 43	0.03 ± 0.01	-0.05 ± 0.01	0.15 ± 0.03	-0.08 ± 0.01	-0.22 ± 0.02	0.03 ± 0.01	0.13 ± 0.02	-0.18 ± 0.03
	-0.05 ± 0.01	-0.01 ± 0.01	-0.02 ± 0.04	-0.08 ± 0.03	0.12 ± 0.01	0.01 ± 0.03	0.02 ± 0.01	-0.26 ± 0.03
SAI 116	0.16 ± 0.01	-0.03 ± 0.01	0.19 ± 0.10	-0.02 ± 0.01	-0.04 ± 0.02	0.04 ± 0.01	0.06 ± 0.02	-0.11 ± 0.02
	-0.03 ± 0.01	-0.01 ± 0.01	-0.09 ± 0.08	-0.09 ± 0.02	0.12 ± 0.03	0.06 ± 0.05	0.01 ± 0.01	0.03 ± 0.03
ASCC 21	-0.18 ± 0.01	-0.04 ± 0.07	0.07 ± 0.05	-0.07 ± 0.01	-0.06 ± 0.14	-0.08 ± 0.03	0.31 ± 0.10	0.20 ± 0.10
	0.17 ± 0.09	-0.06 ± 0.09	—	0.05 ± 0.20	-0.00 ± 0.05	-0.28 ± 0.09	-0.05 ± 0.02	0.01 ± 0.14
Ruprecht 82	-0.03 ± 0.01	—	0.19 ± 0.04	-0.03 ± 0.01	-0.03 ± 0.02	0.02 ± 0.01	0.12 ± 0.03	-0.08 ± 0.03
	-0.00 ± 0.01	-0.01 ± 0.02	—	-0.04 ± 0.03	0.02 ± 0.01	-0.01 ± 0.04	-0.03 ± 0.01	0.09 ± 0.03
Collinder 69	-0.12 ± 0.04	-0.07 ± 0.03	-0.89 ± 0.68	-0.06 ± 0.05	-0.10 ± 0.13	-0.07 ± 0.06	0.00 ± 0.19	0.01 ± 0.07
	-0.02 ± 0.09	-0.04 ± 0.13	0.00 ± 0.09	-0.07 ± 0.22	-0.02 ± 0.05	-0.45 ± 0.39	-0.05 ± 0.05	0.20 ± 0.12
FSR 0816	-0.10 ± 0.02	—	—	0.19 ± 0.04	-0.25 ± 0.14	0.29 ± 0.19	-0.06 ± 0.08	-1.99 ± 0.18
	0.34 ± 0.05	—	—	-0.06 ± 0.14	0.36 ± 0.09	—	-0.17 ± 0.15	0.25 ± 0.16
NGC 2355	-0.14 ± 0.01	—	0.03 ± 0.05	-0.04 ± 0.01	-0.02 ± 0.02	-0.02 ± 0.01	0.04 ± 0.03	0.01 ± 0.03
	0.01 ± 0.01	-0.04 ± 0.02	—	-0.00 ± 0.04	-0.03 ± 0.02	0.02 ± 0.05	-0.02 ± 0.01	-0.01 ± 0.04
NGC 1980	-0.08 ± 0.04	-0.06 ± 0.06	—	-0.08 ± 0.09	-0.17 ± 0.18	-0.08 ± 0.06	—	0.06 ± 0.02
	0.01 ± 0.19	-0.11 ± 0.02	—	-0.02 ± 0.12	-0.06 ± 0.03	-0.54 ± 0.41	-0.10 ± 0.07	0.11 ± 0.05

Continued on next page

Table D.1 – Continued

Cluster name	[Fe/H] (dex)	[O/Fe] (dex)	[Na/Fe] (dex)	[Mg/Fe] (dex)	[Al/Fe] (dex)	[Si/Fe] (dex)	[S/Fe] (dex)	[K/Fe] (dex)
	[Ca/Fe] (dex)	[Ti/Fe] (dex)	[V/Fe] (dex)	[Cr/Fe] (dex)	[Mn/Fe] (dex)	[Co/Fe] (dex)	[Ni/Fe] (dex)	[Cu/Fe] (dex)
FSR 0494	-0.01 ± 0.01	—	-0.17 ± 0.07	-0.03 ± 0.02	-0.01 ± 0.04	-0.05 ± 0.02	-0.01 ± 0.05	-0.06 ± 0.09
	0.01 ± 0.02	-0.01 ± 0.04	—	0.00 ± 0.06	-0.01 ± 0.03	-0.14 ± 0.08	-0.02 ± 0.02	-0.06 ± 0.06
Berkeley 79	0.32 ± 0.01	0.00 ± 0.01	0.22 ± 0.04	0.02 ± 0.01	-0.04 ± 0.02	0.00 ± 0.01	-0.01 ± 0.03	0.01 ± 0.03
	-0.00 ± 0.01	0.07 ± 0.02	0.15 ± 0.05	-0.06 ± 0.03	0.17 ± 0.01	0.06 ± 0.03	0.07 ± 0.01	0.03 ± 0.03
FSR 0656	-0.32 ± 0.01	0.02 ± 0.02	0.22 ± 0.06	0.05 ± 0.02	0.06 ± 0.03	0.03 ± 0.01	0.15 ± 0.05	0.10 ± 0.05
	0.05 ± 0.02	0.03 ± 0.03	—	0.03 ± 0.05	-0.03 ± 0.02	0.06 ± 0.06	0.05 ± 0.02	0.18 ± 0.05
NGC 358	-0.31 ± 0.01	—	0.36 ± 0.07	0.04 ± 0.02	0.14 ± 0.03	0.02 ± 0.02	0.01 ± 0.05	0.06 ± 0.05
	0.04 ± 0.02	-0.06 ± 0.03	—	-0.10 ± 0.06	-0.05 ± 0.03	-0.12 ± 0.07	0.01 ± 0.02	-0.04 ± 0.06
Chupina 5	0.09 ± 0.01	-0.00 ± 0.01	0.02 ± 0.04	0.01 ± 0.01	-0.02 ± 0.02	-0.01 ± 0.01	0.02 ± 0.03	0.04 ± 0.03
	0.00 ± 0.01	0.02 ± 0.02	—	0.09 ± 0.03	0.05 ± 0.01	0.03 ± 0.04	0.03 ± 0.01	-0.02 ± 0.03
King 7	-0.13 ± 0.05	-0.03 ± 0.03	0.13 ± 0.10	-0.03 ± 0.01	-0.11 ± 0.04	-0.00 ± 0.01	0.10 ± 0.03	-0.04 ± 0.06
	-0.01 ± 0.02	-0.05 ± 0.03	0.34 ± 0.20	-0.06 ± 0.08	0.05 ± 0.03	-0.03 ± 0.04	-0.07 ± 0.02	0.08 ± 0.06
NGC 2158	-0.21 ± 0.02	0.02 ± 0.07	0.05 ± 0.09	0.02 ± 0.03	-0.00 ± 0.03	0.01 ± 0.02	0.07 ± 0.08	0.06 ± 0.05
	0.03 ± 0.03	-0.04 ± 0.04	-0.13 ± 0.05	-0.06 ± 0.09	-0.03 ± 0.03	-0.05 ± 0.16	-0.02 ± 0.02	0.03 ± 0.10
Teutsch 10	-0.27 ± 0.01	—	0.19 ± 0.05	-0.00 ± 0.01	-0.16 ± 0.02	-0.13 ± 0.01	0.11 ± 0.04	0.07 ± 0.04
	0.09 ± 0.02	0.09 ± 0.03	—	0.08 ± 0.04	0.10 ± 0.02	0.15 ± 0.06	-0.01 ± 0.02	0.44 ± 0.05
Teutsch 51	-0.33 ± 0.02	—	0.10 ± 0.13	0.02 ± 0.02	0.09 ± 0.05	0.03 ± 0.04	0.04 ± 0.09	0.03 ± 0.13
	0.04 ± 0.03	-0.01 ± 0.05	—	-0.00 ± 0.11	-0.05 ± 0.04	-0.10 ± 0.10	0.00 ± 0.03	-0.27 ± 0.18
NGC 2420	-0.19 ± 0.03	0.04 ± 0.03	-0.02 ± 0.11	-0.00 ± 0.02	0.01 ± 0.03	-0.00 ± 0.02	0.04 ± 0.05	0.04 ± 0.04
	0.05 ± 0.03	0.01 ± 0.06	0.11 ± 0.14	0.02 ± 0.06	-0.01 ± 0.02	-0.23 ± 0.32	-0.02 ± 0.02	-0.01 ± 0.10
NGC 2318	-0.03 ± 0.01	—	0.10 ± 0.04	-0.06 ± 0.01	-0.05 ± 0.02	0.01 ± 0.01	0.09 ± 0.03	-0.07 ± 0.03
	-0.01 ± 0.01	-0.02 ± 0.02	—	-0.03 ± 0.03	0.01 ± 0.01	-0.02 ± 0.04	-0.02 ± 0.01	0.08 ± 0.03
Teutsch 84	0.20 ± 0.01	-0.08 ± 0.02	0.06 ± 0.07	-0.03 ± 0.01	-0.04 ± 0.04	0.02 ± 0.01	0.03 ± 0.04	-0.05 ± 0.04
	0.00 ± 0.01	0.01 ± 0.02	—	0.02 ± 0.04	0.04 ± 0.02	0.03 ± 0.10	0.04 ± 0.02	0.08 ± 0.04
ASCC 16	-0.05 ± 0.05	-0.06 ± 0.02	-0.80 ± 0.05	-0.06 ± 0.06	-0.14 ± 0.07	-0.08 ± 0.04	0.04 ± 0.11	0.04 ± 0.02
	-0.03 ± 0.07	-0.10 ± 0.09	—	-0.05 ± 0.08	-0.05 ± 0.12	-0.46 ± 0.10	-0.04 ± 0.04	0.13 ± 0.09

Continued on next page

Table D.1 – Continued

Cluster name	[Fe/H] (dex)	[O/Fe] (dex)	[Na/Fe] (dex)	[Mg/Fe] (dex)	[Al/Fe] (dex)	[Si/Fe] (dex)	[S/Fe] (dex)	[K/Fe] (dex)
	[Ca/Fe] (dex)	[Ti/Fe] (dex)	[V/Fe] (dex)	[Cr/Fe] (dex)	[Mn/Fe] (dex)	[Co/Fe] (dex)	[Ni/Fe] (dex)	[Cu/Fe] (dex)
NGC 752	-0.04 ± 0.01	-0.03 ± 0.01	-0.00 ± 0.04	-0.09 ± 0.01	-0.05 ± 0.02	-0.02 ± 0.01	-0.06 ± 0.03	-0.03 ± 0.03
	0.01 ± 0.01	-0.06 ± 0.02	—	-0.00 ± 0.03	-0.02 ± 0.01	-0.11 ± 0.04	-0.04 ± 0.01	-0.08 ± 0.03
NGC 7789	-0.01 ± 0.02	-0.03 ± 0.03	-0.18 ± 0.48	-0.02 ± 0.04	-0.04 ± 0.07	-0.00 ± 0.04	0.05 ± 0.05	0.05 ± 0.09
	0.01 ± 0.05	-0.03 ± 0.04	-0.15 ± 0.04	-0.01 ± 0.04	0.01 ± 0.03	-0.03 ± 0.04	-0.02 ± 0.05	0.03 ± 0.06
Chupina 4	-0.00 ± 0.01	—	0.08 ± 0.04	-0.02 ± 0.01	-0.04 ± 0.02	-0.04 ± 0.01	0.01 ± 0.03	-0.15 ± 0.03
	0.02 ± 0.01	-0.01 ± 0.02	—	0.07 ± 0.04	0.04 ± 0.02	-0.00 ± 0.05	0.03 ± 0.01	-0.09 ± 0.04
Berkeley 19	-0.32 ± 0.01	0.03 ± 0.02	-0.11 ± 0.05	0.07 ± 0.01	0.03 ± 0.03	0.01 ± 0.01	0.07 ± 0.05	0.02 ± 0.05
	0.00 ± 0.02	-0.02 ± 0.02	-0.21 ± 0.06	-0.03 ± 0.05	-0.04 ± 0.02	-0.05 ± 0.05	-0.03 ± 0.02	0.06 ± 0.05
NGC 6819	0.05 ± 0.03	-0.01 ± 0.03	0.07 ± 0.09	-0.01 ± 0.01	-0.04 ± 0.03	0.00 ± 0.03	0.00 ± 0.03	-0.04 ± 0.07
	0.01 ± 0.02	0.01 ± 0.03	0.04 ± 0.13	0.01 ± 0.03	0.05 ± 0.03	0.02 ± 0.06	0.02 ± 0.02	0.04 ± 0.06
NGC 1981	-0.18 ± 0.01	-0.10 ± 0.01	—	-0.10 ± 0.01	-0.35 ± 0.02	-0.09 ± 0.01	—	—
	-0.10 ± 0.01	—	—	—	—	-0.40 ± 0.09	0.11 ± 0.02	0.27 ± 0.04
NGC 6383	-0.39 ± 0.03	—	-1.79 ± 0.09	-0.45 ± 0.03	-0.35 ± 0.05	-0.46 ± 0.03	—	-1.46 ± 0.06
	0.55 ± 0.04	—	—	—	-0.08 ± 0.05	-0.43 ± 0.12	-0.10 ± 0.04	-0.72 ± 0.09
ASCC 20	0.02 ± 0.01	-0.09 ± 0.01	—	-0.04 ± 0.01	-0.16 ± 0.02	-0.04 ± 0.01	—	—
	-0.07 ± 0.01	—	—	—	—	-0.55 ± 0.08	-0.03 ± 0.03	0.08 ± 0.04
NGC 2682	0.01 ± 0.03	-0.01 ± 0.02	0.04 ± 0.07	-0.00 ± 0.02	-0.01 ± 0.02	-0.00 ± 0.02	-0.01 ± 0.05	-0.03 ± 0.03
	0.01 ± 0.02	-0.01 ± 0.03	0.04 ± 0.08	0.03 ± 0.05	0.03 ± 0.02	-0.02 ± 0.07	0.02 ± 0.01	-0.03 ± 0.06
Chupina 3	0.01 ± 0.02	—	—	0.03 ± 0.02	0.07 ± 0.04	0.01 ± 0.02	-0.02 ± 0.06	-0.03 ± 0.09
	-0.02 ± 0.03	—	—	0.04 ± 0.10	0.02 ± 0.03	0.08 ± 0.19	0.02 ± 0.03	-0.24 ± 0.18
IC 166	-0.10 ± 0.03	0.01 ± 0.02	0.03 ± 0.20	0.03 ± 0.04	-0.05 ± 0.16	0.00 ± 0.03	0.06 ± 0.10	0.02 ± 0.07
	0.03 ± 0.04	0.02 ± 0.10	—	-0.04 ± 0.09	0.00 ± 0.03	-0.19 ± 0.42	0.00 ± 0.03	-0.12 ± 0.30
NGC 2324	-0.19 ± 0.02	-0.05 ± 0.01	0.14 ± 0.04	-0.04 ± 0.03	-0.03 ± 0.03	-0.01 ± 0.02	0.07 ± 0.07	0.03 ± 0.05
	0.02 ± 0.02	0.03 ± 0.07	0.00 ± 0.04	0.00 ± 0.04	0.00 ± 0.02	-0.14 ± 0.15	-0.04 ± 0.02	0.14 ± 0.04
Platais 4	-0.31 ± 0.01	0.02 ± 0.01	0.04 ± 0.04	0.05 ± 0.01	0.04 ± 0.02	0.05 ± 0.01	0.05 ± 0.03	0.03 ± 0.03
	0.03 ± 0.01	0.02 ± 0.02	0.05 ± 0.05	0.01 ± 0.03	0.02 ± 0.02	-0.03 ± 0.04	0.02 ± 0.01	0.14 ± 0.03

Continued on next page

Table D.1 – Continued

Cluster name	[Fe/H] (dex)	[O/Fe] (dex)	[Na/Fe] (dex)	[Mg/Fe] (dex)	[Al/Fe] (dex)	[Si/Fe] (dex)	[S/Fe] (dex)	[K/Fe] (dex)
	[Ca/Fe] (dex)	[Ti/Fe] (dex)	[V/Fe] (dex)	[Cr/Fe] (dex)	[Mn/Fe] (dex)	[Co/Fe] (dex)	[Ni/Fe] (dex)	[Cu/Fe] (dex)
Czernik 23	-0.28 ± 0.01	—	0.16 ± 0.05	0.01 ± 0.01	-0.07 ± 0.02	0.01 ± 0.01	0.20 ± 0.04	-0.06 ± 0.04
	0.04 ± 0.02	-0.05 ± 0.03	—	-0.06 ± 0.04	0.02 ± 0.02	-0.21 ± 0.05	-0.05 ± 0.02	0.10 ± 0.04
NGC 4337	0.24 ± 0.03	-0.02 ± 0.02	0.23 ± 0.03	0.01 ± 0.01	0.01 ± 0.03	0.03 ± 0.01	-0.00 ± 0.04	-0.04 ± 0.04
	0.00 ± 0.02	0.05 ± 0.03	0.05 ± 0.03	-0.03 ± 0.06	0.10 ± 0.03	0.04 ± 0.05	0.05 ± 0.01	0.03 ± 0.03
NGC 2447	-0.08 ± 0.01	—	0.11 ± 0.04	-0.02 ± 0.01	0.01 ± 0.02	0.01 ± 0.01	0.07 ± 0.03	-0.05 ± 0.03
	0.02 ± 0.01	-0.04 ± 0.02	—	-0.00 ± 0.03	0.01 ± 0.02	-0.05 ± 0.04	-0.05 ± 0.01	-0.01 ± 0.04
Berkeley 53	-0.08 ± 0.02	-0.04 ± 0.02	0.14 ± 0.05	-0.02 ± 0.01	-0.09 ± 0.09	0.01 ± 0.01	0.03 ± 0.06	0.04 ± 0.04
	0.02 ± 0.04	-0.02 ± 0.03	-0.06 ± 0.11	-0.02 ± 0.08	-0.00 ± 0.03	-0.02 ± 0.05	-0.03 ± 0.01	0.01 ± 0.05
NGC 1912	-0.14 ± 0.01	—	0.04 ± 0.04	-0.09 ± 0.01	-0.08 ± 0.02	-0.02 ± 0.01	0.18 ± 0.03	-0.12 ± 0.03
	-0.02 ± 0.01	0.04 ± 0.02	—	-0.05 ± 0.04	0.02 ± 0.02	-0.07 ± 0.05	-0.04 ± 0.01	0.06 ± 0.04
NGC 1857	-0.14 ± 0.01	—	0.03 ± 0.04	-0.07 ± 0.01	-0.01 ± 0.02	0.01 ± 0.01	0.14 ± 0.03	-0.11 ± 0.03
	-0.01 ± 0.01	-0.02 ± 0.02	—	-0.13 ± 0.03	-0.01 ± 0.02	-0.04 ± 0.04	-0.06 ± 0.01	0.24 ± 0.04
FSR 0304	-0.07 ± 0.01	0.07 ± 0.02	0.00 ± 0.15	0.06 ± 0.04	0.10 ± 0.06	0.02 ± 0.03	0.15 ± 0.10	0.02 ± 0.08
	0.04 ± 0.03	0.02 ± 0.05	0.14 ± 0.07	-0.04 ± 0.05	0.01 ± 0.02	0.03 ± 0.06	0.03 ± 0.02	0.06 ± 0.05
NGC 2304	-0.12 ± 0.02	-0.02 ± 0.01	-0.08 ± 0.10	-0.03 ± 0.01	0.01 ± 0.03	-0.00 ± 0.01	-0.02 ± 0.04	0.07 ± 0.04
	0.05 ± 0.02	0.04 ± 0.03	0.12 ± 0.05	0.06 ± 0.05	-0.01 ± 0.02	0.02 ± 0.06	-0.04 ± 0.02	0.02 ± 0.06
Ruprecht 147	0.12 ± 0.03	-0.05 ± 0.03	0.11 ± 0.03	-0.01 ± 0.02	0.02 ± 0.04	-0.00 ± 0.05	0.02 ± 0.06	0.04 ± 0.08
	-0.01 ± 0.04	-0.07 ± 0.09	0.01 ± 0.07	0.02 ± 0.09	0.04 ± 0.03	0.14 ± 0.20	0.01 ± 0.02	-0.09 ± 0.20
Teutsch 5	-0.35 ± 0.01	—	-0.40 ± 0.06	0.07 ± 0.01	0.08 ± 0.02	-0.07 ± 0.01	-0.06 ± 0.04	0.06 ± 0.04
	0.05 ± 0.02	0.03 ± 0.03	—	-0.08 ± 0.05	-0.03 ± 0.02	0.01 ± 0.06	0.02 ± 0.02	-0.11 ± 0.05
FSR 1113	-0.30 ± 0.01	0.02 ± 0.03	0.07 ± 0.07	-0.06 ± 0.02	0.04 ± 0.03	0.06 ± 0.02	0.21 ± 0.05	-0.10 ± 0.05
	0.02 ± 0.02	-0.05 ± 0.03	—	0.05 ± 0.06	-0.08 ± 0.03	-0.64 ± 0.07	-0.01 ± 0.02	0.02 ± 0.06
Berkeley 29	-0.49 ± 0.03	0.10 ± 0.02	-0.00 ± 0.06	0.06 ± 0.07	0.06 ± 0.12	0.04 ± 0.03	0.07 ± 0.09	-0.02 ± 0.06
	0.03 ± 0.02	-0.14 ± 0.04	-0.10 ± 0.12	-0.11 ± 0.10	-0.10 ± 0.04	0.16 ± 0.10	0.03 ± 0.02	0.07 ± 0.08
NGC 2240	-0.15 ± 0.01	0.04 ± 0.01	0.00 ± 0.03	0.03 ± 0.01	-0.01 ± 0.02	0.02 ± 0.01	0.03 ± 0.03	-0.01 ± 0.03
	0.01 ± 0.01	—	0.04 ± 0.03	-0.02 ± 0.03	0.06 ± 0.01	0.05 ± 0.03	-0.02 ± 0.01	0.10 ± 0.03

Continued on next page

Table D.1 – Continued

Cluster name	[Fe/H] (dex)	[O/Fe] (dex)	[Na/Fe] (dex)	[Mg/Fe] (dex)	[Al/Fe] (dex)	[Si/Fe] (dex)	[S/Fe] (dex)	[K/Fe] (dex)
	[Ca/Fe] (dex)	[Ti/Fe] (dex)	[V/Fe] (dex)	[Cr/Fe] (dex)	[Mn/Fe] (dex)	[Co/Fe] (dex)	[Ni/Fe] (dex)	[Cu/Fe] (dex)
Berkeley 91	0.09 ± 0.01	-0.02 ± 0.02	-0.03 ± 0.05	-0.02 ± 0.01	0.06 ± 0.03	-0.07 ± 0.01	0.08 ± 0.03	0.02 ± 0.04
	0.04 ± 0.01	0.07 ± 0.02	-0.21 ± 0.06	0.01 ± 0.04	0.04 ± 0.02	-0.12 ± 0.05	0.01 ± 0.01	0.05 ± 0.04
Collinder 220	-0.08 ± 0.01	-0.01 ± 0.01	0.22 ± 0.04	-0.03 ± 0.01	-0.07 ± 0.02	0.03 ± 0.01	0.13 ± 0.03	-0.08 ± 0.03
	-0.00 ± 0.01	-0.03 ± 0.02	—	-0.05 ± 0.03	0.04 ± 0.01	0.01 ± 0.04	-0.06 ± 0.01	0.07 ± 0.03
Haffner 4	-0.16 ± 0.01	—	-0.11 ± 0.07	-0.04 ± 0.02	0.02 ± 0.04	-0.07 ± 0.02	0.07 ± 0.05	-0.01 ± 0.05
	0.03 ± 0.02	0.00 ± 0.04	—	-0.09 ± 0.06	-0.01 ± 0.03	-1.01 ± 0.08	-0.04 ± 0.02	0.06 ± 0.07
FSR 0542	-0.23 ± 0.01	0.02 ± 0.03	-0.05 ± 0.06	0.00 ± 0.02	0.10 ± 0.03	0.01 ± 0.02	0.21 ± 0.05	0.12 ± 0.05
	0.03 ± 0.02	-0.01 ± 0.03	—	0.05 ± 0.06	-0.07 ± 0.03	0.07 ± 0.07	-0.01 ± 0.02	-0.01 ± 0.06
Berkeley 44	-0.00 ± 0.01	0.04 ± 0.01	-0.16 ± 0.03	-0.02 ± 0.01	-0.30 ± 0.02	0.01 ± 0.01	0.02 ± 0.03	-0.15 ± 0.03
	-0.14 ± 0.01	-0.13 ± 0.01	-0.29 ± 0.04	-0.17 ± 0.03	0.06 ± 0.01	0.05 ± 0.03	-0.03 ± 0.01	0.04 ± 0.03
FSR 0942	-0.28 ± 0.01	—	0.13 ± 0.05	0.01 ± 0.01	-0.02 ± 0.02	-0.00 ± 0.01	0.08 ± 0.04	-0.00 ± 0.04
	0.04 ± 0.02	-0.05 ± 0.03	—	-0.18 ± 0.04	-0.06 ± 0.02	-0.19 ± 0.06	-0.06 ± 0.02	0.06 ± 0.05
NGC 7058	0.03 ± 0.04	0.07 ± 0.11	—	-0.07 ± 0.02	-0.07 ± 0.18	-0.11 ± 0.03	-0.04 ± 0.13	0.10 ± 0.04
	0.09 ± 0.05	-0.02 ± 0.16	-0.50 ± 0.56	-0.02 ± 0.08	-0.08 ± 0.03	0.10 ± 0.24	-0.03 ± 0.04	0.06 ± 0.09
Berkeley 33	-0.30 ± 0.01	—	0.17 ± 0.06	-0.09 ± 0.04	-0.07 ± 0.02	-0.08 ± 0.02	0.12 ± 0.04	-0.04 ± 0.04
	0.05 ± 0.02	0.01 ± 0.09	—	0.07 ± 0.05	0.08 ± 0.03	-0.71 ± 0.13	-0.02 ± 0.04	0.21 ± 0.09
Melotte 22	-0.00 ± 0.05	-0.03 ± 0.03	—	-0.04 ± 0.06	-0.15 ± 0.09	-0.05 ± 0.05	-0.01 ± 0.05	-0.01 ± 0.04
	-0.01 ± 0.08	-0.06 ± 0.14	0.05 ± 0.05	-0.06 ± 0.15	-0.05 ± 0.07	-0.20 ± 0.23	-0.06 ± 0.05	0.08 ± 0.17
NGC 7062	0.01 ± 0.01	—	0.17 ± 0.04	-0.07 ± 0.01	-0.05 ± 0.02	-0.01 ± 0.01	0.00 ± 0.03	-0.05 ± 0.03
	-0.00 ± 0.01	-0.02 ± 0.02	—	-0.08 ± 0.03	-0.00 ± 0.01	0.01 ± 0.04	-0.02 ± 0.01	-0.04 ± 0.03
FSR 0667	-0.02 ± 0.01	—	0.11 ± 0.04	-0.05 ± 0.01	0.01 ± 0.02	0.04 ± 0.01	0.05 ± 0.03	-0.08 ± 0.03
	0.02 ± 0.01	-0.06 ± 0.02	—	-0.10 ± 0.03	0.00 ± 0.02	-0.06 ± 0.04	-0.06 ± 0.01	-0.05 ± 0.04
Czernik 18	-0.07 ± 0.02	—	—	-0.08 ± 0.02	-0.07 ± 0.06	-0.09 ± 0.02	0.36 ± 0.08	-0.02 ± 0.08
	0.05 ± 0.04	-0.21 ± 0.11	—	0.57 ± 0.14	-0.14 ± 0.04	—	-0.06 ± 0.04	0.22 ± 0.16

Appendix E

Figure Set For Figure 2.2

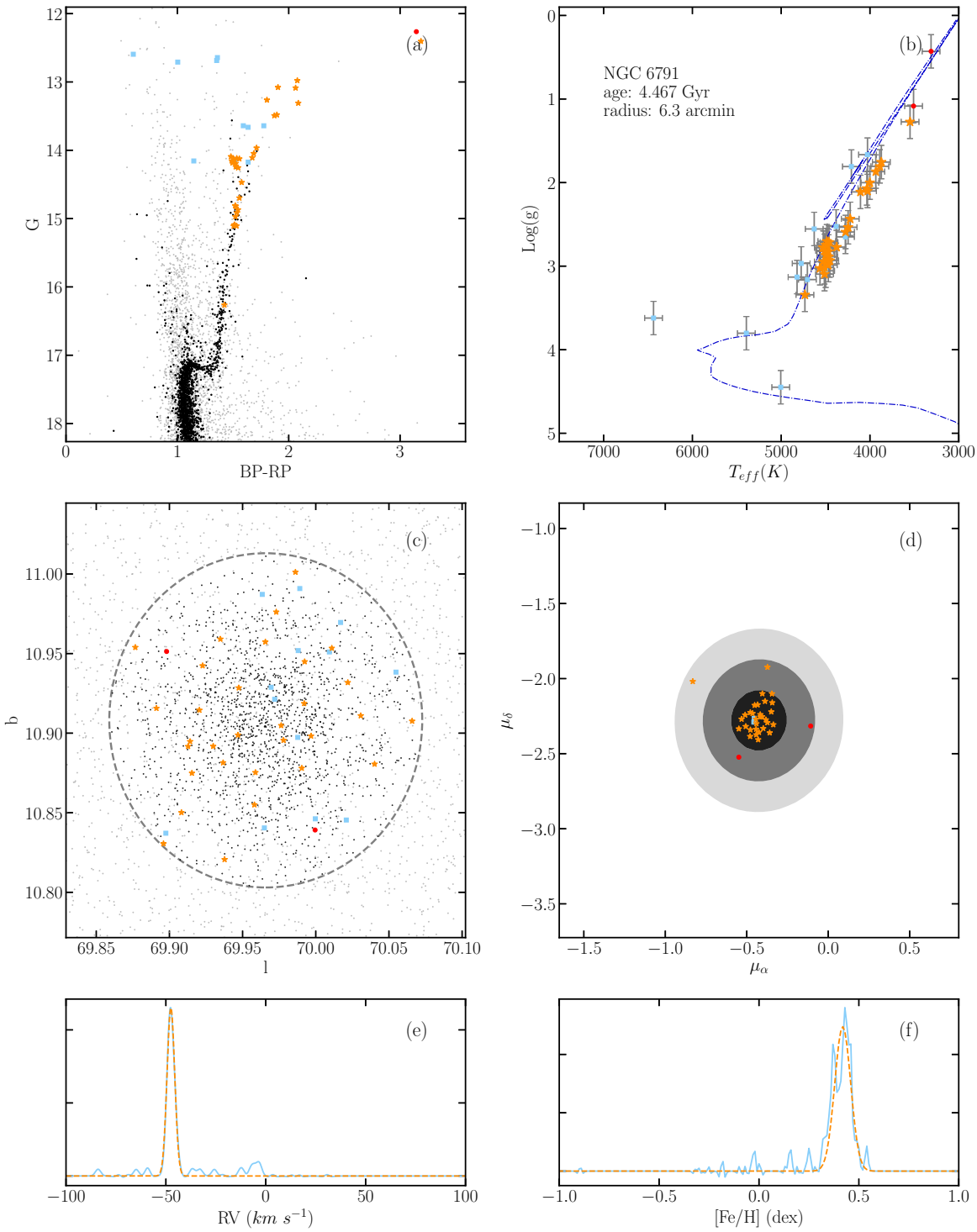

Figure E.1: Summary for NGC 6791

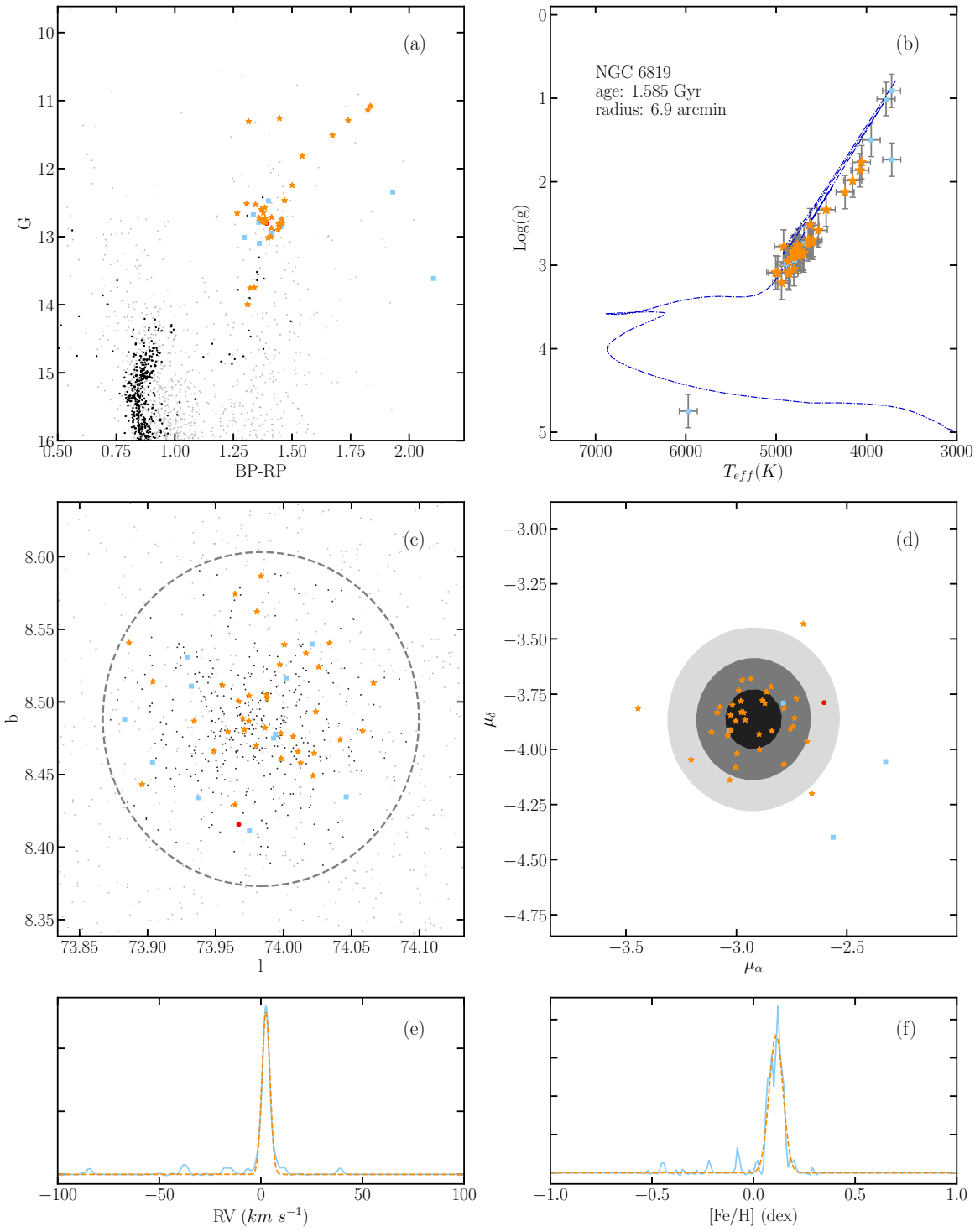

Figure E.2: Summary for NGC 6819

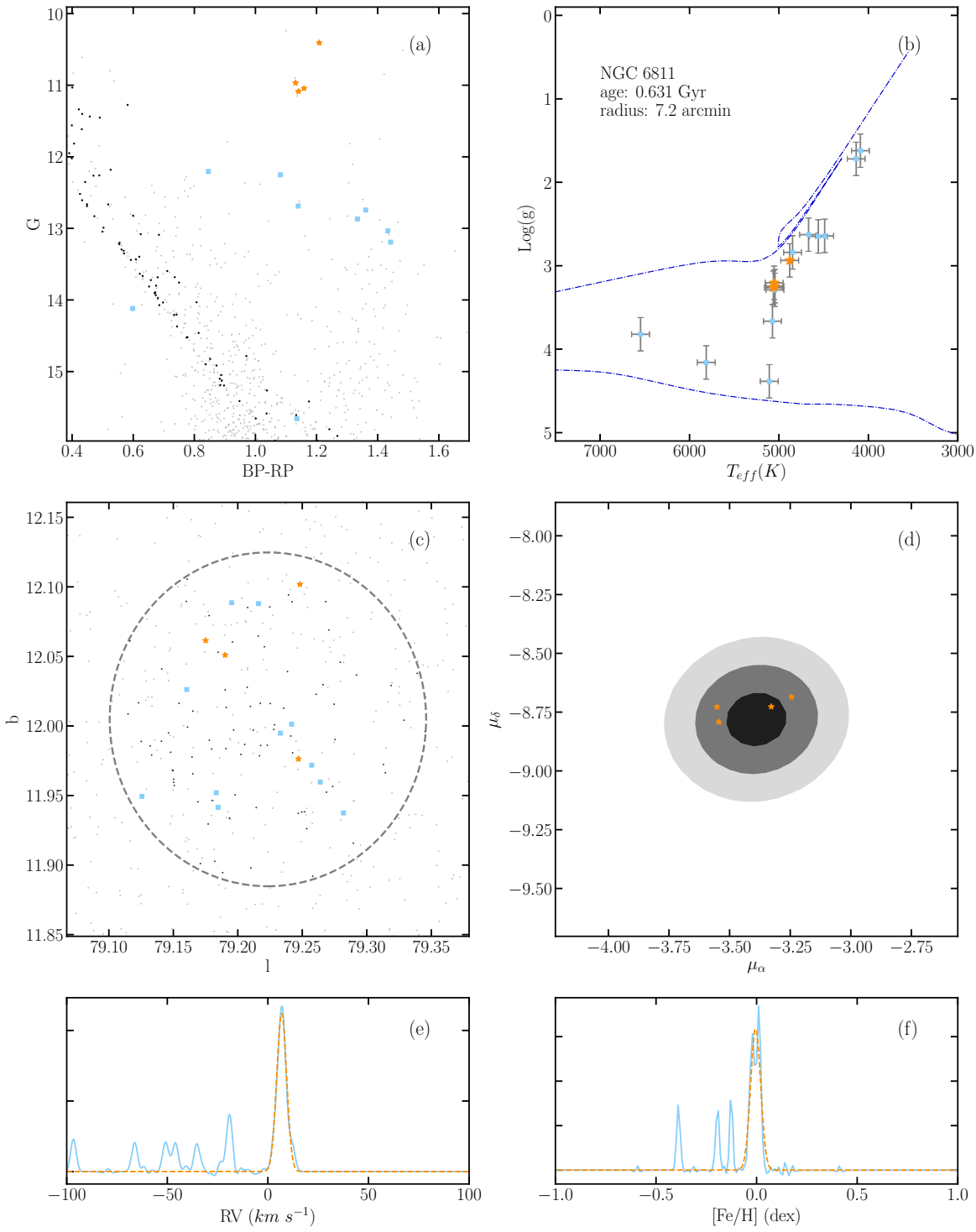

Figure E.3: Summary for NGC 6811

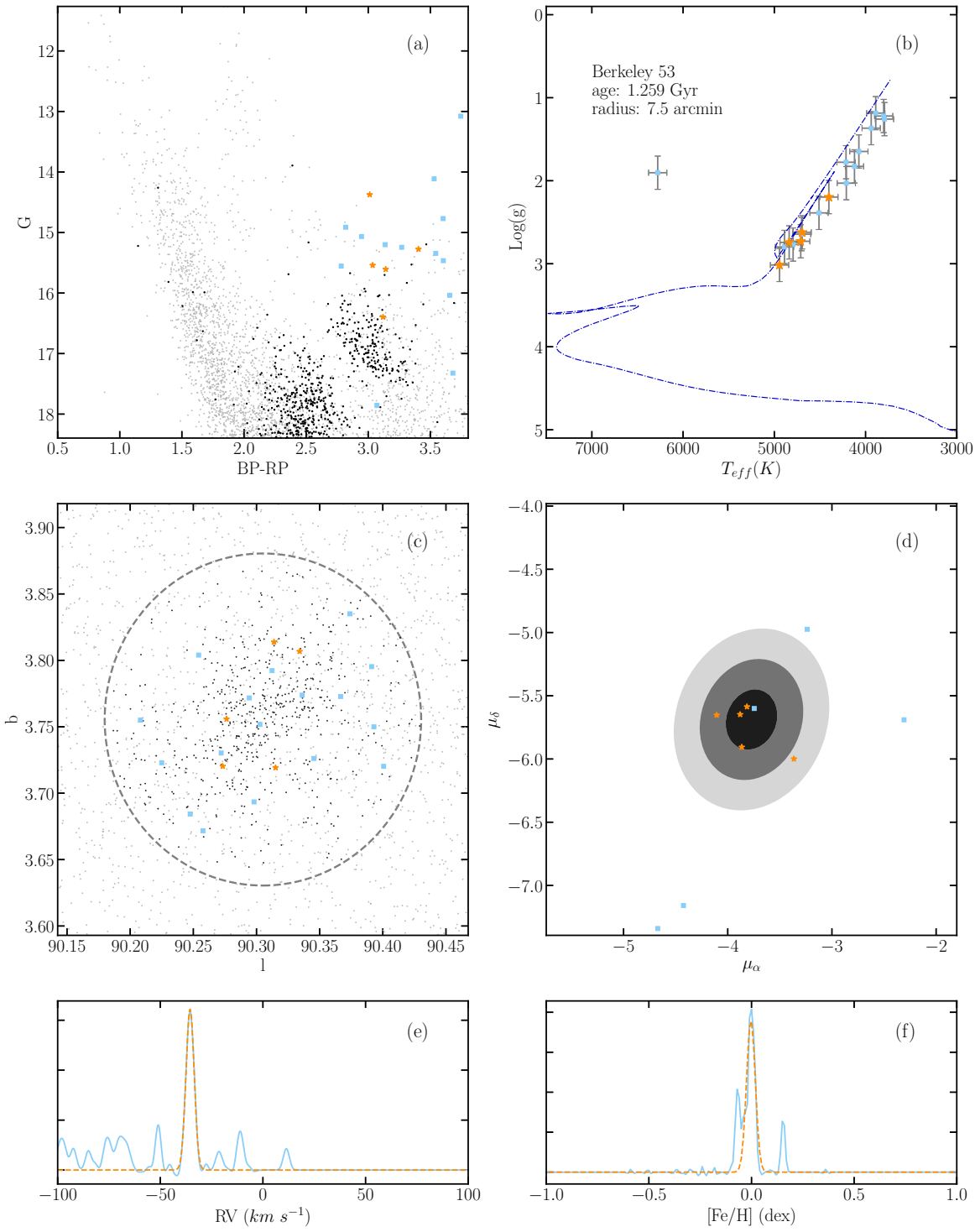

Figure E.4: Summary for Berkeley 53

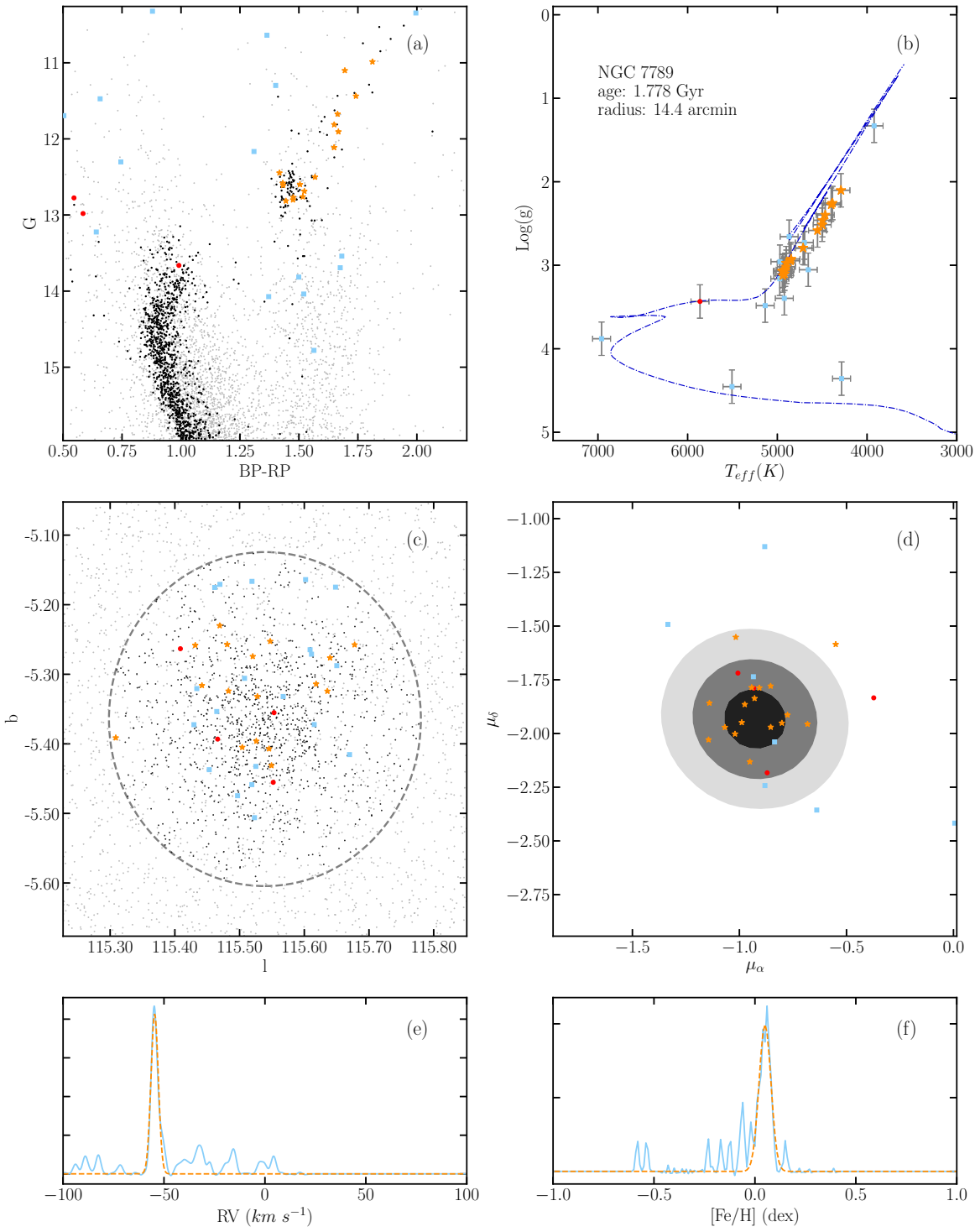

Figure E.5: Summary for NGC 7789

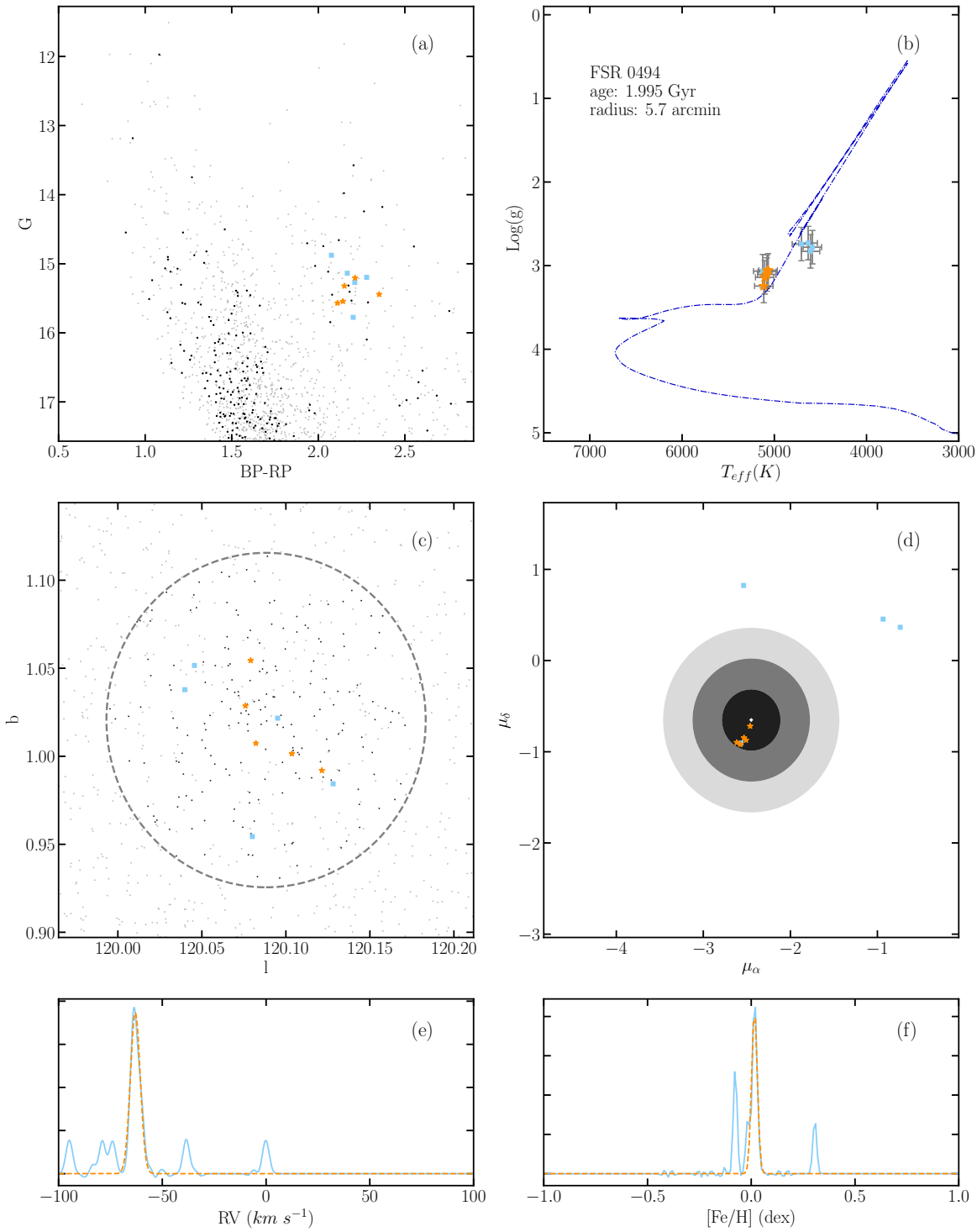

Figure E.6: Summary for FSR 0494

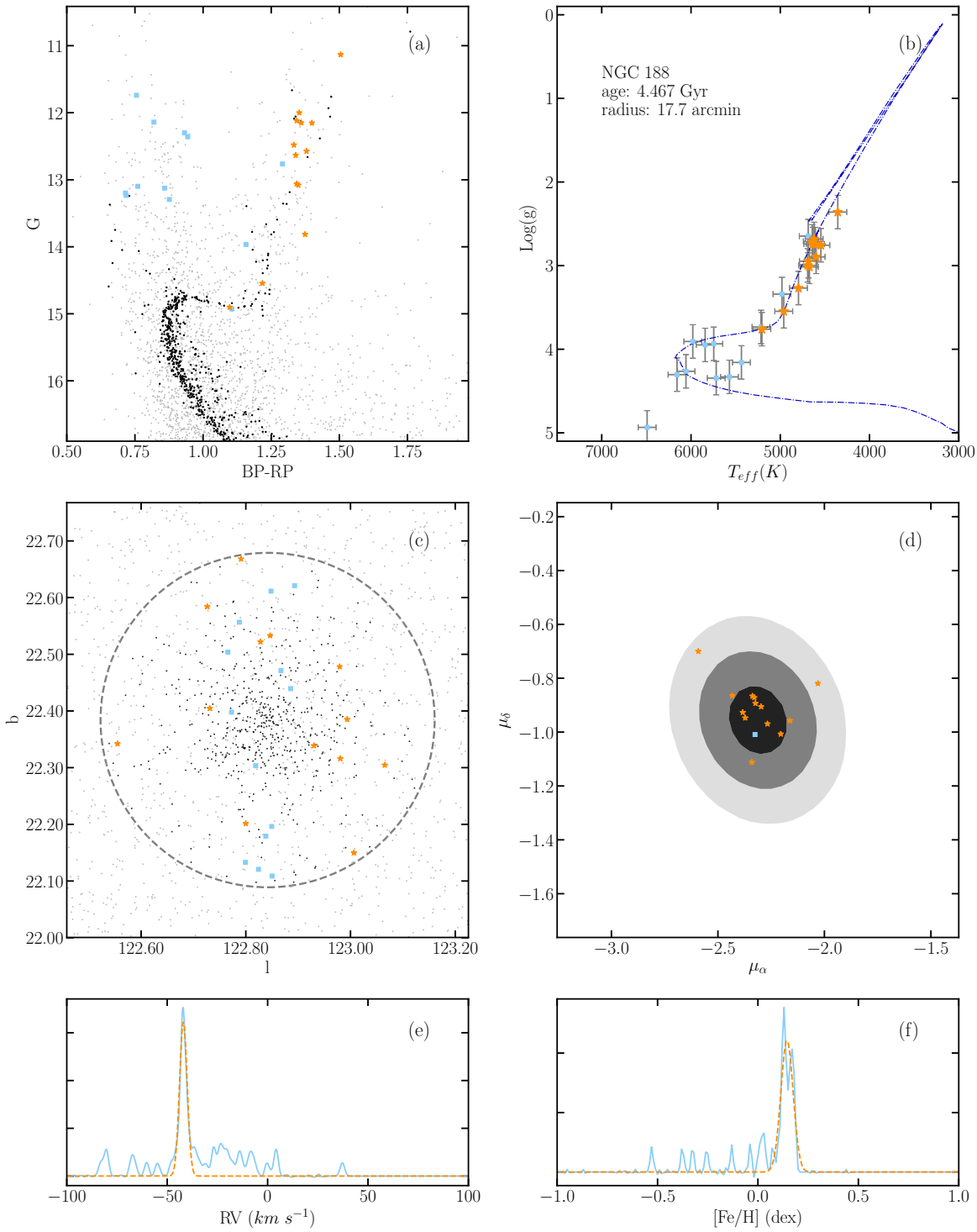

Figure E.7: Summary for NGC 188

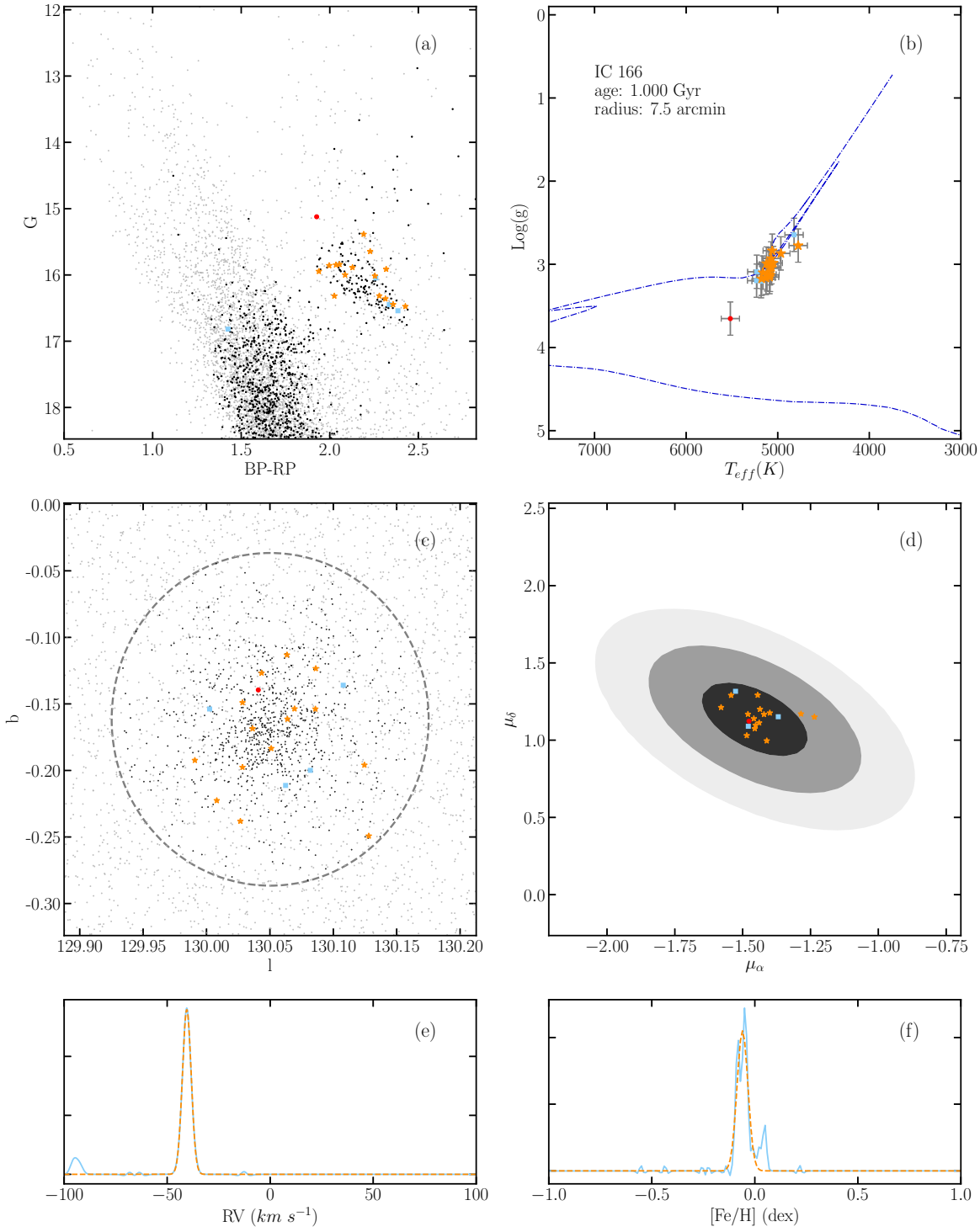

Figure E.8: Summary for IC 166

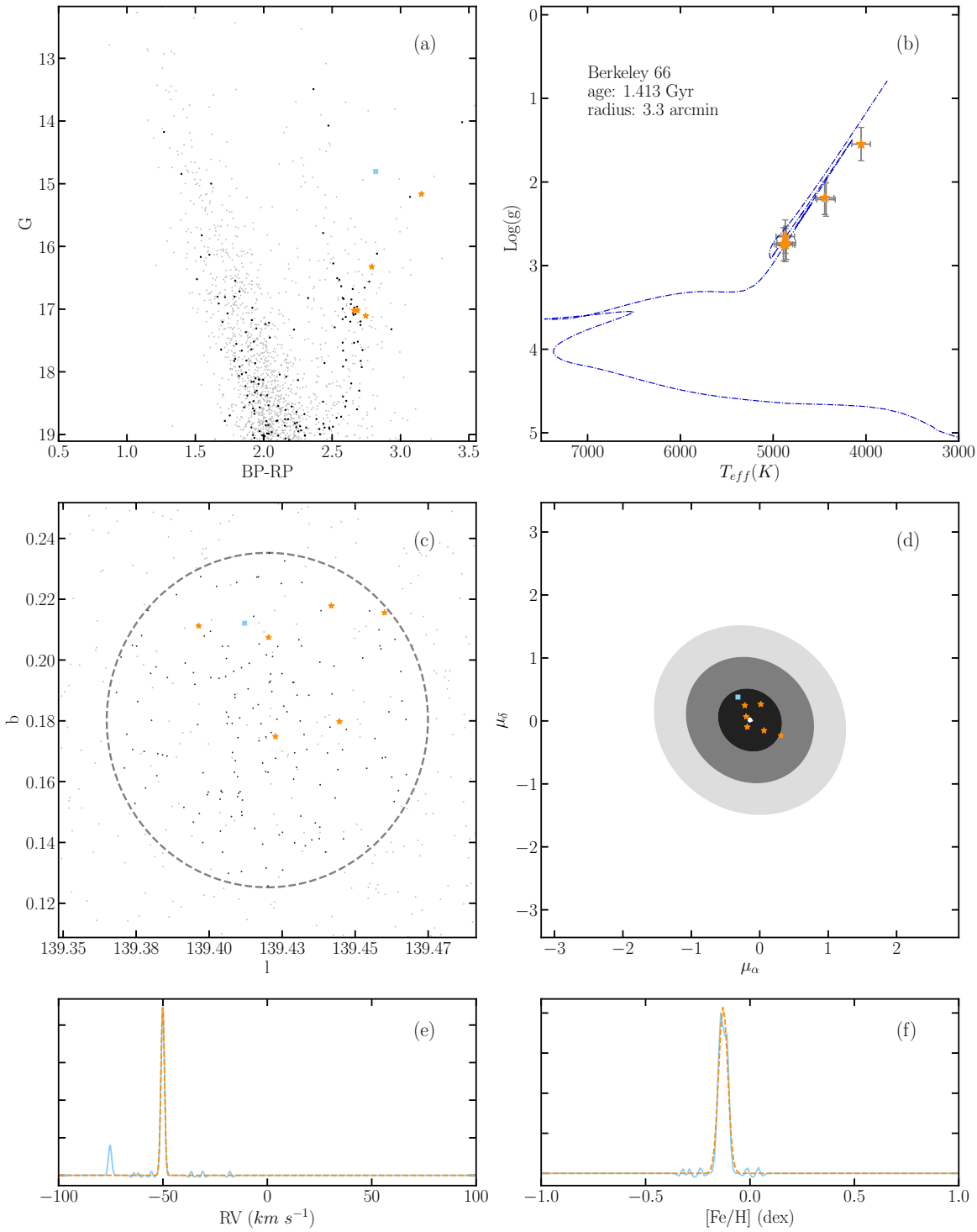

Figure E.9: Summary for Berkeley 66

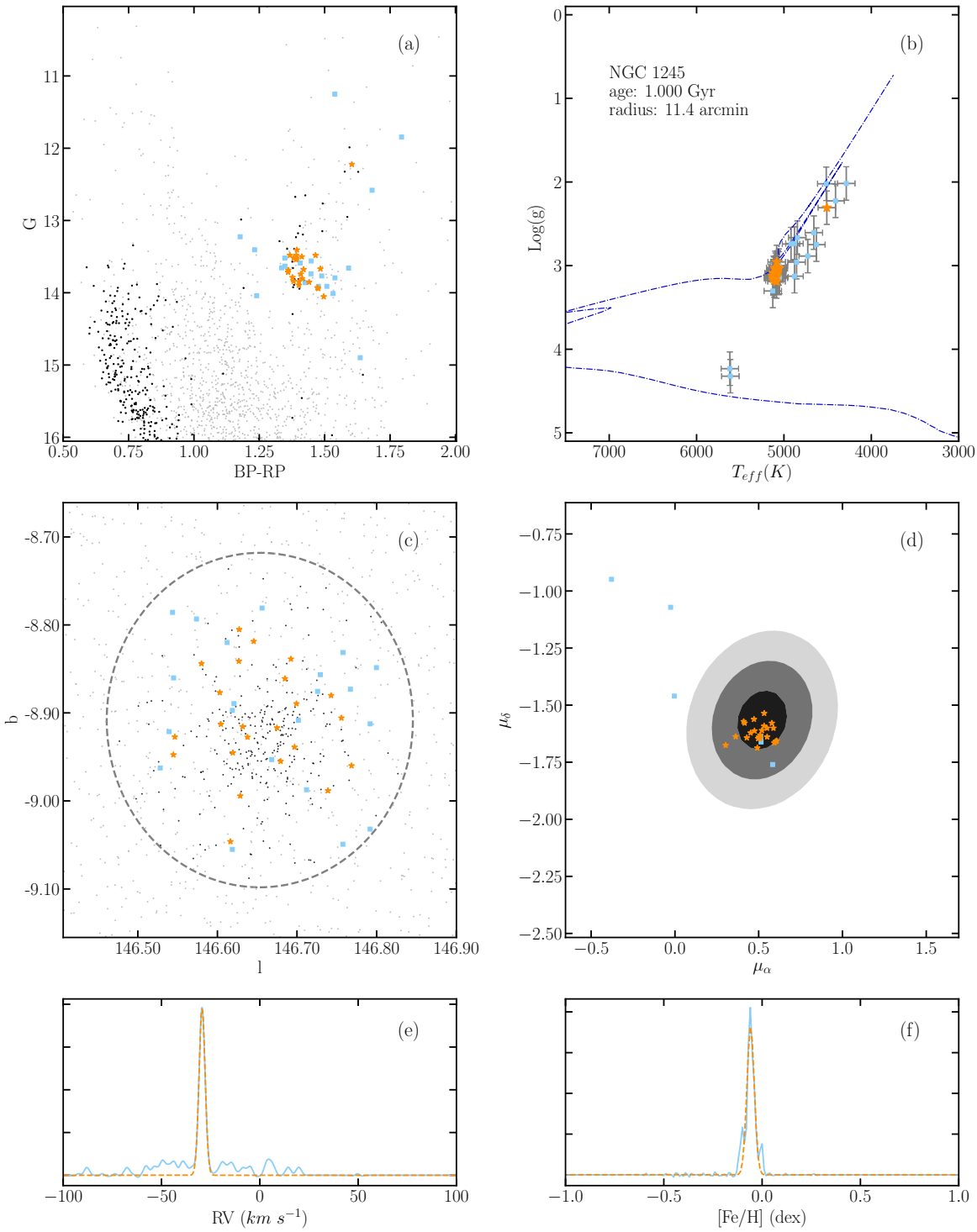

Figure E.10: Summary for NGC 1245

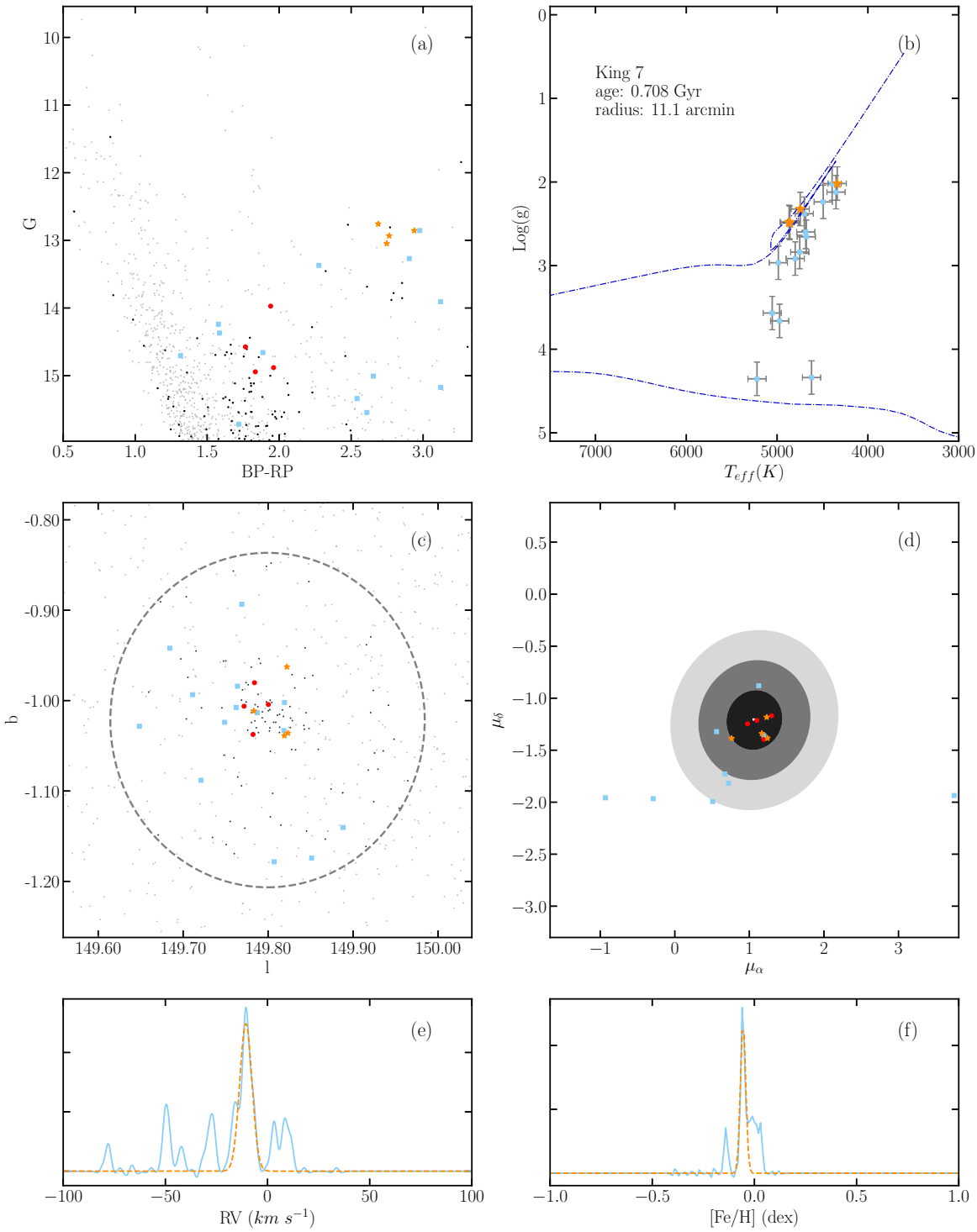

Figure E.11: Summary for King 7

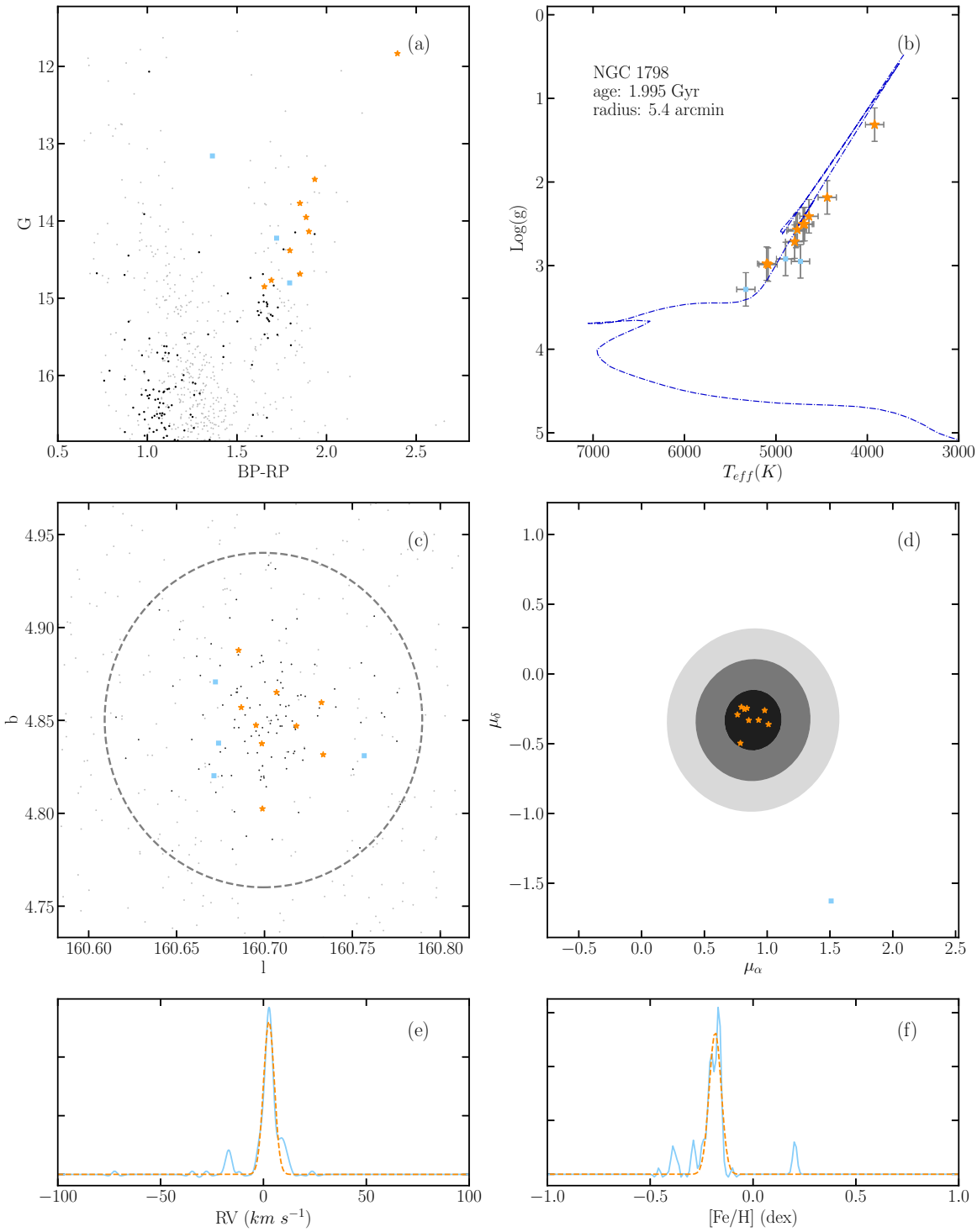

Figure E.12: Summary for NGC 1798

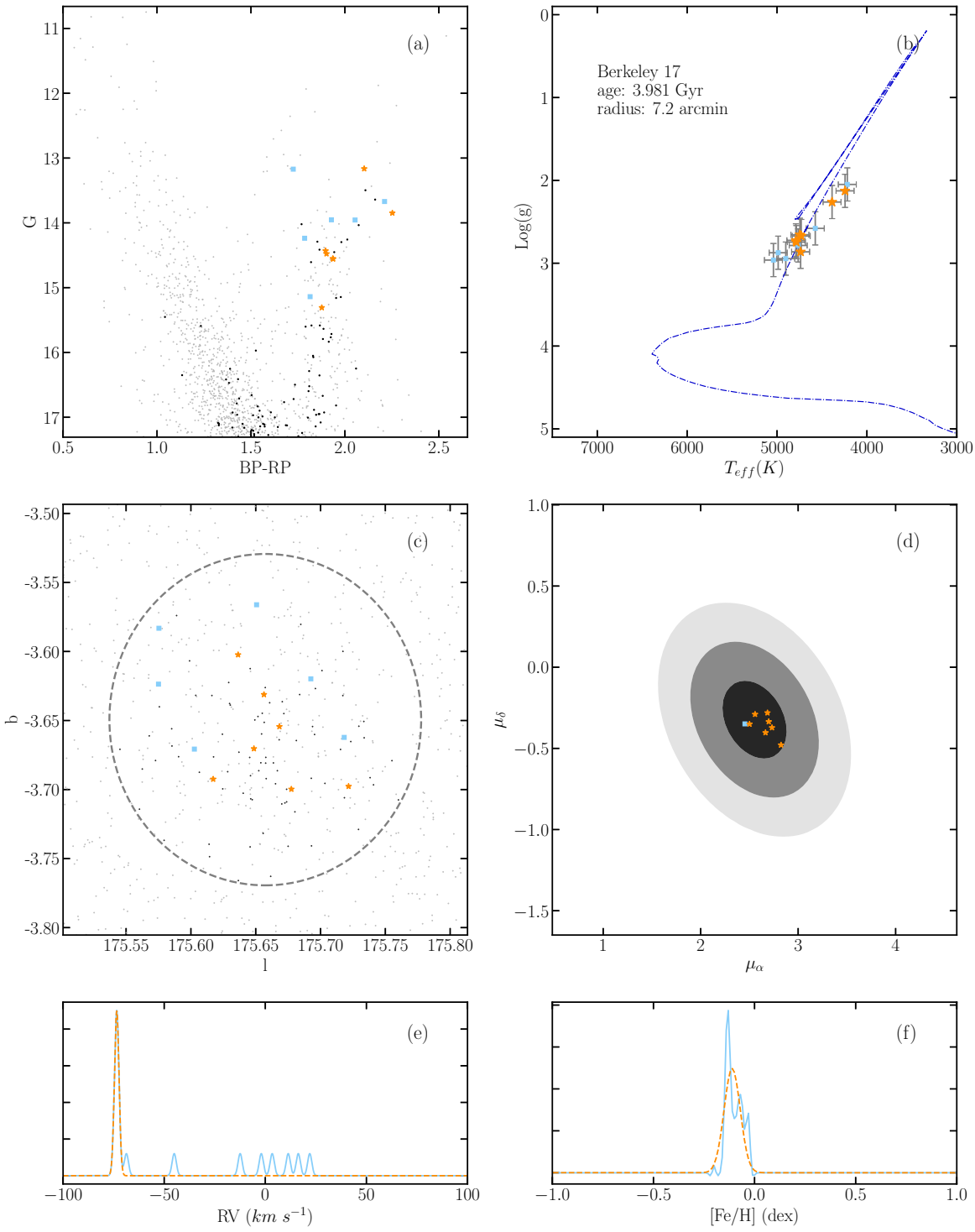

Figure E.13: Summary for NGC Berkeley 17

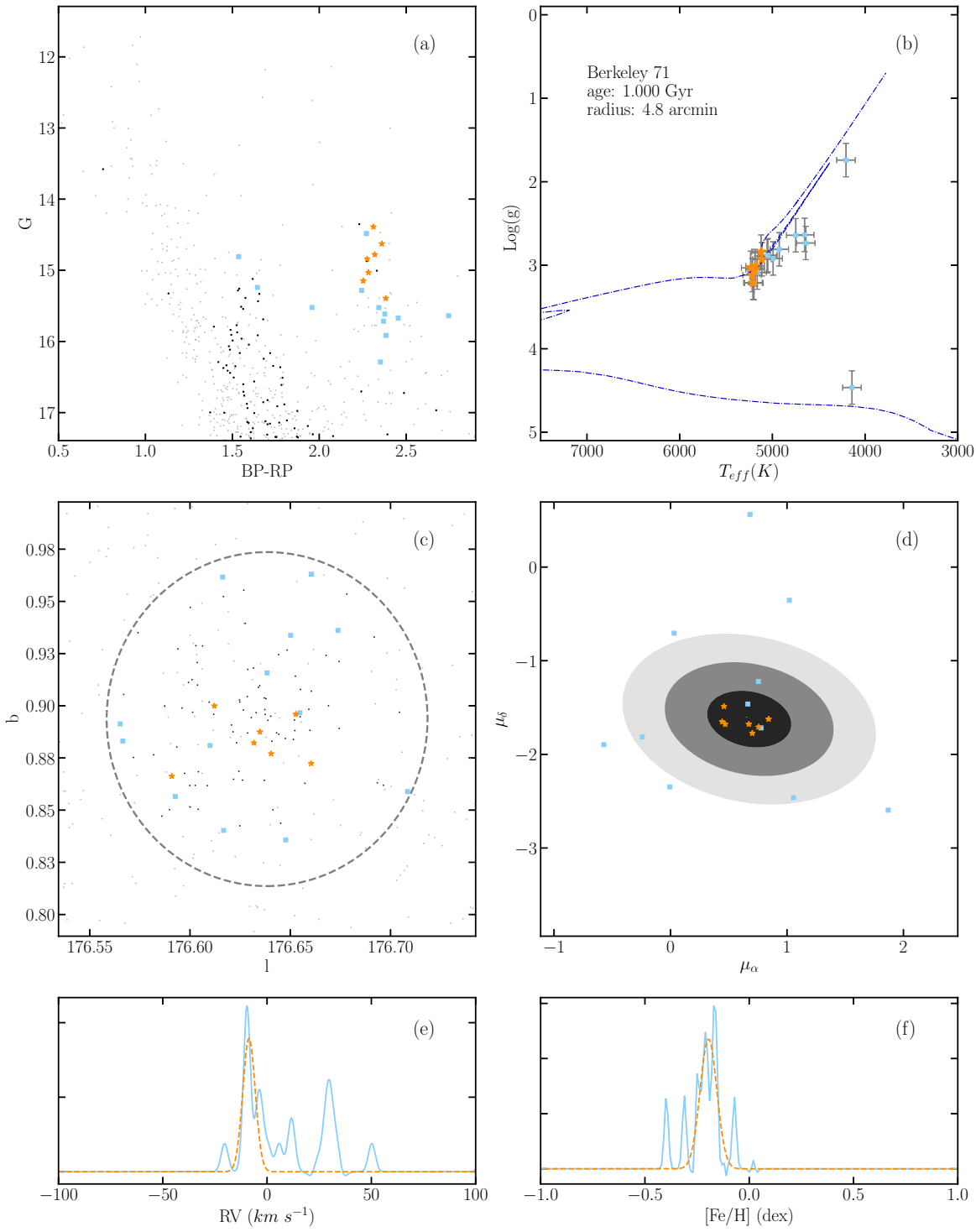

Figure E.14: Summary for Berkeley 71

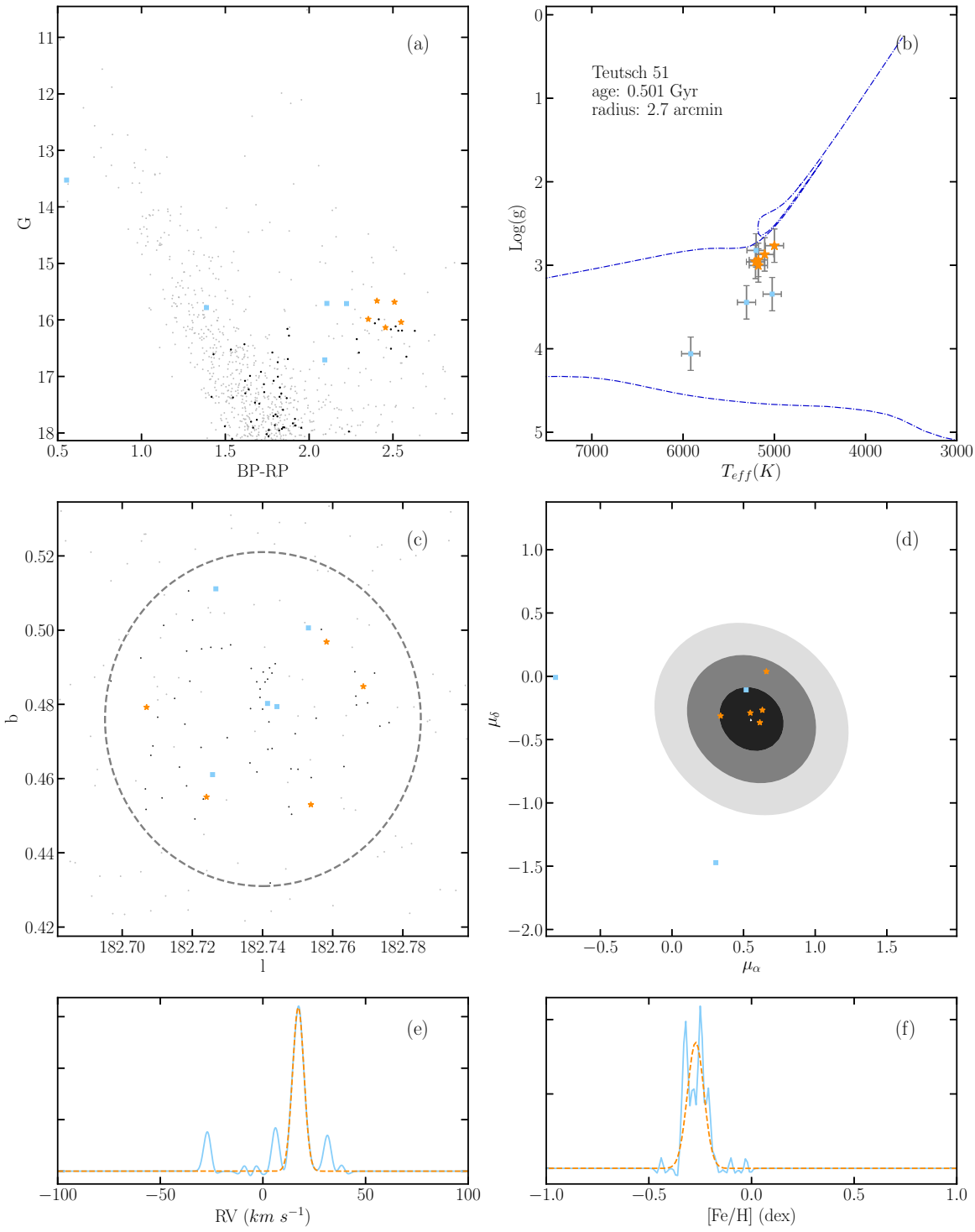

Figure E.15: Summary for Teutsch 51

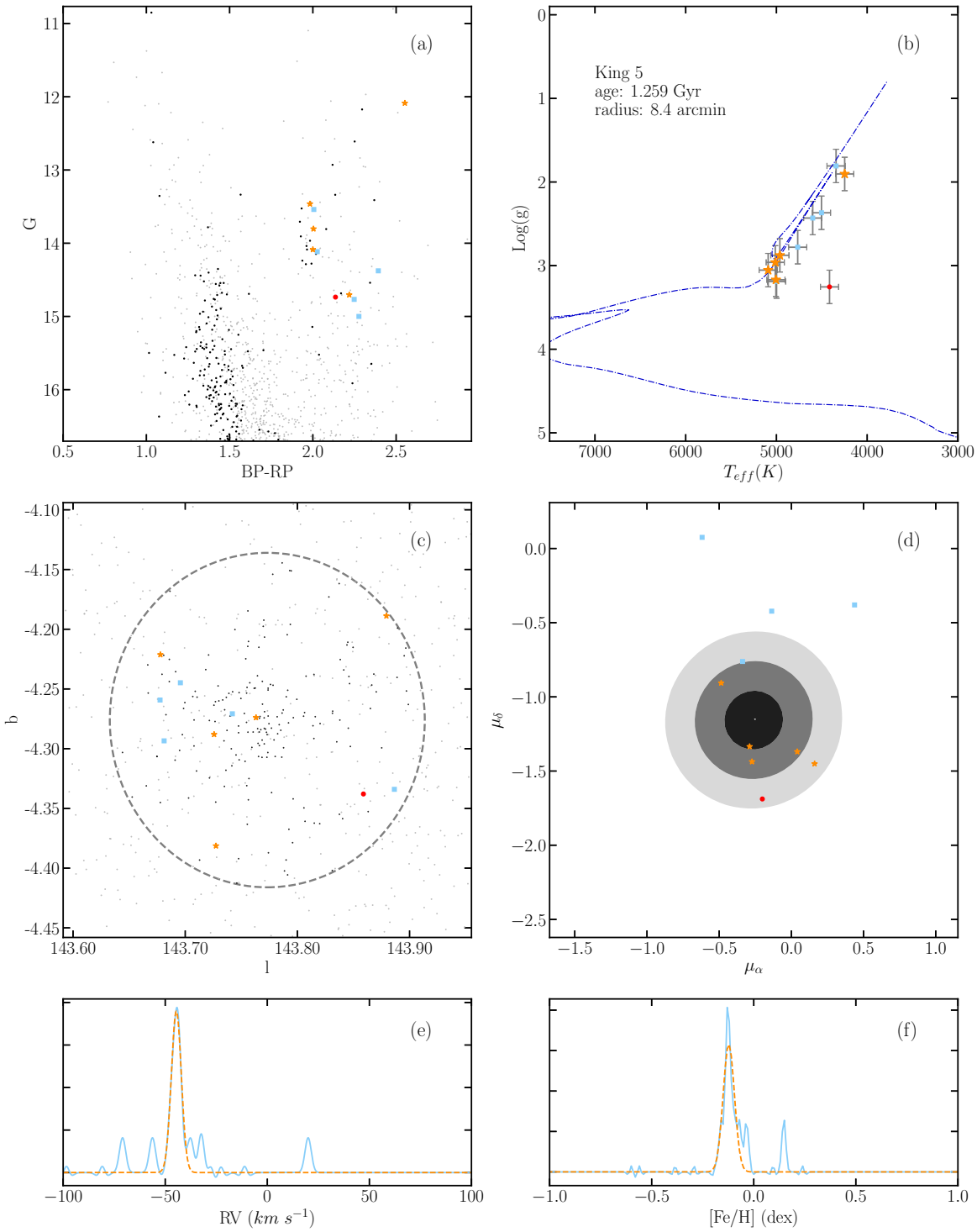

Figure E.16: Summary for King 5

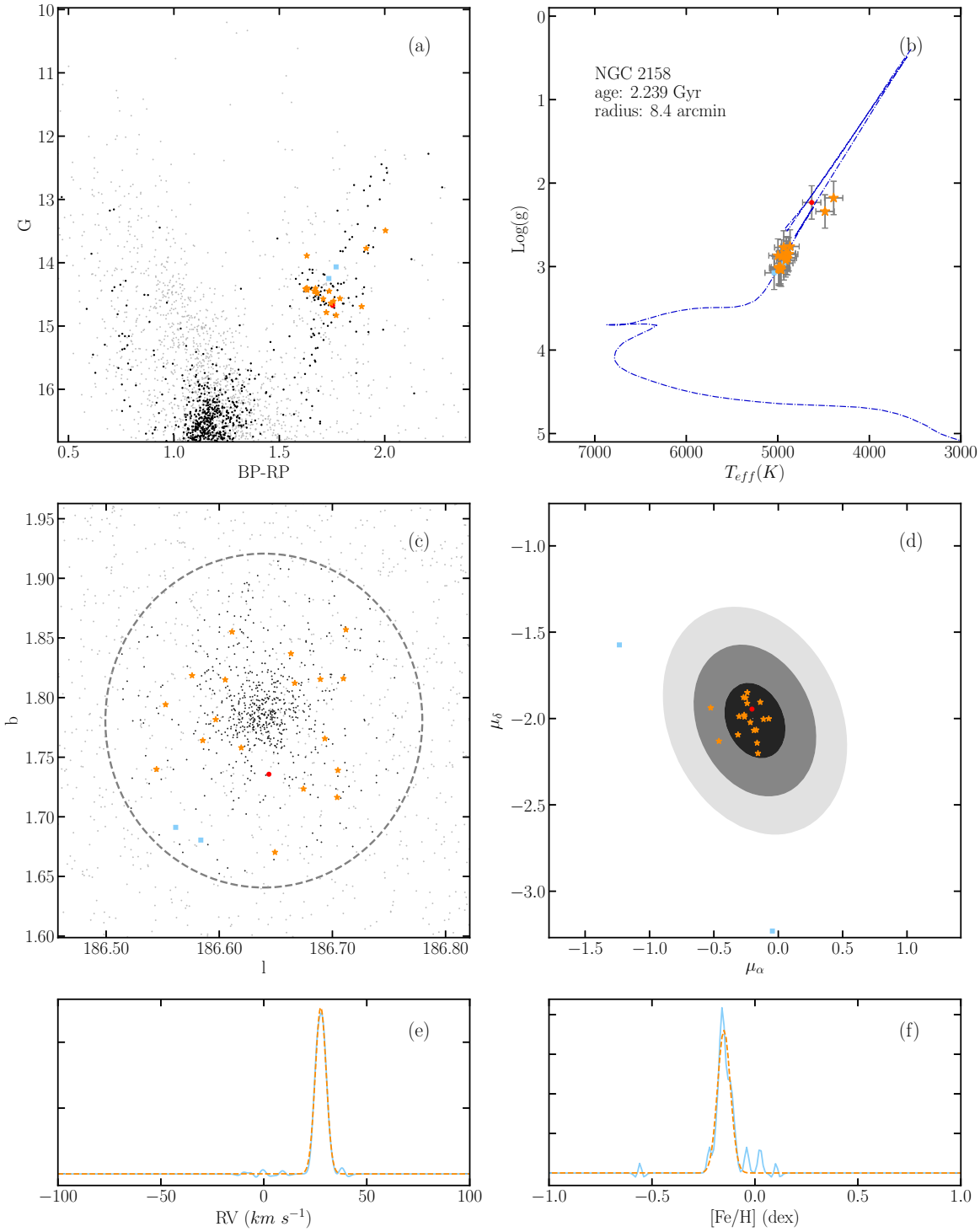

Figure E.17: Summary for NGC 2158

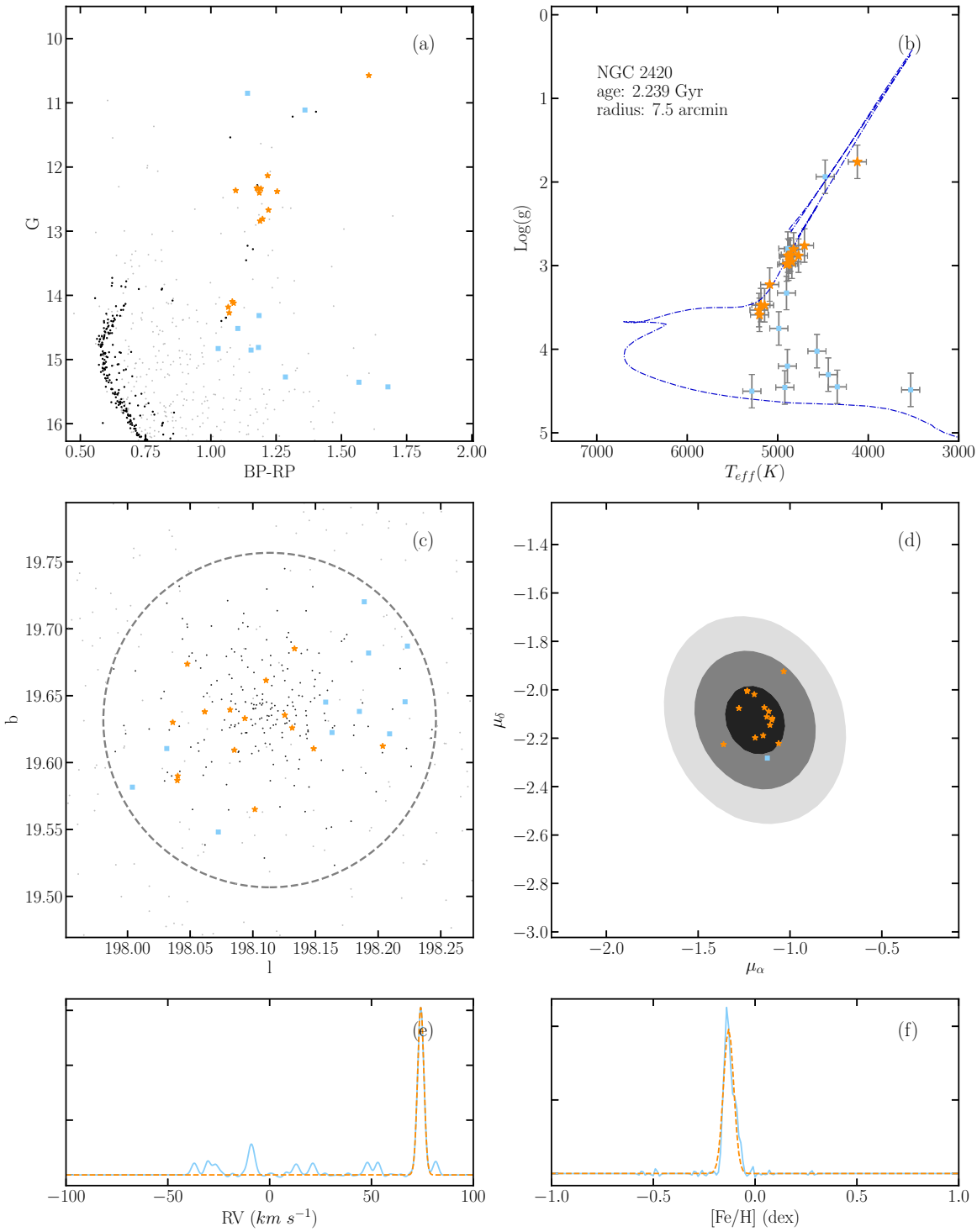

Figure E.18: Summary for NGC 2420

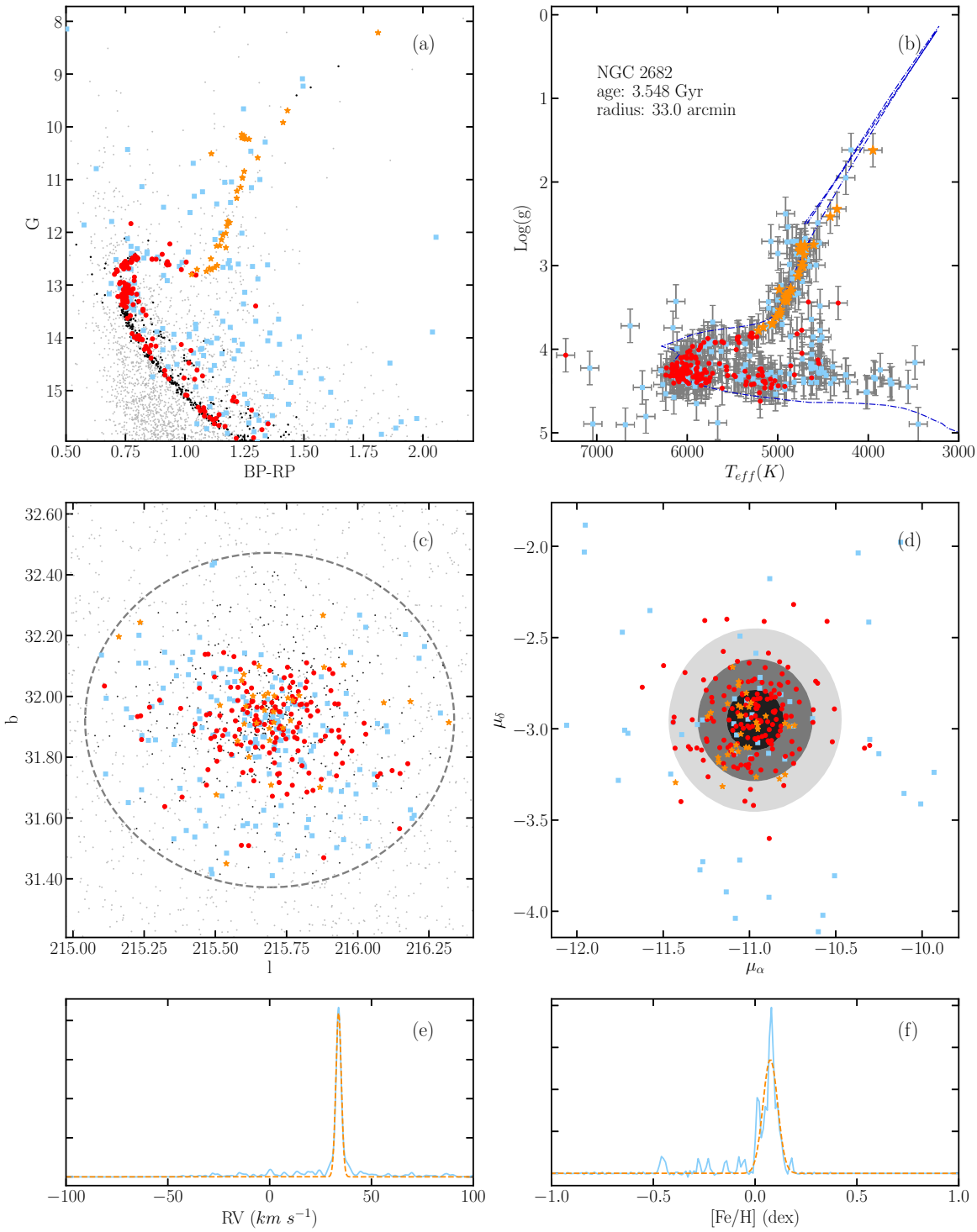

Figure E.19: Summary for NGC 2682

Bibliography

Abolfathi, B., Aguado, D. S., Aguilar, G., Allende Prieto, C., Almeida, A., Tasnim Ananna, T., Anders, F., Anderson, S. F., Andrews, B. H., Anguiano, B., & et al. 2018, Astrophysical Journal Supplement, 235, 42

Ahumada, R., Allende Prieto, C., Almeida, A., Anders, F., Anderson, S. F., Andrews, B. H., Anguiano, B., Arcodia, R., Armengaud, E., & Aubert, M. 2019, arXiv e-prints, arXiv:1912.02905

Anders, F., Chiappini, C., Minchev, I., Miglio, A., Montalbán, J., Mosser, B., Rodrigues, T. S., Santiago, B. X., Baudin, F., Beers, T. C., da Costa, L. N., García, R. A., García-Hernández, D. A., Holtzman, J., Maia, M. A. G., Majewski, S., Mathur, S., Noels-Grotsch, A., Pan, K., Schneider, D. P., Schultheis, M., Steinmetz, M., Valentini, M., & Zamora, O. 2017, Astronomy and Astrophysics, 600, A70

Anguiano, B., Majewski, S. R., Allende-Prieto, C., Meszaros, S., Jönsson, H., García-Hernández, D. A., Beaton, R. L., Stringfellow, G. S., Cunha, K., & Smith, V. V. 2018, Astronomy and Astrophysics, 620, A76

Bailer-Jones, C. A. L., Rybizki, J., Fouesneau, M., Mantelet, G., & Andrae, R. 2018, The Astronomical Journal, 156, 58

Basu, S., Grundahl, F., Stello, D., Kallinger, T., Hekker, S., Mosser, B., García, R. A., Mathur, S., Brogaard, K., Bruntt, H., Chaplin, W. J., Gai, N., Elsworth, Y., Esch, L., Ballot, J., Bedding, T. R., Gruberbauer, M., Huber, D., Miglio, A., Yildiz, M., Kjeldsen, H., Christensen-Dalsgaard, J., Gilliland, R. L., Fanelli, M. M., Ibrahim, K. A., & Smith, J. C. 2011, The Astrophysical Journal Letters, 729, L10

Blanton, M. R., Bershady, M. A., Abolfathi, B., Albareti, F. D., Allende Prieto, C., Almeida, A., Alonso-García, J., Anders, F., Anderson, S. F., Andrews, B., & et al. 2017, The Astronomical Journal, 154, 28

Bovy, J. 2015, Astrophysical Journal Supplement, 216, 29

Bowen, I. S. & Vaughan, A. H., J. 1973, Applied Optics, 12, 1430

Bragaglia, A., Carretta, E., Gratton, R. G., Tosi, M., Bonanno, G., Bruno, P., Calì, A., Claudi, R., Cosentino, R., Desidera, S., Farisato, G., Rebeschini, M., & Scuderi, S. 2001, The Astronomical Journal, 121, 327

Bragaglia, A., Sestito, P., Villanova, S., Carretta, E., Randich, S., & Tosi, M. 2008, Astronomy and Astrophysics, 480, 79

Bragaglia, A., Sneden, C., Carretta, E., Gratton, R. G., Lucatello, S., Bernath, P. F., Brooke, J. S. A., & Ram, R. S. 2014, The Astrophysical Journal, 796, 68

Bressan, A., Marigo, P., Girardi, L., Salasnich, B., Dal Cero, C., Rubele, S., & Nanni, A. 2012, Monthly Notices of the Royal Astronomical Society, 427, 127

Brogaard, K., VandenBerg, D. A., Bruntt, H., Grundahl, F., Frandsen, S., Bedin, L. R., Milone, A. P., Dotter, A., Feiden, G. A., Stetson, P. B., Sandquist, E., Miglio, A., Stello, D., & Jessen-Hansen, J. 2012, Astronomy and Astrophysics, 543, A106

Bundy, K., Bershady, M. A., Law, D. R., Yan, R., Drory, N., MacDonald, N., Wake, D. A., Cherinka, B., Sánchez-Gallego, J. R., Weijmans, A.-M., Thomas, D., Tremonti, C., Masters, K., Coccato, L., Diamond-Stanic, A. M., Aragón-Salamanca, A., Avila-Reese, V., Badenes, C., Falcón-Barroso, J., Belfiore, F., Bizyaev, D., Blanc, G. A., Bland-Hawthorn, J., Blanton, M. R., Brownstein, J. R., Byler, N., Cappellari, M., Conroy, C., Dutton, A. A., Emsellem, E., Etherington, J., Frinchaboy, P. M., Fu, H., Gunn, J. E., Harding, P., Johnston, E. J., Kauffmann, G., Kinemuchi, K., Klaene, M. A., Knapen, J. H., Leauthaud, A., Li, C., Lin, L., Maiolino, R., Malanushenko, V., Malanushenko, E., Mao, S., Maraston, C., McDermid, R. M., Merrifield, M. R., Nichol, R. C., Oravetz, D., Pan, K., Parejko, J. K., Sanchez, S. F., Schlegel, D., Simmons, A., Steele, O., Steinmetz, M., Thanjavur, K., Thompson, B. A., Tinker, J. L., van den Bosch, R. C. E., Westfall, K. B., Wilkinson, D., Wright, S., Xiao, T., & Zhang, K. 2015, The Astrophysical Journal, 798, 7

Burger, D., Stassun, K. G., Pepper, J., Siverd, R. J., Paegert, M., De Lee, N. M., & Robinson, W. H. 2013, Astronomy and Computing, 2, 40

Cantat-Gaudin, T., Anders, F., Castro-Ginard, A., Jordi, C., Romero-Gomez, M., Soubiran, C., Casamiquela, L., Tarricq, Y., Moitinho, A., Vallenari, A., Bragaglia, A., Krone-Martins, A., & Kounkel, M. 2020, arXiv e-prints, arXiv:2004.07274

Cantat-Gaudin, T., Jordi, C., Vallenari, A., Bragaglia, A., Balaguer-Núñez, L., Soubiran, C., Bossini, D., Moitinho, A., Castro-Ginard, A., Krone-Martins, A., Casamiquela, L., Sordo, R., & Carrera, R. 2018, Astronomy and Astrophysics, 618, A93

Carraro, G., Ng, Y. K., & Portinari, L. 1998, Monthly Notices of the Royal Astronomical Society, 296, 1045

Carraro, G., Villanova, S., Demarque, P., McSwain, M. V., Piotto, G., & Bedin, L. R. 2006, The Astrophysical Journal, 643, 1151

Carrera, R., Bragaglia, A., Cantat-Gaudin, T., Vallenari, A., Balaguer-Núñez, L., Bossini, D., Casamiquela, L., Jordi, C., Sordo, R., & Soubiran, C. 2019, Astronomy and Astrophysics, 623, A80

Carrera, R. & Pancino, E. 2011, Astronomy and Astrophysics, 535, A30

Carretta, E., Bragaglia, A., & Gratton, R. G. 2007, Astronomy and Astrophysics, 473, 129

Casamiquela, L., Blanco-Cuaresma, S., Carrera, R., Balaguer-Núñez, L., Jordi, C., Anders, F., Chiappini, C., Carbajo-Hijarrubia, J., Aguado, D. S., del Pino, A., Díaz-Pérez, L., Gallart, C., & Pancino, E. 2019, Monthly Notices of the Royal Astronomical Society, 490, 1821

Casamiquela, L., Carrera, R., Blanco-Cuaresma, S., Jordi, C., Balaguer-Núñez, L., Pancino, E., Anders, F., Chiappini, C., Díaz-Pérez, L., Aguado, D. S., Aparicio, A., Garcia-Dias, R., Heiter, U., Martínez-Vázquez, C. E., Murabito, S., & del Pino, A. 2017, Monthly Notices of the Royal Astronomical Society, 470, 4363

Chen, Y. Q. & Zhao, G. 2020, Monthly Notices of the Royal Astronomical Society

Chiappini, C. 2009, in IAU Symposium, Vol. 254, The Galaxy Disk in Cosmological Context, ed. J. Andersen, Nordströara, B. m, & J. Bland -Hawthorn, 191–196

Cohen, J. G. 1980, The Astrophysical Journal, 241, 981

Cunha, K., Frinchaboy, P. M., Souto, D., Thompson, B., Zasowski, G., Allende Prieto, C., Carrera, R., Chiappini, C., Donor, J., García-Hernández, D. A., García Pérez, A. E., Hayden, M. R., Holtzman, J., Jackson, K. M., Johnson, J. A., Majewski, S. R., Mészáros, S., Meyer, B., Nidever, D. L., O'Connell, J., Schiavon, R. P., Schultheis, M., Shetrone, M., Simmons, A., Smith, V. V., & et al. 2016, Astronomische Nachrichten, 337, 922

Cunha, K., Smith, V. V., Hasselquist, S., Souto, D., Shetrone, M. D., Allende Prieto, C., Bizyaev, D., Frinchaboy, P., García-Hernández, D. A., Holtzman, J., Johnson, J. A., Jőnsson, H., Majewski, S. R., Mészáros, S., Nidever, D., Pinsonneault, M., Schiavon, R. P., Sobeck, J., Skrutskie, M. F., Zamora, O., Zasowski, G., & Fernández-Trincado, J. G. 2017, The Astrophysical Journal, 844, 145

Cunha, K., Smith, V. V., Johnson, J. A., Bergemann, M., Mészáros, S., Shetrone, M. D., Souto, D., Allende Prieto, C., Schiavon, R. P., Frinchaboy, P., Zasowski, G., Bizyaev, D., Holtzman, J., García Pérez, A. E., Majewski, S. R., Nidever, D., Beers, T., Carrera, R., Geisler, D., Gunn, J., Hearty, F., Ivans, I., Martell, S., Pinsonneault, M., Schneider, D. P., Sobeck, J., Stello, D., Stassun, K. G., Skrutskie, M., & Wilson, J. C. 2015, The Astrophysical Journal Letters, 798, L41

Cutri, R. M., Skrutskie, M. F., van Dyk, S., Beichman, C. A., Carpenter, J. M., Chester, T., Cambresy, L., Evans, T., Fowler, J., Gizis, J., Howard, E., Huchra, J., Jarrett, T., Kopan, E. L., Kirkpatrick, J. D., Light, R. M., Marsh, K. A., McCallon, H., Schneider, S., Stiening, R., Sykes, M., Weinberg, M., Wheaton, W. A., Wheelock, S., & Zacarias, N. 2003, 2MASS All Sky Catalog of point sources.

Daflon, S. & Cunha, K. 2004, The Astrophysical Journal, 617, 1115

Dias, W. S., Alessi, B. S., Moitinho, A., & Lépine, J. R. D. 2002, Astronomy and Astrophysics, 389, 871

Donati, P., Bragaglia, A., Carretta, E., D'Orazi, V., Tosi, M., Cusano, F., & Carini, R. 2015, Monthly Notices of the Royal Astronomical Society, 453, 4185

Dreyer, J. L. E. 1888, Memoirs of the Royal Astronomical Society, 49, 1

Eisenstein, D. J., Weinberg, D. H., Agol, E., Aihara, H., Allende Prieto, C., Anderson, S. F., Arns, J. A., Aubourg, É., Bailey, S., Balbinot, E., & et al. 2011, The Astronomical Journal, 142, 72

Esteban, C., García-Rojas, J., & Pérez-Mesa, V. 2015, Monthly Notices of the Royal Astronomical Society, 452, 1553

Foreman-Mackey, D., Hogg, D. W., Lang, D., & Goodman, J. 2013, Publications of the Astronomical Society of the Pacific, 125, 306

Friel, E. D. 1995, The Annual Review of Astronomy and Astrophysics, 33, 381

Friel, E. D., Jacobson, H. R., & Pilachowski, C. A. 2010, The Astronomical Journal, 139, 1942

Friel, E. D. & Janes, K. A. 1993, Astronomy and Astrophysics, 267, 75

Friel, E. D., Janes, K. A., Tavarez, M., Scott, J., Katsanis, R., Lotz, J., Hong, L., & Miller, N. 2002, The Astronomical Journal, 124, 2693

Frinchaboy, P., Zasowski, G., Jackson, K., Johnson, J. A., Majewski, S. R., Shetrone, M., Rocha, A., & SDSS-III Collaboration. 2010, in JENAM 2010, Joint European and National Astronomy Meeting, 136

Frinchaboy, P. M. & Majewski, S. R. 2008, The Astronomical Journal, 136, 118

Frinchaboy, P. M., Thompson, B., Jackson, K. M., O'Connell, J., Meyer, B., Zasowski, G., Majewski, S. R., Chojnowksi, S. D., Johnson, J. A., Allende Prieto, C., Beers, T. C., Bizyaev, D., Brewington, H., Cunha, K., Ebelke, G., García Pérez, A. E., Hearty, F. R., Holtzman, J., Kinemuchi, K., Malanushenko, E., Malanushenko, V., Marchante, M., Mészáros, S., Muna, D., Nidever, D. L., Oravetz, D., Pan, K., Schiavon, R. P., Schneider, D. P., Shetrone, M., Simmons, A., Snedden, S., Smith, V. V., & Wilson, J. C. 2013, The Astrophysical Journal Letters, 777, L1

Fujii, M. S. & Baba, J. 2012, Monthly Notices of the Royal Astronomical Society, 427, L16

Gaia Collaboration, Brown, A. G. A., Vallenari, A., Prusti, T., de Bruijne, J. H. J., Babusiaux, C., Bailer-Jones, C. A. L., Biermann, M., Evans, D. W., Eyer, L., & et al. 2018, Astronomy and Astrophysics, 616, A1

Gaia Collaboration, Prusti, T., de Bruijne, J. H. J., Brown, A. G. A., Vallenari, A., Babusiaux, C., Bailer-Jones, C. A. L., Bastian, U., Biermann, M., Evans, D. W., & et al. 2016, Astronomy and Astrophysics, 595, A1

García Pérez, A. E., Allende Prieto, C., Holtzman, J. A., Shetrone, M., Mészáros, S., Bizyaev, D., Carrera, R., Cunha, K., García-Hernández, D. A., Johnson, J. A., Majewski, S. R., Nidever, D. L., Schiavon, R. P., Shane, N., Smith, V. V., Sobeck, J., Troup, N., Zamora, O., Weinberg, D. H., Bovy, J., Eisenstein, D. J., Feuillet, D., Frinchaboy, P. M., Hayden, M. R., Hearty, F. R., Nguyen, D. C., O'Connell, R. W., Pinsonneault, M. H., Wilson, J. C., & Zasowski, G. 2016, The Astronomical Journal, 151, 144

Geller, A. M., Mathieu, R. D., Braden, E. K., Meibom, S., Platais, I., & Dolan, C. J. 2010, The Astronomical Journal, 139, 1383

Geller, A. M., Mathieu, R. D., Harris, H. C., & McClure, R. D. 2008, The Astronomical Journal, 135, 2264

Genovali, K., Lemasle, B., Bono, G., Romaniello, M., Fabrizio, M., Ferraro, I., Iannicola, G., Laney, C. D., Nonino, M., Bergemann, M., Buonanno, R., François, P., Inno, L., Kudritzki, R. P., Matsunaga, N., Pedicelli, S., Primas, F., & Thévenin, F. 2014, Astronomy and Astrophysics, 566, A37

Gunn, J. E., Siegmund, W. A., Mannery, E. J., Owen, R. E., Hull, C. L., Leger, R. F., Carey, L. N., Knapp, G. R., York, D. G., Boroski, W. N., Kent, S. M., Lupton, R. H., Rockosi, C. M., Evans, M. L., Waddell, P., Anderson, J. E., Annis, J., Barentine, J. C., Bartoszek, L. M., Bastian, S., Bracker, S. B., Brewington, H. J., Briegel, C. I., Brinkmann, J., Brown, Y. J., Carr, M. A., Czarapata, P. C., Drennan, C. C., Dombeck, T., Federwitz, G. R., Gillespie, B. A., Gonzales, C., Hansen, S. U., Harvanek, M., Hayes, J., Jordan, W., Kinney, E., Klaene, M., Kleinman, S. J., Kron, R. G., Kresinski, J., Lee, G., Limmongkol, S., Lindenmeyer, C. W., Long, D. C., Loomis, C. L., McGehee, P. M., Mantsch, P. M., Neilsen, Jr., E. H., Neswold, R. M., Newman, P. R., Nitta, A., Peoples, Jr., J., Pier, J. R., Prieto, P. S., Prosapio, A., Rivetta, C., Schneider, D. P., Snedden, S., & Wang, S.-i. 2006, The Astronomical Journal, 131, 2332

Hasselquist, S., Shetrone, M., Cunha, K., Smith, V. V., Holtzman, J., Lawler, J. E., Allende Prieto, C., Beers, T. C., Chojnowski, D., Fernández-Trincado, J. G., García-Hernández, D. A., Hearty, F. R., Majewski, S. R., Pereira, C. B., Placco, V. M., Villanova, S., & Zamora, O. 2016, The Astrophysical Journal, 833, 81

Hayden, M. R., Bovy, J., Holtzman, J. A., Nidever, D. L., Bird, J. C., Weinberg, D. H., Andrews, B. H., Majewski, S. R., Allende Prieto, C., Anders, F., Beers, T. C., Bizyaev, D., Chiappini, C., Cunha, K., Frinchaboy, P., García-Herńand ez, D. A., García Pérez, A. E., Girardi, L., Harding, P., Hearty, F. R., Johnson, J. A., Mészáros, S., Minchev, I., O'Connell, R., Pan, K., Robin, A. C., Schiavon, R. P., Schneider, D. P., Schultheis, M., Shetrone, M., Skrutskie, M., Steinmetz, M., Smith, V., Wilson, J. C., Zamora, O., & Zasowski, G. 2015, The Astrophysical Journal, 808, 132

Hole, K. T., Geller, A. M., Mathieu, R. D., Platais, I., Meibom, S., & Latham, D. W. 2009, The Astronomical Journal, 138, 159

Holtzman, J. A., Hasselquist, S., Shetrone, M., Cunha, K., Allende Prieto, C., Anguiano, B., Bizyaev, D., Bovy, J., Casey, A., Edvardsson, B., Johnson, J. A., Jönsson, H., Meszaros, S., Smith, V. V., Sobeck, J., Zamora, O., Chojnowski, S. D., Fernandez-Trincado, J., Garcia-Hernandez, D. A., Majewski, S. R., Pinsonneault, M., Souto, D., Stringfellow, G. S., Tayar, J., Troup, N., & Zasowski, G. 2018, The Astronomical Journal, 156, 125

Holtzman, J. A., Shetrone, M., Johnson, J. A., Allende Prieto, C., Anders, F., Andrews, B., Beers, T. C., Bizyaev, D., Blanton, M. R., Bovy, J., Carrera, R., Chojnowski, S. D., Cunha, K., Eisenstein, D. J., Feuillet, D., Frinchaboy, P. M., Galbraith-Frew, J., García Pérez, A. E., García-Hernández, D. A., Hasselquist, S., Hayden, M. R., Hearty, F. R., Ivans, I., Majewski, S. R., Martell, S., Meszaros, S., Muna, D., Nidever, D., Nguyen, D. C., O'Connell, R. W., Pan, K., Pinsonneault, M., Robin, A. C., Schiavon, R. P., Shane, N., Sobeck, J., Smith, V. V., Troup, N., Weinberg, D. H., Wilson, J. C., Wood-Vasey, W. M., Zamora, O., & Zasowski, G. 2015, The Astronomical Journal, 150, 148

Jacobson, H. R., Pilachowski, C. A., & Friel, E. D. 2011, The Astronomical Journal, 142, 59

Janes, K. A. 1979, Astrophysical Journal Supplement, 39, 135

Jönsson, H., Allende Prieto, C., Holtzman, J. A., Feuillet, D. K., Hawkins, K., Cunha, K., Mészáros, S., Hasselquist, S., Fernández-Trincado, J. G., García-Hernández, D. A., Bizyaev, D., Carrera, R., Majewski, S. R., Pinsonneault, M. H., Shetrone, M., Smith, V., Sobeck, J., Souto, D., Stringfellow, G. S., Teske, J., & Zamora, O. 2018, The Astronomical Journal, 156, 126

Kharchenko, N. V., Piskunov, A. E., Schilbach, E., Röser, S., & Scholz, R.-D. 2013, Astronomy and Astrophysics, 558, A53

Kounkel, M., Covey, K., Suárez, G., Román-Zúñiga, C., Hernandez, J., Stassun, K., Jaehnig, K. O., Feigelson, E. D., Peña Ramírez, K., Roman-Lopes, A., Da Rio, N., Stringfellow, G. S., Kim, J. S., Borissova, J., Fernández-Trincado, J. G., Burgasser, A., García-Hernández, D. A., Zamora, O., Pan, K., & Nitschelm, C. 2018, The Astronomical Journal, 156, 84

Kubryk, M., Prantzos, N., & Athanassoula, E. 2015, Astronomy and Astrophysics, 580, A127

Lindegren, L., Hernández, J., Bombrun, A., Klioner, S., Bastian, U., Ramos-Lerate, M., de Torres, A., Steidelmüller, H., Stephenson, C., Hobbs, D., Lammers, U., Biermann, M., Geyer, R., Hilger, T., Michalik, D., Stampa, U., McMillan, P. J., Castañeda, J., Clotet, M., Comoretto, G., Davidson, M., Fabricius, C., Gracia, G., Hambly, N. C., Hutton, A., Mora, A., Portell, J., van Leeuwen, F., Abbas, U., Abreu, A., Altmann, M.,

Andrei, A., Anglada, E., Balaguer-Núñez, L., Barache, C., Becciani, U., Bertone, S., Bianchi, L., Bouquillon, S., Bourda, G., Brüsemeister, T., Bucciarelli, B., Busonero, D., Buzzi, R., Cancelliere, R., Carlucci, T., Charlot, P., Cheek, N., Crosta, M., Crowley, C., de Bruijne, J., de Felice, F., Drimmel, R., Esquej, P., Fienga, A., Fraile, E., Gai, M., Garralda, N., González-Vidal, J. J., Guerra, R., Hauser, M., Hofmann, W., Holl, B., Jordan, S., Lattanzi, M. G., Lenhardt, H., Liao, S., Licata, E., Lister, T., Löffler, W., Marchant, J., Martin-Fleitas, J. M., Messineo, R., Mignard, F., Morbidelli, R., Poggio, E., Riva, A., Rowell, N., Salguero, E., Sarasso, M., Sciacca, E., Siddiqui, H., Smart, R. L., Spagna, A., Steele, I., Taris, F., Torra, J., van Elteren, A., van Reeven, W., & Vecchiato, A. 2018, Astronomy and Astrophysics, 616, A2

Linden, S. T., Pryal, M., Hayes, C. R., Troup, N. W., Majewski, S. R., Andrews, B. H., Beers, T. C., Carrera, R., Cunha, K., Fernández-Trincado, J. G., Frinchaboy, P., Geisler, D., Lane, R. R., Nitschelm, C., Pan, K., Allende Prieto, C., Roman-Lopes, A., Smith, V. V., Sobeck, J., Tang, B., Villanova, S., & Zasowski, G. 2017, The Astrophysical Journal, 842, 49

Luo, A. L., Zhao, Y.-H., Zhao, G., Deng, L.-C., Liu, X.-W., Jing, Y.-P., Wang, G., Zhang, H.-T., Shi, J.-R., Cui, X.-Q., Chu, Y.-Q., Li, G.-P., Bai, Z.-R., Wu, Y., Cai, Y., Cao, S.-Y., Cao, Z.-H., Carlin, J. L., Chen, H.-Y., Chen, J.-J., Chen, K.-X., Chen, L., Chen, X.-L., Chen, X.-Y., Chen, Y., Christlieb, N., Chu, J.-R., Cui, C.-Z., Dong, Y.-Q., Du, B., Fan, D.-W., Feng, L., Fu, J.-N., Gao, P., Gong, X.-F., Gu, B.-Z., Guo, Y.-X., Han, Z.-W., He, B.-L., Hou, J.-L., Hou, Y.-H., Hou, W., Hu, H.-Z., Hu, N.-S., Hu, Z.-W., Huo, Z.-Y., Jia, L., Jiang, F.-H., Jiang, X., Jiang, Z.-B., Jin, G., Kong, X., Kong, X., Lei, Y.-J., Li, A.-H., Li, C.-H., Li, G.-W., Li, H.-N., Li, J., Li, Q., Li, S., Li, S.-S., Li, X.-N., Li, Y., Li, Y.-B., Li, Y.-P., Liang, Y., Lin, C.-C., Liu, C., Liu, G.-R., Liu, G.-Q., Liu, Z.-G., Lu, W.-Z., Luo, Y., Mao, Y.-D., Newberg, H., Ni, J.-J., Qi, Z.-X., Qi, Y.-J., Shen, S.-Y., Shi, H.-M., Song, J., Song, Y.-H., Su, D.-Q., Su, H.-J., Tang, Z.-H., Tao, Q.-S., Tian, Y., Wang, D., Wang, D.-Q., Wang, F.-F., Wang, G.-M., Wang, H., Wang, H.-C., Wang, J., Wang, J.-N., Wang, J.-L., Wang, J.-P., Wang, J.-X., Wang, L., Wang, M.-X., Wang, S.-G., Wang, S.-Q., Wang, X., Wang, Y.-N., Wang, Y., Wang, Y.-F., Wang, Y.-F., Wei, P., Wei, M.-Z., Wu, H., Wu, K.-F., Wu, X.-B., Wu, Y.-Z., Xing, X.-Z., Xu, L.-Z., Xu, X.-Q., Xu, Y., Yan, T.-S., Yang, D.-H., Yang, H.-F., Yang, H.-Q., Yang, M., Yao, Z.-Q., Yu, Y., Yuan, H., Yuan, H.-B., Yuan, H.-L., Yuan, W.-M., Zhai, C., Zhang, E.-P., Zhang, H.-W., Zhang, J.-N., Zhang, L.-P., Zhang, W., Zhang, Y., Zhang, Y.-X., Zhang, Z.-C., Zhao, M., Zhou, F., Zhou, X., Zhu, J., Zhu, Y.-T., Zou, S.-C., & Zuo, F. 2015, Research in Astronomy and Astrophysics, 15, 1095

Magrini, L., Randich, S., Donati, P., Bragaglia, A., Adibekyan, V., Romano, D., Smiljanic, R., Blanco-Cuaresma, S., Tautvaišienė, G., Friel, E., Overbeek, J., Jacobson, H., Cantat-Gaudin, T., Vallenari, A., Sordo, R., Pancino, E., Geisler, D., San Roman, I., Villanova, S., Casey, A., Hourihane, A., Worley, C. C., Francois, P., Gilmore, G., Bensby, T., Flaccomio, E., Korn, A. J., Recio-Blanco, A., Carraro, G., Costado, M. T., Franciosini, E., Heiter, U., Jofré, P., Lardo, C., de Laverny, P., Monaco, L., Morbidelli, L., Sacco, G., Sousa, S. G., & Zaggia, S. 2015, Astronomy and Astrophysics, 580, A85

Magrini, L., Randich, S., Kordopatis, G., Prantzos, N., Romano, D., Chieffi, A., Limongi, M., François, P., Pancino, E., Friel, E., Bragaglia, A., Tautvaišienė, G., Spina, L., Overbeek, J., Cantat-Gaudin, T., Donati, P., Vallenari, A., Sordo, R., Jiménez-Esteban, F. M., Tang, B., Drazdauskas, A., Sousa, S., Duffau, S., Jofré, P., Gilmore, G., Feltzing, S., Alfaro, E., Bensby, T., Flaccomio, E., Koposov, S., Lanzafame, A., Smiljanic, R., Bayo, A., Carraro, G., Casey, A. R., Costado, M. T., Damiani, F., Franciosini, E., Hourihane, A., Lardo, C., Lewis, J., Monaco, L., Morbidelli, L., Sacco, G., Sbordone, L., Worley, C. C., & Zaggia, S. 2017, Astronomy and Astrophysics, 603, A2

Majewski, S. R., Schiavon, R. P., Frinchaboy, P. M., Allende Prieto, C., Barkhouser, R., Bizyaev, D., Blank, B., Brunner, S., Burton, A., Carrera, R., Chojnowski, S. D., Cunha, K., Epstein, C., Fitzgerald, G., García Pérez, A. E., Hearty, F. R., Henderson, C., Holtzman, J. A., Johnson, J. A., Lam, C. R., Lawler, J. E., Maseman, P., Mészáros, S., Nelson, M., Nguyen, D. C., Nidever, D. L., Pinsonneault, M., Shetrone, M., Smee, S., Smith, V. V., Stolberg, T., Skrutskie, M. F., Walker, E., Wilson, J. C., Zasowski, G., Anders, F., Basu, S., Beland, S., Blanton, M. R., Bovy, J., Brownstein, J. R., Carlberg, J., Chaplin, W., Chiappini, C., Eisenstein, D. J., Elsworth, Y., Feuillet, D., Fleming, S. W., Galbraith-Frew, J., García, R. A., García-Hernández, D. A., Gillespie, B. A., Girardi, L., Gunn, J. E., Hasselquist, S., Hayden, M. R., Hekker, S., Ivans, I., Kinemuchi, K., Klaene, M., Mahadevan, S., Mathur, S., Mosser, B., Muna, D., Munn, J. A., Nichol, R. C., O'Connell, R. W., Parejko, J. K., Robin, A. C., Rocha-Pinto, H., Schultheis, M., Serenelli, A. M., Shane, N., Silva Aguirre, V., Sobeck, J. S., Thompson, B., Troup, N. W., Weinberg, D. H., & Zamora, O. 2017, The Astronomical Journal, 154, 94

Majewski, S. R., Zasowski, G., & Nidever, D. L. 2011, The Astrophysical Journal, 739, 25

Mermilliod, J. C., Mayor, M., & Udry, S. 2008, Astronomy and Astrophysics, 485, 303

Mészáros, S., Allende Prieto, C., Edvardsson, B., Castelli, F., García Pérez, A. E., Gustafsson, B., Majewski, S. R., Plez, B., Schiavon, R., Shetrone, M., & de Vicente, A. 2012, The Astronomical Journal, 144, 120

Minchev, I., Anders, F., Recio-Blanco, A., Chiappini, C., de Laverny, P., Queiroz, A., Steinmetz, M., Adibekyan, V., Carrillo, I., Cescutti, G., Guiglion, G., Hayden, M., de Jong, R. S., Kordopatis, G., Majewski, S. R., Martig, M., & Santiago, B. X. 2018, Monthly Notices of the Royal Astronomical Society, 481, 1645

Minchev, I., Chiappini, C., & Martig, M. 2013, Astronomy and Astrophysics, 558, A9

—. 2014, Astronomy and Astrophysics, 572, A92

Minchev, I., Matijevic, G., Hogg, D. W., Guiglion, G., Steinmetz, M., Anders, F., Chiappini, C., Martig, M., Queiroz, A., & Scannapieco, C. 2019, Monthly Notices of the Royal Astronomical Society, 487, 3946

Netopil, M., Paunzen, E., Heiter, U., & Soubiran, C. 2016, Astronomy and Astrophysics, 585, A150

Nidever, D. L., Holtzman, J. A., Allende Prieto, C., Beland, S., Bender, C., Bizyaev, D., Burton, A., Desphande, R., Fleming, S. W., García Pérez, A. E., Hearty, F. R., Majewski, S. R., Mészáros, S., Muna, D., Nguyen, D., Schiavon, R. P., Shetrone, M., Skrutskie, M. F., Sobeck, J. S., & Wilson, J. C. 2015, The Astronomical Journal, 150, 173

Nomoto, K., Kobayashi, C., & Tominaga, N. 2013, The Annual Review of Astronomy and Astrophysics, 51, 457

Origlia, L., Valenti, E., Rich, R. M., & Ferraro, F. R. 2006, The Astrophysical Journal, 646, 499

Overbeek, J. C., Friel, E. D., & Jacobson, H. R. 2016, The Astrophysical Journal, 824, 75

Pancino, E., Carrera, R., Rossetti, E., & Gallart, C. 2010, Astronomy and Astrophysics, 511, A56

Quillen, A. C., Nolting, E., Minchev, I., De Silva, G., & Chiappini, C. 2018, Monthly Notices of the Royal Astronomical Society, 475, 4450

Raboud, D., Grenon, M., Martinet, L., Fux, R., & Udry, S. 1998, Astronomy and Astrophysics, 335, L61

Reddy, A. B. S., Giridhar, S., & Lambert, D. L. 2012, Monthly Notices of the Royal Astronomical Society, 419, 1350

—. 2013, Monthly Notices of the Royal Astronomical Society, 431, 3338

—. 2015, Monthly Notices of the Royal Astronomical Society, 450, 4301

Reddy, A. B. S., Lambert, D. L., & Giridhar, S. 2016, Monthly Notices of the Royal Astronomical Society, 463, 4366

Riello, M., De Angeli, F., Evans, D. W., Busso, G., Hambly, N. C., Davidson, M., Burgess, P. W., Montegriffo, P., Osborne, P. J., Kewley, A., Carrasco, J. M., Fabricius, C., Jordi, C., Cacciari, C., van Leeuwen, F., & Holland, G. 2018, Astronomy and Astrophysics, 616, A3

Sellwood, J. A. 2014, Reviews of Modern Physics, 86, 1

Sestito, P., Bragaglia, A., Randich, S., Pallavicini, R., Andrievsky, S. M., & Korotin, S. A. 2008, Astronomy and Astrophysics, 488, 943

Smith, V. V. & Suntzeff, N. B. 1987, The Astronomical Journal, 93, 359

Soubiran, C., Cantat-Gaudin, T., Romero-Gómez, M., Casamiquela, L., Jordi, C., Vallenari, A., Antoja, T., Balaguer-Núñez, L., Bossini, D., Bragaglia, A., Carrera, R., Castro-Ginard, A., Figueras, F., Heiter, U., Katz, D., Krone-Martins, A., Le Campion, J. F., Moitinho, A., & Sordo, R. 2018, Astronomy and Astrophysics, 619, A155

Souto, D., Allende Prieto, C., Cunha, K., Pinsonneault, M., Smith, V. V., Garcia-Dias, R., Bovy, J., García-Hernández, D. A., Holtzman, J., Johnson, J. A., Jönsson, H., Majewski, S. R., Shetrone, M., Sobeck, J., Zamora, O., Pan, K., & Nitschelm, C. 2019, The Astrophysical Journal, 874, 97

Souto, D., Cunha, K., Smith, V., Allende Prieto, C., Pinsonneault, M., Zamora, O., García-Hernández, D. A., Mészáros, S., Bovy, J., García Pérez, A. E., Anders, F., Bizyaev, D., Carrera, R., Frinchaboy, P. M., Holtzman, J., Ivans, I., Majewski, S. R., Shetrone, M., Sobeck, J., Pan, K., Tang, B., Villanova, S., & Geisler, D. 2016, The Astrophysical Journal, 830, 35

Souto, D., Cunha, K., Smith, V. V., Allende Prieto, C., García-Hernández, D. A., Pinsonneault, M., Holzer, P., Frinchaboy, P., Holtzman, J., Johnson, J. A., Jönsson, H., Majewski, S. R., Shetrone, M., Sobeck, J., Stringfellow, G., Teske, J., Zamora, O., Zasowski, G., Carrera, R., Stassun, K., Fernand ez-Trincado, J. G., Villanova, S., Minniti, D., & Santana, F. 2018, The Astrophysical Journal, 857, 14

Spina, L., Randich, S., Magrini, L., Jeffries, R. D., Friel, E. D., Sacco, G. G., Pancino, E., Bonito, R., Bravi, L., Franciosini, E., Klutsch, A., Montes, D., Gilmore, G., Vallenari, A., Bensby, T., Bragaglia, A., Flaccomio, E., Koposov, S. E., Korn, A. J., Lanzafame, A. C., Smiljanic, R., Bayo, A., Carraro, G., Casey, A. R., Costado, M. T., Damiani, F., Donati, P., Frasca, A., Hourihane, A., Jofré, P., Lewis, J., Lind, K., Monaco, L., Morbidelli, L., Prisinzano, L., Sousa, S. G., Worley, C. C., & Zaggia, S. 2017, Astronomy and Astrophysics, 601, A70

Stassun, K. G. & Torres, G. 2018, The Astrophysical Journal, 862, 61

Tautvaišiene, G., Edvardsson, B., Tuominen, I., & Ilyin, I. 2000, Astronomy and Astrophysics, 360, 499

Twarog, B. A., Ashman, K. M., & Anthony-Twarog, B. J. 1997, The Astronomical Journal, 114, 2556

von Hippel, T., Jefferys, W. H., Scott, J., Stein, N., Winget, D. E., De Gennaro, S., Dam, A., & Jeffery, E. 2006, The Astrophysical Journal, 645, 1436

Wilson, J. C., Hearty, F., Skrutskie, M. F., Majewski, S. R., Schiavon, R., Eisenstein, D., Gunn, J., Holtzman, J., Nidever, D., Gillespie, B., Weinberg, D., Blank, B., Henderson, C., Smee, S., Barkhouser, R., Harding, A., Hope, S., Fitzgerald, G., Stolberg, T., Arns, J., Nelson, M., Brunner, S., Burton, A., Walker, E., Lam, C., Maseman, P., Barr, J., Leger, F., Carey, L., MacDonald, N., Ebelke, G., Beland, S., Horne, T., Young, E., Rieke, G., Rieke, M., O'Brien, T., Crane, J., Carr, M., Harrison, C., Stoll, R., Vernieri, M., Shetrone, M., Allende-Prieto, C., Johnson, J., Frinchaboy, P., Zasowski, G., Garcia

Perez, A., Bizyaev, D., Cunha, K., Smith, V. V., Meszaros, S., Zhao, B., Hayden, M., Chojnowski, S. D., Andrews, B., Loomis, C., Owen, R., Klaene, M., Brinkmann, J., Stauffer, F., Long, D., Jordan, W., Holder, D., Cope, F., Naugle, T., Pfaffenberger, B., Schlegel, D., Blanton, M., Muna, D., Weaver, B., Snedden, S., Pan, K., Brewington, H., Malanushenko, E., Malanushenko, V., Simmons, A., Oravetz, D., Mahadevan, S., & Halverson, S. 2012, in Proceedings of the SPIE, Vol. 8446, Ground-based and Airborne Instrumentation for Astronomy IV, 84460H

Wilson, J. C., Hearty, F. R., Skrutskie, M. F., Majewski, S. R., Holtzman, J. A., Eisenstein, D., Gunn, J., Blank, B., Henderson, C., Smee, S., Nelson, M., Nidever, D., Arns, J., Barkhouser, R., Barr, J., Beland, S., Bershady, M. A., Blanton, M. R., Brunner, S., Burton, A., Carey, L., Carr, M., Colque, J. P., Crane, J., Damke, G. J., Davidson, J. W., J., Dean, J., Di Mille, F., Don, K. W., Ebelke, G., Evans, M., Fitzgerald, G., Gillespie, B., Hall, M., Harding, A., Harding, P., Hammond, R., Hancock, D., Harrison, C., Hope, S., Horne, T., Karakla, J., Lam, C., Leger, F., MacDonald, N., Maseman, P., Matsunari, J., Melton, S., Mitcheltree, T., O'Brien, T., O'Connell, R. W., Patten, A., Richardson, W., Rieke, G., Rieke, M., Roman-Lopes, A., Schiavon, R. P., Sobeck, J. S., Stolberg, T., Stoll, R., Tembe, M., Trujillo, J. D., Uomoto, A., Vernieri, M., Walker, E., Weinberg, D. H., Young, E., Anthony-Brumfield, B., Bizyaev, D., Breslauer, B., De Lee, N., Downey, J., Halverson, S., Huehnerhoff, J., Klaene, M., Leon, E., Long, D., Mahadevan, S., Malanushenko, E., Nguyen, D. C., Owen, R., Sánchez-Gallego, J. R., Sayres, C., Shane, N., Shectman, S. A., Shetrone, M., Skinner, D., Stauffer, F., & Zhao, B. 2019, Publications of the Astronomical Society of the Pacific, 131, 055001

Wright, E. L., Eisenhardt, P. R. M., Mainzer, A. K., Ressler, M. E., Cutri, R. M., Jarrett, T., Kirkpatrick, J. D., Padgett, D., McMillan, R. S., Skrutskie, M., Stanford, S. A., Cohen, M., Walker, R. G., Mather, J. C., Leisawitz, D., Gautier, III, T. N., McLean, I., Benford, D., Lonsdale, C. J., Blain, A., Mendez, B., Irace, W. R., Duval, V., Liu, F., Royer, D., Heinrichsen, I., Howard, J., Shannon, M., Kendall, M., Walsh, A. L., Larsen, M., Cardon, J. G., Schick, S., Schwalm, M., Abid, M., Fabinsky, B., Naes, L., & Tsai, C.-W. 2010, The Astronomical Journal, 140, 1868

Yamaguchi, H., Badenes, C., Foster, A. R., Bravo, E., Williams, B. J., Maeda, K., Nobukawa, M., Eriksen, K. A., Brickhouse, N. S., Petre, R., & Koyama, K. 2015, The Astrophysical Journal Letters, 801, L31

Yong, D., Carney, B. W., & Friel, E. D. 2012, The Astronomical Journal, 144, 95

Yong, D., Carney, B. W., & Teixera de Almeida, M. L. 2005, The Astronomical Journal, 130, 597

Zamora, O., García-Hernández, D. A., Allende Prieto, C., Carrera, R., Koesterke, L., Edvardsson, B., Castelli, F., Plez, B., Bizyaev, D., Cunha, K., García Pérez, A. E., Gustafsson, B., Holtzman, J. A., Lawler, J. E., Majewski, S. R., Manchado, A., Mészáros, S., Shane, N., Shetrone, M., Smith, V. V., & Zasowski, G. 2015, The Astronomical Journal, 149, 181

Zasowski, G., Cohen, R. E., Chojnowski, S. D., Santana, F., Oelkers, R. J., Andrews, B., Beaton, R. L., Bender, C., Bird, J. C., Bovy, J., Carlberg, J. K., Covey, K., Cunha, K., Dell'Agli, F., Fleming, S. W., Frinchaboy, P. M., García-Hernández, D. A., Harding, P., Holtzman, J., Johnson, J. A., Kollmeier, J. A., Majewski, S. R., Mészáros, S., Munn, J., Muñoz, R. R., Ness, M. K., Nidever, D. L., Poleski, R., Román-Zúñiga, C., Shetrone, M., Simon, J. D., Smith, V. V., Sobeck, J. S., Stringfellow, G. S., Szigetiáros, L., Tayar, J., & Troup, N. 2017, The Astronomical Journal, 154, 198

Zasowski, G., Johnson, J. A., Frinchaboy, P. M., Majewski, S. R., Nidever, D. L., Rocha Pinto, H. J., Girardi, L., Andrews, B., Chojnowski, S. D., Cudworth, K. M., Jackson, K., Munn, J., Skrutskie, M. F., Beaton, R. L., Blake, C. H., Covey, K., Deshpande, R., Epstein, C., Fabbian, D., Fleming, S. W., Garcia Hernandez, D. A., Herrero, A., Mahadevan, S., Mészáros, S., Schultheis, M., Sellgren, K., Terrien, R., van Saders, J., Allende Prieto, C., Bizyaev, D., Burton, A., Cunha, K., da Costa, L. N., Hasselquist, S., Hearty, F., Holtzman, J., García Pérez, A. E., Maia, M. A. G., O'Connell, R. W., O'Donnell, C., Pinsonneault, M., Santiago, B. X., Schiavon, R. P., Shetrone, M., Smith, V., & Wilson, J. C. 2013, The Astronomical Journal, 146, 81

Zasowski, G., Schultheis, M., Hasselquist, S., Cunha, K., Sobeck, J., Johnson, J. A., Rojas-Arriagada, A., Majewski, S. R., Andrews, B. H., Jönsson, H., Beers, T. C., Chojnowski, S. D., Frinchaboy, P. M., Holtzman, J. A., Minniti, D., Nidever, D. L., & Nitschelm, C. 2019, The Astrophysical Journal, 870, 138

Zhang, J., Zhao, J., Oswalt, T. D., Fang, X., Zhao, G., Liang, X., Ye, X., & Zhong, J. 2019, The Astrophysical Journal, 887, 84

VITA

Personal Background	John Richard Donor III Bedford, TX Son of John and Amy Donor Married Rachel Christine Du Frane, June 17, 2017
Education	Diploma, Lawrence D. Bell High School, Hurst, TX, 2010 Bachelor of Arts, Physics, Austin College, Sherman, TX, 2014 Master of Science, Physics, Texas Christian University, Fort Worth, TX, 2017
Experience	Summer research assistant, Austin College, Sherman, TX, 2013 Teaching assistantship, Texas Christian University, Fort Worth, 2014-2017 SDSS Research assistantship, Texas Christian University, Fort Worth, 2018-2020
Professional Memberships	American Astronomical Society

ABSTRACT

OBSERVABLE CONSTRAINTS ON GALACTIC CHEMICAL EVOLUTION USING A UNIFORM SAMPLE OF OPEN CLUSTERS

by John R Donor III, 2020
Department of Physics and Astronomy
Texas Christian University

Peter M. Frinchaboy III, Associate Professor of Physics

Models of Galactic evolution are key to our understanding of not just our Galaxy but galaxies in general. Verifying observable constraints for these models is crucial. Open clusters are among the best tracers for establishing these constraints as they are reliable tracers for chemistry and age for which an accurate distance can also be determined. Previous work using open clusters however has relied on samples constructed from multiple studies, introducing significant uncertainty into any measurements made. We present methodology for targeting open cluster member stars, and establishing a probability for their membership within a cluster. Using this criteria, we establish a large, uniform sample of open clusters leveraging the APOGEE survey. This sample of 128 clusters, 71 of which we designate "high quality", is used to measure Galactic abundance gradients in 16 elements. Since our sample covers a wide age range, the evolution of the abundance gradients over time is also considered. We compare to previous work and a chemical evolution model, finding reasonable agreement with our results. Finally we discuss open cluster radial migration, a poorly understood topic, and find agreement with previous work that open clusters tend to migrate away from the Galactic center.